The response of Arabidopsis to low potassium availability

HETHERINGTON, FLORA,MARY

The response of *Arabidopsis* to low potassium availability

Flora Mary Hetherington

Submitted for the qualification of Doctor of Philosophy

Department of Biosciences, Durham University

September 2017

Abstract

The potassium ion (K^+) is vital for plant growth and development, and K^+ deficiency leads to reductions in crop yields. Given the significance of K^+ deficiency in agriculture, it is important to understand the mechanisms by which K^+ is taken into the plant and also how K^+ deficiency impacts on the architecture of the root system, both of which will influence the ability of the crop to forage for K^+ in the soil. The overall objective of the work described in this thesis is to uncover the mechanisms by which plant hormones control the root architectural responses to low K^+ in the Arabidopsis accession Col-0. This question has been investigated using a combination of microscopy, genetics, chemical intervention, transcriptomics and analysis of the published literature.

In response to low K^+ *Arabidopsis* reduces its lateral root (LR) growth, and it was established that this reduction in growth is mediated through a reduction in cell division in the LR meristems. Analysis of RNA-Seq data allowed the identification of gene transcriptional changes in response to low K^+. These data were then used to form hypotheses about the hormonal control of the reduction in LR growth. Data in this thesis allowed the identification of a role for the hormone gibberellin (GA) and for DELLA proteins in the modulation of LR growth in response to K^+ starvation. These data were also used to identify the CBF1 transcription factor as a potential regulator of changes in cellular GA levels in response to low K^+. The roles of reactive oxygen species (ROS), ethylene, auxin and abscisic acid (ABA) in the regulation of the root architectural responses to low K^+ were investigated but no clear regulatory effects were identified. A role for ethylene and low K^+ in the root gravitropic response was also identified. A model is proposed that describes the link between low K^+ availability and root architectural changes mediated by altered GA signalling pathways.

Table of contents

List of Figures

List of Tables

List of Appendices

Statement of authorship

I certify that all of the work described in this thesis is my own original research unless otherwise acknowledged in the text or by references, and has not been previously submitted for a degree in this or any other university.

Statement of copyright

List of Abbreviations

The standard scientific conventions for protein and gene naming have been followed: wild type genes and proteins are in capitals and mutants are denoted by lower case, gene names are italicized whereas protein names are not.

Standard scientific abbreviations have been used for units of weight, length, amount, molarity, temperature and time.

Standard chemical element symbols, nucleic acid and amino acid codes are used.

½ MS10	Half strength Murashige & Skoog media
ABA	Abscisic acid
ACC	1-aminocyclopropane-1-carboxylic acid
Ag^{2+}	Silver ions (used in this thesis in the form of silver thiosulphate)
Col-0	Columbia
CSLM	Confocal scanning laser microscopy
DAG	Days after germination
DEGs	Differentially expressed genes
DMSO	Dimethyl sulfoxide
DNA	Deoxyribonucleic acid
DPI	Diphenylene iodonium
Fe	Iron
GA	Gibberellic acid
GFP	Green fluorescent protein
GO	Gene ontology
GUS	β-glucuronidase
IAA	Indole-3-acetic acid
JA	Jasmonic acid

K^+	Potassium
LC-MS	Liquid chromatography-mass spectrometry
Log_2fc	Log_2 fold change
LR	Lateral root
LRP	Lateral root primordia
LSFM	Light sheet fluorescence technology
NGS	next generation sequencing
NPA	N-1-naphthylphthalamic acid
PAC	Paclobutrazol
PAT	Polar auxin transport
PCR	Polymerase chain reaction
PR	Primary root
QC	Quiescent centre
qRT-PCR	Quantitative real time PCR
RNA	Ribonucleic acid
RNA-Seq	RNA Sequencing
ROS	Reactive oxygen species
RSA	Root system architecture
sdH2O	Sterile distilled water
T-DNA	Transfer DNA
TF	Transcription factor
VGI	Vertical growth index
WT	Wild type
YFP	Yellow fluorescent protein

Acknowledgements

First, I need to thank Keith for being such a fantastic supervisor. You supported me and guided me at every step of the way, allowing me to go off on scientific tangents, but always knowing when to reign me in. You managed to turn every negative result into something positive and meetings with you always made me so excited to get back into the lab. A huge thank you as well to Jen for your invaluable technical knowhow and for always being around for a chat. Thank you both for the friendship, the laughs, the drinks, and the jazz, it really has been wonderful.

Next, I need to thank all the members of Labs 1004 and 1003 over the many years. James, 'the knower of all things', thanks so much for the drinks, the dancing and for teaching me everything I know. Anna, you welcomed me into the lab and into your friendship group, those first few years wouldn't have been the same without you. Amy, thank you for always knowing that there isn't a problem that can't be solved by a trip to Fabio's, you're going to be a fab PG rep, good luck with everything. Miguel, thanks so much for your help with my RNA-Seq data, and Peter, thank you for keeping me going these past couple of years. Your knowledge and advice have been immensely helpful, and you (mostly) know just how to cheer me up when I'm in a grump. Thanks also to Little Sam, Big Sam, Vinny, Kat, Devina, Helen, Ahmed, Martin, Pat, Greg, Dave, Johan, Joey, Grace and Shauni for making the lab such a fun place to work.

A massive thank you to all my friends from Cuths over the years. It's been a whirlwind of formals, gin, adventures and silent discos, and you all provided me with the escape and perspective I sometimes needed from the lab. John, despite our rocky beginnings, you've been an amazing friend, living with you has been wonderful, thanks so much for everything. Heather and Tom, the worst influences, but the best memories, I couldn't have done it without you two.

Mum and Dad, how can I thank you both enough for everything you have done to help me through this PhD. Thank you so much for your unwavering support, for always being at the end of the phone or email, and for inspiring me to become a scientist in the first place.

Chapter 1 Introduction

1.1 Potassium

Potassium (K^+) is one of the most important nutrients that plants need to survive. It is the most abundant cation in higher plants, making up 2–10% of the dry weight of a plant (Leigh & Jones, 1984), and is known to be essential for many functions in the plant, including enzyme activation, stomatal activity, photosynthesis, protein synthesis and the transport of sugars, water and nutrients (see Prajapati & Modi, 2012 for a review). A key role for sufficient K^+ nutrition in plant resistance to various abiotic and biotic stresses has also been identified; these include disease resistance, drought, salt, low temp and reactive oxygen species (ROS) (reviewed in M. Wang *et al.*, 2013). All these examples highlight the essential nature of this nutrient in plant growth and survival.

Despite being one of the most abundant elements on the earth, its availability to plants is often limited. Typically, the concentration of K^+ in soil is between 0.1 mM to 6 mM (Adams, 1971) although acidic soils and intensive farming can lead to the depletion of K^+ in soils. As a result, large areas of the world's agricultural land are K^+-deficient, including three-quarters of the paddy soils of China and two-thirds of the wheat belt of southern Australia (Romheld & Kirkby, 2010). This deficiency leads to reductions in crop growth, which translates to significantly reduced yields (Amtmann & Rubio, 2012). To alleviate this problem, it is necessary to apply large amounts of K^+ fertilizer to the soils. Potassium in soil solution, as is applied in fertilizer form, is rapidly depleted by crops, therefore requiring regular application to maintain levels of growth. With increased food demands requirements for, and consumption of, potash fertilizer are set to increase dramatically (FAO, 2015).

K^+ starved soil is a problem particularly in developing countries, as the addition of K^+ fertilisers is often neglected or not possible for economic reasons. A recent NAAIAP report (2014) has highlighted this problem in Kenya, and describes large areas of K^+-deficient soils. This has been attributed to the omission of K^+ from fertiliser application since the 1960s, due to the assumption that it was not a limiting factor for growth (Kanyanjua & Ayaga, 2006). K^+ starvation not only leads to reduced yields, but also impacts on the nutritional content of crops and animal fodder. In addition to its importance in plants, K^+ is an essential nutrient in the human body, where it is involved in the maintenance of the volume of body fluid, the balance of acid and electrolytes and the maintenance of normal cellular functioning (Young, 2001).

World Health Organisation (WHO) reports have linked reduced K^+ in the diet to increased risk of cardiovascular disease, stroke and coronary heart diseases (World Health Organization, 2012). This report also highlighted that the average K^+ consumption in many countries is lower than the recommended daily intake (World Health Organization, 2012). Therefore, the K^+ content of crop plants is of great importance.

Given the importance of K^+ deficiency on crops it is therefore important to understand the mechanisms by which K^+ is taken into the plant and the way in which the architecture of the roots affects the ability to forage for K^+ in the soil. Even with the addition of K^+ to fields, the availability of K^+ for uptake by plant roots is affected by many different factors. Variables such as soil water availability, soil density, soil pH and the presence of NH_4^+ and Na^+ (Jung *et al.*, 2009) also limit the extent of K^+ uptake, and therefore plants have developed mechanisms to enable them to withstand periods of K^+ deficiency.

1.2 K^+ uptake and sensing

To date there have been 71 K^+ channels and transporters characterized in Arabidopsis; these are classified into three families of transporters (KUP/HAK/KT, HKT and CPA) and two families of channels (*Shaker* and Tandem-Pore K^+ (TPK)/ K_{ir}-like; Gierth & Mäser, 2007; Marcel *et al.*, 2010; Voelker *et al.*, 2010; Wang & Wu, 2010; Chanroj *et al.*, 2012; Gomez-Porras *et al.*, 2012). Depending on the external K^+ concentration ($[K^+]_{ext}$), high or low affinity uptake mechanisms are used to maintain K^+ levels within the plant; high affinity acts at $[K^+]_{ext}$ <0.2 mM and low affinity acts at $[K^+]_{ext}$ >0.3 mM (Maathuis & Sanders, 1994; Schroeder *et al.*, 1994; Epstein *et al.,* 1963). This suggests that the plant is able to accurately sense $[K^+]_{ext}$ and readjust uptake mechanisms to adapt to the external concentration.

The sensing mechanism for $[K^+]_{ext}$ has not yet been identified in plants, but there are currently a number of different, non-mutually exclusive hypotheses, all of which involve the plasma membrane (PM). One hypothesis postulates the direct electrical polarization of the membrane as a result of the change in flow of K^+. Hyperpolarization of the membrane potential under low $[K^+]_{ext}$ occurs only minutes after a decrease in $[K^+]_{ext}$ (Schroeder & Fang, 1991; Maathuis & Sanders, 1993; Nieves-Cordones *et al.*, 2008), therefore this hyperpolarization could act as one of the earliest sensing signals to low K^+. An alternative hypothesis suggests that K^+ sensors are located at the PM of epidermal root cells due to their proximity with the $[K^+]_{ext}$ environment. The GORK shaker channel, and the K^+ transporter AKT1 have both been suggested as potential K^+ sensors in roots, because of their expression in the root hairs and root epidermis,

respectively (Sentenac *et al.*, 1992; Lagarde *et al.*, 1996; Johansson *et al.*, 2006). The identification of the nitrate (NO_3^-) sensor CHL1 (Ho *et al.*, 2009) further supports the potential for a role for AKT1 as a K^+ sensor, as they share a number of similarities. Both CHL1 and AKT1 have dual affinity properties for their specific ions (Hirsch *et al.*, 1998; Spalding *et al.*, 1999; Ho *et al.*, 2009), and are known to be regulated by the same set of CIPK-CBL (Calcineurin B-like (CBL)-interacting protein kinases and partners) (Li *et al.*, 2006; Xu *et al.*, 2006; Cheong *et al.*, 2007; Ho *et al.*, 2009; Tsay *et al.*, 2011). Recent advances have also linked Ca^{2+} signals to AKT1 activation under low K^+ (Behera *et al.*, 2017) and used root growth responses in the *akt1* mutant to suggest that the mutant is unable to perceive low K^+ (Li *et al.,* 2017). However, there is still much work to be done in order to understand the K^+ sensing mechanism(s) in plants. The work described in this thesis will focus on the events following K^+ perception, rather than K^+ sensing itself.

1.3 Responses of plants to nutrient starvation

In response to nutrient starvation there are typically two adaptive mechanisms employed by the plant to increase nutrient acquisition. The first is through the regulation of nutrient transporters, channels and their transport properties. The second is through the alteration of plant morphology. The latter involves the reprogramming of developmental processes in the roots, for example leading to increased lateral root (LR) branching and root hair growth to facilitate nutrient uptake through increased root surface area. Of the identified transporters and channels, only the K^+ transporter HAK5 is reported to be consistently upregulated in response to low K^+ levels (Ahn *et al.*, 2004; Gierth *et al.*, 2005). It is believed to be the major component of the high affinity K^+ uptake mechanism and, due to its rapid and consistent upregulation, much research has focussed on understanding how low soil K^+ leads to this increase in HAK5 expression. Work has demonstrated roles for the hormones ethylene and cytokinin, and for reactive oxygen species (ROS) in HAK5 expression (Shin & Schachtman, 2004; Jung *et al.*, 2009; Nam *et al.*, 2012). In addition, the affinity of HAK5 for K^+ has also been shown to be modified by protein phosphorylation (Ragel *et al.*, 2015). The roles of other K^+ channels have also been characterized in response to low soil K^+ (for a review see Ashley *et al.*, 2006). However, there has been less work investigating the role of root architectural changes leading to increased K^+-scavenging capacity in the response to low K^+. This topic will form the main focus of the work described in this thesis.

1.4 Root system architecture

Roots are essential for the sensing and uptake of water and nutrients from the soil but their physical location in the soil, and associated technical difficulties of biological analysis, has left them under-researched compared with the above-ground parts of the plant. A number of high profile review articles have declared roots to be the key to the 'next green revolution' and therefore an important factor in the maintenance of food security as populations increase dramatically (Lynch, 2007; Herder *et al.*, 2010). One of the below-ground characteristics of plants identified as a promising feature for enabling the so called 'new green revolution' is root system architecture (RSA).

RSA describes the spatial configuration of the root system and the exact arrangement of the root axes through the growth medium (Lynch, 1995). The main components of the root system are the primary root (PR), lateral roots (LRs), root hairs, seminal roots and adventitious roots (Smith & De Smet, 2012). The combinations of these different components of the root system vary between species, a difference that can be seen dramatically between monocotyledonous and dicotyledonous plants (Smith & De Smet, 2012). Root systems of dicots typically display a hierarchical tree structure, where one PR gives rise to LRs, and these LRs produce a branching pattern of higher order LRs (Kellermeier *et al.*, 2013) (Fig. 1-1A). By contrast, monocots such as grasses and cereals, form a much more complex fibrous root system, often with adventitious roots, such as crown roots, constituting a large proportion of the total root system (Smith & De Smet, 2012) (Fig. 1-1B).

In addition to between-species variation in root architecture there is also a large amount of within-species variability. Roots display phenotypic plasticity, which allows the plant to change its growth in response to changing environmental conditions, such as the availability of soil water and nutrients, and stresses such as salinity (López-Bucio *et al.*, 2003; Comas *et al.*, 2013; Galvan-Ampudia *et al.*, 2013). It is this dynamic nature of RSA that determines the survival of plants in the continuously changing microenvironment they experience as they grow. Identification of root traits that increase the nutrient- and water-foraging capacity of a plant is essential for breeding programmes focused on increasing crop productivity and survivability in a future of limited resources and against a backdrop of a changing climate. Traits such as rooting depth, gravitropic setpoint angle, root hair distribution and length, and the level of root branching have all been identified as key elements of RSA relevant for crop productivity (Paez-Garcia *et al.*, 2015). The importance of this area of research has recently been highlighted by RSA research resulting in increased shoot and yield attributes in maize (Hammer

et al., 2009; Lynch & Brown, 2012). Therefore, increasing knowledge of the RSA and the factors controlling RSA are key for increasing crop productivity in future breeding programmes.

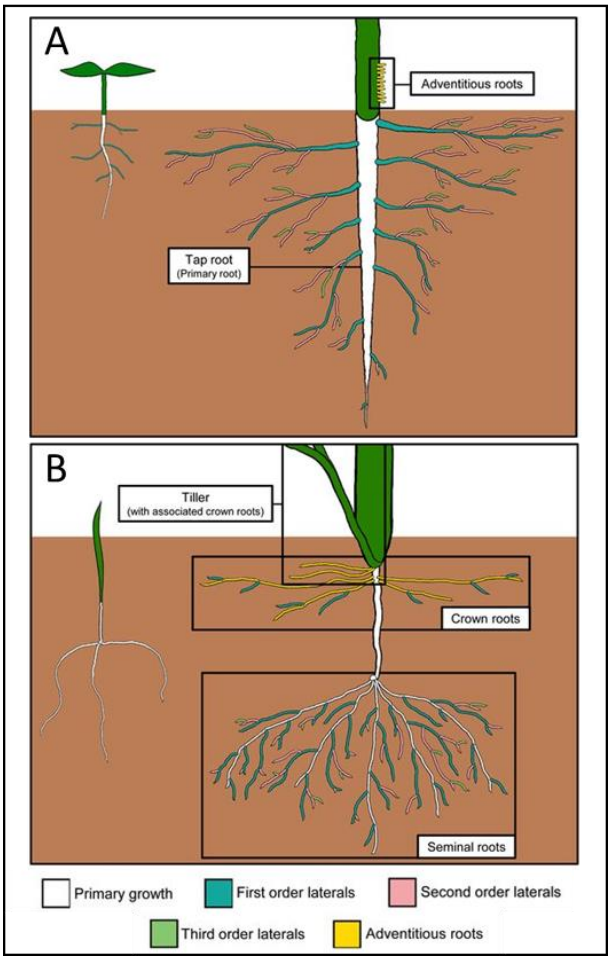

Fig. 1-1: Typical root architectures of dicot (A) (tomato) and monocot (B) (wheat) root systems, in both seedlings (left) and mature plants (right). Different root types are labelled in different colours. Adapted from Atkinson *et al.* (2014).

1.5 Arabidopsis as a model for root development

Arabidopsis thaliana has been used in plant science research for over 100 years, but it was not until the late 1970s/1980s that it was fully accepted as a model species across the research community. Traits such as short lifecycle, small size, ability to self-fertilize and diploid genome, led to its wide usage, and being the first published plant genome (The Arabidopsis Genome Initiative, 2000) cemented it as a key resource for molecular and developmental research. In addition to the above-mentioned traits, Arabidopsis also presents an ideal model for root analysis. Displaying the typical dicotyledonous hierarchical tree RSA (Kellermeier *et al.*, 2013), it is small enough to grow on the surface of agar plates and has almost translucent roots with a diameter of only 100–150 µM. These features allow the characterization of RSA changes to various stimuli, and make microscopic analysis and quantification of changes very easy.

1.5.1 Structure and growth

The Arabidopsis root has a highly ordered structure (Dolan *et al.*, 1993). A transverse section displays a radial symmetry with concentric ring cell files, consisting of the epidermis, the cortex and the endodermis, all surrounding the vascular tissue, or stele, which is made up of pericycle, phloem, xylem and procambium (Scheres *et al.*, 1995) (Fig. 1-2). All of these distinct cell types originate from a pool of stem cell initials at the root tip. These cells are in contact with, and under the control of, the cells of the quiescent centre (QC), which act to maintain their undifferentiated state (Dolan *et al.*, 1993; van den Berg *et al.*, 1997; Van Berg *et al.*, 1998). Together the stem cells and QC make up the stem cell niche (SCN) (Fig. 1-2). Each cell file originates through asymmetric cell division from its specified stem-cell initial, thereby creating a self-renewing cell and a daughter cell. The cells undergo repeated cell division in the meristematic zone, before division stops and elongation begins in the elongation zone. The boundary between these two zones is referred to as the transition zone. The final zone is referred to as the differentiation zone, in which root hairs, vascular tissues and the Casparian strip develop (Verbelen *et al.*, 2006; Sanz *et al.*, 2009; Petricka *et al.*, 2012) (Fig. 1-2). This repeated cell division and elongation creates the basis of apical root growth, pushing the root tip further into the soil (Dolan *et al.*, 1993; Beemster & Baskin, 1998; Petricka *et al.*, 2012).

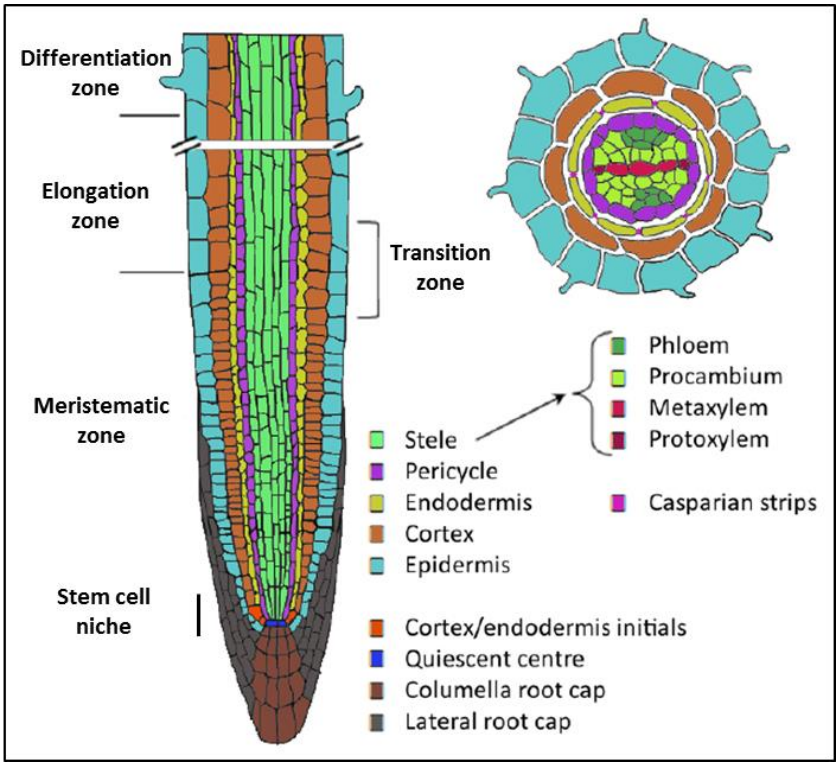

Fig. 1-2: Structure of the Arabidopsis root. Longitudinal section through the root (left), cross section of the root taken from the differentiation zone (right). Different cell types marked in different colours and developmental zones indicated. Image adapted from De Smet *et al.* (2015).

1.5.2 LR development

LRs develop from xylem pole pericycle cells, the priming of which occurs in the PR meristem. These primed cells then gain founder cell identity and go on to develop into LRs (Dubrovsky *et al.*, 2001; Benková *et al.*, 2003; De Smet *et al.*, 2007). These founder cells then undergo a series of periclinal and anticlinal cell divisions to form the LR primordium (LRP). Malamy & Benfey (1997) defined eight stages of LR development (Fig. 1-3A,B) each with specific anatomical characteristics and cell divisions (Malamy & Benfey, 1997). Initial anticlinal divisions of pericycle founder cells make a single layered primordium (stage I), then periclinal divisions create two layers (stage II). Combinations of both anticlinal and periclinal divisions then create the characteristic dome shape of the LRP (stages II–VII) (Fig. 1-3A,B). Stage VIII marks the emergence of the LRP from the PR, after which the meristem is activated and the LR continues to grow through tip-based growth, as described in the PR (Malamy & Benfey, 1997; Casimiro *et al.*, 2001; Dubrovsky *et al.*, 2001) (Fig. 1-3C). A number of plant hormones have important roles in the control of LR development, and auxin works centrally in the coordination of this developmental process (discussed further in section 1.7.1).

1.6 What is currently known about how K^+ affects root architecture?

K^+ deficiency is known to have an adverse impact on plant growth, both of the above ground tissue as well as the roots (Chérel *et al.*, 2014). The changes in root architecture of many crop plants have not been investigated due to the difficulty in cultivating and measuring root systems of crop species in controlled conditions; however, *A. thaliana* has been used as a model species to investigate the effects of K^+ starvation on growth and development of root systems. Work over many years has reported that in response to K^+ starvation there is inhibition of LR initiation and development (Armengaud *et al.*, 2004; Shin & Schachtman, 2004), an increase in root hair elongation (López-Bucio *et al.*, 2003; Desbrosses *et al.*, 2003; Jung *et al.*, 2009), inhibition of growth of the PR (Jung *et al.*, 2009; Kim *et al.*, 2010), and a mild agravitropic response (Vicente-Agullo *et al.*, 2004). Work by Kellermeier *et al.* (2013) reported a phenotypic gradient of growth responses to K^+ starvation in different accessions of *A. thaliana* explaining conflicting results published in previous papers. This phenotypic gradient has two extremes, based on the trade-off between growth of the PR and LRs. In the Kellermeier *et al*. paper two strategies were defined (Fig. 1-4): the first strategy results in the maintenance of the growth of the PR as K^+ decreases but restricts the growth of the LRs, whereas the second strategy restricts the growth of the PR in favour of elongation of LRs (Kellermeier *et al.*, 2013) (Fig. 1-4). Despite identifying this gradient, the architectures were not explored in detail and the mechanisms that govern the responses were not elucidated. The

ecological significance of these different strategies was also not discussed in the work and little is known about the optimal RSA for potassium foraging.

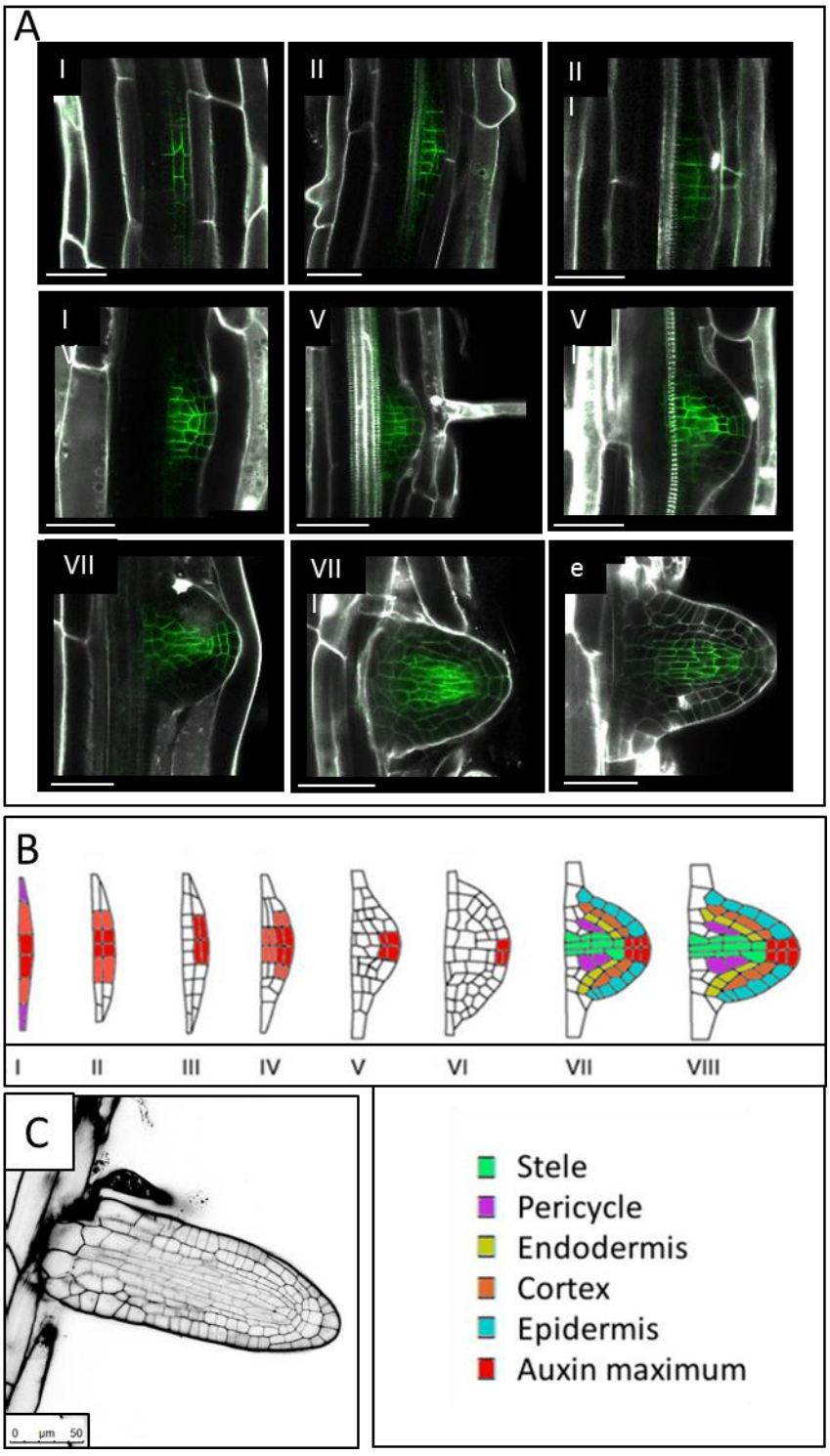

Fig. 1-3: Lateral root (LR) development in Arabidopsis. (A) Stages of lateral root primordia (LRP) development, stages 1- VII and e (emergence), as defined by Malamy & Benfey (1997). Cells visualized using *proPIN1::PIN1:GFP,* green is GFP, white is propidium iodide stain. Scale bars = 50 µm. (B) Different cell types in the developing LRPs, stages as described, Malamy & Benfey (1997). Figure adapted from (De Smet *et al.,* 2015). (C) LR after emergence from the primary root and after establishment of the meristem. Black, propidium iodide stain. Scale bar = 50 µm

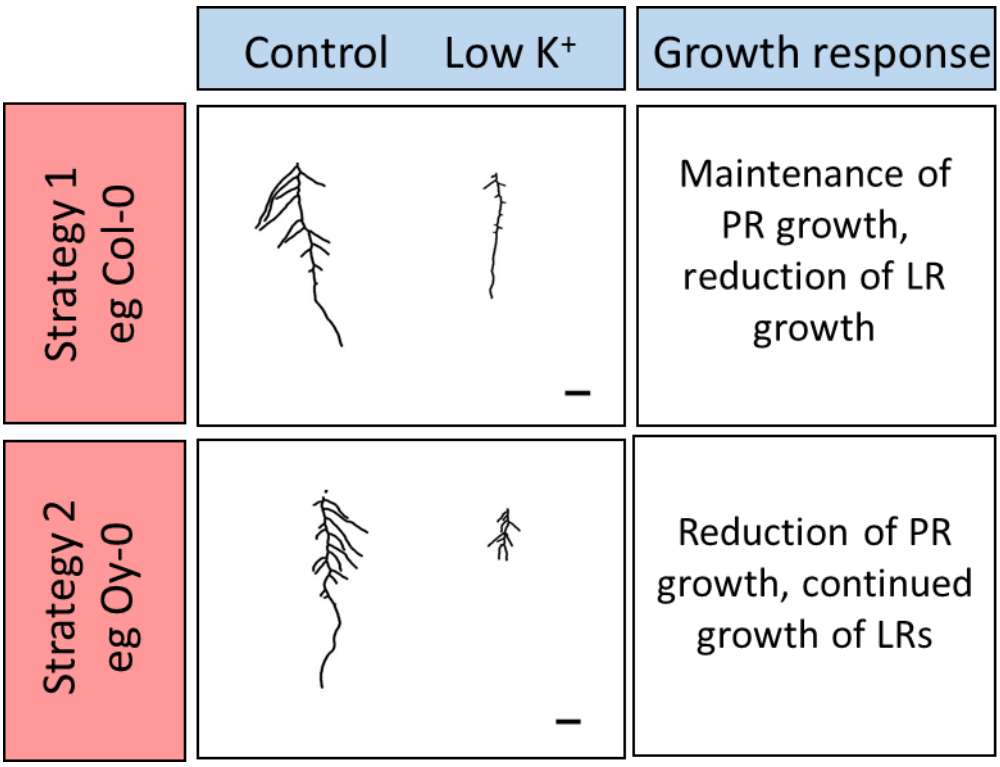

Fig. 1-4: Typical root architectural responses to low K^+ of 'strategy 1' and 'strategy 2' Arabidopsis accessions grown on control and low K^+ media. Images and definitions of growth responses from Kellermeier *et al.* (2013). Representative images taken 12 d after germination (DAG). Scale bars = 1 cm. Accessions represented Col-0 and Oystese-0 (Oy-0). PR, primary root; LR, lateral root.

1.7 Plant hormones as regulators of root growth

Hormones are ubiquitous across the plant and animal kingdoms and are defined as 'a chemical substance produced by one tissue with the primary function of exerting a specific effect of functional value on another tissue' (Huxley, 1935). Plant hormones are essential in governing and coordinating the developmental responses of the plant to external cues, such as light, temperature and nutrition. Investigations into the impacts of hormones on plant development have been ongoing since the late 1800s, with the plant hormone auxin initially being described by Charles Darwin in 'The power of movement in plants' (albeit chemically undefined at that point) (Darwin, 1880). More recently four other hormones, ethylene, gibberellin (GA), cytokinin and abscisic acid (ABA) have joined auxin to be collectively known as the classical five plant hormones. Synergistic or antagonistic interactions between different combinations of these hormones are key in coordinating processes such as LR formation (Chang *et al.*, 2013), PR growth (Dello Ioio *et al.*, 2008; Perilli *et al.*, 2010) and root hair development (Rahman *et al.*, 2002), as well as playing important roles in several developmental processes in the above-

ground tissues. Mutant screens and observations of specific mutants in Arabidopsis have allowed the discoveries of many of the hormonal perception and downstream signalling pathways, however there is still much that is unknown.

1.7.1 Auxin

Auxins are a class of plant hormones known to be essential in the coordination and control of almost all aspects of plant development and growth. The regulation of these processes is coordinated through directional transport and through auxin-specific regulation of gene transcription.

1.7.1.1 Directional auxin transport

The distribution of auxin in the root is controlled by polar auxin transport (PAT). This polar transport exhibited by auxin is unique among all plant hormones, and provides positional information for developmental processes. PAT is facilitated by the asymmetrical localization of membrane proteins inserted into the PM (Rubery & Sheldrake, 1974; Raven, 1975). These proteins belong to three main families; PIN-Formed (PIN), P-Glycoprotein (PGP), and AUX/LAX. Members of the AUX/LAX family act as influx carries, pumping auxin into cells. Of these proteins, AUX1 is the most studied (Bennett *et al.*, 1996; Marchant *et al.*, 1999; Yang *et al.*, 2006; Péret *et al.*, 2012). The PIN family act as an important group of efflux carriers (Friml, 2003; Petrášek *et al.*, 2006; Wisniewska *et al.*, 2006), and the PGP family has been less well characterised although they are thought to act independently but in coordination with the PINs (Mravec *et al.*, 2008). Auxin is transported acropetally through the vasculature of the PR mainly by AUX1 and PIN1 (Gälweiler *et al.*, 1998) (Fig. 1-5A). The proteins are localized to the apical and basal sides of the cells respectively, creating polar transport of auxin that correlates with the known directionality of the auxin flow (Swarup *et al.*, 2001). As auxin is transported to the root tip it is targeted to the root columella cells by PIN4, which is positioned on the distal side of the cells of the central root meristem (Friml *et al.*, 2002a) (Fig. 1-5A). Auxin accumulates in the first layers of columella cells, and during normal growth, the auxin is then directed symmetrically on both sides of the root by PIN3 and PIN7. Auxin is then transported in a basipetal direction to the elongation zone by AUX1 and PIN2 (Luschnig *et al.*, 1998; Müller *et al.*, 1998) (Fig. 1-5A), where it inhibits cell elongation (Wolverton *et al.*, 2002). This directional transport at the root tip is referred to as the reverse fountain model.

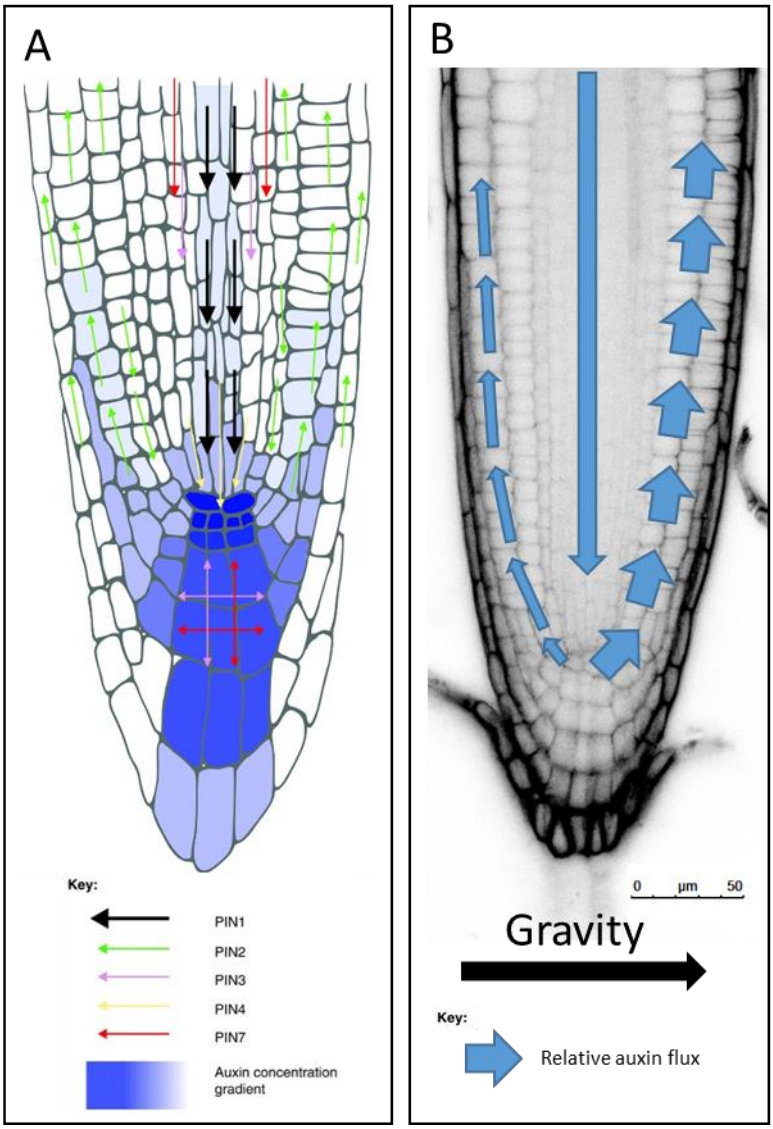

Fig. 1-5: (A) The reverse-fountain model of auxin transport in an Arabidopsis primary root tip, showing auxin distribution (blue gradient) and the direction of flow shown by the arrows mediated by the different PIN proteins involved. Figure from Křeček *et al.* (2009). AUX/LAX proteins are not included in this diagram. Black arrows show direction of acropetal auxin transport. Green arrows show direction of basipetal auxin transport. (B) In response to gravity auxin flux is redirected asymmetrically to the lower side of the root. The thickness of arrows depicts the relative auxin flux.

1.7.1.2 Auxin regulation of gene transcription

Auxin regulates transcription by rapidly stabilizing the interaction between Aux/IAA transcription factors and F-box proteins of the TRANSPORT INHIBITOR RESPONSE 1/ AUXIN SIGNALLING F-BOX (TIR1/AFB) family (Tan *et al.*, 2007). The F-box proteins act as the substrate selection subunit of the SCF-type ubiquitin protein ligase complex, thereby leading to the ubiquitination and removal of the inhibitory Aux/IAA by the 26S proteasome in an auxin-dependent manner (Fig. 1-6) (Gray *et al.*, 2001; Smalle & Vierstra, 2004; Dharmasiri *et al.*,

2005; Kepinski & Leyser, 2005; Dos Santos Maraschin *et al.*, 2009). Removal of the Aux/IAA transcriptional repressors (Ulmasov *et al.*, 1997) allows Auxin Response Factors (ARFs) to homodimerize and bind to the promoter regions of auxin regulated genes (Boer *et al.*, 2014; Mironova *et al.*, 2014), regulating the level of gene expression (Fig. 1-6).

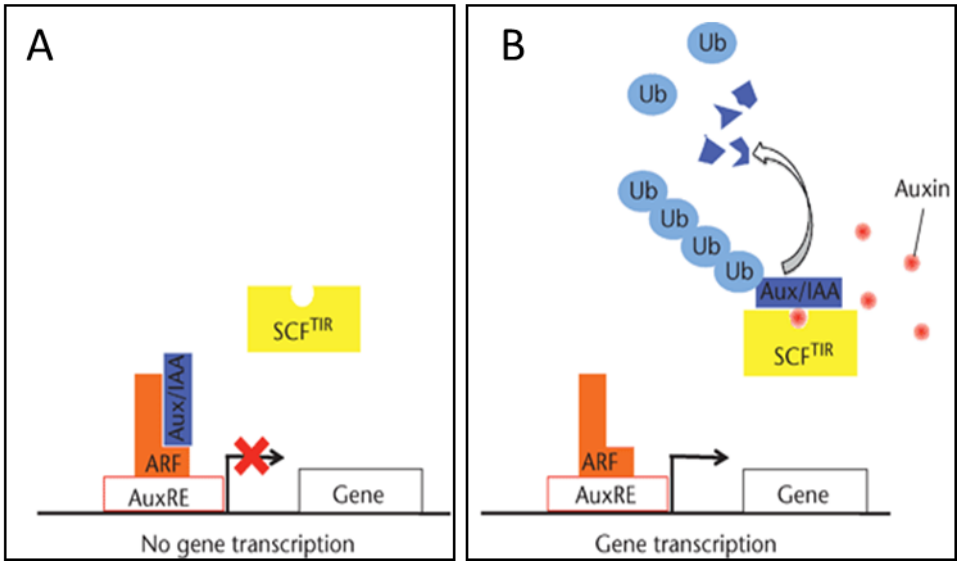

Fig. 1-6: Regulation of gene transcription by auxin, as described in text. (A) Aux/IAA transcription repressor inhibits gene transcription. (B) Auxin binding to the SCF^{TIR} complex promotes the interaction between the Aux/IAA transcriptional repressor and the ubiquitin protein ligase SCF^{TIR} leading to the degradation of AUX/IAA. This allows the transcription of auxin regulated genes by Auxin Response Factor (ARF) binding to Auxin Response Element (AuxRE). Figure taken from Morita & Tasaka (2010).

1.7.1.3 Auxin control of RSA

It is through the regulation of gene expression that auxin plays an important role in the control of RSA. Its directional transport sets up concentration gradients that are regulatory (Sabatini *et al.*, 1999). Auxin has an essential role in the control of meristem size, and growth of the root, and it is known to promote cell division and cell elongation and inhibit differentiation (Dello Ioio *et al.*, 2007, 2008; Moubayidin *et al.*, 2010; Perrot-Rechenmann, 2010), whilst at high concentrations it is known to inhibit root elongation (Eliasson *et al.*, 1989). Auxin is also known to control the development of LRs through multiple auxin-signalling modules. It coordinates the priming of LR initials (De Rybel *et al.*, 2010; Xuan *et al.*, 2016), LR initiation (Fukaki *et al.*, 2002, 2005; Okushima *et al.*, 2005), development of the LRP (Benková *et al.*, 2003; Hirota *et al.*, 2007; De Smet *et al.*, 2008) and emergence of the LR from the PR (Swarup *et al.*, 2008; also see Lavenus *et al.*, 2013 for a comprehensive review of the role of auxin at each stage of development). Another RSA trait that auxin plays an important role in is the plant's response to gravity. Following a gravistimulation event, auxin is directed asymmetrically at the root tip

towards the downward facing side of the root (Fig. 1-5B), through the redistribution of the PIN3 and PIN7 proteins in the root columella cells (Friml *et al.*, 2002b; Kleine-Vehn *et al.*, 2010). The accumulation of auxin on one side of the root leads to differential cell expansion, which results in the root bending towards the direction of gravity.

1.7.2 Ethylene

Ethylene is a gaseous plant hormone known for its important agricultural roles in senescence and ripening, as well as its role as a modulator of a plants' responses to biotic and abiotic stresses. The ethylene signal is perceived by a family of five receptors located at the endoplasmic reticulum (ER), ETHYLENE RESPONSE1 (ETR1), ETR2, ETHYLENE RESPONSE SENSOR1 (ERS1), ERS2, and ETHYLENE INSENSITIVE4 (EIN4) (Hua & Meyerowitz, 1998). In their active state (ethylene not bound), these receptors activate the Raf-like kinase (CONSTITUTIVE TRIPLE RESPONSE 1) CTR1 (Kieber *et al.*, 1993; Clark *et al.*, 1998), which in turn phosphorylates the ETHYLENE INSENSITIVE 2 (EIN2) protein (Alonso *et al.*, 1999). EIN2 is inactive in its phosphorylated state and remains localized to the ER, inhibiting downstream signalling (Ju *et al.*, 2012) (Fig. 1-7A). The binding of ethylene to the receptors leads to their inactivation, releasing the inhibitory effect on downstream elements of the pathway. As a result of this relieved suppression, EIN2 is proteolytically processed so that the carboxyl terminal end (C-END) is cleaved and migrates to the nucleus where it stabilises EIN3 leading to the accumulation of EIN3 (An *et al.*, 2010; Ju *et al.*, 2012; Qiao *et al.*, 2012; Wen *et al.,* 2012). EIN3 activates the transcription of *ETHYLENE RESPONSE FACTOR 1 (ERF1)* and other ethylene regulated target genes (Solano *et al.*, 1998) (Fig. 1-7B).

In the root, ethylene is known to inhibit root elongation and LR development as well as stimulating root hair formation resulting in the production of characteristic short fat hairy roots upon ethylene treatment. Ethylene control of root growth is thought to be largely mediated by the regulation of auxin biosynthesis and transport. Ethylene stimulates the expression of auxin biosynthesis genes and members of the auxin transport machinery (Swarup *et al.*, 2007; Negi *et al.*, 2008; Stepanova *et al.*, 2008; Lewis *et al.*, 2011). This leads to ethylene induced auxin accumulation and inhibition of cell expansion of cells exiting the root meristem (Ruzicka *et al.*, 2007; Swarup *et al.*, 2007; Stepanova *et al.*, 2008). Ethylene has also been proposed to play a role in the inhibition of cell division in the root meristem (Street *et al.*, 2015), and in the regulation of stem cell proliferation and quiescence at the root tip (Ortega-Martínez *et al.*, 2007).

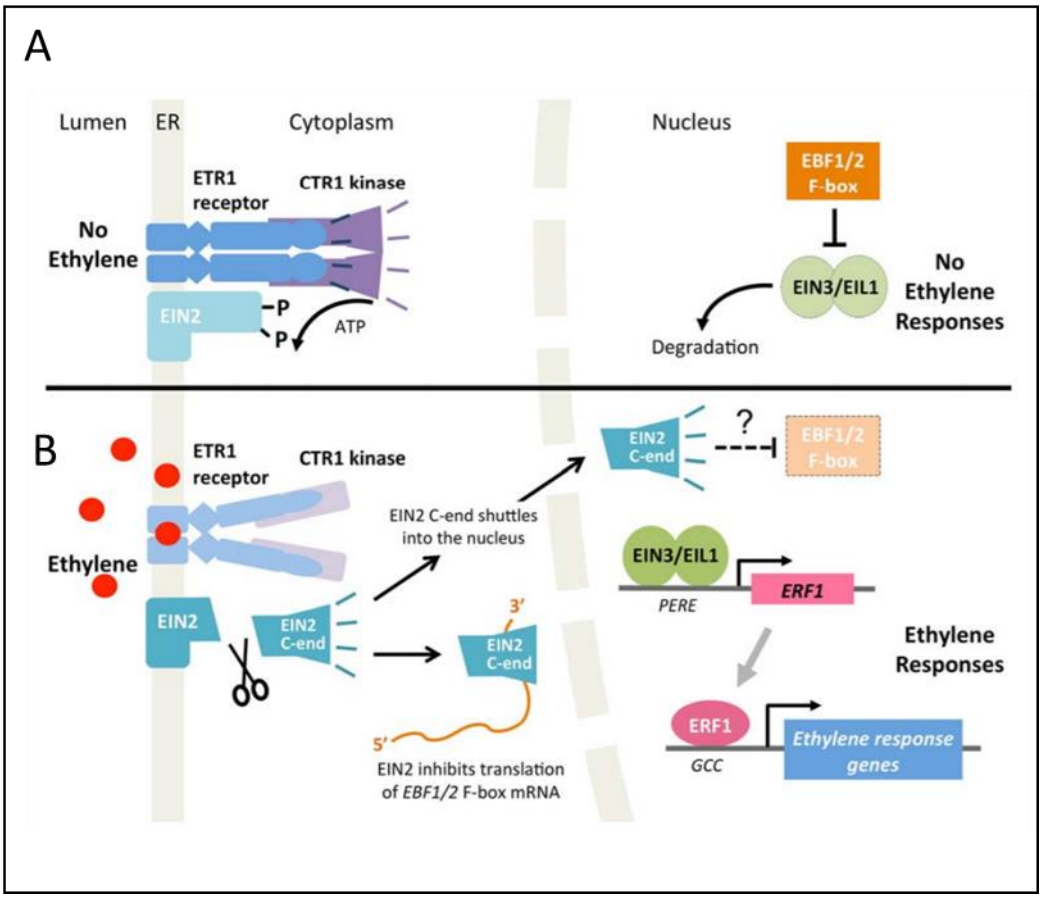

Fig. 1-7: The ethylene signalling pathway as described in the text. (A) In the absence of ethylene, the receptors activate CTR1, which phosphorylates EIN2, halting downstream signalling. EIN3 is degraded. (B) Binding of ethylene to the receptor results in the proteolytic release of the EIN2 C-END, which migrates to the nucleus. In the nucleus, it stabilizes EIN3 and EIN3 activates the transcription of *ETHYLENE RESPONSE FACTOR 1 (ERF1)* and other ethylene regulated target genes. Figure taken from Chang (2016).

1.7.3 Gibberellic acid

Gibberellins (GAs) are a class of tetracyclic diterpenoid hormones regulating many processes such as germination, root and shoot growth, flowering and fruit development (Fleet & Sun, 2005; Yamaguchi, 2008; Brian, 1959), and are best known for their role in promoting growth. Over a hundred GAs have been identified in higher plants and fungi (MacMillan, 2002), however only GA_1, GA_3, GA_4 and GA_7 are considered biologically active (Hedden & Phillips, 2000). Of these, the predominant bioactive forms are GA_1 and GA_4 (Sponsel & Hedden, 2010). The GA signal is perceived by the soluble GA receptor GA-INSENSITIVE DWARF1 (GID1) (Ueguchi-Tanaka *et al.*, 2005). GA-bound GID1 proteins interact with growth repressing DELLA proteins, forming a GA-GID1-DELLA complex. (Griffiths *et al.*, 2006; Nakajima *et al.*, 2006; Murase *et al.*, 2008). This interaction targets the DELLA proteins for degradation via E3 ubiquitin ligases such as $SCF^{SLY1/SNZ}$ in Arabidopsis (McGinnis *et al.*, 2003; Dill *et al.*, 2004; Fu *et*

al., 2004; Dohmann *et al.*, 2010; Ariizumi *et al.*, 2011). The pathway has been referred to as the relief of restraint, or relief of repression model, whereby DELLAs restrain plant growth, and GA promotes growth by overcoming DELLA-mediated growth restraint (Gao *et al.*, 2011) (Fig. 1-8).

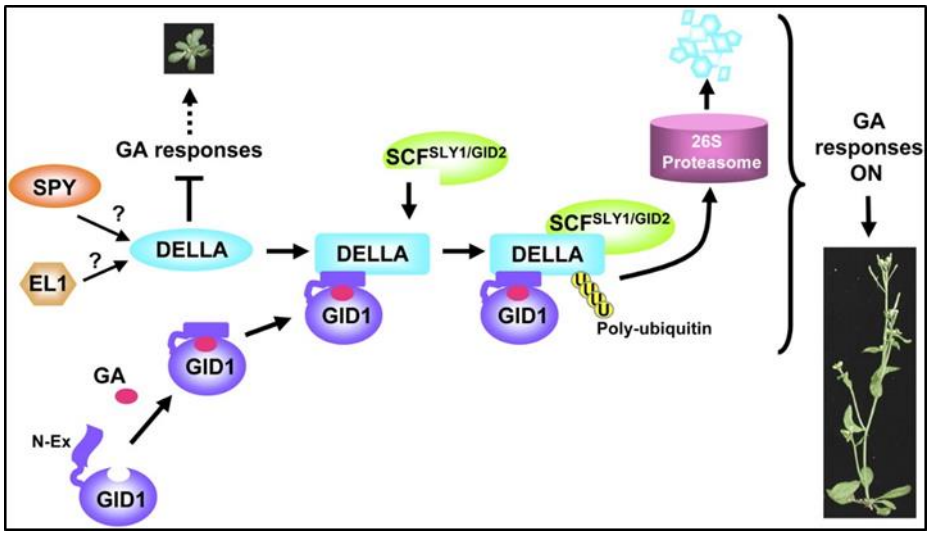

Fig. 1-8: Model of gibberellin (GA) signalling, as described in the text. GA binds to the GID1 GA receptor, which forms a GA-GID1-DELLA complex with DELLA proteins. This targets the DELLAs for degradation via the ubiquitin-proteasome pathway. In the absence of GA, DELLA proteins are stabilized and repress GA responses. Figure taken from (Sun, 2010).

In Arabidopsis there are five DELLA proteins; GAI, RGA, RGL1, RGL2 and RGL3, all sharing the DELLA-motif as well as the C-terminal GRAS domain (Peng *et al.*, 1997; Ikeda *et al.*, 2001; Silverstone *et al.*, 2001; Lee *et al.*, 2002; Wen & Chang, 2002). They act as key repressors of GA-responsive growth by inhibiting GA-regulated gene expression (Sun & Gubler, 2004) by interacting with transcription factors (TFs) such as PHYTOCHROME INTERACTING FACTORS (PIFs) and SCARECROW-LIKE3 (SCL3) (Zentella *et al.*, 2007; Feng *et al.*, 2008; de Lucas *et al.*, 2008; Heo *et al.*, 2011; Zhang *et al.*, 2011). GA homeostasis is regulated through the biosynthesis and deactivation of bioactive GAs. The system is strongly influenced by developmental and environmental cues, and three families of dioxygenases, the GA 3-oxidases (GA3ox), GA 20-oxidases (GA20ox) and the GA 2-oxidases (GA2ox), have been identified as the primary sites of this regulation (Colebrook *et al.*, 2014). The GA3oxs and GA20oxs act in the final step of GA biosynthesis, and the GA2oxs deactivate GAs, therefore regulation of the expression of these genes provides a mechanism for GA homeostasis (Thomas *et al.*, 1999; Yamaguchi, 2008). In the control of RSA, GA is known to increase root elongation, modulate meristem size and promote cell division through the degradation of DELLAs (Ubeda-Tomás *et al.*, 2008; Achard *et al.*, 2009; Moubayidin *et al.*, 2010). Various stresses, such as cold, salt and osmotic stress, are known to induce reduced GA levels and stabilised DELLAs, resulting in

reduced root growth responses (Achard *et al.*, 2008a; Magome *et al.*, 2008; Dubois *et al.*, 2013; Zhou *et al.*, 2017).

1.7.4 Abscisic acid (ABA)

Another of the five major plant hormones that is known for its regulatory roles in root growth is ABA (Harris, 2015). It has been shown to regulate root meristem function, through inhibition of cell differentiation in the QC thereby maintaining the pool of stem cells (Zhang *et al.*, 2010). It has also been shown to increase the rate of root elongation through modulation of the elongation zone and through inhibiting ROS accumulation (Sharp *et al.,* 1994; Sharp *et al.*, 2004). It is also known to play a role in the regulation of LR development, at the stage of initiation (Ariel *et al.*, 2010; Van Norman *et al.*, 2014) emergence (Ariel *et al.*, 2010), and meristem activation (Signora *et al.*, 2001).

In the ABA signalling cascade, ABA binds to members of the PYR/PYL/RCAR receptor family creating a surface for protein phosphatases (PP2Cs) to bind (Ma *et al.*, 2009; Park *et al.*, 2009). When unbound, PPC2s act to inhibit the autophosphorylation of the SnRK2 family (SNF1-RELATED PROTEIN KINASE) of kinases, preventing their activation of ABA-RESPONSIVE ELEMENT BINDING FACTOR (ABF) transcription factors (Furihata *et al.*, 2006; Yoshida *et al.*, 2006, 2015) (Fig. 1-9A). The binding of PP2Cs to the PYR/PYL/RCAR receptor when ABA is present, leads to its inactivation and release of its negative regulatory effect on the autophosphorylation of the SnRK2s, allowing the activation of ABFs. This subsequently leads to transcriptional initiation at ABA-responsive promoter elements (ABREs) (Choi *et al.*, 2000; Uno *et al.*, 2000; Furihata *et al.*, 2006) (Fig. 1-9B).

1.7.5 Reactive oxygen species (ROS)

Significant evidence has accumulated supporting the premise that ROS can act as signalling molecules serving a functional role similar to hormones. ROS, such as singlet oxygen ($^1O_2$), superoxide (O_2^-), hydrogen peroxide (H_2O_2) and hydroxyl radical ($HO^{\cdot}$), are constantly produced in plants through metabolic processes such as photosynthesis and respiration. However, their reactive nature means that at high levels, they can be very detrimental to the plant, leading to cell death and damage to DNA, lipids and proteins. For this reason, ROS levels are tightly regulated through detoxification and scavenging systems (Bowler *et al.*, 1994; Caverzan *et al.*, 2012; Sofo *et al.*, 2015). As well as causing detrimental effects, it has emerged that ROS also play a role in the regulation of responses to developmental and environmental signals. One of the areas in which ROS is known to have roles is the control of root development. ROS has been shown to reduce the number of dividing cells in the root meristem, play a role in defining

the transition zone (Passardi *et al.*, 2006; Tsukagoshi *et al.*, 2010) and also in repressing the size of the meristem itself (Tsukagoshi, 2012). ROS has also been strongly implicated in root hair development (Foreman *et al.*, 2003), and in the regulation of LR emergence (Manzano *et al.*, 2014). There is still much that is unknown about how the levels and localization of ROS affects developmental processes, however it is likely to be important in many processes.

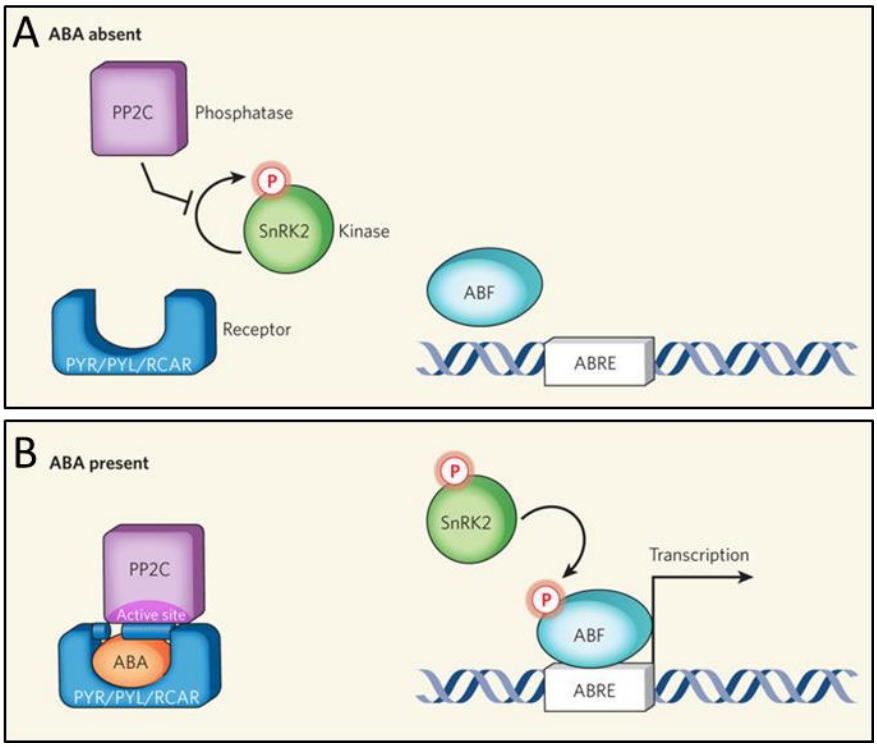

Fig. 1-9: The abscisic acid (ABA) signalling cascade, as described in the text. (A) In the absence of ABA, PP2Cs autophosphorylate SnRK2 proteins, which prevents them from activating ABF regulated gene transcription. (B) In the presence of ABA, ABA binds to the PYR/PYL/RCAR family of receptors, forming a surface for the binding of PP2C proteins. The PP2Cs are sequestered and this relieves the inhibition on the downstream pathway components. ABFs are able to activate transcription at ABA-responsive promoter elements (ABREs). Figure taken from Sheard & Zheng (2009).

1.7.6 Hormonal crosstalk

As discussed above, hormones and ROS have specific roles in the regulation of root growth, however it is through the crosstalk between them that the plant maintains growth and development, and integrates and responds to environmental signals. The hormones already mentioned, as well as cytokinin, brassinosteroids, strigolactones, jasmonates and salicylic acid all communicate in different regions of the developing roots to control the rate of cell division, elongation and differentiation. It is beyond the scope of this thesis to describe every proposed interaction in detail; however, recent review articles have summarised the evidence to date

describing the crosstalk models influencing root growth (Takatsuka & Umeda, 2014; Pacifici *et al.*, 2015) and Fig. 1-10 elegantly displays the complexity involved.

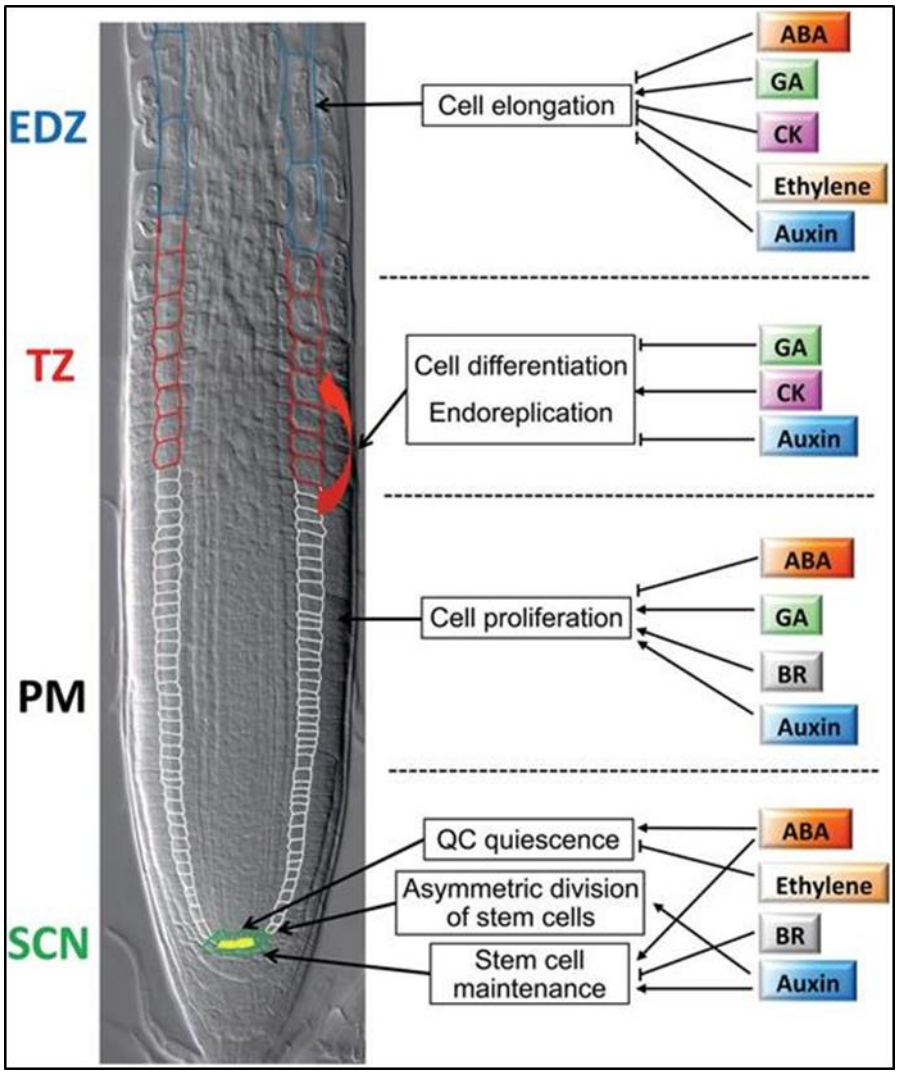

Fig. 1-10: Hormonal control of cell elongation, differentiation, proliferation and regulation of the quiescent centre (QC) in different developmental zones of the Arabidopsis primary root tip. EDZ, elongation/differentiation zone; TZ, transition zone; PM, proximal meristem; SCN, stem cell niche; ABA, abscisic acid; GA, gibberellic acid; CK, cytokinin; BR, brassinosteroids. Figure taken from Takatsuka & Umeda (2014).

1.8 What is known about hormonal crosstalk in response to K^+ deficiency?

As already discussed, much of the work surrounding K^+ starvation has focused on the changes in K^+ transporter levels and uptake kinetics, leading to the elucidation of key hormonal signalling pathways involved in the regulation of these factors. The rapid upregulation of the K^+ transporter HAK5 has been one of the best characterized. Here there is strong evidence suggesting an increase in ethylene and ROS leads to the induction of HAK5 transcription (Jung *et al.*, 2009; Nam *et al.*, 2012). However, much less is known about the hormonal control of the

architectural changes displayed in response to low K^+. As well as being a key early step in the activation of HAK5, ethylene and ROS have also been linked to an increased elongation of root hairs (Pitts *et al.*, 1998; Jung *et al.*, 2009) and in a reduction in PR growth (Jung *et al.*, 2009) in response to low K^+. In this case, increased ethylene leads to increased ROS levels, however it has been recognised that there is also an ethylene-independent increase in ROS in response to low K^+ (Jung *et al.*, 2009).

There is also mounting evidence to suggest that auxin plays a key role in the response to K^+ deficiency. Observations of gene expression changes (Armengaud *et al.*, 2004) and the identification of a K^+ transporter that also behaves like an auxin efflux facilitator (TRH1/AtKUP4) (Vicente-Agullo *et al.*, 2004) provided the basis for a link between auxin and K^+ deficiency. The agravitropic nature of the *trh1* mutant has been shown to be attenuated when grown on low K^+ (Vicente-Agullo *et al.*, 2004) which more recently has been attributed to a mislocalization of auxin transport carriers, leading to impaired auxin transport (Rigas *et al.*, 2013).

Auxin has also been linked to the development of LRs under low K^+ conditions through reduced LR density observed in response to low K^+ in the auxin signalling mutant (*MYB77*; Shin *et al.*, 2007). A reduction in the concentration of free IAA and reduced basipetal auxin transport in response to K^+ stress has also been observed (Shin *et al.*, 2007). It is therefore likely that auxin is playing a role in the response to low K^+ in Arabidopsis. Cytokinin synthesis mutants have also identified a role for cytokinin in the response to low K^+ pathway, displaying enhanced K^+ starvation response (Nam *et al.*, 2012).

Hormonal crosstalk interactions are often very complex networks and tightly regulated. Much is still unknown about how hormonal signals lead to the diverse range of adaption strategies deployed by plants as a coping mechanism in response to K^+ starvation.

1.9 Aims and objectives

The overall objective of the work described in this thesis was to uncover the hormonal control of root architectural responses to low K^+ in the Arabidopsis accession Col-0. In order to investigate this question, the first aim of the work was to characterize the root architectural response of Col-0 to low K^+ (Chapter 3). The second aim was to identify gene expression differences between seedlings grown on high (2 mM) and low (0.005 mM) [K^+] for short periods of time (Chapter 4). Using these data, the aim was to create hypotheses about the

hormonal control of root architectural changes in response to low K^+ (Chapter 4). Next, the work aimed test these hypotheses experimentally to identify the roles of hormones in the root architectural changes (Chapter 5). The final results chapter (Chapter 6) aimed to utilise RNA-Seq data to explore possible upstream events regulating changes in hormone levels in response to low K^+. Together, the work in the four experimental chapters utilises experimental and bioinformatics data as well as literature-based searches to increase the understanding of the root architectural responses to low K^+ and the means by which they are regulated.

Chapter 2 Materials and Methods

2.1 Materials

2.1.1 Chemical suppliers

All chemicals were obtained from SIGMA (Poole, UK) or Fisher Scientific Ltd (Loughborough, UK) unless otherwise stated.

2.1.2 Plant material

Arabidopsis thaliana wild type (WT) Columbia (Col-0) seeds were obtained from lab stocks. All mutants and reporter lines are in Col-0 background and from lab stocks, unless otherwise stated.

2.1.2.1 Reporter lines

The reporter lines were obtained as follows: *pDR5rev::3XvenusN7* (Heisler *et al.*, 2005); *proRGA::RGA::GFP* (Silverstone *et al.*, 2001) Ari Sadanandom (Durham University, UK); *QC25::GUS, proPIN1::PIN1:GFP* (Benková *et al.*, 2003) and *proPIN2::PIN2::GFP* courtesy of Ben Scheres (Utrecht University, the Netherlands); *WOX5::GFP* courtesy of Chunli Chen (Huazhong Agricultural University, Wuhan, China); *pAtHAK5::GUS/GFP* courtesy of Frans Maathuis (York University, UK) (Gierth *et al.*, 2005). HyPer courtesy of Marc & Heather Knight (Durham University, UK)(Belousov *et al.*, 2006). *35S::DII-VENUS-N7* (Brunoud *et al.*, 2012) and *CYCB1;2:GUS* were obtained from the Nottingham Arabidopsis Stock Centre (NASC) (http://arabidopsis.info/).

2.1.2.2 Mutant lines

Mutant lines were obtained as follows: *aux1-22* courtesy of Claire Grierson (University of Bristol, UK); *ga2ox quintuple* mutant courtesy of Steve Thomas (Rothamsted Research, UK)(Rieu *et al.*, 2008); *sfr6-1* and *erf5 erf6* courtesy of Marc & Heather Knight (Durham University, UK)(Knight *et al.*, 2009); *atrbohF* and *atrbohD/F* mutants courtesy of Alistair Hetherington (University of Bristol, UK); *atrbohD-3* and *aux1-7 DR5::GUS* were obtained from NASC. SALK_056756, SM_3.32872, SALK_054092, SALK_087356, SALK_127471, GK-843H09 were also obtained from NASC.

2.1.2.3 Genetic cross progeny

Progeny of crossing: *aux1-7* x *35S::DII-VENUS-N7* and *aux1-7 x proPIN2::PIN2::GFP*

2.1.3 Genotyping insertion lines

Insertion lines were genotyped by running two parallel PCR reactions using three primers; a forward primer (Fw), a reverse primer (Rev) and an insertion-specific primer (Fig. 2-1B). PCR conditions are described in section 2.8.2. One PCR reaction was set up using the Fw and Rev primer set, and the second PCR was set up with the Rev primer and the insertion specific primer. Primer sets were designed so that different sized bands would be created in each case. Homozygous plants would display a band in one of the other PCR reactions, whereas a heterozygous line would display bands in both (Fig. 2-1C). Details of insertion lines and primer combinations required for genotyping displayed in Table 2-1 below. Primer sequences listed (Appendix I).

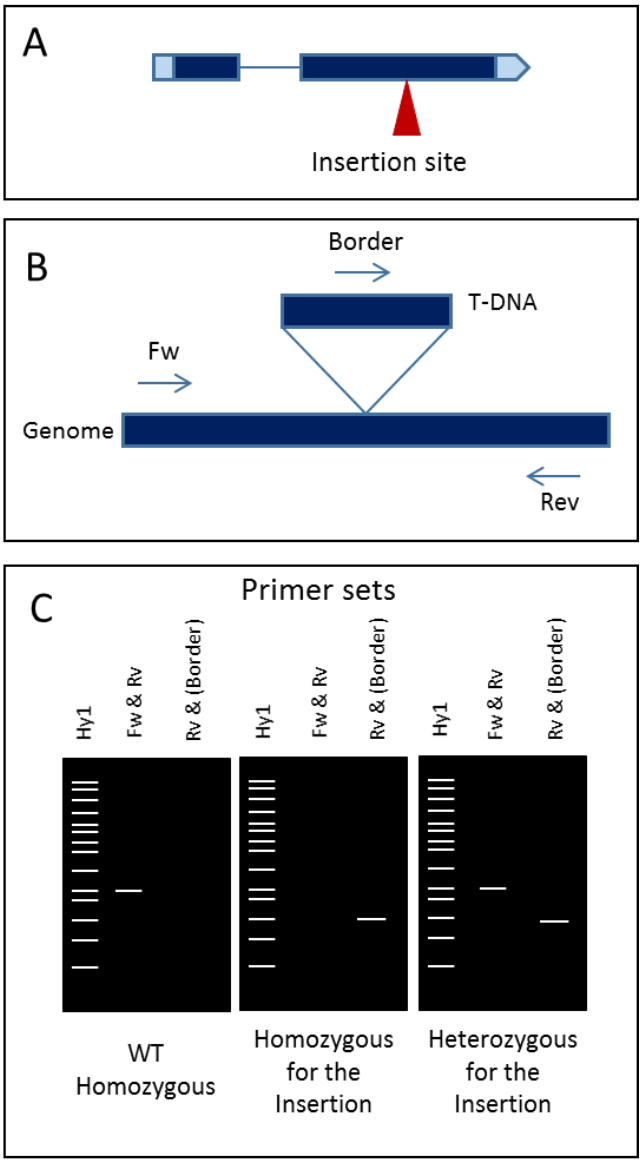

Fig. 2-1: Workflow for the genotyping of T-DNA insertion lines. (A) identification of insertion site. (B) Primer design. DNA extraction is performed and PCR with specific primers is

completed & run on gel to determine genotype (C). Border (B,C) refers to the specific primer for each T-DNA insertion type.

Seed line	Locus	Associated gene name	Insertion specific primer	WT band size	Mutant band size
atrbohD-3	*AT5G47910*		dSpm1	732	~660
atrbohF	*AT1G64060*		dSpm11	924	~700
atrbohDF			dSpm1 & dSpm11 (*)	(see above)	
SALK_127471	*AT5G39670*	*CML46*	LBb1.3	1117	584–848
SM_3.32872	*AT1G80840*	*WRKY40*	Spm32	1127	448–748
SALK_087356	*AT4G17490*	*ERF6*	LBb1.3	1005	462–762
SALK_054092	*AT1G27730*	*STZ*	LBb1.3	1092	493–793

(*) two PCR reactions, one for each mutation

Table 2-1: Details of insertion lines with associated loci, gene name, primer combinations used for genotyping and sizes of bands expected if the insertion was present/absent.

2.1.4 Genetic crosses

Genetic crosses between Arabidopsis plants were made under the Zeiss STEMI SV8 dissecting stereomicroscope (Carl Zeiss, Cambridge, UK). Large unopened flower buds were emasculated to remove all immature anthers using fine forceps. All other siliques and flowers were removed. Mature pollen from the male plant was then transferred manually using forceps and brushed against the stigma of the female plant. The stem was labelled using Micropore™ tape, and plants were returned to the growth cabinet. Siliques were removed upon maturity but before senescence and pod shatter.

2.2 Plant tissue culture

2.2.1 Seed sterilisation

To ensure that seeds were sterile and free from surface contamination seeds were placed in 1.5-ml Eppendorf® tubes and washed with 70% v/v ethanol for 1 min. The ethanol was then replaced with concentrated bleach (Tesco, UK) with a drop of 0.1% v/v Tween20 as wetting agent for 15 min. The seeds were then rinsed four times with sterile deionised water and then left in 1 ml of sterile distilled water (sdH_2O) and stratified for 4–7 d in the dark at 4°C to encourage and synchronise germination.

2.2.2 Culture media

Half strength Murashige and Skoog media (½ MS10) (Murashige & Skoog, 1962)
2.2 g/L half strength Murashige and Skoog medium (SIGMA M5519), 10 g/L sucrose, adjusted to pH 5.7 with 1M KOH, 8 g/L agar.

2.2.2.1 High and low K^+ media

A stock of growth medium was made up with zero potassium: the stock consisted of 1.497 mM $CaCl_2$, 0.363 mM $Ca(H_2PO_4)_2$, 10.3 mM NH_4N0_3, 0.7506 mM $MgSO_4.7H_2O$, 29.21 mM sucrose, 50 ml/L half strength MS Vitamins 10× and 500 µl/L half strength Murashige and Skoog basal salt micronutrients from 1000× stock (for full list of ingredients in the MS vitamins and basal salt micronutrients, see the SIGMA websites listed below:
ttp://www.sigmaaldrich.com/catalog/product/sigma/m7150?lang=en&region=GB
http://www.sigmaaldrich.com/catalog/product/sigma/m0529?lang=en&region=GB
The solution was adjusted to pH 5.7 with 1 M NaOH solution. Different concentrations of K^+ ions were added to the media using K_2SO_4 to achieve final K^+ concentrations of 2 mM and 0.005 mM.Half strength Murashige and Skoog medium has a final K^+ concentration of 10 mM.

2.2.2.2 High and low phosphate media

High and low phosphate media were made as described in Jiang *et al.* (2007). Four-day-old seedlings were transferred to low P medium (10 µM NaH_2PO_4) or high P medium (1 mM NaH_2PO_4), which was supplemented with: 2.0 mM NH_4NO_3, 1.9 mM KNO_3, 0.3 mM $CaCl_2{\cdot}2H_2O$, 0.15 mM $MgSO_4{\cdot}7H_2O$, 5 μM KI, 100 μM H_3BO_3, 100 μM $MnSO_4{\cdot}H_2O$, 30 μM $ZnSO_4{\cdot}7H_2O$, 1 μM $Na_2MoO_4{\cdot}2H_2O$, 0.1 μM $CuSO_4{\cdot}5H_2O$, 0.1 μM $CoCl_2{\cdot}6H_2O$, 100 μM $FeSO_4{\cdot}7H_2O$, 100 μM $Na_2EDTA{\cdot}2H_2O$, 1% Sucrose. The solution was adjusted to pH 5.7 using KOH.

2.2.2.3 High and low nitrate media

High and low nitrate media were made up as described in Mounier *et al.* (2014). Four-day-old seedlings were transferred to low N medium (0.05 mM KNO_3) or high N medium (10 mM KNO_3), which was supplemented with: 0.5 mM $CaSO_4$, 0.5 mM $MgCl_2$, 1 mM KH_2PO_4, 2.5 mM MES (2-[morpholino]ethanesulphonic acid), 50 μM NaFeEDTA, 50 μM H_3BO_3, 12 μM $MnCl_2$, 1 μM $CuCl_2$, 1 μM $ZnCl_2$, 0.03 μM NH_4MoO_4. The solution was adjusted to pH 5.7 using KOH.

9 g/L SIGMA agar (A-1296) was added to all the growth media solutions to create solid media and the media were autoclaved at 121°C for 20 min before use.

2.2.3 Plant growth conditions

All experiments were conducted using solid growth media in growth rooms or growth cabinets under long day conditions, 16 h light: 8 h dark at 22°C (*c*. 3000 lux).

Seeds were grown for 4 d on horizontal sterile 10 × 10 cm^2 square Petri dishes containing 50 ml of solid ½ MS10 growth medium and sealed around the edges with Micropore^{TM} tape. The seedlings were then transferred to vertical 10 × 10 cm^2 square Petri dishes containing 50 ml of the solid K^+ media for a further 8 d, or the seedlings were transferred to vertical ½ MS10 plates for a further 5 d before being moved to K^+ media for time-course experiments. The vertical 10 × 10 cm^2 square Petri dishes were placed vertically into cardboard racks constructed to allow light to the shoots but not to the roots. All biological replicates for each experiment were conducted at the same time unless otherwise stated in the thesis. Technical replicates are specified when used.

For the RNASeq experiment the growth conditions were as follows: Col-0 seedlings were grown for 4 d on ½ MS10 horizontal plates, followed by 7 d on ½ MS10 vertical plates. The seedlings were then transferred to plates containing ether 2 mM or 0.005 mM K^+. Tissue was collected after 3 h and 30 h.

For growth in soil, seedlings were grown in 24-well trays in a 5: 1 mixture of Gem multipurpose compost and horticultural silver sand (LBS Horticulture Ltd, UK). Plants were grown at 21°C, with a 16-h photoperiod. The systemic insecticide Intercept (Levinton Horticulture Ltd, UK) was applied to all compost (60 mg per 24-well tray) before seeds were sown.

2.3 Phytohormones

Stock solutions for all the phytohormones were made up at 10 mM, filter sterilised and stored at −20°C before use. Details of the stock solutions are shown in Table 2-2 below.

Hormone	Notes	Method of preparation
1-aminocyclopropane-1-carboxylic acid (ACC)	An ethylene precursor	Dissolve 10.1 mg 1-aminocyclopropane-1-carboxylic acid in 10 ml sdH_2O
Silver thiosulphate (AgS_2O_3)	Binds to the copper atom in ETR1 to inhibit ethylene responses	Combine 5 ml $AgNO_3$ at 3.4 mg/ml and 5 ml of NaS_2O_3 at 12.7 mg/ml
Indole-3-acetic acid (IAA)	The principal free auxin in plants	Dissolve 17.5 mg indole-3-acetic acid in 1 ml in 98% ethanol, top up to 10 ml with sdH_2O
Abscisic acid (ABA)		Dissolve 22.6 mg of ABA in 10 ml methanol
Fluridon	An inhibitor of abscisic acid biosynthesis	Dissolve 32.9 mg of fluridon in 10 ml of methanol
Diphenylene iodonium (DPI)	An inhibitor of NADPH oxidase and other flavin containing enzymes	Dissolve 31.5 mg diphenyleneiodonium chloride in 10 ml DMSO
Paclobutrazol (PAC)	GA inhibitor	Dissolve 2.9 mg paclobutrazol in 10 ml 98% ethanol
Gibberellic acid (GA_3)		Dissolve 34.6 mg Gibberellic acid in 2 ml 98% ethanol and top up to 10 ml with dsH_2O
***N*-1-naphthylphthalamic acid (NPA)**	An inhibitor of polar auxin transport	Dissolve 27.3 mg (*N*-1-naphthylphthalamic acid) in 10 ml DMSO

Table 2-2: Method of preparation of phytohormone stock solutions. All made up 10 mM.

2.4 Root architecture assays

2.4.1 Primary and lateral root length analysis

Vertical plates were scanned using a flatbed scanner Epson Expression 1680Pro (Epson, UK) at resolution 600 dpi. Primary root (PR) length, lateral root (LR) number and LR length were analysed from these images using ImageJ (Schneider *et al.*, 2012) with the plugin SmartRoot (Lobet *et al.*, 2011), an analysis tool specifically designed for the quantitative analysis of root-system architecture (RSA). All LRs were measured when they were long enough to be picked up by the analysis software (*c.* >200 µm). Data from ImageJ was then transferred to Microsoft Excel to produce graphs. Anchor roots (defined as roots emerging from the hypocotyl–root junction; Ingram *et al.*, 2011) were discounted from analysis.

2.4.2 Vertical growth index

To assess the degree of positive gravitropism exhibited by the seedlings, the vertical growth index (VGI) was used. It is calculated as:

$$VGI = \frac{CH_Y}{RL}$$

where CH_Y is the depth of the root apex penetration, and RL is the root length (Vicente-Agullo *et al.*, 2004) (Fig. 2-2).

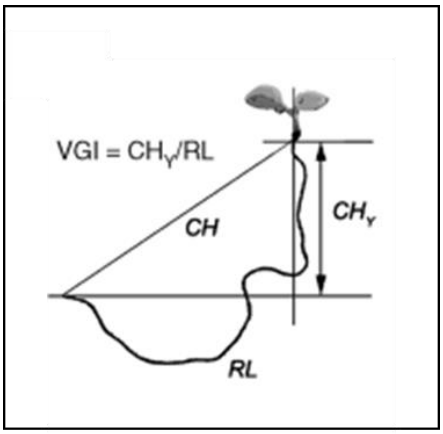

Fig. 2-2: Vertical Growth Index, defined as the ratio between the vertical projection (CH_y) of the base-to-tip chord CH and the root length RL, figure taken from Vicente-Agullo *et al.* (2004).

2.4.3 Total LR counts & LR progression analysis

Localised auxin accumulation in the PR is required for the first cellular divisions involved in LR development. These very early stages can, therefore, be marked and observed using auxin reporters such as *DR5::GUS* (Sabatini *et al.*, 1999). By GUS staining developing LRs it was possible to count LRs at all stages of development (Fig. 3-4B). In cases where *DR5::GUS* could not be used (mutant analysis), lugol staining was used to visualize areas of LRP development as these areas appeared a much darker colour under the lugol staining conditions compared to the areas of the PR around the developing site. Roots were examined using compound light microscopy (see the Materials and Methods section 2.11.1). LR progression analysis used these techniques to count and identify the stages of development of each LR along each PR, allowing the influence of stresses and hormones on LR development to be analysed.

2.5 Statistical analysis

All statistical analyses were performed in IBM SPSS Statistics for Windows, Version 22 (Armonk, NY, USA; IBM Corp.). The 0.05 level of significance was used. The one-way analysis of variance (ANOVA) and Tukey Pairwise comparison post hoc test were used to determine significance between the means of three or more independent groups. An independent samples *t*-test was used to determine significance between the means of two independent groups.

2.6 Histochemical staining

2.6.1 GUS staining

The reporter gene GUS (beta-glucuronidase) is used as a histochemical reporter gene for the localization of promoter activity in transgenic plants (Jefferson *et al.*, 1987). Activity of the enzyme is localised by incubating tissues in the colourless substrate X-Gluc, which is converted to a blue precipitate in tissues expressing the GUS enzyme.

Single whole seedlings were submerged in a staining solution of 1 mM N-N-dimethylformamide in 100 mM sodium phosphate (pH 7.0), 10 mM EDTA, 0.5 mM potassium ferrocyanide, 0.5 mM potassium ferricyanide, 0.1% v/v Triton X buffer as described by Topping & Lindsey (1997) in a 1.5-ml Eppendorf tube®. Time-course experiments were carried out to identify the optimum time for staining for each GUS line and buffer solution prior to the experiment. The reaction was stopped by replacing the reaction mix with 98% ethanol. Before imaging, the seedlings were rehydrated by replacing the ethanol with water, then the tissue was cleared by transferring the seedling to a slide with chloral hydrate solution (8 g chloral hydrate, 1 ml glycerol, 2 ml water). A coverslip was placed over the top. Slides were imaged using compound light microscopy (see the Materials and Methods section 2.11.1).

2.6.2 Lugol staining

Whole individual seedlings were immersed in Lugol solution (SIGMA, UK) for 5 min before being transferred to dsH_2O to wash. The seedlings were then mounted on a microscope slide in chloral hydrate solution, the aerial parts of the plant were removed using a scalpel blade and the root tissue was imaged using compound light microscopy (see the Materials and Methods section 2.11.1).

2.7 Nucleic acid isolation

2.7.1 Genomic DNA extraction (Edwards Prep; Edwards *et al.*, 1991)

A leaf disk was placed in an Eppendorf tube, frozen in liquid nitrogen and ground using a micro pestle. 400 µl of extraction buffer (200 mM Tris-HCl pH 7.5, 250 mM NaCl, 25 mM EDTA, 0.5% w/v SDS) was added before the sample was vortexed for 5 s. The sample was then centrifuged at 15000 x ***g*** for 4 min and 300 µl of the supernatant was removed and mixed with 300 µl isopropanol to precipitate the DNA. The sample was left at room temperature for 2 min before centrifuging at 15000 x ***g*** for 5 min. The supernatant was discarded and 200 µl of 70% ethanol

was added in order to wash away salts. The sample was centrifuged for 5 min at 15000 x ***g*** before the ethanol was removed and the pellet was allowed to dry on the bench overnight. DNA was resuspended in 30 µl sterile water and stored at −20°C

2.7.2 RNA extraction / DNase treatment / cDNA synthesis

A maximum of 100 mg of plant tissue was placed in a 1.5 ml Eppendorf® tube and flash frozen in liquid nitrogen; the sample could then be stored at −80°C until required. Tissue was ground in the Eppendorf® tube by a micro pestle before RNA extraction. RNA extraction was carried out using the SIGMA Spectrum™ Plant Total RNA Kit following the manufacturer's instructions. The procedure extracts RNA using a process of lysis, filtration, binding of the RNA to a column, washing and eluting. An on-column DNA digest was also carried out for all samples (SIGMA). The extracted RNA was analysed using a Nanodrop 1000 spectrophotometer (ThermoFisher Scientific, Hemel Hempstead, UK).

cDNA synthesis was carried out using 5 ng of RNA in a 20 µl reaction mixture. The reactions used SuperScript® III First-Strand Synthesis Supermix (Invitrogen Ltd, Paisley, UK) following the manufacturer's protocol and primed with Oligo$(dT)_{20}$. The cDNA samples were diluted with sterile distilled water in a ratio of 1 : 4 before use in PCR and qRT-PCR.

PCR amplification with *ACT2* primers (see Appendix I for primer sequences) designed over an intron were used to test whether cDNA samples were contaminated with genomic DNA. Contaminated samples were taken though another DNase treatment step (Promega RQ1 DNase) before cDNA was resynthesized.

2.7.3 Tissue extraction and sample preparation for RNA-Seq experiment

Tissue of between 20 mg and 100 mg was flash frozen in liquid nitrogen. Two metal ball bearings were added to each microcentrifuge tube of frozen tissue. The tissue was ground using the TissueLyser II (QIAGEN®, Manchester, UK) before 1 ml of Trizol (TRI Reagent® SIGMA) was added to each tube. Samples were incubated at room temperature for 5 min before 0.2 ml chloroform was added to each tube. Samples were vortexed then incubated at RT for 3 min. The tubes were then centrifuged at 15000 x ***g*** for 15 min at 4°C and 400 ml of the colourless upper phase was transferred to a fresh microcentrifuge tube. 400 ml of 70% ethanol was then added and vortexed to mix. 700 ml of the sample was then transferred to the binding column from the Spectrum™ Plant Total RNA Kit (SIGMA). Samples were centrifuged at 14,000 x ***g*** and flow-through discarded. 300 ml of Wash 1 solution from Spectrum™ Plant Total RNA Kit, was added to the column and centrifuged at 14,000 x ***g***. The rest of protocol was completed

following manufacturer's instructions including a DNase treatment step using On-Column DNase 1 Digestion Set (SIGMA).

RNA samples were analysed using the NanoDrop® ND-1000 spectrophotometer (ThermoFisher Scientific) and Agilent 2200 TapeStation. RNA samples with RNA integration number equivalent (RIN^e) above 7.0 were taken forward to library preparation (Appendix II).

Library preparation was completed using NEBNext® Ultra™ Directional RNA Library Prep Kit for Illumina® protocol for use with NEBNext Poly(A) mRNA Magnetic Isolation Module (NEB #E7490) following the manufacturer's instructions (NEB, Hitchin, UK). Total RNA starting material of between 100 ng and 1 µg was used. mRNA was isolated, fragmented and primed, cDNA was synthesised and end prep was performed. NEBNext Adaptor was ligated and the ligation reaction was purified using AMPure XP Beads. PCR enrichment of adaptor ligated DNA was conducted using NEBNext Multiplex Oligos for Illumina (Set 1, NEB #E7335). The PCR reaction was purified using Agencourt AMPure XP Beads. Library quality was then assessed using a DNA analysis ScreenTape on the Agilent Technologies 2200 TapeStation. qPCR was then completed for sample quantification using NEBNext® Library Quant Kit Quick Protocol Quant kit for Illumina®. Samples were all diluted to 10 nM. 7 µl of each 10 nM sample was pooled together and all were run on one lane using the Illumina HiSeq 2500, through the DSB Genomics facility in Durham University.

2.8 Polymerase chain reaction PCR

2.8.1 Primers

Primers were designed using Primer-BLAST (http://www.ncbi.nlm.nih.gov/tools/primer-blast/) and synthesised by MWG Eurofins (http://www.eurofinsdna.com/). The full list of primers used can be found in Appendix I.

2.8.2 Standard PCR

The following reaction mix (Table 2-3) was made up per reaction using MyTaq™ Mix (Bioline).

10× Reaction Buffer	4 µl
Bioline Taq	0.1 µl
Forward Primer	0.5 µl
Reverse Primer	0.5 µl
Template	0.4 µl
RNase/DNase free water	14.5 µl

Table 2-3: Reaction mix per reaction for standard PCR, using MyTaq™ Mix (Bioline).

The following program (Table 2-4) was run using an Applied G-Storm GS1 PCR machine.

	Temperature (°C)	Time	Number of cycles
Initial denaturation	95	1 min	1
Denaturation	95	15 s	25–60
Annealing	(variable depending on primer sets)	15 s	
Extension	72	15 s	
Final extension	72	1 min	1
Refrigerate	4	Hold	1

Table 2-4: Program used for standard PCR using an Applied G-Storm GS1 PCR machine.

2.8.3 Quantitative RT-PCR (qRT-PCR)

AT1G13320 was used as a reference gene for all qRT-PCR analyses. It was selected due to its stable expression profile across a wide range of developmental and environmental conditions (Czechowski *et al.*, 2005), and its consistency across K^+ concentrations. qRT-PCR reactions were conducted using a total volume of 20 µl and consisting of 10 µl 2× SensiFAST SYBR® No-ROX Mix, 0.4 µl of each 20 µM forward and reverse primer, 0.5 µl of diluted cDNA sample and 8.7 µl H_2O. Reactions were run on a Rotor-Gene Q Machine, (QIAGEN®) as follows (Table 5):

	Temperature (°C)	Time
Hold	95	2 min
40 × Cycles	95	5 s
	58	10 s
	72	10 s
Melt curve	50 – 95	Increasing by 0.2°C every 5 s

Table 2-5: Program used for Quantitative RT-PCR (qRT-PCR), run using a Rotor-Gene Q Machine, (QIAGEN®)

Expression analysis was conducted using the Rotorgene Q Series software v1.7. Relative normalised levels of transcript of each gene was calculated relative to each housekeeping gene

and analysed by comparative quantification using an assumption-free, linear regression analysis approach (Ramakers *et al.*, 2003).

2.9 Gel electrophoresis

After completion of PCR reactions, DNA samples were separated by size using gel electrophoresis to identify PCR products. Agarose Multi-Purpose (Bioline) was dissolved in 1× TAE buffer (diluted 1 in 10 from 10× TAE Buffer: 242 g Tris, 37.2 g $Na_2EDTA.2H_2O$, 57.1 ml glacial acetic acid, in 5 L) to produce a 1% w/v gel. Ethidium bromide was added to a concentration of 0.5 µg/ml. 5× DNA loading buffer (Bioline) was mixed with PCR product and loaded into the gel with a separate lane for appropriate Hyperladder. The gel was run for *c*. 40 min at 80 V. Gels were imaged using a BioRad Gel-Doc 1000 (BioRad).

2.10 Bioinformatic analysis

2.10.1 Analysis of RNA-Seq data

Results from the Illumina HiSeq 2500 were processed using the following steps (Fig. 2-3); Trimmomatic (Bolger *et al.*, 2014) was used to cut down and remove low quality reads, TopHat2 (Kim *et al.*, 2013) was used for the alignment of reads against TAIR10 (EnsemblePlants), SAMtools (Li *et al.*, 2009) indexed and sorted the binary sequence alignment files (BAM files) then converted them into readable (SAM) files. HTSeq 0.6.1 (Anders *et al.*, 2015) was used to estimate gene counts, then EdgeR (Robinson *et al.*, 2010; McCarthy *et al.*, 2012) normalised gene counts and estimated differential expression between sample groups. A *P*-value of ≤ 0.5 and a log fold change ≥0.5 were selected to identify differentially expressed genes (DEGs) (Fig. 2-3).

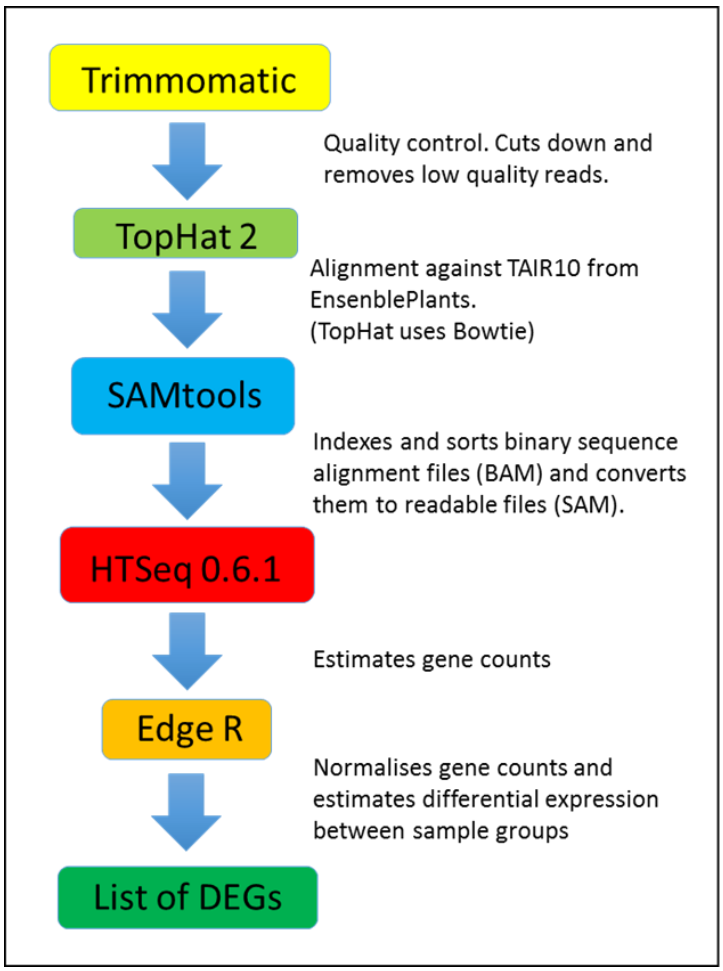

Fig. 2-3: Workflow of RNA-Seq data analysis.

2.10.2 Bioinformatic analysis of transcriptomic data

Online bioinformatics tools were used for the analysis of the RNA Seq data. Listed in table below (Table 2-6).

Tool	Reference / Website	Function
BioVenn	(http://www.biovenn.nl/index.php) (Hulsen *et al.*, 2008)	Comparison and visualization of biological lists using area-proportional Venn diagrams
AgriGO	(http://bioinfo.cau.edu.cn/agriGO/) (Du *et al.*, 2010; Tian *et al.,* 2017)	Gene Ontology analysis tool
REViGO	(http://revigo.irb.hr/) (Supek *et al.*, 2011)	Summarization and visualization tool for long lists of gene ontology terms
Plant reactome	(http://plantreactome.gramene.org/) (Naithani *et al.*, 2017)	Database of plant metabolic and regulatory pathways, allowing analysis of gene sets
AtTFDB-Arabidopsis	(http://arabidopsis.med.ohio-state.edu/AtTFDB/) (Davuluri *et al.,* 2003; Yilmaz *et al.*, 2011)	Identification of transcription factors & links to interaction tools (GRG-X)

transcription factor database		
GRG-X- Grassius Regulatory Grid eXplorer	(http://arabidopsis.med.ohio-state.edu/grgx/)	Visual assessment of regulatory networks of transcription factors
STRING	(https://string-db.org/) (Szklarczyk *et al.*, 2017)	Database of known and predicted protein-protein interactions
DAVID (Database for Annotation, Visualization and Integrated Discovery)	(https://david-d.ncifcrf.gov/home.jsp) (Huang *et al.*, 2009a,b)	Comprehensive set of functional annotation tools for investigators to understand biological meaning behind large list of genes. (Used in this thesis mostly for gene ID conversion)
TAIR (The Arabidopsis Information Resource)	(https://www.arabidopsis.org/)	Database of genetic and molecular biology data for the model higher plant *Arabidopsis thaliana*
UniProt	(http://www.uniprot.org/)	Comprehensive, high-quality and freely accessible resource of protein sequence and functional information.

Table 2-6: Online bioinformatics tools used for analysis of transcriptomics data. Name, website link, reference (where appropriate) and function stated.

2.11 Microscopy

2.11.1 Compound light microscopy

Histological tissue sections were examined using a Zeiss Axioskop compound microscope (Carl Zeiss, Cambridge, UK), equipped with a QImaging Retiga-2000r camera (Photometrics, Marlow, UK) using a ×20 objective.

2.11.2 Confocal scanning laser microscopy (CSLM)

To reveal cell organization, roots were stained in 0.5 µg/mL propidium iodide (PI) solution for 1 min 30 s, then washed for the same time in sdH_2O. Roots were then mounted on slides in sdH_2O, a 1.5-mm cover slip was placed on top, secured by Micropore™ tape and imaged using the Leica SP5 TCS confocal microscope (www.leica-microsystems.com) using either ×40 or ×63 oil immersion objectives. Excitation of flurophores was performed as follows: GFP 488 nm using the Argon laser, YFP 514 nm using the Argon laser, propidium iodide 548 nm using the HeNe laser.

2.11.3 Analysis of confocal images

Images were originally opened in LAS AF Lite software (v2.63 build 8173 http://www.leica-microsystems.com/products/microscope-software/life-sciences/las-af-advanced-fluorescence/). Images were exported in Tiff form and opened in Image J for analysis. Images were taken from at least six individual roots for each analysis. Analysis was conducted as follows:

2.11.3.1 Analysis of meristem size:

The straight-line tool was used to draw a line and measure from the quiescent centre (QC) to the end of the meristem (defined as the first cell that was twice the length of the immediately preceding cell; González-García *et al.*, 2011).

2.11.3.2 Analysis of *pDR5rev::3XvenusN7* & *proRGA::RGA::GFP* lines:

The polygon tool was used to draw around the meristem of the LRs and the mean green channel intensity was calculated using the colour histogram tool. Background was measured and subtracted from the value.

2.11.3.3 Analysis of *aux1-7* x *35S::DII-VENUS-N7, aux1-7 x proPIN2::PIN2::GFP & WOX5::GFP* lines:

Images were analysed by eye for general pattern, presence or absence of fluorescence.

2.11.4 Stereo microscopy

Seedlings were imaged through the Petri dish lid to avoid contamination of the samples. The Leica M165 FC Fluorescent Stereo Microscope was used and images were taken using a Leica DFC 420C camera.

Images of the ROS reporter HyPer line (Belousov *et al.*, 2006) were analysed using the ImageJ software by drawing a line from the place where the LR meets the PR down to the tip of the LR. The plot profile tool was used to calculate the grey value for each point down the length of the measured line. The grey value indicates the brightness of each pixel, used as a measure for HyPer fluorescence. The LRs measured were not equal lengths and therefore the data needed transforming for comparison. Distance along the root was therefore transformed into relative distance along the LR, 0 representing the LR to PR junction and 100 the LR tip.

Chapter 3 Characterization of the root architectural changes in response to K^+ starvation

3.1 Introduction

When plants are faced with nutrient starvation in the soil they adapt the architecture of their root systems to utilise their remaining resources to search for more favourable soil environments. The root architectural changes, and the signalling pathways involved in mediating these changes, have been extensively investigated in response to nutrients such as phosphate and nitrate (see Shahzad & Amtmann, 2017 for a review). However, the mechanisms causing changes to root architecture in response to potassium starvation are less well understood (Shahzad & Amtmann, 2017).

Kellermeier *et al.* (2013) recently described a phenotypic gradient of root architectural responses to K^+ starvation in Arabidopsis accessions (Fig. 1-4). This gradient results from a trade-off between the primary root (PR) growth and lateral root (LR) growth, with some accessions displaying reduced LR growth accompanied by increased PR growth, and others maintaining LR growth with an attenuation in PR growth (Kellermeier *et al.*, 2013). The Arabidopsis accession Columbia (Col-0) was identified as compromising LR growth in favour of PR growth (Kellermeier *et al.*, 2013). Col-0 was chosen for all analyses presented here in order to maintain consistency in architectural phenotypes and because there are extensive genetic resources available for this accession.

The work in this chapter describes the characterization of the response of root architecture to low K^+ in Col-0; first to verify the results described in Kellermeier *et al.* (2013) and second, to pinpoint the developmental stage at which the low K^+ signalling pathway acts. The role of K^+ in the root architectural trait of gravitropism will then be investigated through the use of agravitropic mutants, and the roles of hormones in this response will be characterized.

3.2 Results

3.2.1 Root phenotypic growth changes of the PR and LRs in response to K^+ starvation

3.2.1.1 Col-0 maintains PR growth but reduces LR growth in response to K^+ starvation

The analysis of root system architecture (RSA) traits revealed that in response to 8 d low K^+, Col-0 seedlings showed a reduction in the length of the PR (Fig. 3-1A), reduction in the number of LRs (Fig. 3-1B) and a reduction in the length of the LRs (Fig. 3-1C). To further characterize

the growth response over time a time-course experiment was set up in which seedlings were grown for 7 d on ½ MS10 media then transferred to K^+ treatment media (2 mM of 0.005 mM). Seedlings were photographed from 7 days after germination (DAG) to 12 DAG to observe the pattern of growth on the control and K^+ starved media. The results of this experiment showed that the number of LRs under both 2 mM and 0.005 mM K^+ increased gradually over the 6 d, with a larger total number of LRs under the unstressed (control) conditions (Fig. 3-2B). However, the growth of the LRs under low [K^+], in contrast to the control conditions, did not increase over time, instead staying at a very low rate throughout (Fig. 3-2A). Under K^+ stress PR growth was maintained at a reduced but constant rate throughout the 6 d of analysis (Fig. 3-2C). These data support the Col-0 phenotype described by Kellermeier *et al.* (2013) of a maintenance of PR growth, with attenuation of LR growth.

3.2.1.2 LR density is not changed in response to low K^+

To further investigate the reduction in LR number (Fig. 3-1B) in response to low K^+, light microscopy was used to characterise LR development pre-emergence from the PR (Fig. 1-3A,B). Auxin accumulation occurs at the sites of new LRs (Benková *et al.*, 2003) and by using the auxin-responsive *DR5::GUS* reporter line, visualization of the early stages of LR development (stages 0–5) (Fig. 1-3A,B) can be seen as characteristic blue staining along the PR (Fig. 3-4B). Seedlings were grown for 4 d on ½ MS10 followed by 8 d on either high or low K^+ media, and by counting auxin maxima and LRs at all stages of development, it was found that there was still a reduction in the number of LRs under K^+ stress compared with control conditions (Fig. 3-3A); however, the reduction in number was less than that seen when counting only emerged LRs (Fig. 3-1B). Density of LRs was calculated by dividing the LR number by the PR length and no difference between the two K^+ conditions was observed (Fig. 3-3B), suggesting that the difference in LR number was an artefact of the reduced PR length. These data suggest that low K^+ was causing an attenuation of LR growth at an early stage of development.

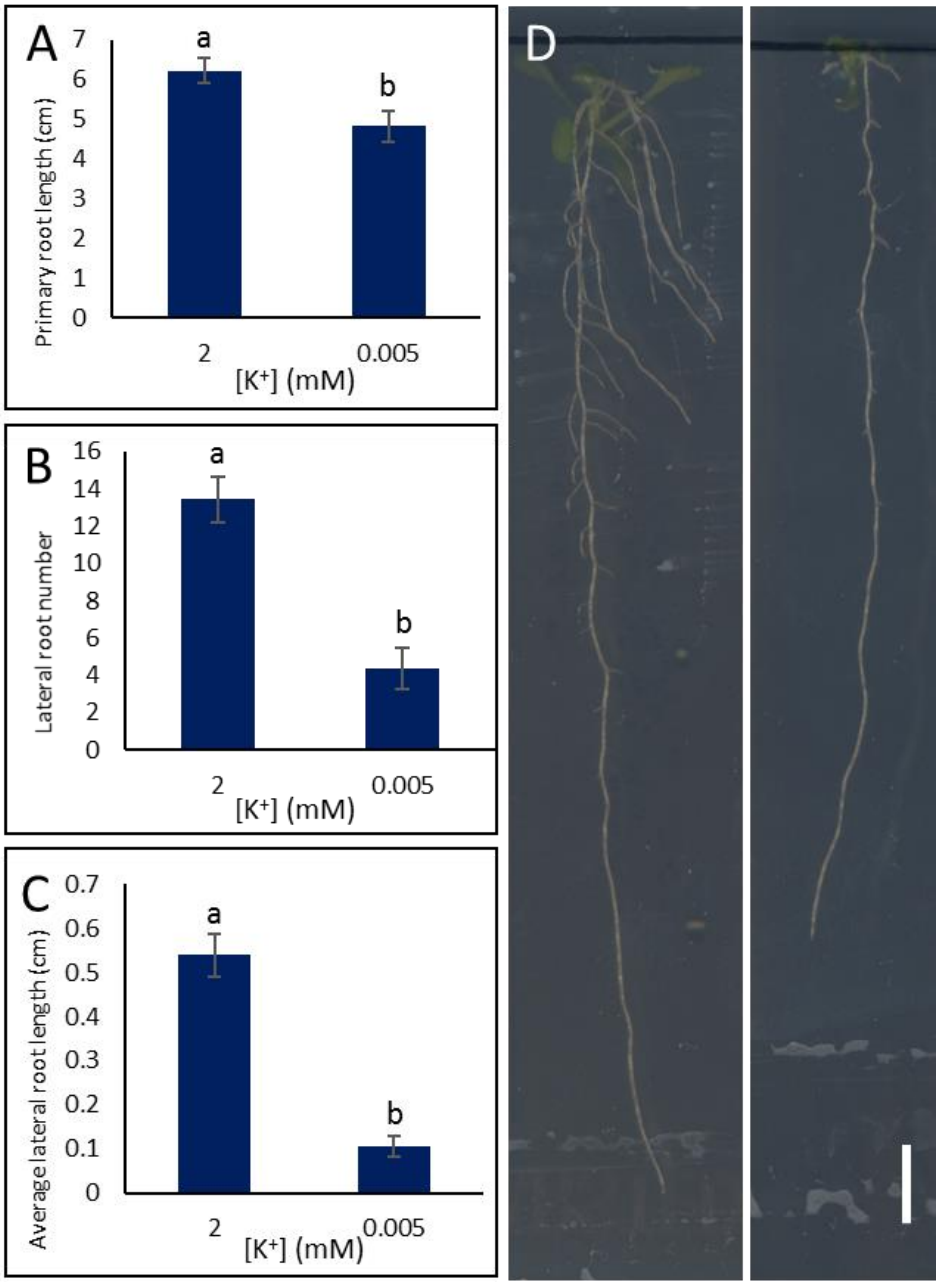

Fig. 3-1: Typical root architecture seen in *Arabidopsis thaliana* wild type accession Col-0, grown for 4 d on horizontal ½ MS10 agar plates followed by 8 d on vertical agar plates supplemented with either 2 mM and 0.005 mM K^+. (A) Primary root length, (B) emerged lateral root number, (C) average lateral root length. Values are averages of at least 14 individual seedlings per treatment ± SE, $n \geq 14$. Letters indicate significance with independent samples *t* test (*P*-value <0.05) (A) *P*= 0.009, (B) *P*= 0.000, (C) *P*= 0.000. (D) Typical root architectural 2 mM (left) and 0.005 mM (right).

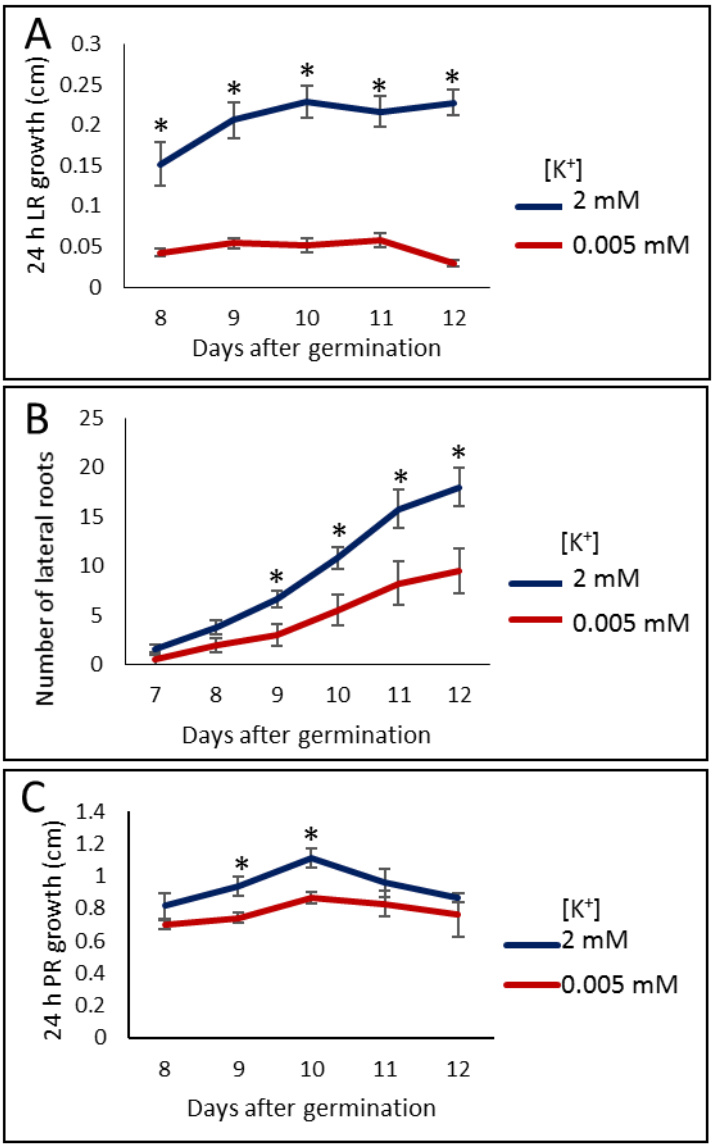

Fig. 3-2: Root growth analysis of Col-0 seedlings grown for 7 d on ½ MS10 media before being transferred to media with either 2 mM or 0.005 mM [K^+]. (A) Average lateral root growth over 24 h, (B) number of emerged lateral roots after each day, (C) primary root growth over 24 h. Values are averages of at least 5 individual seedlings per treatment ± SE, $n \geq 5$. Asterisks indicate significance between 2 mM and 0.005 mM at each point calculated using the independent samples *t* test *(P*-value <0.05).

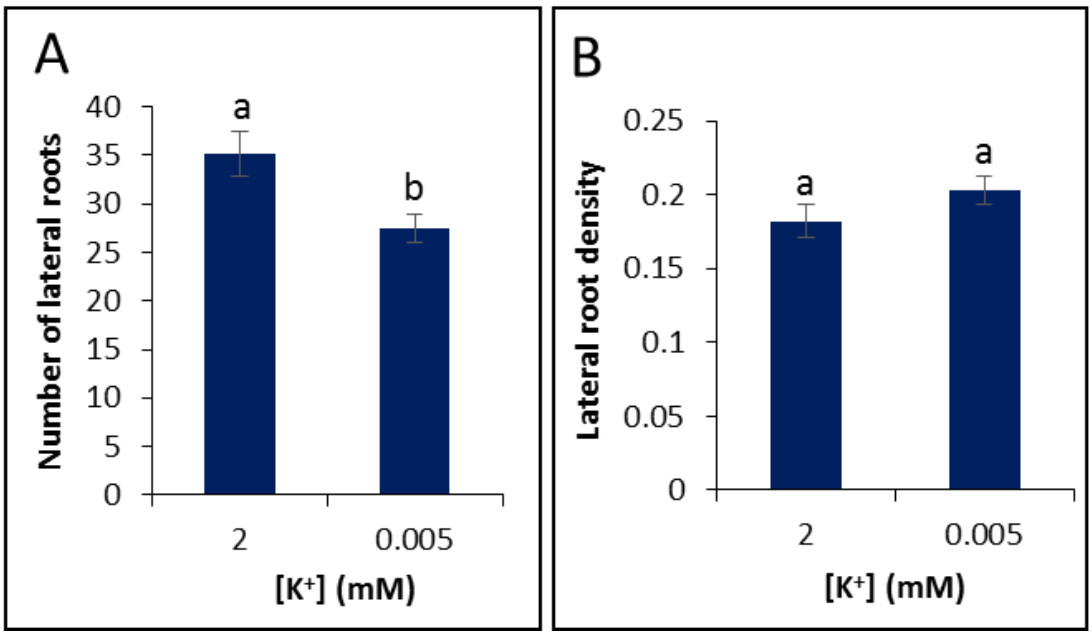

Fig. 3-3: Lateral root analysis of seedlings grown for 4 d on ½ MS10 followed by 8 d on either high or low K^+ media. Light microscopy and the auxin-responsive *DR5::GUS* reporter line allows all lateral root primordia and lateral roots to be counted along the length of the primary root. (A) Average number of lateral root primordia and lateral roots per seedling. (B) Average LR density (PR length/ total lateral roots) per seedling. Values are averages of at least 10 individual seedlings per treatment ± SE, $n \geq 10$. Letters indicate significance with independent samples *t* test (*P*-value <0.05); (A) $P = 0.013$, (B) $P = 0.167$.

3.2.1.3 K^+ starvation is causing a reduction in LR elongation

LR development is a complex process controlled at every step by interactions between different hormones (discussed in the introduction section 1.7). It was therefore important to characterize the stage at which development was inhibited by low K^+. Using the light microscope and the *DR5::GUS* reporter line, the number of LRs and LR primordia (LRP) were counted at each stage of development along each PR after 8 d growth on high and low K^+ conditions (Fig. 3-4). The average number of LRs at each stage of development remained roughly the same between the two conditions until after emergence from the PR (Fig. 3-4A). Following emergence, the number of LRs longer than 1 mm was significantly higher in the high K^+ treatment than in the low K^+, with a larger number of the LRs in the low K^+ treatment in the 200 µm to 1 mm categories (Fig. 3-4A).

The transition from lateral root primordia (LRP) to LR occurs after the formation of the functional LR meristem, at which point the LR grows via cell divisions at the LR root apex as opposed to division of the basal cells as in earlier stages (Malamy & Benfey, 1997). The transition corresponds to a length of LR of *c*. 100–200 µm (Fig. 1-3Ae). The results here suggest

that LR development remains normal throughout LRP development and that interference by low K^+ takes place after the development of the LR meristem. The elongation of the LRs appears to be affected by the low K^+ treatment as there was an accumulation of LRs in categories < 1 mm, whereas under control conditions, most LRs elongate further than 1 mm (Fig. 3-4A).

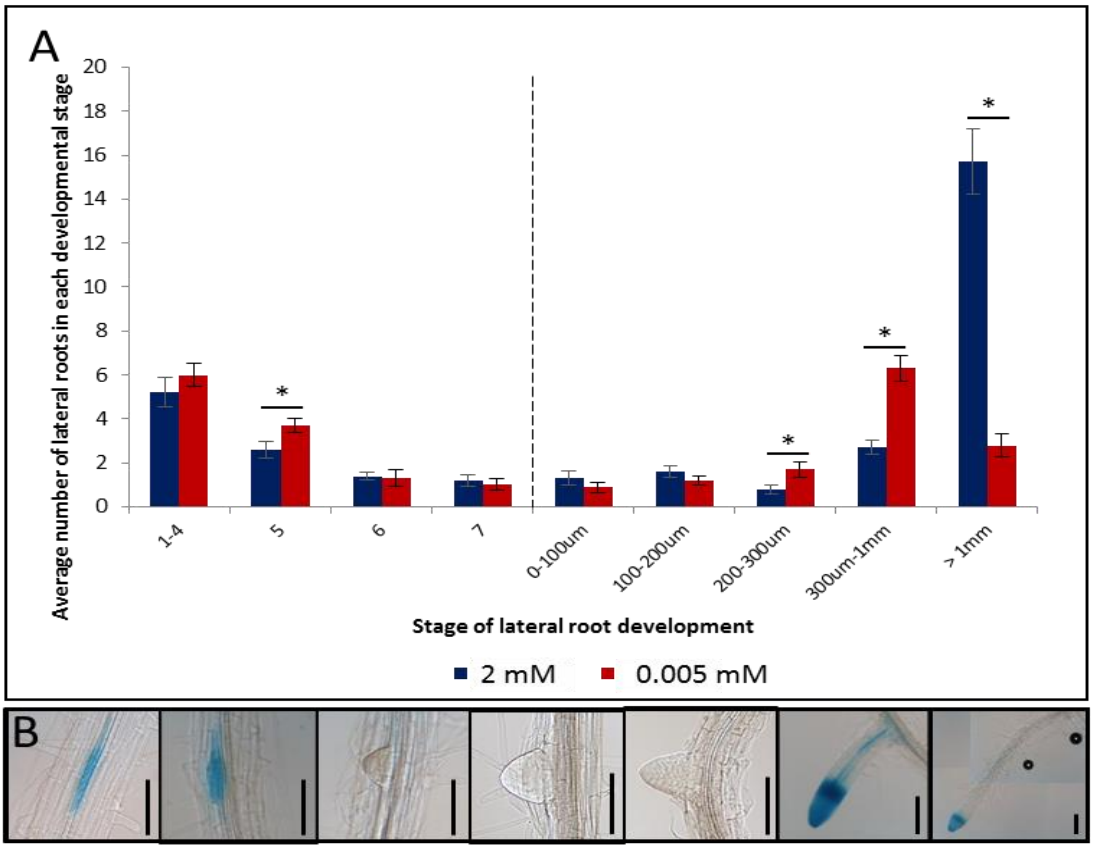

Fig. 3-4: Lateral root (LR) progression analysis**.** Light microscopy and the auxin-responsive *DR5::GUS* reporter line allow all LR primordia and LRs to be counted along the length of the PR. Col-0 seedlings analysed 12 DAG, 8 d of K^+ treatment (2 mM or 0.005 mM). Primordial stage as defined in Malamy & Benfey, (1997). (A) Average number of LRs in each stage of development on each PR, dotted line indicates point of emergence from the PR. (B) Typical *DR5::GUS* staining pattern of LR development, stages shown are (left-right) 1-4, 5, 6, 7, 0-100 µm, 300 µm-1 mm, >1mm. Scale bars = 100 µm. Values are averages of at least 10 individual seedlings ± SE, $n \geq 10$. Stars indicate significance with independent samples *t* test *(P*-value <0.05). Categories and associated *P* values; 1-4 *(P*= 0.361), 5 (*P* = 0.049), 6 (*P* = 0.806), 7 (*P* = 0.584), 1-100 µm (*P* = 0.340), 100-200 µm (*P* = 0.246), 200-300 µm (*P* = 0.045), 300 µm- 1 mm (*P* = 0.000), >1 mm (*P* = 0.000).

3.2.1.4 LR meristem size is reduced under K^+ starvation

The growth of the LR, as in the PR, is maintained by the rate of cell division, differentiation and elongation in the meristem. A reduction in LR growth in response to low K^+ could therefore be regulated by a modulation of meristem activity. Confocal imaging was used to investigate

meristem size in LRs grown in control or low K^+ conditions. The meristem size was calculated as the region of isodiametric cells extending from the quiescent centre (QC) to the cell that was twice the length of the immediately preceding cell (González-García *et al.*, 2011). The boundary of the transition zone is different in each cell type therefore in all analyses undertaken here, the cortex cell file was used to define the boundary. The length of the meristematic zone in the LRs was reduced after 8 d low K^+ stress (Fig. 3-5).

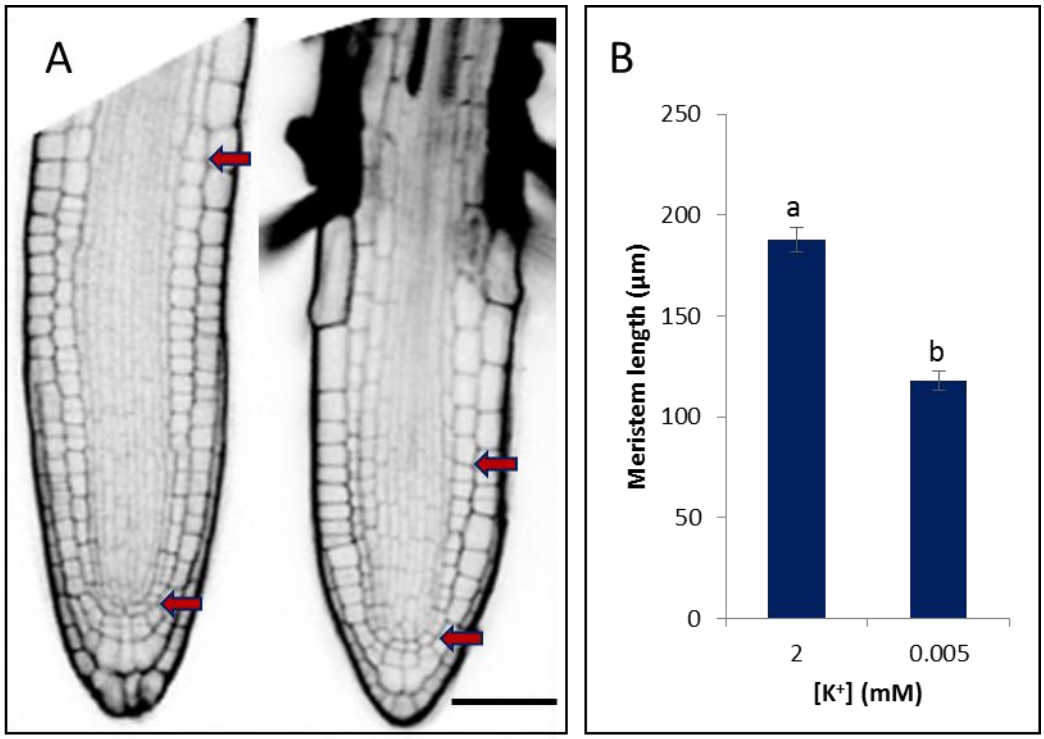

Fig. 3-5: (A) Typical LR meristems of Col-0 seedlings grown for 4 d ½ MS10 then 8 d on 2 mM $[K^+]$ (left) or 0.005 mM $[K^+]$. Images taken using confocal microscopy, cell walls stained using propidium iodide stain. Arrows denote meristem size. Scale bar = 50 µm. (B) Average length of LR meristems of LRs between 300 µm and 1 mm in length. Meristem border defined as region of isodiametric cells from the QC up to the cell that was twice the length of the immediately preceding cell (calculated from the cortex cell layer). Values are averages of at least 18 LRs taken from at least 15 individual seedlings ± SE, $n \geq 18$. Letters indicate significance with independent samples *t* test (*P* -value <0.05) (*P* =0.000).

3.2.1.5 Identity of the QC is maintained in LRs under K^+ starvation

A reduction in the size of the LR meristem in response to low K^+ could be caused by a reduced/impaired stem cell niche activity, a reduced meristematic cell division potential or a change in the rate of elongation/differentiation in the elongation/ transition zone. These were therefore investigated using light and confocal microscopy.

If the pool of stem cells at the tip of the LR are not maintained then the cells at the tip will terminally differentiate and stop the growth of the LR. To investigate if the activity of the LR stem cell niche was still maintained under 8 d low K^+ stress, the promoter activity of the QC-specific marker lines *QC25::GUS* and *WOX5::GFP* were investigated using histochemical staining and fluorescence microscopy, respectively (Sabatini *et al.*, 2003; Sarkar *et al.*, 2007). Histochemical staining of *QC25::GUS* showed a higher percentage of LRs with *QC25* promoter activity under low K^+ in the 300 µm–1 mm LR length, and no difference between treatments in LRs over 1 mm (Fig. 3-6 B,C). Promoter activity of *WOX5* was investigated using the stereo microscope and showed fluorescence in all LRs of all seedlings (*n*=9) over 200 µm, under both stressed (low K^+) and non-stressed (control) conditions. Confocal microscopy was used to investigate the expression pattern of *WOX5* within the LR meristems and no difference was found between the different K^+ conditions (Fig. 3-6A). *WOX5* acts to initiate and maintain identity of the QC (Forzani *et al.*, 2014) therefore its continued promoter activity, as well as the activity of *QC25*, in the QC after 8 d of stress, suggests that the identity of the QC is maintained under low K^+ conditions.

Starch granules are a marker of differentiation in columella cells while inactivity of the QC can lead to early differentiation of cells in close proximity to the QC (van den Berg *et al.*, 1997). Lugol staining identifies starch grains through their post staining dark blue/black colour under the light microscope. In this study lugol staining was carried out to investigate the differentiation of the cells of the LR meristems under high and low K^+ (Fig. 3-6D). No difference was observed between the K^+ treatments (2 mM or 0.005 mM) (Fig. 3-6D) after 8 d growth, further supporting the presence of a functional root meristem.

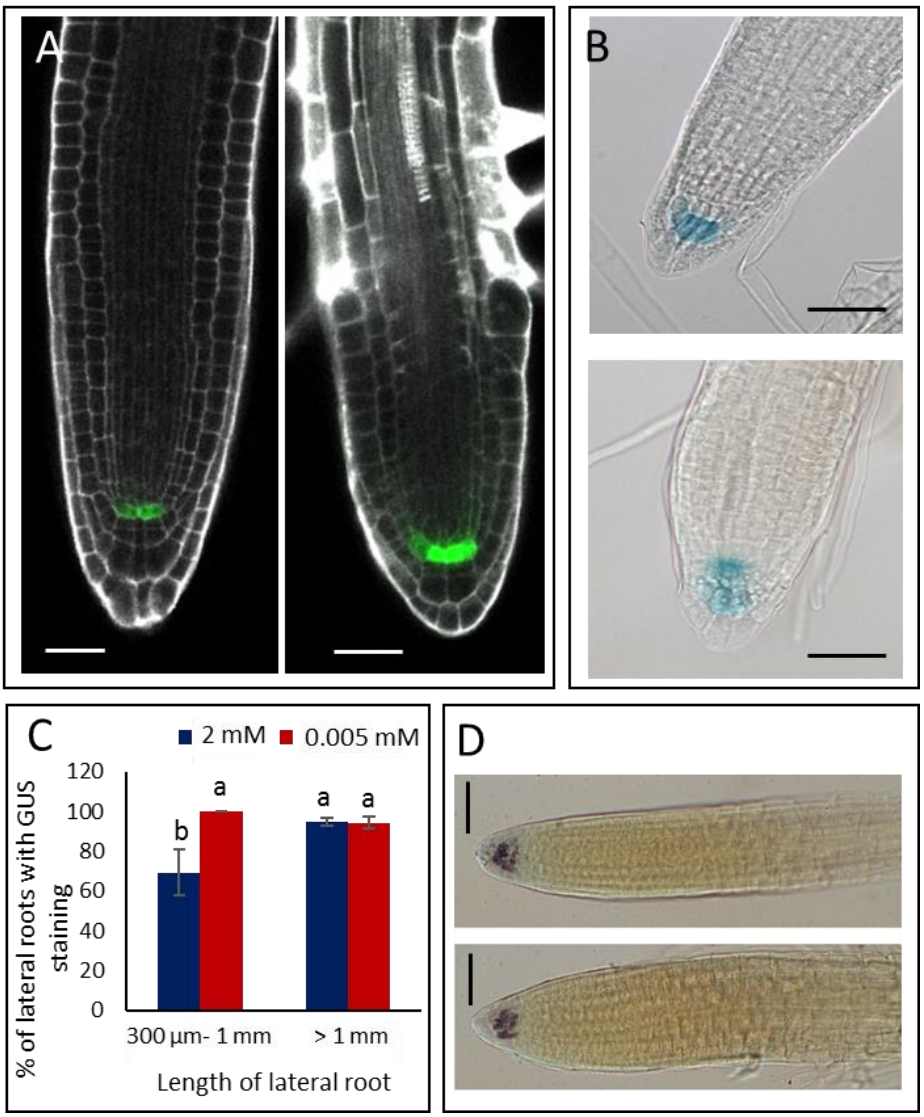

Fig. 3-6: Lateral root (LR) meristem activity of seedlings grown for 4 d on ½ MS10 followed by 8 d on high (2 mM) or low (0.005 mM) [K^+]. (A) Representative images of *WOX5::GFP* expression in LRs over 200 µm, [K^+] 2 mM (left) and 0.005 mM (right). Scale bars = 50 µm. (B) Typical GUS staining pattern of *QC25::GUS* in LR tips when grown on high and low [K^+] (upper and lower, respectively). Scale bars = 100 µM. (C) The average % of LRs on each *QC25::GUS* seedling with visible blue GUS staining. Values are averages of at least 10 individual seedlings per treatment ± SE, $n \geq 10$. Letters indicate significance with independent samples *t* test (*P* -value <0.05). (D) Typical lugol staining pattern of LRs grown on high (upper) and low (lower) [K^+] Scale bars = 50 µm.

3.2.1.6 Cell division is reduced in LR meristems under K^+ starvation

Meristematic cell division in the LRs was investigated under high and low K^+ conditions using the *CYCB1;2:GUS* marker. Mitotic cyclins such as *CYCB1;2* are only expressed from the G2 to M transition of the cell cycle; therefore, when fused with a reporter gene such as glucuronidase (GUS) they can be used as markers for cell division (Bulankova *et al.*, 2013). The root systems of *CYCB1;2:GUS* seedlings were stained for GUS activity, and the distance from the first stained

cell nearest the LR tip, to the one furthest from the tip was measured. This measurement gives an estimate of the proximal meristem as further support for the confocal image analysis (Fig. 3-5). A count of stained cells in the LR meristems was also made as a measurement of the number of dividing cells. A reduced area of cell division was observed in response to low K^+ at all stages of LR growth over 100 µm (Fig. 3-7C), and a reduced number of dividing cells in response to low K^+ was observed in LRs of between 300 µm–1 mm and also over 1 mm in length (Fig. 3-7B). This suggests that the reduced growth of the LRs is, at least in part, due to a reduced cell division potential in the meristematic zone of the LRs.

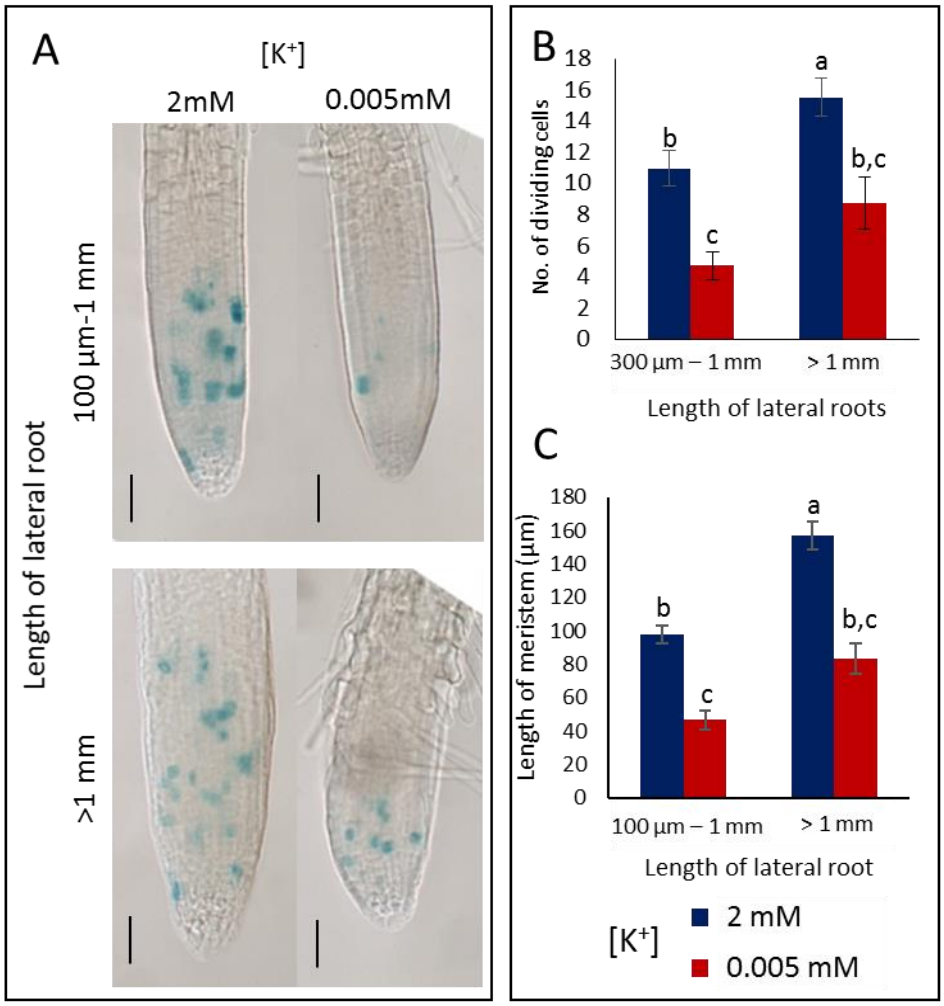

Fig. 3-7: *CYCB1;2:GUS* line grown for 4 d ½ MS10 followed by 8 d K^+ treatment (2 mM or 0.005 mM). (A) Typical GUS staining pattern of *CYCB1;2:GUS;* the staining shows a reduced area of cell division in low [K^+]. Scale bars = 50 µm. (B) Average number of dividing cells recorded as cells stained blue in *CYCB1;2:GUS* line. (C) Average length of meristem size measured as the length of area with dividing cells (stained blue in *CYCB1;2:GUS* line). Values are averages taken from at least 32 LRs taken from at least 10 individual seedlings ± SE, $n \geq 32$. Letters indicate significance with a Tukey Pairwise comparison $P < 0.05$.

3.2.1.7 Cell elongation in the transition zone of LRs is unaffected by K^+ starvation

After undergoing division in the meristematic zone of the root, cells enter the transition/elongation zone where they begin to elongate. The length of the first seven cells of the elongation zone were measured in order to investigate the elongation rate in response to low K^+. No significant difference was seen in the length of the first seven cells between the high and low K^+ conditions after 8 d growth (Fig. 3-8) suggesting that elongation rate is not affected by the low K^+ treatment.

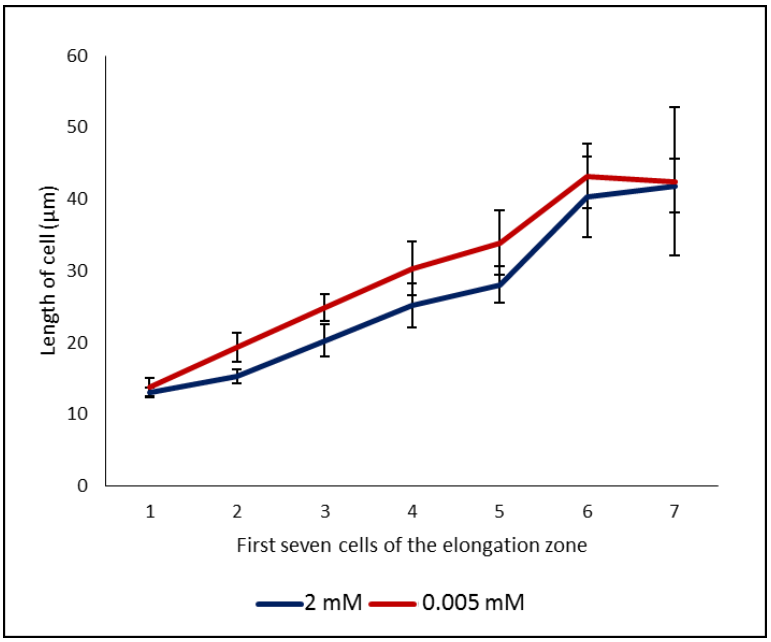

Fig. 3-8: Length of the first seven cells of the elongation zone of lateral roots grown for 4 d ½ MS10 followed by 8 d on 2 mM or 0.005 mM [K^+]. Measurements taken from at least 6 different seedlings. $n \geq 11$ for all apart from 7, where $n = 6$. Values are averages $\pm$ SE. Independent samples *t* test found no significance between [K^+] at any of the cells ($P < 0.05$). 1 ($P = 0.597$), 2 ($P = 0.1$), 3 ($P = 0.121$), 4 ($P = 0.306$), 5 ($P = 0.268$), 6 ($P = 0.695$), 7 ($P = 0.953$).

3.2.3 Potassium and gravitropism

The ability of a plant to sense and respond to gravity is essential in determining the root system architecture. Whilst some recent work has begun investigating the behaviour of LRs in response to this signal (Guyomarc'h *et al.,* 2012), the trait has been studied extensively in the PR. A link between potassium and gravitropism has been made a number of times previously in the literature (eg. Vicente-Agullo *et al.*, 2004; Ashley *et al.*, 2006), therefore the role of potassium in the PR gravitropic response was investigated.

3.2.3.1 K^+ starvation attenuates the level of agravitropism displayed in auxin transport mutants

Vicente-Agullo *et al.* (2004), suggested a role for K^+ in gravitropism through observations looking at TRH1, a K^+ transporter that also behaves like an auxin efflux facilitator. Under control K^+ conditions the *trh1* mutant is severely agravitropic, but when grown on low [K^+] the agravitropic phenotype is attenuated and the roots grow in a much more gravity-orientated way (Vicente-Agullo *et al.*, 2004). The vertical growth index (VGI) (Fig. 2-2) was used to show that the same response was also seen in another two agravitropic mutants, the auxin transport mutants *aux1-7* (Fig. 3-9B), and *eir1* (otherwise known as *pin2*) after 8 d growth (Fig. 3-9D). A difference in gravitropic response between K^+ treatments was not observed in the *aux1-22* mutant (Fig. 3-9C); however, this mutant is much less agravitropic when grown on standard growth medium, suggesting that low K^+ has a limited effect in this mutant background. The VGI was also calculated for Col-0 plants, where it was found that K^+ seems to have no effect when gravitropism is not impaired (Fig. 3-9A).

3.2.3.2 The attenuation of the agravitropic nature of the mutants is not a general nutrient stress response

To investigate whether this attenuation of agravitropic nature was a K^+-specific response or a general response to nutrient deficiency, *aux1-7* was grown on high and low phosphate (1 mM and 0.01 mM) (Jiang *et al.*, 2007) (Fig. 3-9E) and high and low nitrate (10 mM and 0.005 mM) (Mounier *et al.*, 2014) for 8 d (Fig. 3-9F). There was no significant difference in the gravitropic response between the phosphate conditions (Fig. 3-9E) or the nitrate conditions (Fig. 3-9F), suggesting that the attenuated agravitropic nature is a K^+-specific response.

3.2.3.3 Gravitropism is not rescued in the agravitropic mutants through addition of IAA or NPA

Next the impact of different hormones on the *aux1* gravitropic response was investigated. In previous work 80 nM IAA has been shown to rescue the agravitropic phenotype of the *trh1* mutant (Vicente-Agullo *et al.*, 2004). However, in the current investigation, adding 200 nM IAA to the *aux1-7* growth media did not rescue the gravitropic response under control conditions (2 mM K^+) (Fig. 3-10C). To investigate whether low K^+ restores the gravitropic response through restoration of polar auxin transport, the growth medium was supplemented with 10 µM of the auxin transport inhibitor *N*-1-naphthylphthalamic acid (NPA). This addition did not significantly reduce the VGI when grown on low K^+ (Fig. 3-10C) this result suggests that that low K^+ is not rescuing gravitropism by restoring polar auxin transport.

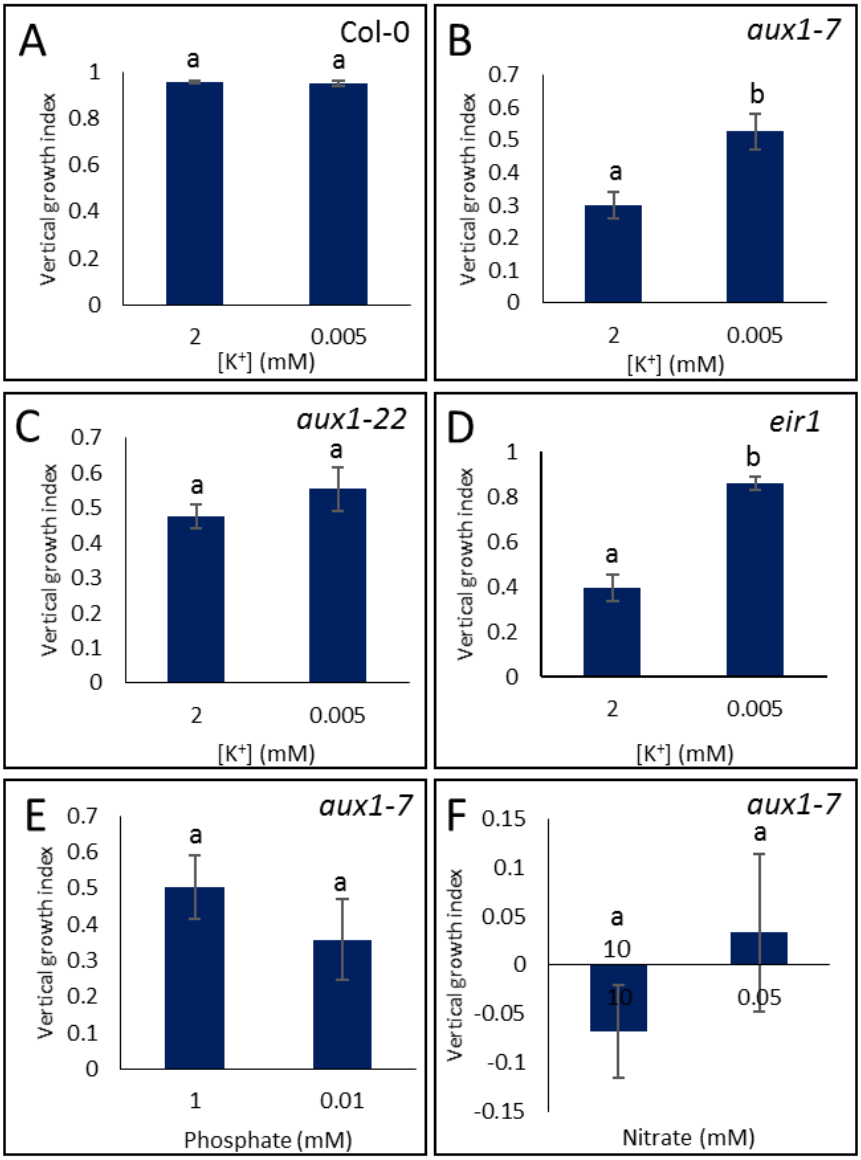

Fig. 3-9: Vertical growth index (VGI) calculated for seedlings following 4 d growth on ½ MS10 then 8 d growth on high or low nutrient concentration treatments. Values are averages of (*n*) individual seedlings ± SE. Letters indicate significance with independent samples *t* test (*P* - value <0.05). (A) Col-0, *P* =0.653, *n*≥16, (B) *aux1-7*, *P* =0.001, *n*≥32, (C) *aux1-22*, *n*≥10, *P* = 0.282, (D) *eir1*, *n*≥8, *P* = 0.008, (E) *aux1-7* grown on high and low phosphate media (1 mM or 0.01 mM) *P* = 0.242, *n*≥8, (F) *aux1-7* grown on high and low nitrate media (10 mM or 0.05 mM) *P* = 0.124 *n*≥10.

3.2.3.4 Ethylene signalling plays a role in the restoration of gravitropism in the agravitropic mutant *aux1-7*

As there has been a documented increase in ethylene in response to low K^+ in Arabidopsis (Jung *et al.*, 2009), the role of ethylene in this gravitropic response was investigated here. The addition of the ethylene blocker silver thiosulphate (referred to as Ag^{2+}) (1 µM) to the growth medium for 8 d led to a severe agravitropic response in *aux1-7* under both high and low K^+

treatments, with no restoration of gravitropism (Fig. 3-10B). Supplementation with 200 nM of the ethylene precursor 1-aminocyclopropane-1-carboxylic acid (ACC), restored gravitropism in the *aux1-7* mutant under both high and low [K^+] after 8 d (Fig. 3-10B). These two findings suggest a role for ethylene in the restoration of gravitropism in the agravitropic mutant *aux1-7*.

To determine the stage at which ethylene might influence the gravitropic response, the shorter-term effects of reorientation to gravity were investigated. *aux1-7* and Col-0 seedlings were grown vertically on ½ MS10 for 7 d. They were then transferred onto treatment plates so that they were perpendicular to the direction of gravity. They were then left to grow for 72 h and the angle of growth of the PR away from horizontal was measured every 24 h (Fig. 3-11A).

Compared with the WT, the reorientation to gravity of *aux1-7* in all treatments was greatly impaired (Fig. 3-11B). The addition of ACC or Ag^{2+} to the media did not have any obvious effects on the reorientation angle in either high or low K^+ conditions (Fig. 3-11B), suggesting that ethylene may be acting at a later stage in the response to gravity. However, due to the large variation in angle of growth, and the relatively small sample size (n=10 per treatment), it is difficult to determine conclusively whether ethylene has a role in the early response to gravity.

3.2.3.5 Initial data do not suggest change in auxin localization or PIN2 distribution in the *aux1-7* mutant in response to low K^+

Auxin distribution is known to be impaired in the *aux1-7* mutant and as ethylene is known to stimulate auxin biosynthesis and transport in Arabidopsis roots (Ruzicka *et al.*, 2007; Swarup *et al.*, 2007), it was hypothesised that an increase in ethylene may lead to an increase in tip-derived auxin. To investigate this hypothesis *aux1-7* plants were crossed with plants containing the *35S::DII-VENUS-N7* auxin reporter (Brunoud *et al.*, 2012). AUX1 is known to act with the auxin efflux carrier PIN2 to coordinate auxin redistribution in response to gravistimulation (Marchant *et al.*, 1999). The localization of PIN2 was investigated in the meristem of the PR by crossing the *aux1*-7 mutant with the *proPIN2::PIN2::GFP* protein fusion. Initial investigations (n≥4) did not observe differences in the auxin distribution (Fig. 3-12A,B) or the general PIN2 localization pattern (Fig. 3-12C,D) in the *aux1-7* mutant in response to low K^+ treatment for 8 d. It would be profitable in the future to carry out this experiment over shorter time periods, and to investigate the polar localization of PIN2. Previous reports have identified ectopic localization of PIN1 in agravitropic mutants (Rigas *et al.*, 2013) and it would, therefore, be interesting to investigate the potential role of ethylene in this response.

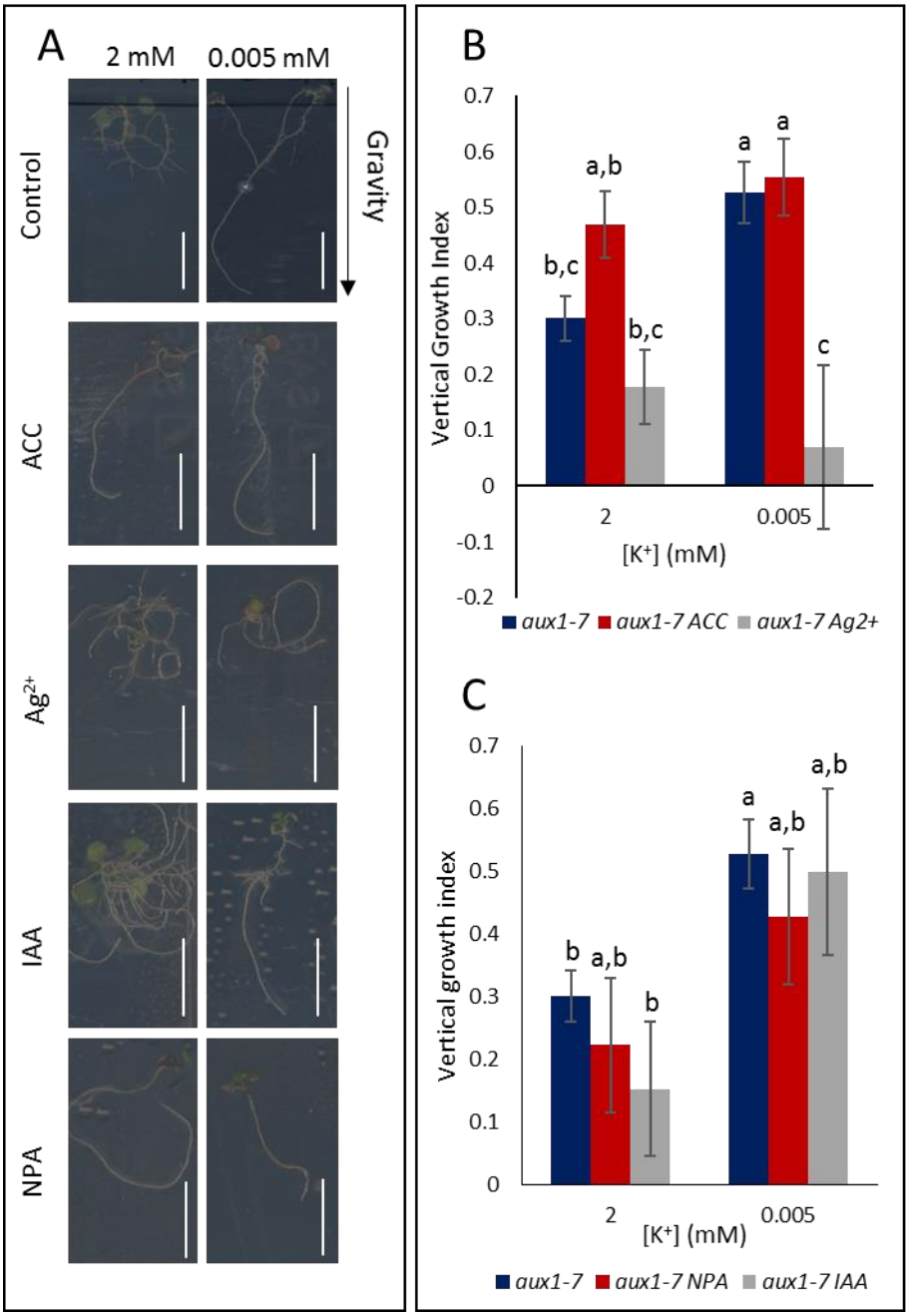

Fig. 3-10: The influence of hormones in restoring the vertical growth index (VGI) of *aux1-7* grown for 4 d on ½ MS10 followed by 8 d vertically on media with high or low [K^+] and supplemented with; 200 nM ACC, 1 µM Ag^{2+}, 200 nM IAA, 10 µM NPA. (A) Typical root growth architectures of *aux1-7* seedlings. Scale bars = 1 cm. (B, C) VGI of *aux1-7* grown on supplemented media. Values are averages of at least 9 individual seedlings ± SE, $n \geq 9$. Letters indicate significance with a Tukey Pairwise comparison $P < 0.05$.

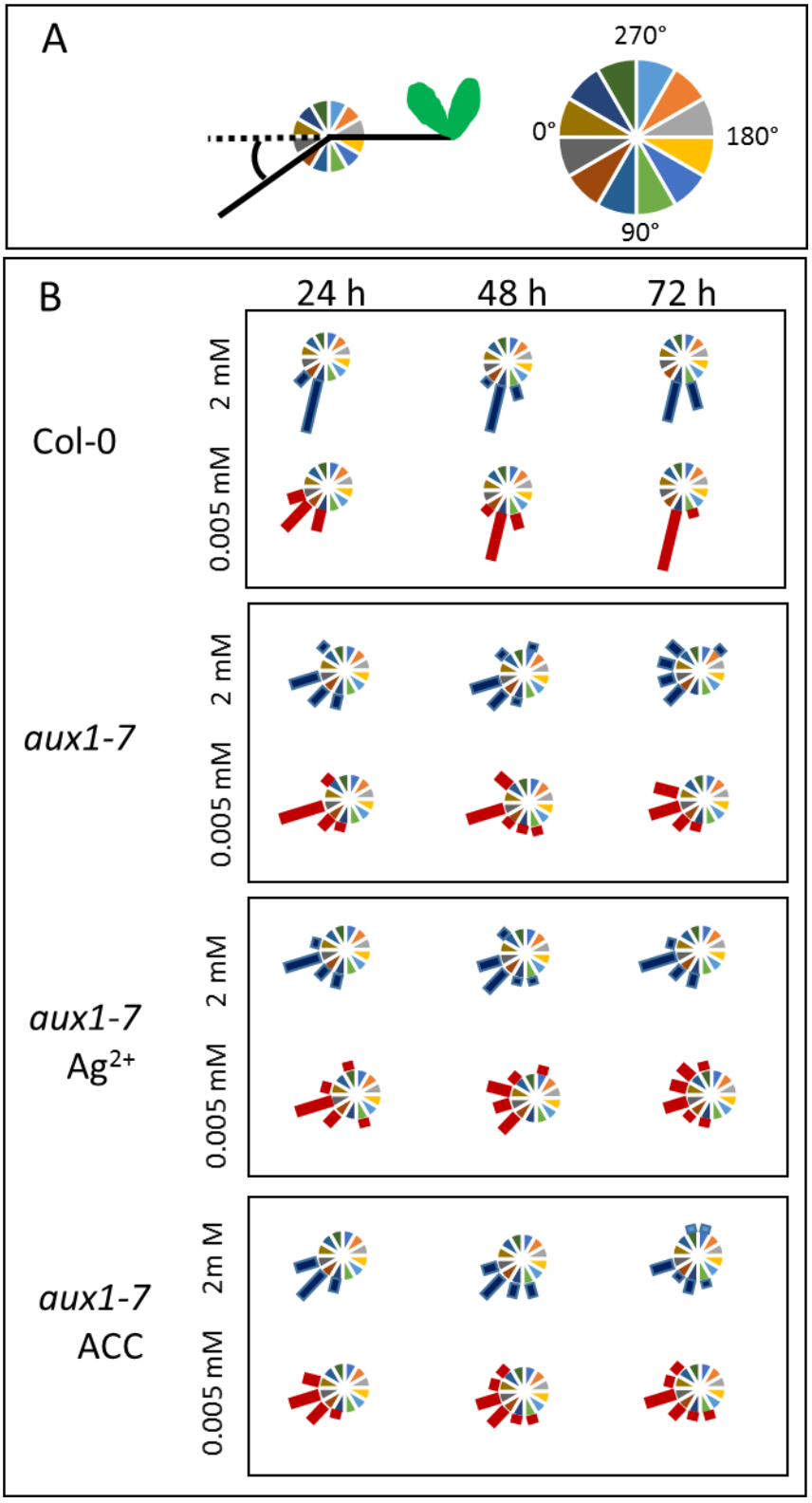

Fig. 3-11: (B) Gravitropic response of Col-0 and *aux1-7* seedlings after reorientation by 90° to perpendicular to the direction of gravity. Grown vertically on ½ MS10 for 7 d, then transferred onto treatment plates perpendicular to the direction of gravity. Media supplemented with 200 nM ACC, 1 µM Ag^{2+}. Measured as angular departure from the vertical (degrees). Length of bar indicates number of seedlings in each degree category. (A) displays experimental set up. *n*=10 individual seedlings

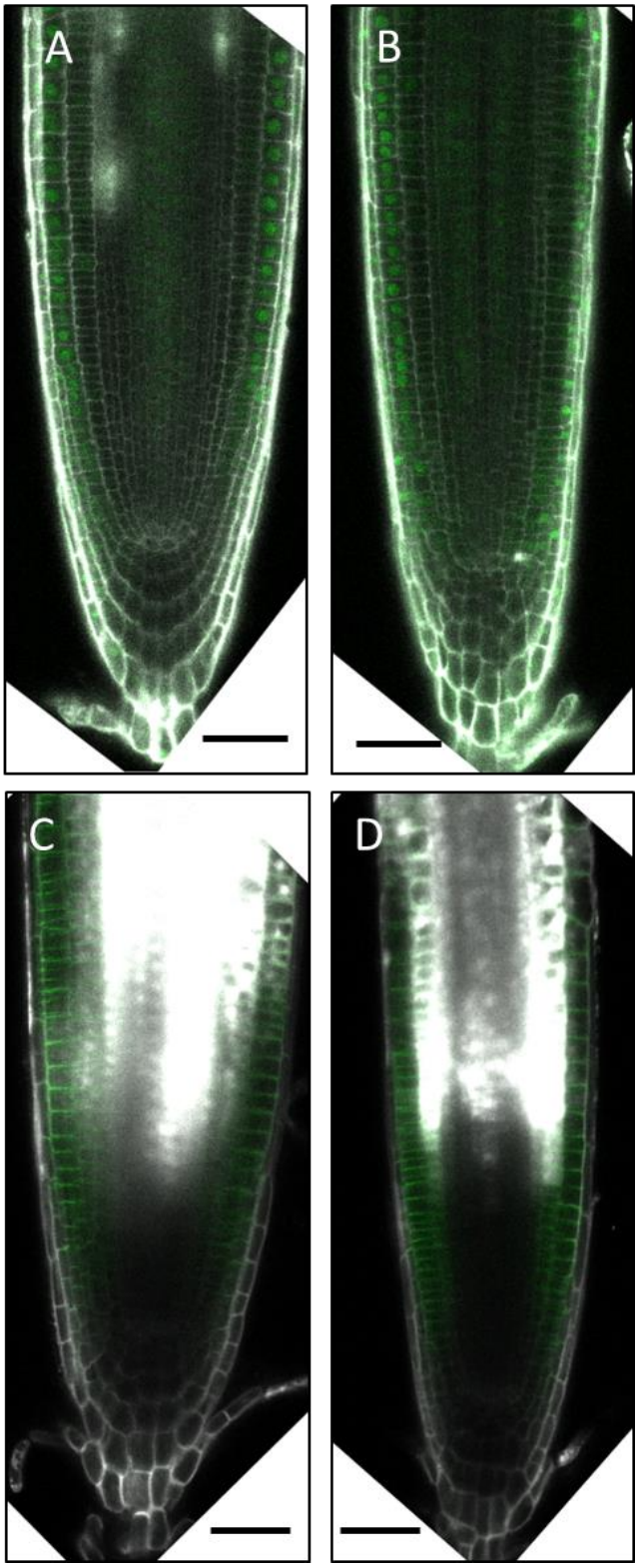

Fig. 3-12: Representative confocal images of the primary roots of *aux1-7 35S::DII-VENUS-N7* (A, B), and *aux1-7 proPIN2::PIN2::GFP* (C, D). White is propidium iodide stain, green is either VENUS (A & B) or GFP (C & D). Seedlings at a total of 12 d after germination (DAG), with 8 d growth on 2 mM (A,C), or 0.005 mM (B,D) [K^+]. Scale bars = 50 µM.

3.3 Summary

Work in this chapter has focussed on the characterization of the root architectural changes that occur in the Arabidopsis accession Col-0 in response to low K^+. In response to K^+ starvation, Col-0 maintains the growth of its PR but reduces the growth of its LRs. It was shown that the density of LRs remains the same under low K^+ conditions, and that development of LRs is normal until after emergence from the PR. Low K^+ was shown to lead to a reduction in the elongation of the LRs after the development of the LR meristem. Furthermore, the reduction in growth of the LRs under K^+ starvation is then mediated through a reduction in cell division in the LR meristem. The results in this chapter also identified a possible role for low K^+ in gravitropism and that gravitropism is partially restored in the agravitropic mutants *aux1-7* and *eir1* when they are grown on low K^+ (after 8 d of treatment). This attenuation was not observed after short time scales but further repeats need to be carried out to establish the short-term response more conclusively. Finally, the results in this chapter suggest a role for increased ethylene in the restoration of gravitropic response; however, the way in which ethylene performs this role was not investigated.

Chapter 4 RNA-Seq analysis investigating the effect of low K^+ on gene expression

4.1 Introduction

In May 2008, a series of five papers were published introducing a novel method of mapping the transcribed regions of an organism's genome using next generation sequencing (NGS) technology. The technique was termed RNA Sequencing (RNA-Seq) (Cloonan *et al.*, 2008; Lister *et al.*, 2008; Mortazavi *et al.*, 2008; Nagalakshmi *et al.*, 2008; Wilhelm *et al.*, 2008). Before the development of NGS, microarrays were used as the primary means of investigating high throughput gene expression profiling. Microarrays measure gene expression via hybridization of known gene sequences to fluorescently tagged probes – the stronger the fluorescence the higher the level of expression; however, NGS has several key advantages over microarrays. RNA-Seq does not use a probe sequence, it sequences the whole transcriptome and, therefore, does not rely on prior knowledge about the gene sequences, allowing, for example, the identification of microRNAs and alternatively spliced transcripts. This also makes it possible to use the technique on non-model species where little or no data have been previously collected (Wang *et al.*, 2009). RNA-Seq also bypasses the problems caused by cross hybridization and noise that are issues in microarray analysis. Without these problems interpretation of results is much more straightforward (Chee-Seng *et al.,* 2010).

The experimental procedure of RNA-Seq involves the isolation of RNA from a tissue and generation of a double stranded cDNA by reverse transcription with either random hexamers or oligo (dT) primers. Fragmentation and attachment of adaptors to either one or both ends of the cDNA fragments is carried out and then the molecules are sequenced by a NGS platform. The reads are then aligned with a reference genome or assembled *de novo* by overlapping sequences (Nagalakshmi *et al.*, 2008).

This chapter describes the data collected from an RNA-Seq experiment conducted with the aim of elucidating changes in gene expression in response to low K^+. The chapter will focus on uncovering hormonal signalling pathways that could provide the link between low K^+ and the reduction in lateral root (LR) growth. The chapter will also aim to provide a general overview of the gene expression changes in response to low K^+, and hypothesise about what could be resulting from these gene changes.

The first section of the chapter will describe the generation of the list of differentially expressed genes (DEGs). Gene ontology (GO) analysis will then be used to provide a general overview of the data. Other bioinformatics tools (methods section 2.10.2) are then used to investigate the data further and the remainder of the chapter describes hypotheses to account for the responses to low K^+. Later chapters (Chapters 5 & 6) will describe how these hypotheses have been tested.

4.2 Generation of the list of differentially expressed genes (DEGs) through RNA-Seq

The aim of the RNA-Seq experiment was to document changes in gene expression, and to use these data to understand signalling pathways associated with the early stages of the K^+-sensing and -signalling mechanism. For this reason, samples were taken from early timepoints (3 h and 30 h) after K^+ treatment (2 mM or 0.005 mM [K^+]). RNA-Seq analyses were performed on three independent biological replicates for each treatment and timepoint. See the methods section (2.2.3, 2.7.3, 2.10., Fig. 2-3) for full growth conditions, library preparation and the steps conducted to process the data. A *P*-value of ≤ 0.5 and a $\log_2$ fold change ($\log_2$fc) ≥0.5 (equivalent to 0.15 fold difference) were selected to identify differentially expressed genes (DEGs) between the high and low K^+ conditions at each of the timepoints (Fig. 4-1A). In total, there were 187 upregulated genes and 206 downregulated genes after 3 h K^+ starvation and 416 upregulated genes and 195 downregulated genes after 30 h K^+ starvation (Fig. 4-1B), with only 6 common downregulated genes between the treatments and 62 between the upregulated treatments (Fig. 4-1C).

These low numbers of DEGs and relatively small fold changes (Fig. 4-1A,B), fit with previously published microarray data showing that, unlike nitrate or phosphate deficiency, K^+ deficiency does not lead to major alterations in transcript abundance (Maathuis *et al.*, 2003; Gierth *et al.*, 2005; Ma *et al.*, 2012). A large increase in the number of DEGs from 3 h to 30 h (Fig. 4-1B) suggests that an increased transcriptional response to low K^+ is stimulated over time.

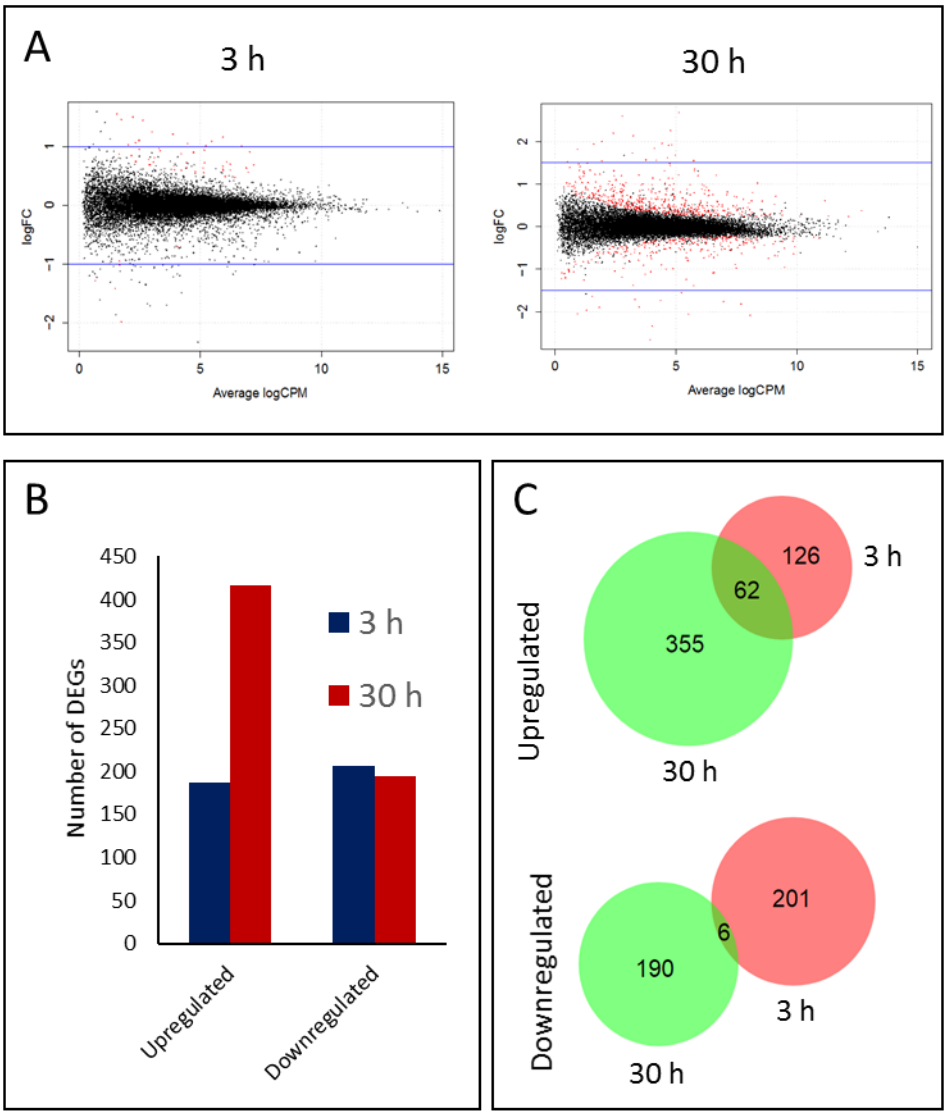

Fig. 4-1: Genes differentially expressed in low K^+ (0.005 mM) compared with control (2 mM) after 3 h and 30 h treatment identified through RNA-Seq. 3 independent biological replicates used per sample. *P*-value ≤ 0.5 and a $\log_2$ fold change ($\log_2$fc) ≥0.5. (A) Differentially expressed genes (DEGs) as estimated by the processing software EdgeR (Robinson *et al.*, 2010). Red dots are significant DEGs, black dots are non-significant. CPM (counts per million). (B) Histogram of significant DEGs separated into up- and down-regulated genes at the two K^+ time treatments. (C) Venn diagrams of common genes between the treatments separated into up- and down-regulated genes, created using BioVenn (Hulsen *et al.*, 2008).

To verify the data produced by the RNA-Seq experiment, qRT-PCR was conducted on three DEGs identified from the RNA-Seq data. qRT-PCR was performed on three independent biological replicates (independent from the samples used for the RNA-Seq experiment) after 30 h high and low K^+ treatment. The genes chosen from the RNA-Seq experiment were *HAK5, ERF6* and *STZ* (also known as *ZAT10),* all of which were selected because of their significant

log_2fc upregulation after 30 h K^+ starvation. *HAK5* (2.60 log_2fc), *ERF6* (0.84 log_2fc), *STZ* (0.79 log_2fc). qRT-PCR analysis of these genes corresponded with the RNA-Seq data for the 30 h timepoint, with all genes showing significant upregulation in response to low K^+ (Fig. 4-2).

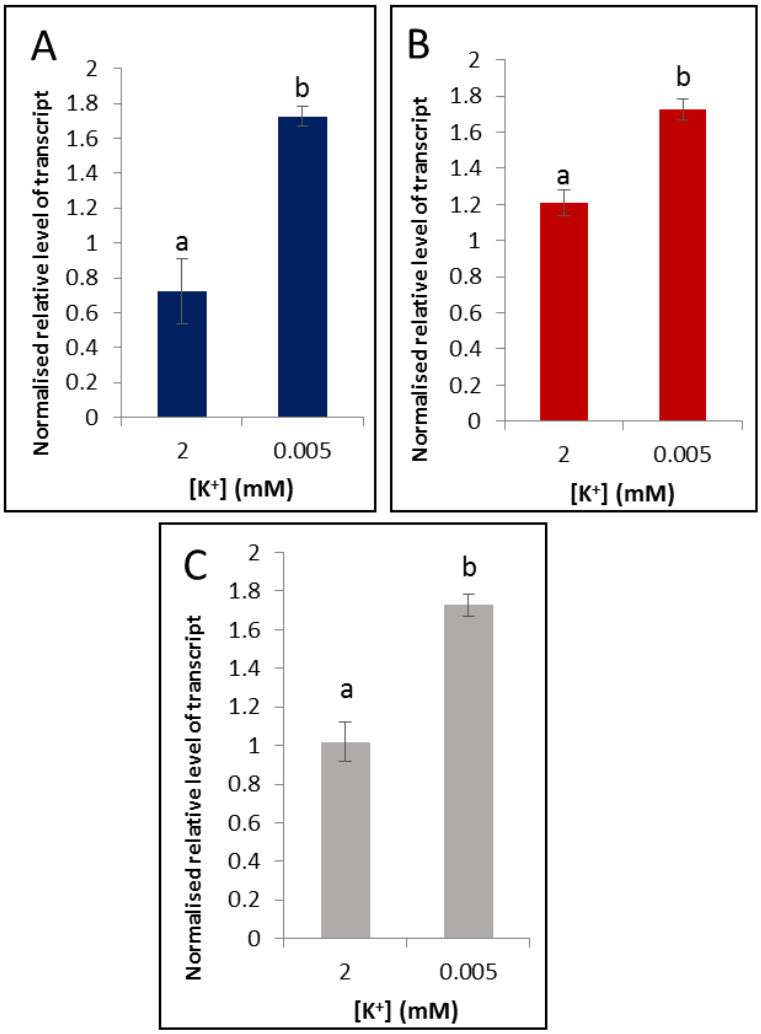

Fig. 4-2: Relative normalised levels of transcript of *HAK5* (A)*, ERF6* (B) and *STZ* (C) after 30 h K^+ treatment (2 mM or 0.005 mM [K^+]), determined by qRT-PCR. Normalised against *AT1G13320*. Values are means ± SE. Three biological repeats and three technical repeats used. Letters indicate significance between 2 mM and 0.005 mM with independent samples *t* test (*P*-value <0.05).

4.3 General overview of the data

4.3.1 Gene ontology (GO) analysis of the DEGs

In order to interpret the differential expression data collected from the RNA-Seq experiment, a gene ontology (GO) enrichment analysis was carried out using the online tool agriGO (Du *et al.*, 2010; Tian *et al.* 2017). This allows the identification of GO terms that occur frequently in the list of DEGs, to reveal the biological processes that are being regulated in response to low K^+

treatment. The outputs from GO analyses are often difficult to interpret and can be confounded by redundancies within the lists of GO terms (Supek *et al.*, 2011). Therefore, the agriGO data was further analysed using the online tool REVIGO, which summarises the list of GO terms and reduces functional redundancies allowing the visualization of the data in easy to interpret formats (Supek *et al.*, 2011). By grouping together semantically similar GO terms into clusters, then identifying a single GO term as a representative for that cluster, the long list of GO terms is reduced into a much more accessible format (Supek *et al.*, 2011). The treemap outputs (Figs 4-3 to 4-6) display each cluster as a rectangle, then groups them further, based on colours, into superclusters, with the sizes of rectangles representing the *P*-values. Obsolete terms, defined as a term that is out of scope, misleadingly named or defined or describes a concept that would be better represented in another way, are still often included however, and must be viewed with caution. The agriGO and REVIGO analysis provides a quick overview of the data which then allows identification of potential pathways and processes.

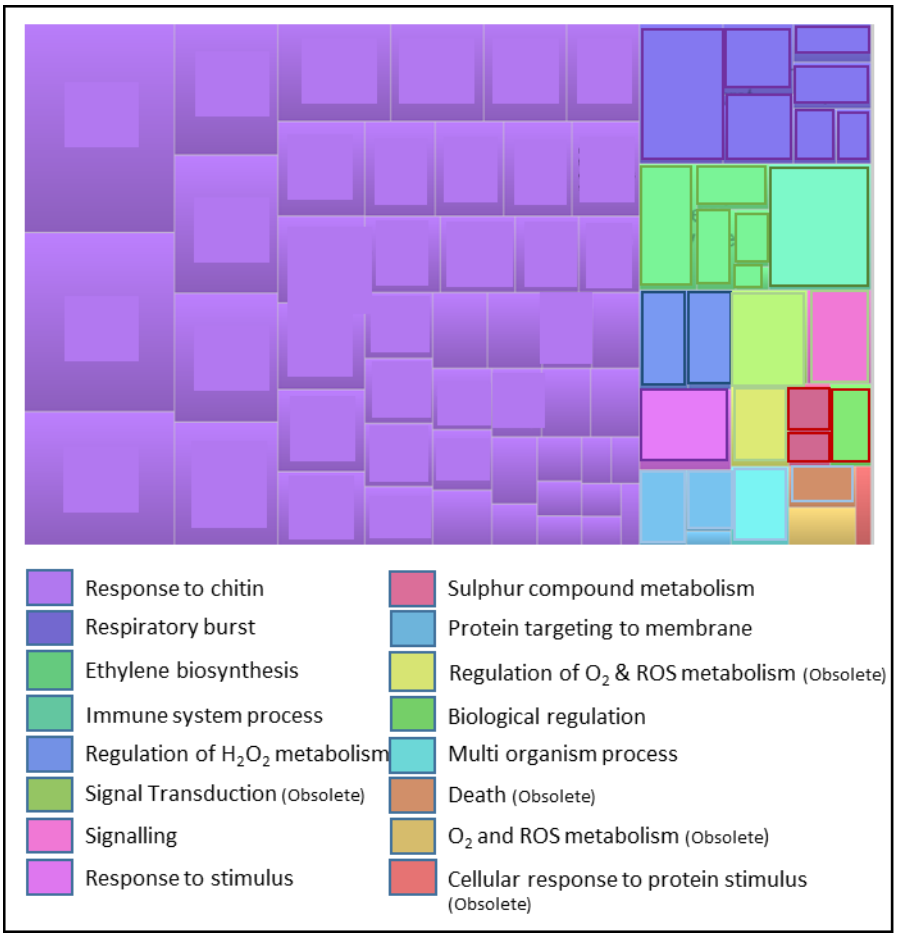

Fig. 4-3: Treemap output from REVIGO (Supek *et al.,* 2011) of the genes identified as significantly upregulated after 3 h K^+ starvation, following RNA-Seq experiment. *P*-value ≤ 0.5 and a $\log_2$ fold change ($\log_2$fc) ≥0.5. Each rectangle represents a gene ontology (GO) term cluster and each colour represents a supercluster of related clusters. The superclusters are listed in the key below the treemap. Obsolete terms represent misleadingly named or defined terms. Sizes of rectangles reflect the –log10 *P*-value of each cluster.

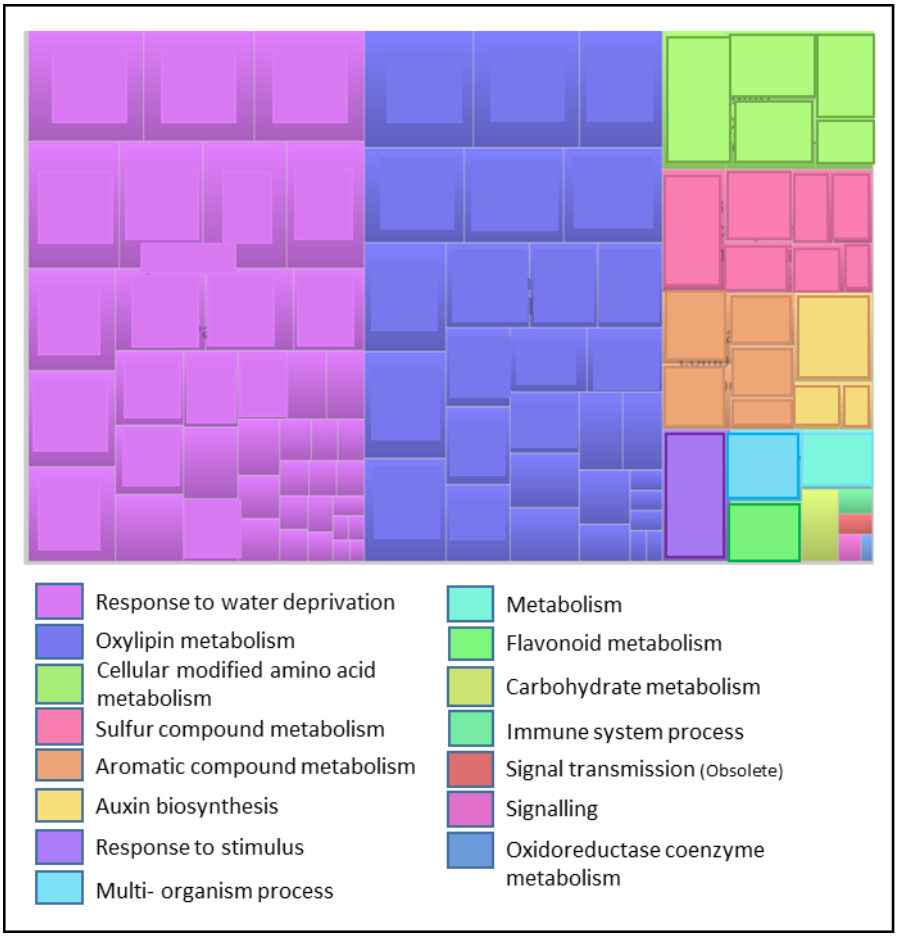

Fig. 4-4: Treemap output from REVIGO (Supek *et al.,* 2011) of the genes identified as significantly downregulated after 3 h K^+ starvation, following RNA-Seq experiment. *P*-value ≤ 0.5 and a $\log_2$ fold change ($\log_2$fc) ≥0.5. Each rectangle represents a gene ontology (GO) term cluster and each colour represents a supercluster of related clusters. The superclusters are listed in the key below the treemap. Obsolete terms represent misleadingly named or defined terms. Sizes of rectangles reflect the –log10 *P*-value of each cluster

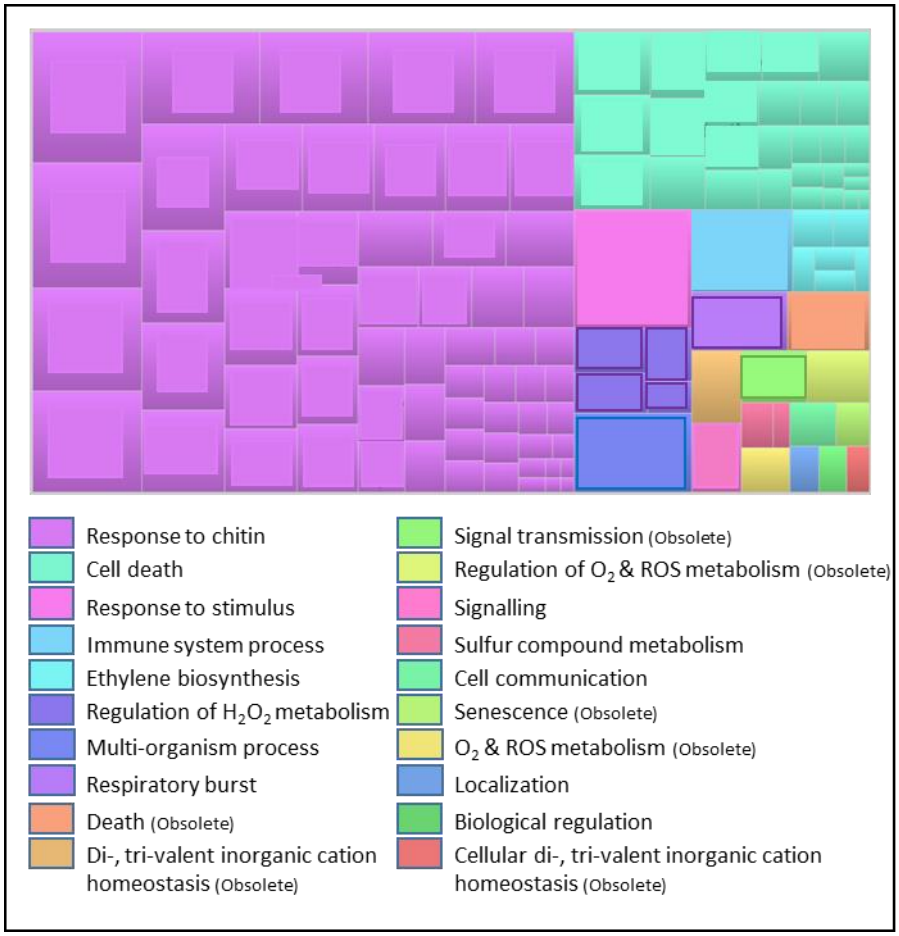

Fig. 4-5: Treemap output from REVIGO (Supek *et al.,* 2011) of the genes identified as significantly upregulated after 30 h K^+ starvation, following RNA-Seq experiment. *P*-value ≤ 0.5 and a $\log_2$ fold change ($\log_2$fc) ≥0.5. Each rectangle represents a gene ontology (GO) term cluster and each colour represents a supercluster of related clusters. The superclusters are listed in the key below the treemap. Obsolete terms represent misleadingly named or defined terms. Sizes of rectangles reflect the –log10 *P*-value of each cluster.

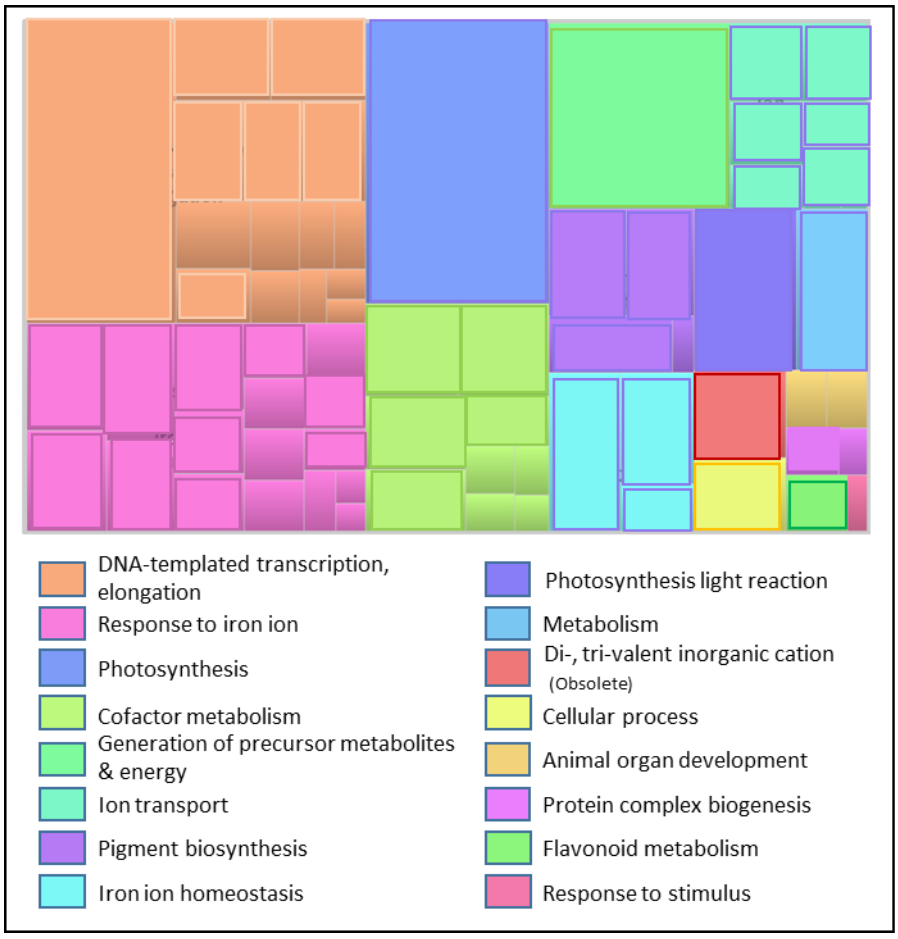

Fig. 4-6: Treemap output from REVIGO (Supek *et al.,* 2011) of the genes identified as significantly downregulated after 30 h K^+ starvation, following RNA-Seq experiment. *P*-value ≤ 0.5 and a $\log_2$ fold change ($\log_2$fc) ≥0.5. Each rectangle represents a gene ontology (GO) term cluster and each colour represents a supercluster of related clusters. The superclusters are listed in the key below the treemap. Obsolete terms represent misleadingly named or defined terms. Sizes of rectangles reflect the –log10 *P*-value of each cluster.

4.3.2 Hypothesis generation from GO analysis

The treemaps suggest that there is a strong upregulation of genes involved in the response to pathogens following transfer to low K^+, as seen by 'response to chitin' being the largest supercluster in each of the upregulated treemaps (Figs 4-3, 4-5). Both upregulated DEG treemaps also hold superclusters referring to 'immune system process', 'response to stimulus' and 'multi organism process' (Figs 4-3, 4-5). The treemaps also identified that there was enrichment in the biosynthesis of the hormones ethylene (3 h up and 30 h upregulation) (Figs 4-3, 4-5) and auxin (3 h downregulation) (Fig. 4-4). As hormones are key in the orchestration of many developmental processes and responses to biotic and abiotic stresses, the enrichment of these GO terms suggests that there could be increased hormone signalling in response to K^+ starvation. GO terms relating to reactive oxygen species (ROS) were also enriched in the upregulated data. As ROS is known to be important in the response to many abiotic and biotic stresses, the overpresentation of ROS-signalling/generation genes in the DEGs suggest that ROS signalling may be activated in response to low K^+. Genes involved in the 'response to the iron ion', and 'iron ion homeostasis', were also identified from the 30 h downregulated data (Fig. 4-6), suggesting a potential link between the Fe and K^+ pathways. Additionally, the downregulation of photosynthesis was also suggested from the 30 h data (Fig. 4-6).

GO analysis provides a very useful basis from which to generate hypotheses about the biological processes that may be being regulated in response to low K^+ in Col-0. The next part of this chapter will use bioinformatics tools and literature analysis to investigate the gene expression changes associated with the enrichments identified by the GO analysis.

4.4 Bioinformatic investigation into pathogens, photosynthesis and iron

4.4.1 Response to pathogens

An overlap in transcript profiles between K^+ starvation and response to pathogen/herbivory has previously been identified (Armengaud *et al.*, 2010), and together with a reversible increase in jasmonic acid (JA) levels (Armengaud *et al.*, 2004; Cao *et al.*, 2006), have been used to suggest that defence pathways are upregulated during K^+-limiting conditions (Armengaud *et al.*, 2010). The data presented here support this suggestion, showing upregulation of members of the JA biosynthesis pathway after 30 h (Fig. 4-7B). Interestingly, however, the early K^+ deprivation timepoint shows a downregulation of members of the JA biosynthesis pathway (Fig. 4-7A), suggesting a transient repression to the initial stress response.

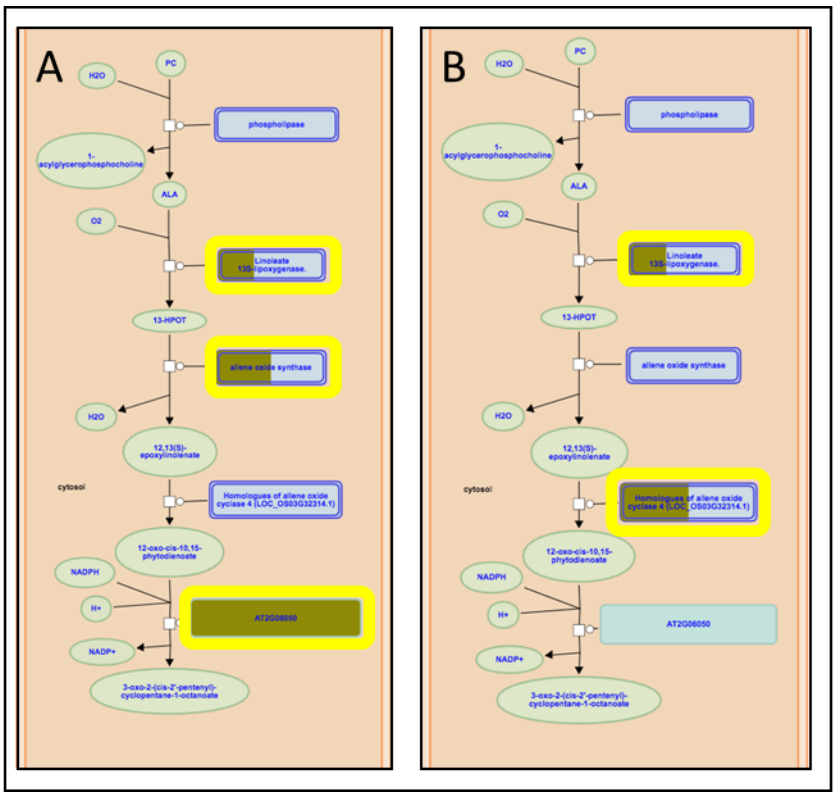

Fig. 4-7: Output from the plant reactome online analysis tool (Naithani *et al.*, 2017) from analysis of RNA-Seq data identifying which genes in the jasmonic acid biosynthesis pathway are transcriptionally changed in response to low K^+. Yellow boxes show where genes from the RNA-Seq data were identified in the JA biosynthesis pathway. (A) Identified genes from the 3 h downregulated genes *AT1G17420 (LOX3), AT2G06050 (OPR3), AT4G15440 (CYP74B2).* (B) Identified genes from the 30 h upregulated data *AT3G25770 (AOC2), AT3G25760 (AOC1), AT3G45140 (LOX2).*

4.4.2 Photosynthesis

The REVIGO treemaps identified downregulation in genes associated with the GO term 'photosynthesis' (Fig. 4-6), and when the 30 h downregulated DEGs were run through the initial GO analysis (agriGO), photosynthesis had the lowest *P*-value of any GO terms (3.6e-23 and FDR of 5.56e-20) (Appendix III) with 32 genes out of the 189 genes inputted with a significant photosynthesis GO term (Table in appendix III).

Of the 32 genes highlighted by GO analysis, a number are known to play important roles in the photosynthetic machinery. With three Photosystem II reaction centre proteins (PSBC, PSCD and PSBJ), four NADH dehydrogenases (NDHJ, NDHB, NDHC and NDHK), and a light-harvesting chlorophyll–protein complex II (LHB1B1) all showing downregulation of expression in response to low K^+ (Fig. 4-8). The data here suggest that reduced photosynthesis could be partly controlled through the downregulation of genes associated with the photosynthetic machinery.

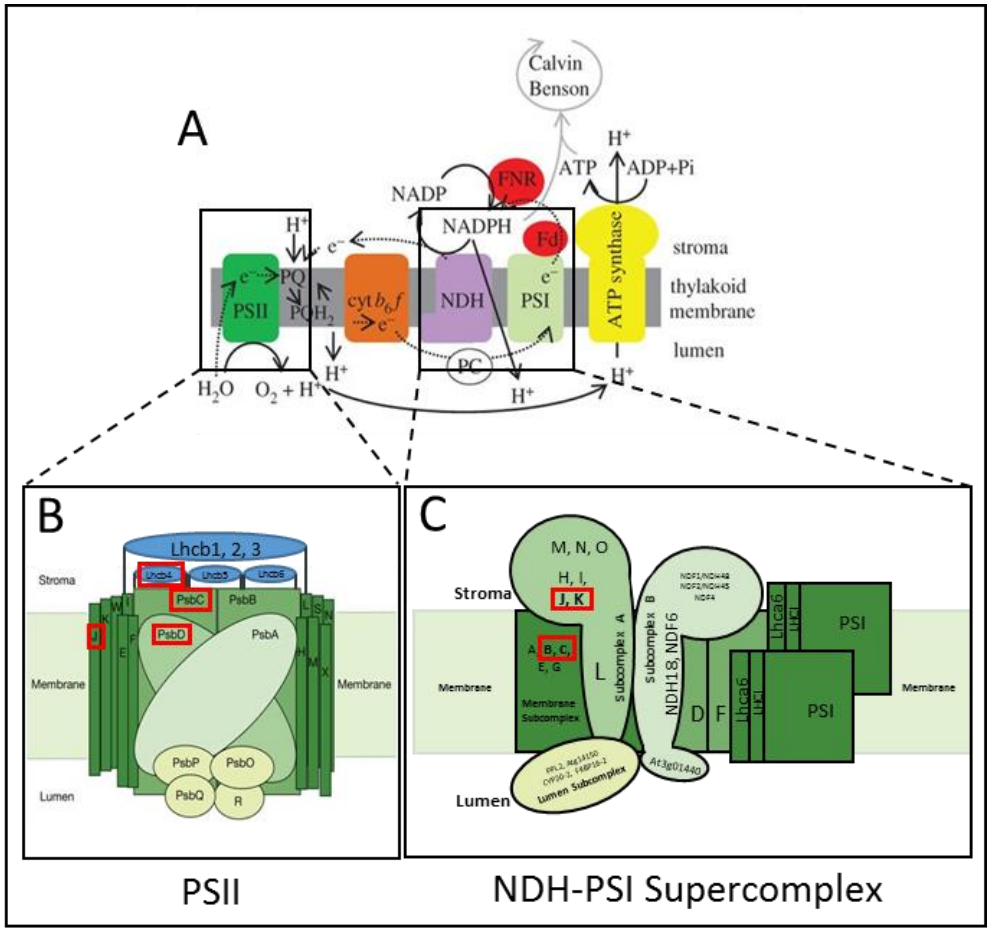

Fig. 4-8: (A) Schematic of the photosynthetic electron transfer chain adapted from (Queval & Foyer, 2012). (B) Schematic of the proteins making up photosystem II (adapted from (Calderone *et al.*, 2003) and (Allakhverdiev *et al.*, 2010). (C) Schematic of the NDH–PSI supercomplex in chloroplasts, based on a diagram in (Peng *et al.*, 2011). Red squares identify genes downregulated in the RNA-Seq data after 30 h K^+ deprivation.

4.4.3 Iron ion homeostasis

The REVIGO treemaps also identified GO terms relating to iron as two large superclusters in the downregulated 30 h data (Fig. 4-6). When the GO terms were investigated in more detail using agriGO, iron related GO terms were also found to be significant in the upregulated 30 h data, with 'iron ion homeostasis' having a *P*-value of 1.1e-7 and 'cellular response to iron ion starvation' having a *P*-value of 3.4e-7 (Appendix IV). Genes identified by agriGO, as well as literature searches, allowed a potential link between the K^+- and Fe-pathways to be investigated further and genes with proven links to iron signalling were identified (Fig. 4-9B).

There was an upregulation of several genes involved in the Fe-deficiency pathway, including a set of bHLH genes (*bHLH38, bHLH39, bHLH100 and bHLH101*) (Fig. 4-9) known to be induced under low Fe (Yuan *et al.*, 2008; N. Wang *et al.*, 2013), as well as the *FRO2/IRT1* and *ZIF1* genes (Fig. 4-9), which act to reduce Fe(III) to Fe(II), transport Fe into the root and function in Fe homeostasis, respectively (Eide *et al.*, 1996; Robinson *et al.*, 1999; Henriques *et al.*, 2002; Varotto *et al.*, 2002; Vert *et al.*, 2002; Haydon *et al.*, 2012). Supporting a link between the K^+-starvation and Fe-deficiency pathway, there was also downregulation of *Fer1* (Fig. 4-9B), a ferritin which acts in the sequestration of iron to avoid oxidative stress (Ravet *et al.*, 2009). *Fer1* is highly upregulated in response to iron- overload (Ravet *et al.*, 2009), a downregulation of *Fer1* in response to K^+ starvation supports the potential Fe deficiency link. The *NEET* gene (Fig. 4-9B) has also been suggested to play a role in Fe homeostasis, with the *At-NEET* knockdown plants accumulating more Fe (Nechushtai *et al.*, 2012) therefore suggesting a role for *NEET* in homeostasis under Fe excess instead of Fe deficiency.

Downregulation of the *FIT* gene and upregulation of *PYE* and *BTS* (Fig. 4-9) do not fit with the suggested link between low K^+ and Fe deficiency however, as *PYE* and *BTS* act as negative regulators of Fe deficiency (Long *et al.*, 2010; Selote *et al.*, 2015) whereas *FIT* is a positive regulator of the response to Fe deficiency (Colangelo, 2004; Jakoby *et al.*, 2004; Yuan *et al.*, 2005). Therefore the trasncriptional regulation of these genes suggest a link between low K^+ and an increased supply of Fe. Overexpression of *FIT* however, has been found to have no effect on the expression of the downstream targets in the Fe deficiency pathway, *FRO2* and *IRT1* (Yuan *et al.*, 2008; N. Wang *et al.*, 2013), and a number of the downstream genes have been upregulated despite negative regulation from *PYE* and *BTS*. This suggests that these genes are regulated through an alternative or additional mechanism. Together these data may suggest a partially conserved pathway between K^+ and Fe deficiency, or some level of crossover, due to the high number of DEGs identified in the data.

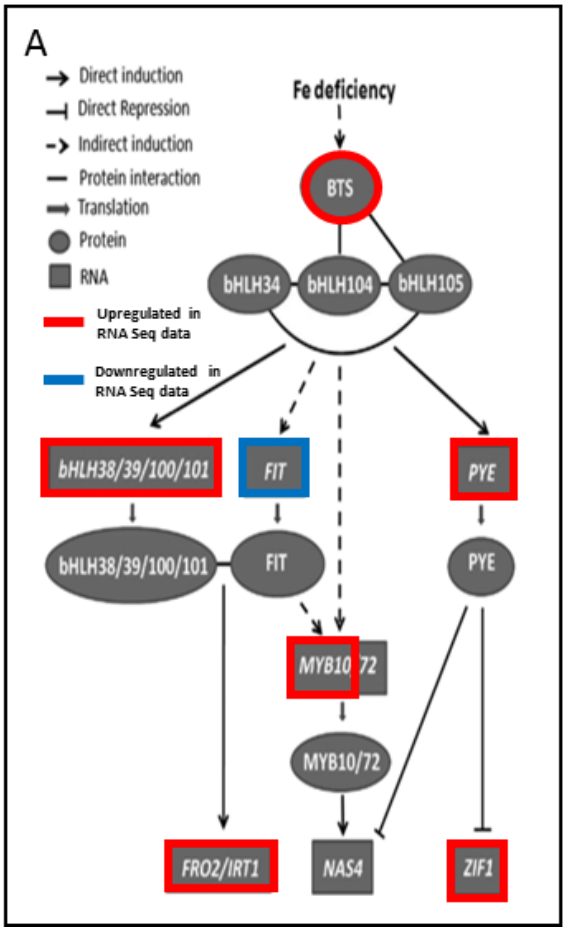

B Gene	AGI	Log_2fc after 30 h <0.05 *P*-value
BTS	*AT3G18290*	0.80
bHLH34	*AT3G23210*	-
bHLH104	*AT4G14410*	-
bHLH105	*AT5G54680*	-
bHLH38	*AT3G56970*	1.96
bHLH39	*AT3G56980*	1.44
bHLH100	*AT2G41240*	1.91
bHLH101	*AT5G04150*	1.73
FIT1	*AT2G28160*	-0.30
PYE	*AT3G47640*	0.70
MYB10	*AT3G12820*	0.82
MYB72	*AT1G56160*	-
FRO2	*AT1G01580*	1.02
IRT1	*AT4G19690*	0.52
NAS4	*AT1G56430*	-
ZIF1	*AT5G13740*	0.57
Fer1	*AT5G01600*	-1.76
NEET	*AT5G51720*	-1.71

Fig. 4-9: (A) Iron (Fe) deficiency pathway adapted from (Li *et al.*, 2016) coloured boxes around gene names denote upregulation (red) or downregulation (blue) in response to 30 h K^+ starvation RNA-Seq data set. (B) Genes with proven associated with Fe signalling identified from RNA-Seq data using agriGO and literature searching with log_2fold change (log_2fc) difference in RNA-Seq data after 30 h K^+ starvation treatment.

4.5 Hormone regulation, evidence from RNA Seq

As described in Chapter 3, there is a reduction in the growth of the LRs in Col-O in response to low K^+. Root architectural changes are often mediated by combinations of the actions of different hormones (see the Introduction section 1.4.1). The RNA-Seq data were therefore investigated in order to identify possible hormonal signalling pathways which are activated in response to low K^+, and could therefore be mediating the reduced LR growth response.

4.5.1 Auxin

4.5.1.1 Regulation of auxin biosynthetic genes in response to low K^+

GO analysis identified an enrichment of terms relating to auxin biosynthesis in the downregulated dataset after 3 h K^+ starvation (Fig. 4-4). As auxin is essential to the regulation of root growth and LR development (see Overvoorde *et al.*, 2010 for a review), its regulation in

response to low K^+ was investigated further. GO analysis as well as the plant reactome online tool (Naithani *et al.*, 2017) were used to identify genes involved in the auxin biosynthetic pathway, with both upregulation and downregulation of genes observed in response to K starvation (Fig. 4-10).

Despite IAA being discovered in the 1930s, its biosynthesis is still not fully understood. There is thought to be both tryptophan (Trp)-independent and -dependent pathways, of which the -dependent pathway has been much better characterized. There have been four proposed Trp-dependent routes to produce IAA: the YUCCA (YUC) pathway, the indole-3-pyruvic acid (IPA) pathway, the indole-3-acetamide (IAM) pathway and the indole-3-acetaldoxime (IAOx) pathway (Fig. 4-10A) (Mashiguchi *et al.*, 2011), with the YUC pathway recently identified as the main biosynthetic pathway in Arabidopsis (Mashiguchi *et al.*, 2011). As the main pathway, genes involved in the conversion of Trp to IAA via IPA (Fig. 4-10A) were sought in the RNA-Seq data. Data presented here identified a downregulation of the auxin biosynthesis gene *YUC8* (Hentrich *et al.*, 2013) after 3 h K^+ starvation. *YUC8* has also been shown to be highly expressed in the vasculature of young LRs (Hentrich *et al.*, 2013). As data in this thesis identified that LR growth is reduced under K^+ starvation, it could be hypothesised that this K^+ treatment could be causing a downregulation of *YUC8* in the young LRs, causing a local reduction in auxin biosynthesis and, therefore, a reduction in growth.

Gene expression changes were also identified in response to low K^+ in the IAOx auxin biosynthesis pathway (Fig. 4-10). Two cytochrome P450 genes involved in the conversion of Trp to IAOx (Zhao *et al.*, 2002) were downregulated after 3 h (*CYP79B3* & *CYP79B2*) (Fig. 4-10C). However, the most highly upregulated gene after the 30 h treatment (*CYP71A12*) (2.68 log_2fc) was identified by the plant reactome online analysis tool as acting in this pathway in the conversion of IAOx to indole-3- acetonitrile (IAN) (Fig. 4-10B). The IAOx pathway (which these genes are thought to be part of) has been suggested to be less important than other pathways in the biosynthesis of IAA, as IAN levels (Fig. 4-10A) have been shown to be more than 100-fold higher than IAA levels in Arabidopsis (Sugawara *et al.*, 2009), and overexpression of nitrilises, which hydrolyze IAN to IAA, does not lead to an increased auxin phenotype (Normanly *et al.*, 1997). The IAOx pathway has also been shown to be important in the production of defence related metabolites such as camalexin and indole glucosionlates (IGs) (Zhao *et al.*, 2002; Glawischnig *et al.*, 2004; Sugawara *et al.*, 2009; Sønderby *et al.*, 2010). As defence related genes exhibit significant changes in expression in response to low K^+, it is possible that gene expression changes in the IAOx pathway reflect a general stress response rather than a specific up- or downregulation of auxin biosynthesis. Further bioinformatic and literature based

investigation into the prominence of *CYP71A12* in the auxin biosynthesis pathway conducted here also suggests that this P450 is more involved with the production of camalexin as a pathogen defence mechanism (Müller *et al.*, 2015) rather than auxin biosynthesis.

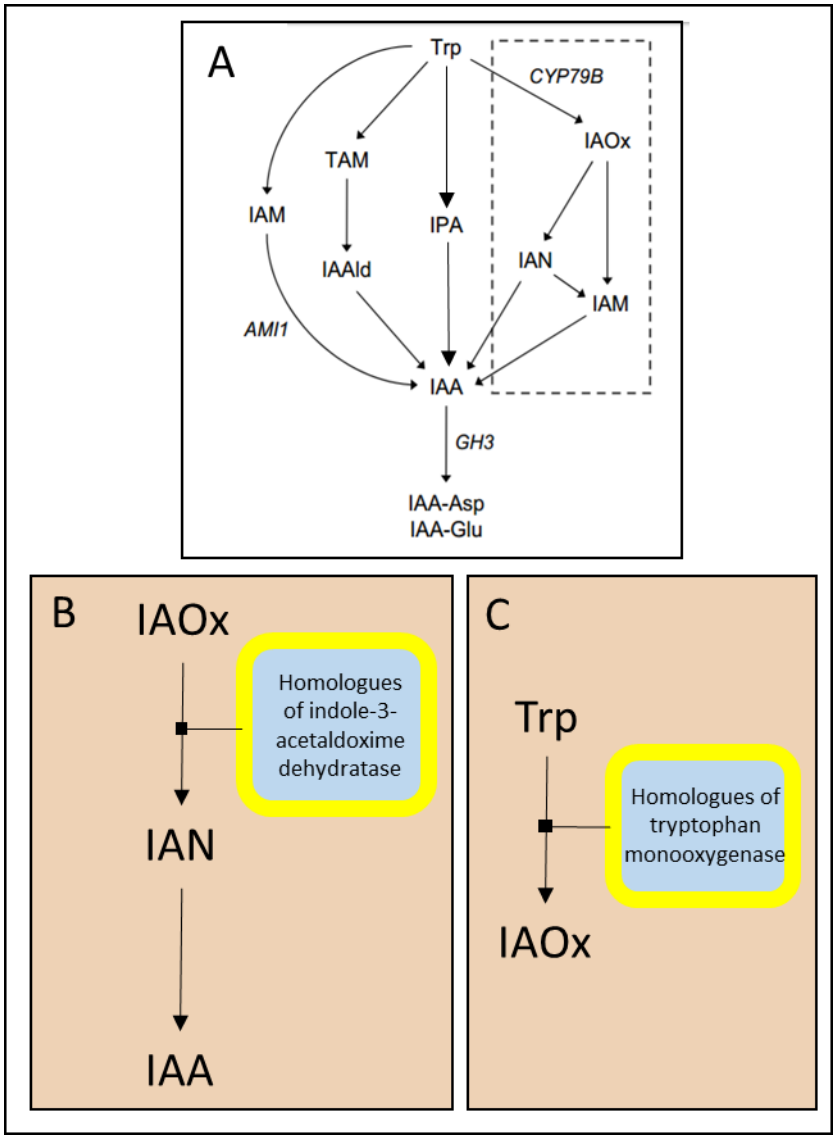

Fig. 4-10: (A) Main IAA biosynthesis pathway in plants, as proposed by Mashiguchi *et al.* (2011). Figure taken and adapted from Mashiguchi *et al.* (2011). The dotted square denotes the IAOx pathway. (B, C) Stylised image of the output from the plant reactome online analysis tool (Naithani *et al.,* 2017) from analysis of RNA-Seq data identifying which genes in the IAA biosynthetic pathway genes are transcriptionally changed in response to low K^+. (B) Yellow box shows where *CYP71A12* was identified in the IAA biosynthesis pathway, upregulated after 30 h K^+ starvation. (C) Yellow box shows where *CYP79B3 & CYP79B2* was identified in the IAA biosynthesis pathway, these genes were downregulated after 3 h K^+ starvation. Indole-3-acetaldoxime and Indole-3-acetonitrile refer to IAOx and IAN respectively in (A). (Further abbreviations see Mashiguchi *et al.* (2011).

4.5.1.2 Regulation of auxin signalling genes in response to low K^+

Due to the complex nature of the auxin biosynthesis expression data, a GO analysis was used to identify auxin-responsive genes, and to identify any evidence for a response to changes in auxin levels in response to low K^+. Once again genes associated with auxin signalling were both up- and downregulated. There was downregulation of a number of auxin-responsive genes (*Saur20, Saur24, Saur22, Saur63* and *IAA29*) after 3 h, however this downregulation was not seen after 30 h. The *IAA-METHYLTRANSFERASE-1 (IAMT1)* gene, which is known to play a role in auxin homeostasis in converting IAA into the non-polar inactive form of IAA, methyl-IAA (MeIAA) (Qin *et al.*, 2005; Li *et al.*, 2008), was also downregulated.

Auxin-responsive genes that were shown to be upregulated in response to K^+ starvation include, *PINOID BINDING PROTEIN 1 (PBP1)*, a calcium binding protein known to interact with PINOID (a key component of auxin signalling), and which is known to be upregulated by auxin (Benjamins *et al.*, 2003), was upregulated after 3 h (0.87 $\log_2$fc) and again, but to a lesser extent (0.64 $\log_2$fc), after 30 h. The genes encoding the BTB and TAZ domain proteins 2 and 5 (*BT2* and *BT5*) were upregulated after 3 h and 30 h, respectively, and these have also been linked to auxin responses. However, these genes are also known to be involved in responses to many abiotic and hormonal signals (Hammer *et al.*, 2009; Mandadi *et al.*, 2009; Canales *et al.*, 2014), making it difficult to link them directly to auxin in this case.

As auxin is essential for many processes in the plant, the auxin-related gene expression changes identified by the GO terms are likely to be involved in many different responses; these potentially range from perception of K^+ through to architectural changes, as well as in a general stress response throughout the whole plant. This wide involvement might explain why there seems to be contradictory up- and downregulation of genes here. Overall the data suggest that there are changes in the regulation of auxin in response to K^+ starvation, but significant additional work is needed in order to identify which pathways, and which parts of the plant, these changes are associated with.

4.5.2 Ethylene

4.5.2.1 Regulation of ethylene biosynthesis in response to low K^+

The hormone ethylene has been identified as a key hormone in the K^+-deprivation pathway, with evidence to suggest upregulation in response to low K^+ (Jung *et al.*, 2009), and downstream regulation of K^+ transporters and ROS (Jung *et al.*, 2009; Nam *et al.*, 2012). However, its role in the reduced LR phenotype has not been investigated; therefore, the RNA-Seq data were investigated here for evidence of ethylene-related transcriptional changes.

GO analysis showed enrichment, in the upregulated data, of a number of ethylene-related terms from the RNA-Seq data, including 'ethylene biosynthesis' (3 h and 30 h) (Figs 4-3, 4-5), 'ethylene-activated signalling pathway' (3 h), 'response to ethylene' (3 h and 30 h) and 'cellular response to ethylene' (30 h). Therefore, the transcriptional regulation of the ethylene biosynthesis pathway was investigated using the Plant reactome database. A key enzyme in the ethylene biosynthetic pathway (*1-AMINOCYCLOPROPANE-1-CARBOXYLIC ACID SYNTHASE 6* (*ACS6*)) (Fig. 4-11) was upregulated by 0.71 log_2fc after 3 h low K^+ treatment, suggesting that, if these transcript changes also represent protein activity, that ethylene biosynthesis is being upregulated within a very short time after the transfer to low K^+ (3 h). The expression of this biosynthesis gene, however, is not significantly different from the control conditions after 30 h, suggesting that the upregulation of ethylene is a very fast and transient reaction to low K^+ treatment.

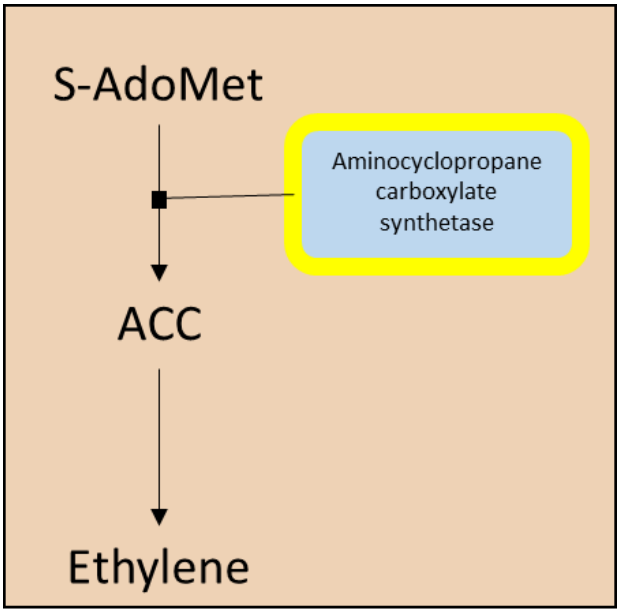

Fig. 4-11: Stylised image of the output from the plant reactome online analysis tool (Naithani *et al.,* 2017) from analysis of RNA-Seq data identifying which genes in the ethylene biosynthetic pathway are transcriptionally changed in response to low K^+. Yellow box shows where *ACS6* was identified in the ethylene biosynthesis pathway. *ACS6* was upregulated after 3 h K^+ starvation.

AGI	Gene name	3 h log_2fc	30 h log_2fc
AT1G05575	*AT1G05575*	0.92	0.83
AT1G18570	*MYB51*	0.73	0.52
AT1G21140	*VTL1*		0.65
AT1G26380	*FOX1*		1.32
AT1G27730	*STZ (ZAT10)*	0.83	0.79
AT1G71030	*MYB-like 2*		0.73
AT1G80840	*WRKY40*	1.11	1.29
AT2G26560	*PLP2*		0.65
AT2G38210	*PDX1L4*	0.52	
AT2G43000	*JUB1 (NAC42)*		1.33
AT3G04640	*AT3G04640*	0.50	0.56
AT3G12900	*MJM20.4*		2.00
AT3G14050	*RSH2*		0.61
AT3G15500	*NAC055 (NAC3)*	0.57	0.96
AT3G28580	*AT3G28580*	0.80	0.79
AT3G44260	*CAF1-9*	0.75	0.86
AT3G48850	*MPT2*		0.78
AT3G55980	*AtC3H47*	1.09	0.63
AT4G11280	*ACS6*	0.71	
AT4G17490	*ERF6*	0.93	0.84
AT4G17500	*ERF1A*		0.66
AT4G19690	*IRT1*		0.52
AT4G29780	*AT4G29780*	0.89	0.88
AT4G34710	*ADC2*		0.71
AT4G37370	*CYP81D8*		0.72
AT5G13080	*WRKY75*		0.74
AT5G22250	*CAF1B*		0.63
AT5G27420	*ATL31*	0.70	0.75
AT5G38900	*AT5G38900*		0.63
AT5G47220	*ERF2*		0.98
AT5G47230	*ERF5*	0.52	
AT5G54190	*PORA*		0.67
AT5G54490	*PBP1*	0.87	0.64
AT5G57220	*CYP81F*		0.64

Table 4-1: List of genes both upregulated by K^+ starvation (either after 3 h or 30 h, or both) and also identified by gene ontology (GO) analysis as relating to ethylene signalling (various GO terms associated with ethylene signalling collated together). Gene names obtained from TAIR.

4.5.2.2 Regulation of ethylene signalling genes in response to low K^+

A number of ethylene response factors (ERFs) known to be induced by ethylene treatment are also upregulated in response to K^+ starvation; *ETHYLENE-RESPONSIVE ELEMENT BINDING FACTOR ERF5* (3 h), *ETHYLENE-RESPONSIVE ELEMENT BINDING FACTOR 1* (*ERF1*) and *ETHYLENE-RESPONSIVE ELEMENT BINDING FACTOR 2* (*ERF2*) (30 h) (Table 4-1). The ERFs are known to be involved in ethylene signalling (Fujimoto *et al.*, 2000), however they can also act through ethylene independent pathways during abiotic stresses (Fujimoto *et al.*, 2000). Their altered expression is, therefore, not necessarily a clear indication of a downstream response regulated by ethylene. Other upregulated genes identified by the GO analysis as relating to ethylene signalling were several WRKY and NAC transcription factors (TFs) (Table 4-1). WRKY TFs, are generally associated with pathogen defence, but expression levels are known also to change upon hormone treatments (Chen & Chen, 2002; Xu, 2004; Zhang *et al.*, 2004; Xie *et al.*, 2006). NAC TFs have been identified as playing a role in the ethylene dependent salt stress signalling pathway (He *et al.*, 2005) as well as in many aspects of ethylene induced fruit ripening (Tigchelaar, 1978; Giovannoni, 2007; Shan *et al.*, 2012; Kou *et al.*, 2016).

4.5.2.3 Identification of downstream ethylene-related targets of transcription factors (TFs)

To look at the potential downstream ethylene targets of the TFs identified by agriGO which relate to ethylene signalling, the Agris AtTFDB- Arabidopsis transcription factor database was used (Davuluri *et al.*, 2003, Yilmaz *et al.*, 2011). Despite having ethylene-related GO terms, no interactions with ethylene-related genes were identified by Agris. Therefore, the search was expanded to look at all the highly upregulated TFs to search for possible TFs in the ethylene signalling cascade. This search identified *ORA47 (AT1G74930*), an AP2-EREBP TF (upregulated by 1.28 $\log_2$fc after 30 h K^+ starvation) as having 17 total direct interactions, many of which were hormone signalling related (Fig. 4-12). Of these interactions two ethylene genes were identified; *1-AMINO-CYCLOPROPANE-1-CARBOXYLATE SYNTHASE 8* (*ACS8*) and *CONSTITUTIVE TRIPLE RESPONSE 1* (*CTR1*). *ACS8* encodes an auxin inducible ACC synthase, and *CTR1* is a negative regulator of the ethylene signal transduction pathway, interacting with the putative ethylene receptors ETR1 and ERS (Clark *et al.*, 1998; Zhang *et al.,* 2017). The upregulation of *ORA47* may, therefore, lead to a downstream change in regulation of ethylene responses.

A

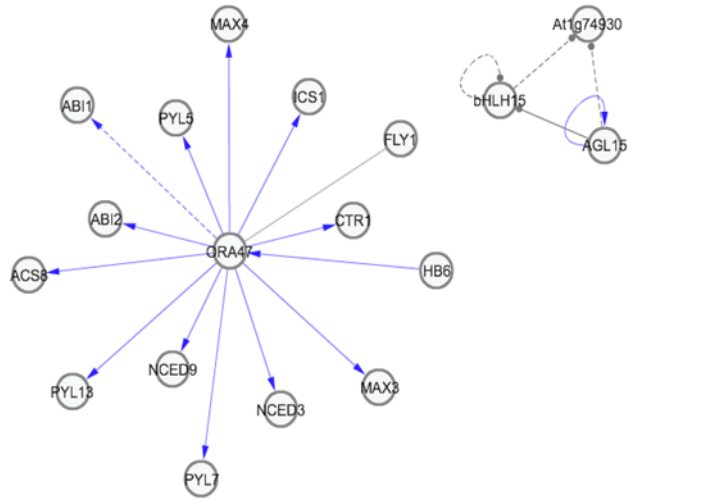

B

Gene name	AGI code	Function
HB6	*AT2G22430*	(HD-Zip I) protein that is a target of the protein phosphatase ABI1 and regulates hormone responses in Arabidopsis.
ABI1	*AT4G26080*	Involved in abscisic acid (ABA) signal transduction.
ABI2	*AT5G57050*	Encodes a protein phosphatase 2C and is involved in ABA signal transduction.
PYL5	*AT5G05440*	Encodes a member of the PYR/PYL/RCAR family of proteins which function as abscisic acid sensors.
PYL13	*AT4G18620*	Encodes a member of the PYR/PYL/RCAR family of proteins which function as abscisic acid sensors.
NCED9	*AT1G78390*	Encodes 9-cis-epoxycarotenoid dioxygenase, a key enzyme in the biosynthesis of abscisic acid.
PYL7	*AT4G01026*	Encodes a member of the PYR/PYL/RCAR family of proteins which function as abscisic acid sensors.
NCED3	*AT3G14440*	Encodes 9-cis-epoxycarotenoid dioxygenase, a key enzyme in the biosynthesis of abscisic acid.
ACS8	*AT4G37770*	Encodes an auxin inducible ACC synthase
CTR1	*AT5G03730*	Negative regulator in the ethylene signal transduction pathway. Interacts with the putative ethylene receptors ETR1 and ERS.

Fig. 4-12: (A) Output from Agris AtTFDB Arabidopsis transcription factor database (Davuluri *et al.*, 2003; Yilmaz *et al.*, 2011) identifying 17 total direct interactions between ORA47 (AT1G74930) and other proteins. *ORA47* an AP2-EREBP transcription factor upregulated by 1.28log_2fc after 30 h K^+ starvation. (B) Table of 10 of the genes identified as interactors with *ORA47* selected due to their known roles in ABA and ethylene signalling. Blue lines represent activation, red lines represent repression, grey lines are uncharacterized but proposed interactions.

In conclusion, RNA-Seq data suggests that ethylene biosynthesis is rapidly and transiently upregulated in response to K^+ starvation and there is evidence to suggest that there are changes in the ethylene signalling pathway. This upregulation of ethylene following K^+ starvation fits with previously published data suggesting that ethylene is involved in the primary response to K^+ deprivation, acting in the upregulation of the high affinity K^+ transporter HAK5 (Jung *et al.*, 2009). However, the role of ethylene in the reduced LR phenotype in response to K^+ starvation has not been investigated. Increased ethylene biosynthesis and activation of TFs could act high up in a cascade to change LR morphology, thereby increasing the K^+ scavenging potential. Further experimental work is needed in order to investigate a role for ethylene in the change in architecture, seen in response to low K^+.

4.5.3 Gibberellin

When investigating the interactions of TFs in the role of ethylene signalling, several pieces of evidence suggested that gibberellin (GA) may be playing a role in the K^+-signalling pathway which was not initially identified by GO analysis. For example, the majority of the upregulated TFs associated with ethylene GO terms had interactions with AGL15 (uncharacterised interactions, only suggested through identification of targets using chromatin immunoprecipitation (ChIP)) (Zheng *et al.*, 2009). AGL15 is known to directly regulate the expression of *GA2ox6*, an enzyme involved in GA catabolism (Wang *et al.*, 2004). The TF *ERF6*, which is transcriptionally upregulated strongly at both 3 h and 30 h has also been suggested to activate *GA2ox6* (Dubois *et al.*, 2015). These data suggest that GA levels could be altered in low K^+ stress.

Further evidence that this might be the case comes from data on the NAC TF (NAC42/JUB1). Although identified by GO analysis as being involved in ethylene signalling (Table 4-1), the analysis also suggested that JUB1 might be involved in the regulation of GA. The Agris AtTFDB (Arabidopsis TF database) suggested that JUB1 interacts with a number of gibberellin-related genes (Fig. 4-13). For example, JUB1 is known to repress *GIBBERELLIN 3 BETA-HYDROXYLASE 1* (*GA3ox1*) (Fig. 4-13), a gene involved in the later steps of the gibberellic acid biosynthetic pathway. JUB1 is also suggested to activate the negative regulators of GA responses, *RGL1* and *GAI* (Fig. 4-13). Both encode members of the DELLA family of proteins that are known to restrain cell proliferation and expansion (from DAVID) (see Achard & Genschik, 2009 for a review). A GA biosynthesis gene *GIBBERELLIN-3-OXIDASE 2* (*GA3ox2*) was also found to be downregulated after 30 h K^+ starvation (-0.51 $\log_2$fc). These data suggest that after 30 h there

is a downregulation of a GA biosynthesis gene and the potential upregulation of TFs involved in the activation of GA degradation and, therefore, reduced GA signalling. This suggests that there may be activation of GA signalling, specifically through reduction in the levels of GA, which could result in the stabilisation of DELLA proteins that might lead to the reduced elongation of LRs in response to low K^+.

A

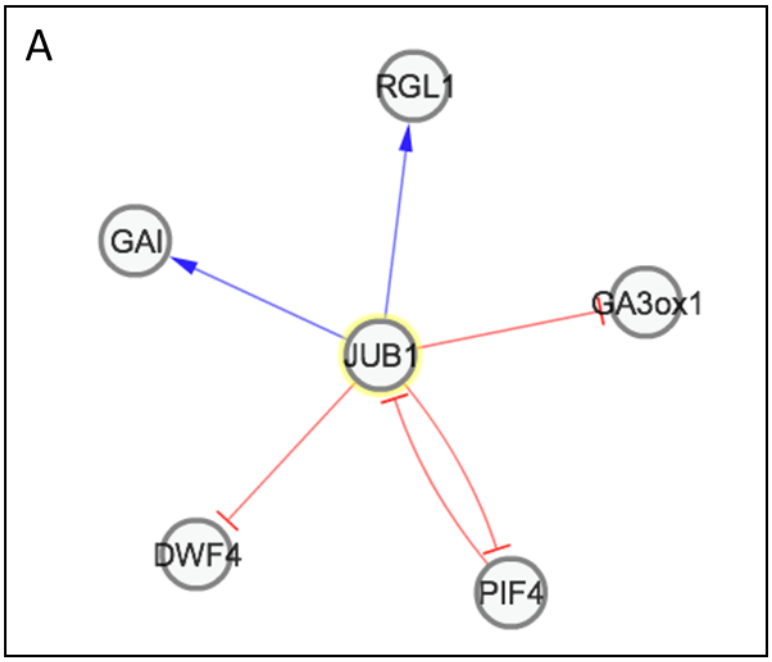

B

Gene name	AGI code	Function
GA3ox1	*AT1G15550*	Involved in later steps of the gibberellic acid (GA) biosynthetic pathway
RGL1	*AT1G66350*	Negative regulator of GA responses and a member of the DELLA proteins that restrain the cell proliferation and expansion that drives plant growth.
GAI	*AT1G14920*	Negative regulator of GA responses and a member of the DELLA proteins that restrain the cell proliferation and expansion that drives plant growth

Fig. 4-13: (A) Output from Agris AtTFDB Arabidopsis transcription factor database (Davuluri *et al.,* 2003; Yilmaz *et al.*, 2011) identifying interactions between JUB1 (NAC42) (AT2G43000) and other proteins. *JUB1* is a H_2O_2 induced NAC transcription factor upregulated by 1.33log_2fc after 30 h K^+ starvation. (B) Table of three of the genes identified as interactors with *JUB1* selected due to their known roles in gibberellin signalling. Blue lines represent activation, red lines represent repression, grey lines are uncharacterized but proposed interactions.

4.5.4 ABA

The TF ORA47 (previously mentioned in relation to ethylene; upregulated by 1.28 log_2fc after 30 h) was also identified as activating a suite of genes involved in ABA signalling, (Fig. 4-12). This suite includes key enzymes in the ABA biosynthesis pathway, NCED9 and NCED3, and members of the PYR/PYL/RCAR family of proteins that have been shown to act as ABA receptors (PYL5, PYL13 and PYL7) (Fig. 4-12) (Ma *et al.*, 2009; Park *et al.*, 2009; Cutler *et al.*, 2010). Two protein phosphatases (PP2Cs) ABI1 and ABI2, which bind to the PYR/PYL/RCAR receptors (Fig. 4-12), and which act as inhibitors of ABA responses (Fujii *et al.*, 2009; Ma *et al.*, 2009; Park *et al.*, 2009) were also identified. A negative regulator of ABA signalling HB6, which acts downstream of ABI1 (Himmelbach *et al.*, 2002) was also identified. However, searches within my data using online tools such as agriGO and Plant reactome did not identify any key components of the ABA-biosynthesis or signalling pathways. This could suggest that the ORA47 TF could be the first in the signalling pathway to stimulate the ABA genes, and that later timepoints after K^+ starvation may see an increase in ABA signalling. Alternatively, it could be that the ABA pathway is not involved in the developmental response to K^+ deficiency.

4.5.5 Reactive oxygen species (ROS)

An increase in ROS after 6 h K^+ starvation has previously been reported and this is associated with an upregulation of the *HAK5* potassium transporter (Jung *et al.*, 2009). However, due to the many different roles that ROS plays in response to abiotic and biotic stresses it is possible that ROS may be functioning in a number of different ways in response to low K^+. The GO treemaps identified ROS/H_2O_2/O_2 metabolism in both of the upregulated DEG data sets (Figs 4-3, 4-5). However, because ROS signalling is involved in many different responses, many genes were identified, which makes interpretation of the data complex. A significant amount of work has been carried out to elucidate pathways of ROS production and scavenging within the plant. Therefore, in order to investigate if there is imbalance in the equilibrium between production and scavenging, these documented pathways were investigated within the RNA-Seq data.

4.5.5.1 Transcriptomic changes in ROS production in response to K^+ starvation

Previous reports have categorised ROS accumulation from three major sources: metabolic background ROS – produced through metabolic processes such as photosynthesis and respiration; ROS produced through metabolic imbalances – caused by changes in environmental conditions; and active ROS production – regulated by specific ROS producing enzymes (see Vaahtera *et al.*, 2013 for a review). Of these categories, active ROS is the easiest to investigate using gene expression data. GO analysis identified 'regulation of H_2O_2 metabolism' as being significantly upregulated at 3 h and 30 h (Figs 4-3,4-5), suggesting an

increase in ROS might be a response to low K^+. However, none of the key ROS producing RBOH genes was up- or downregulated in either of the data sets. Nevertheless, three of the 'NADPH oxidase-like' genes identified in a list of the main ROS genes (Mittler *et al.*, 2004) were upregulated in response to K^+ starvation (*FRO2, FRO3* and *FRO5*). However, there have been no reports that link the *FRO* genes to ROS production, and so their possible role in the low K^+ response remains unclear.

4.5.5.2 Transcriptomic changes in ROS scavenging in response to K^+ starvation

As ROS levels in the plant are regulated through a balance between production and scavenging, the levels of scavenging activity were then investigated in the data. A list of all the main ROS-scavenging genes were taken from Mittler *et al.* (2004), and were compared with the low K^+ RNA-Seq data set. Eight ROS scavenging genes were downregulated in response to low K^+, whereas only three were upregulated (Fig. 4-14A). Once again, due to the complex nature of the ROS production and scavenging system it is difficult to form a clear idea of ROS levels in the plants by simply looking at changes in gene expression of production and scavenging genes.

4.5.5.3 Transcriptomic changes in ROS-responsive genes in response to K^+ starvation

Another way to investigate whether there are changes in ROS levels in the plant is by looking further down the signalling pathway. Gadjev *et al.* (2006) created a transcriptomic footprint by comparing gene expression changes after treatment with different kinds of ROS stress. By comparing this list with the low K^+ data obtained here it was possible to investigate if specific ROS-signalling pathways may be stimulated in response to low K^+ (Fig. 4-14B). The *AT2G43510* gene (upregulated by 1.14 $\log_2$fc after 30 h K^+ starvation) was identified as one of the 'hallmarks for general oxidative stress' from the ROS footprint data, as it was upregulated by more than 5-fold in at least 7 of the 8 experiments described by Gadjev *et al.* (2006). 14 genes upregulated after 3 h and 21 after 30 h were also identified from the ROS footprint data as being upregulated by over 5-fold in at least three of the ROS experiments (Fig. 4-14B) (Full list with expression data in Appendix V). Only the *AT2G29460* gene was identified from the ROS footprint data as being downregulated in the K^+ deprivation RNA-Seq data.

A

AGI code	Log_2fc after 3 h low K^+	Log_2fc after 30 h low K^+	Enzyme family
AT3G62930	0.81		Glutaredoxin family
AT5G14070	0.82		Glutaredoxin family
AT5G20230		0.62	Blue copper binding protein
AT1G19570	-0.50		Dehydroascorbate Reductase (DHAR5)
AT2G40300		-0.99	Ferritin-4, chloroplastic
AT3G56090		-0.59	Ferritin-3, chloroplastic; Ferritin
AT4G25100		-0.74	Superoxide dismutase [Fe], chloroplastic; Superoxide dismutase
AT4G35090		-0.55	Catalase-2; Catalase
AT5G01600		-1.76	Ferritin-1, chloroplastic; Ferritin
AT5G14070		-0.62	Glutaredoxin-C8
AT5G18600		-0.98	Monothiol glutaredoxin-S2

B

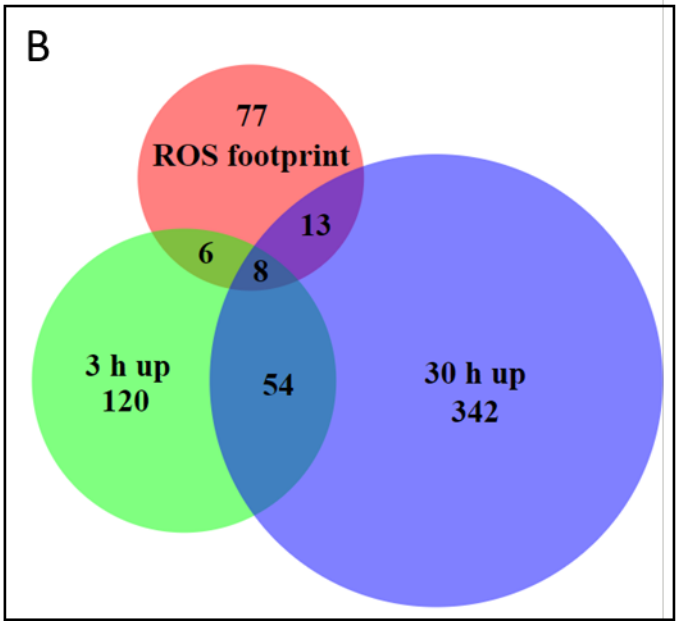

Fig. 4-14: (A) List of genes that act as reactive oxygen species (ROS) scavengers identified in the RNA-Seq data of differentially expressed genes in response to low K^+ after 3 h and 30 h. Log_2fc identified with *P*-value <0.05. List of scavenging genes from Mittler *et al.* (2004). (B) Output from BioVenn online tool (Hulsen *et al.,* 2008) used to identify common genes between genes upregulated in response to 3 h or 30 h K^+ starvation (RNA-Seq data) and genes identified as a ROS transcriptomic footprint (Gadjev *et al.,* 2006). Gene list (Appendix V).

The genes identified in the ROS transcriptomic footprint data have been suggested to respond to oxidative cellular damage (Gadjev *et al.,* 2006), and with a large number also being upregulated in the dataset described here, it suggests that there may be elevated ROS responses to low K^+. Levels of ROS in the plant reflect the balance between production and scavenging. However, with so many different types of ROS, and so many different means of

production, gene expression changes in production, scavenging or ROS-responsive genes cannot alone give a clear picture of the levels and the response to low K^+. However, the overrepresentation of GO terms relating to ROS metabolism, a larger number of downregulated scavenging genes and upregulation of ROS-responsive genes, shown here might suggest that there is an increase in cellular levels of ROS in response to low K^+. In order to understand the role that ROS may be playing in response to low K^+, it is important to investigate further experimentally, and experiments are described in Chapter 5.

4.6 Summary

Work in this chapter has aimed to better understand the gene expression changes that occur in response to low K^+ in the Arabidopsis accession Col-0. In order to do this, an RNA-Seq experiment was carried out and DEGs were identified between the low K^+ and the control at two different timepoints after treatment (3 h and 30 h). GO analysis was utilised to provide a general overview of the data. Other bioinformatics tools and literature searches were used to further investigate the data. As the aim of the thesis is to understand the regulation of the architectural changes to low K^+, the work in this chapter focussed on elucidating the possible regulation of hormonal signalling pathways, and other factors (such as ROS), which would be affecting the reduction in LR growth in response to low K^+.

Data from the RNA-Seq experiment suggested that, in response to low K^+, there are; changes in the regulation of auxin, a rapid and transient upregulation of ethylene biosynthesis, and changes in the ethylene signalling pathway. It was also suggested that there are changes in GA signalling, specifically through reduction in the levels of GA, in response to low K^+. Potentially there is a change in ABA signalling, and changes in the regulation and signalling of ROS levels. Data in this chapter also suggested that there is an overlap in transcript profiles between low K^+ and iron signalling, as well as showing that, in response to low K^+, a number of photosynthetic genes are downregulated, suggesting that a reduction in photosynthesis in response to low K^+ may be mediated, in part, by regulation of gene transcription.

Chapter 5 Hormonal control of lateral root growth in response to low K^+

5.1 Introduction

The previous chapter described the use of transcriptomic data to identify gene expression changes in response to low K^+. Bioinformatic analysis identified gene expression changes which suggested that in response to low K^+ there were changes in ethylene, auxin, abscisic acid (ABA), reactive oxygen species (ROS) and gibberellic acid (GA) signalling (including metabolism of these stimuli). Changes in each of these pathways have been shown to lead to changes in root growth and development, however little work has been carried to link any of these factors to changes in root architecture in response to low K^+. Collation of data from chapter 4, and from the published literature has allowed the construction of (Fig. 5-1) showing pathways hypothesised to lead to reduced lateral root (LR) growth in response to low K^+. Experimental work described in this chapter aimed to investigate the roles of each of these factors in the reduced LR growth phenotype displayed in Col-0 in response to low K^+.

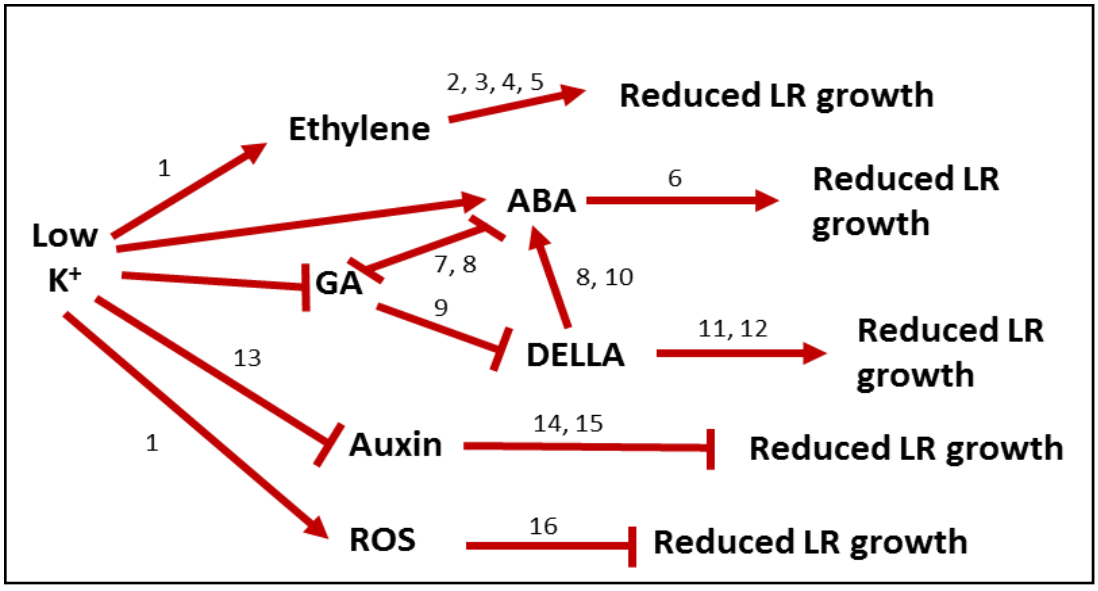

Fig. 5-1: Pathways hypothesised to lead to reduced lateral root (LR) growth in response to low K^+. Hypothesised routes generated from data from Chapter 4 (RNA-Seq experiment) and previously published literature (numbers), linking changes in hormonal signalling to changes in growth. Arrows, hypothesised positive interaction; T-bars, inhibition or a negative relationship. ABA, abscisic acid; GA, gibberellic acid; ROS, reactive oxygen species. Numbers refer to published literature: 1, Shin & Schachtman (2004); 2, Ruzicka *et al.* (2007); 3, Swarup *et al.* (2007); 4, Strader *et al.* (2010); 5, Street *et al.* (2015); 6, De Smet *et al.* (2003); 7, Achard *et al.* (2006); 8, Zentella *et al.* (2007); 9, Sun (2010); 10, Ko *et al.*, (2006); 11, de Lucas *et al.* (2008); 12, Feng *et al.* (2008); 13, Shin *et al.* (2007); 14, Dello Ioio *et al.* (2008); 15, Perrot-Rechenmann (2010); 16, Tsukagoshi *et al.* (2010).

In the work described in this chapter, the use of mutants and phytohormones was a means to manipulate signalling pathways, allowing investigation into their roles in the root architectural response. Gene expression was analysed using qRT-PCR in order to further the transcriptional information uncovered using RNA-Seq. Confocal and stereo microscopy were employed to reveal localization and expression levels of different signalling components in response to low K^+. Together these techniques were used to shed light on the mechanisms that may lead to the reduced LR growth seen in response to low K^+.

5.2 Auxin

Analysis of the RNA-Seq data suggests that there may be changes in auxin signalling and biosynthesis in response to K^+ starvation. The data were not conclusive however, as genes associated with the biosynthesis and signalling pathways were found to be both up- and down-regulated in response to low K^+. Shin *et al.* (2007) identified a reduction in the concentration of free IAA and a reduction in basipetal auxin transport in the roots of seedlings subjected to K^+-stressed conditions. This result suggests that a reduction in auxin may play a role in the root architectural responses to low K^+. Research in this chapter aims to further understand the role of auxin in the LR growth response to K^+ starvation.

5.2.1 Expression of *IAA2* is unchanged in response to K^+ starvation

INDOLE-3-ACETIC ACID INDUCIBLE 2 (IAA2) is upregulated in response to auxin (Lee *et al.*, 2009) therefore its expression level was investigated following low K^+ treatment using qRT-PCR. After 72 h K^+ starvation there was no difference in the expression levels of *IAA2* between the low K^+ and the control (Fig. 5-2). This suggests that auxin signalling levels are not significantly reduced in response to low K^+. It must also be noted however, that both the qRT-PCR and RNA-Seq experiments were carried out on whole seedling tissue, therefore it is not possible to identify localized changes in auxin signalling or accumulation through this method.

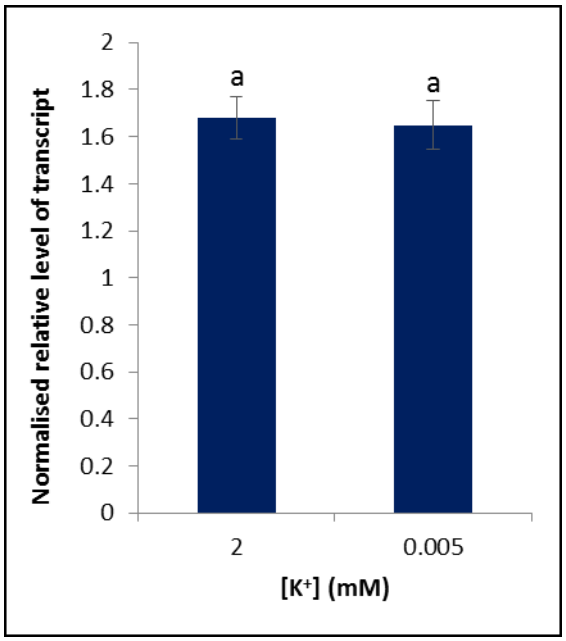

Fig. 5-2: Normalised relative level of transcript of *IAA2* after 72 h K^+ treatment (2 mM or 0.005 mM) determined by qRT- PCR. Samples taken from seedlings 14 days after germination. Normalised against *AT1G13320.* Values are means ± SE. Three biological repeats and three technical repeats used. Independent samples *t*-test determined there was no significant difference between treatments, as denoted by letters (*P*-value <0.05).

5.2.2 Auxin distribution and levels in LR meristems are unaffected by low K^+

The setting up and maintenance of an auxin maximum at the root tip is essential for root growth and development. A reduction in auxin signalling in the primary root (PR) meristem has been shown to reduce cell proliferation and promote early exit from the mitotic cell cycle (Blilou *et al.*, 2005; Dello Ioio *et al.*, 2008; Ishida *et al.*, 2010; Moubayidin *et al.*, 2010). It was hypothesised that a reduction in auxin reduces cell division in the LR meristem in response to low K^+, thereby reducing meristem size and growth. It is possible to visualize auxin levels and distribution in the root using confocal microscopy imaging of the auxin-responsive *pDR5rev* promoter fused to three tandem copies of a rapidly folding YFP, VENUS (Heisler *et al.*, 2005). No differences in the distribution of auxin (Fig. 5-3A), or level of fluorescence (Fig. 5-3B) were identified between high or low K^+ conditions (2 mM or 0.005 mM) in the LR meristems of the *pDR5rev::3xVENUS-N7* line after 8 d treatment (Fig. 5-3). This suggests that the auxin maxima are being maintained at the LR tips even under low K^+ treatment, and that there are no visible changes in accumulation patterns or levels after 8 d low K^+ treatment.

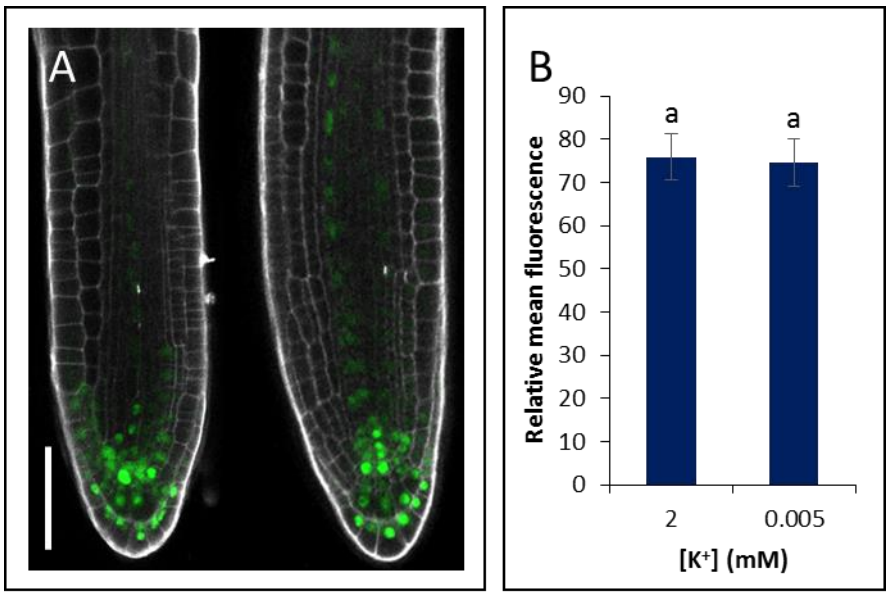

Fig. 5-3: (A) Representative fluorescence in lateral roots (LRs) under 1 mm in length of *pDR5rev::3xVENUS-N7 se*edlings after 4 d growth on ½ MS10 followed by 8 d grown on 2 mM (left) or 0.005 mM (right) [K^+] Scale bar = 50 µm. White is propidium iodide stain, green is VENUS. (B) Relative mean fluorescence of LRs of each treatment measured using ImageJ. Images taken from at least 8 different seedlings per treatment, $n \geq 14$ (*n* denotes number of LRs). Values are means ± SE. Letters indicate significance as calculated with an independent samples *t* test $P=0.159$.

5.2.3 Addition of IAA and NPA are not able to restore LR growth under low K^+

The role of auxin in the LR phenotype was further investigated by supplementing the media with exogenous auxin in the form of IAA, and blocking auxin transport by supplementing the media with NPA. It was hypothesised that if a decrease in auxin was causing a reduction in LR growth in response to low K^+, then the addition of IAA to the media might restore LR growth. If the transport of auxin plays a key role in the reduced LR growth phenotype, then blocking transport with NPA should restore growth.

LR growth was not restored under low K^+ when the media was supplemented with 1 nM IAA, or 5 nM IAA over 3 d (Fig. 5-4A), or 10 nM IAA or 10 µM NPA over 10 d (Fig. 5-4B). 1 µM IAA supplementation also did not alter the distribution of developmental stages seen in a LR progression analysis (Fig. 5-4C) on the basis of using the *DR5::GUS* reporter to highlight LR primordia (LRP). Results show that addition of IAA does not alter LR development under low K^+ when compared with the non-supplemented media (Fig. 3-4; Fig. 5-4C). LR elongation is still impaired under low K^+ conditions after supplementing with IAA, and LRP development remains the same between K^+ conditions throughout (Fig. 5-4C). LR growth was also not restored in the *aux1-7* mutant (Fig. 5-5), suggesting that enhanced auxin transport is not playing an important role in the reduced LR growth response to low K^+.

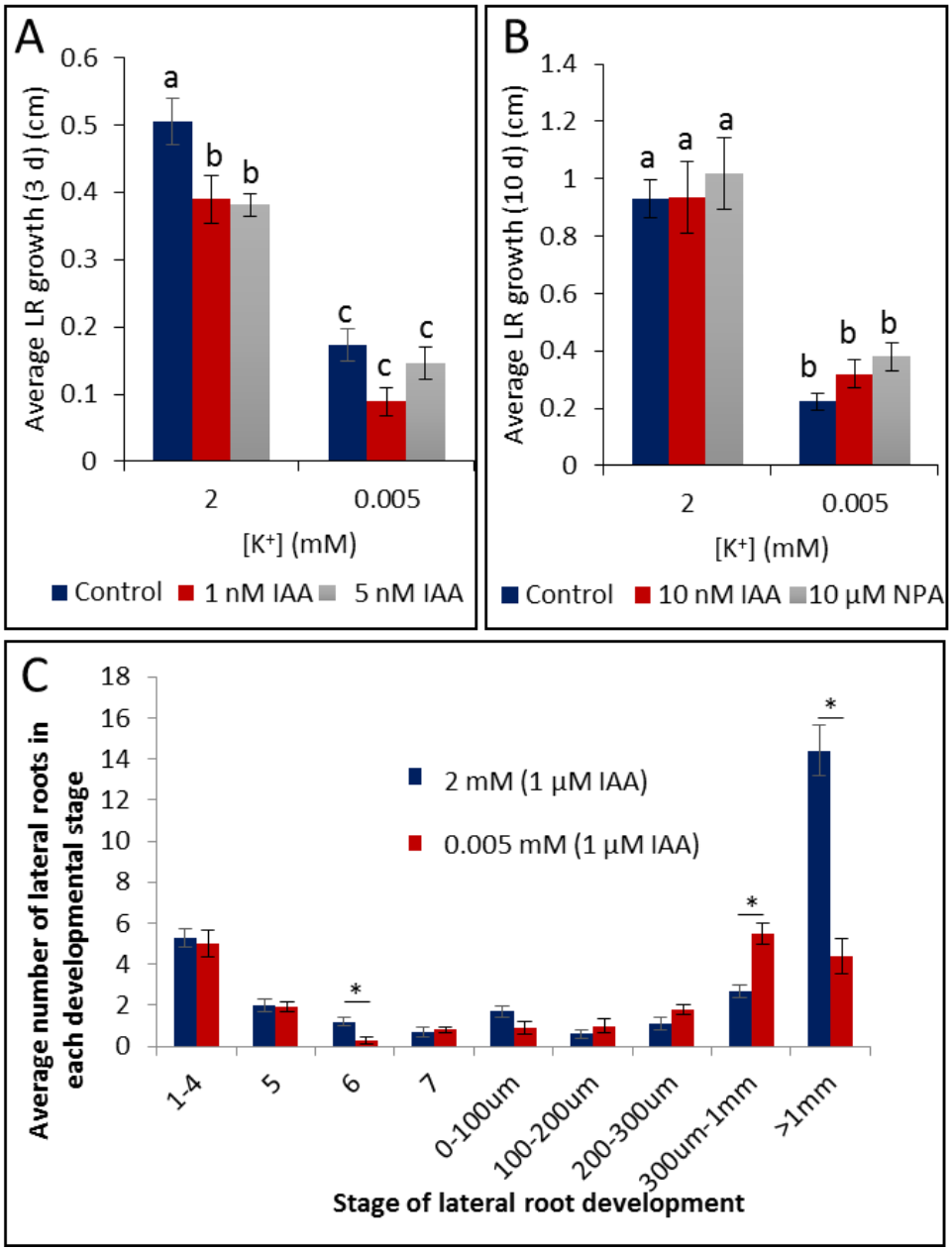

Fig. 5-4: (A) Average lateral root (LR) growth over 3 d following [K^+] treatment (2 mM or 0.005 mM), 12 days after germination (DAG). (B) Average LR length after 10 d treatment, 19 DAG. Values are averages of at least 8 individual seedlings per sample, ± SE. Letters indicate significance with a Tukey Pairwise comparison $P< 0.05$. (C) Light microscopy and the auxin-responsive *DR5::GUS* reporter line allow all lateral root primordia (LRP) and LRs to be counted along the length of the primary root (PR). Col-0 seedlings analysed at 12 DAG, 8 d of K^+ treatment. Primordial stages as defined in Malamy & Benfey (1997). Media supplemented with 1 µM IAA. Values are averages of at least 10 individual seedlings per sample ± SE. Asterisks indicate significance with independent samples *t* test *(P*-value <0.05).

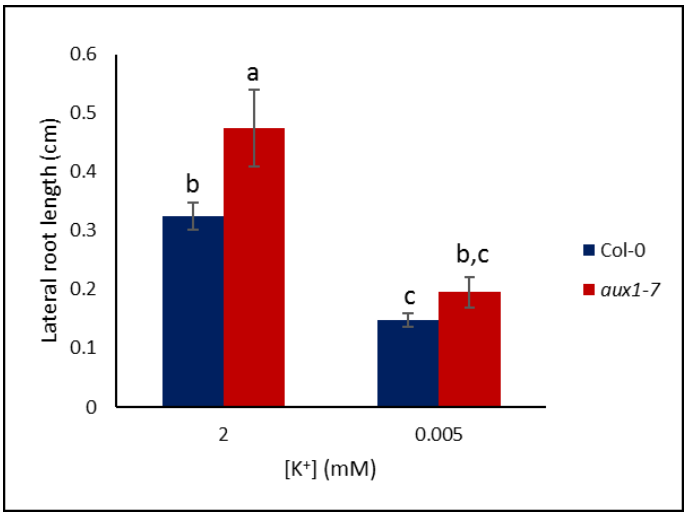

Fig. 5-5: Average lateral root growth after 8 d K^+ treatment (2 mM or 0.005 mM), (12 d after germination (DAG) seedlings) of Col-0 and auxin mutant *aux1-7.* Values are averages of at least 25 individual seedlings ± SE, $n \geq 25$. Letters indicate significance with a Tukey Pairwise comparison $P < 0.05$.

5.2.4 Addition of IAA does not restore LR meristem size under low K^+

The effect of auxin supplementation on cell division and meristem size was also investigated. The *CYCB1;2:GUS* line was used to identify cells undergoing cell division in the meristems of LRs grown on high and low K^+ for 8 d. The length of the area of cell division was measured to give a proxy measurement of meristem size. Addition of 1 nM or 200 nM IAA made no difference to the length of the LR meristems when compared with the control (Fig. 5-6). These results suggest that a decrease in auxin does not cause the reduction in cell division and meristem size in response to low K^+.

5.2.5 Auxin summary

Collectively these data suggest that auxin does not play a role in the reduced LR growth phenotype in response to low K^+, despite the observed changes in gene expression seen in the RNA-Seq data. As the RNA-Seq data represented transcript analysis for whole seedlings, an up- or down-regulation in auxin could be acting elsewhere in the plant in other K^+-deprivation strategies. In conclusion, the evidence presented here suggests no clear role for auxin in the response of root development to low K^+.

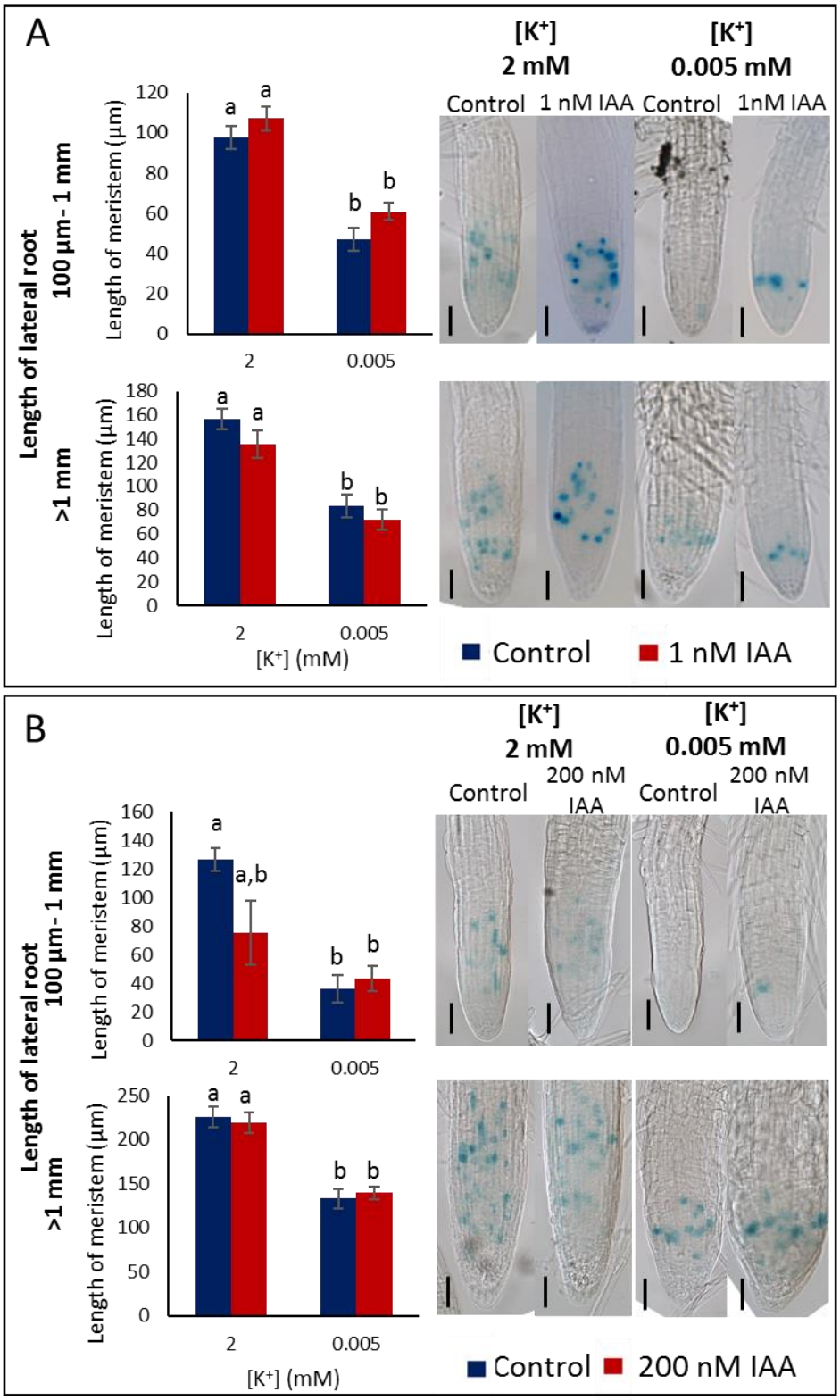

Fig. 5-6: Typical GUS staining pattern of *CYCB1;2:GUS*; the staining shows a reduced area of cell division in low [K^+]. Scale bars = 50 µM. Average length of meristem measured as the length of area with dividing cells (stained blue in *CYCB1;2:GUS* line). Media supplemented with either 1 nM IAA (A), or 200 nM IAA (B) for 8 d. Analysis carried out on seedlings 12 d after germination (DAG). Values in histograms are averages of measurements taken from at least 6 individual seedlings per treatment ± SE, Letters indicate significance with a Tukey Pairwise comparison $P < 0.05$.

5.3 Ethylene

RNA-Seq data showed that in response to low K^+ there was an upregulation of ethylene biosynthesis genes and ethylene signalling genes. This suggested that ethylene may be playing a role in the response to low K^+. Previous work has reported increased ethylene levels in plants starved of K^+ (Shin & Schachtman, 2004), and a key role for ethylene in K^+-stress tolerance has been identified in inducing the high affinity K^+ transporter *HAK5* (Jung *et al.*, 2009). There has been less work on investigating whether there is a role for ethylene in the architectural changes to low K^+. Jung *et al.* (2009) suggested a role for ethylene in the reduced PR growth in response to low K^+; however, this work only looked at ethylene signalling mutants, and further investigation into the mechanism by which ethylene acts was not followed up. The experiments reported here were designed to investigate whether there was a role for ethylene in reducing LR growth in response to low K^+.

5.3.1 Ethylene signalling is increased in response to low K^+

As the RNA-Seq analysis was carried out after short time periods of K^+ starvation (3 h and 30 h), qRT-PCR was used to investigate ethylene signalling after a longer period of low K^+ treatment. RNA was extracted for qRT-PCR analysis from 14-d-old-seedlings, grown for 72 h on 2 mM or 0.005 mM K^+. The expression of *ETHYLENE RESPONSE FACTOR 1* (*ERF1*) was significantly higher in seedlings grown on low K^+ for 72 h, compared with the high K^+ conditions (Fig. 5-7). *ERF1* is one of the immediate targets of EIN3 (Solano *et al.*, 1998) and has been shown to be highly induced by high salt and drought stress (Cheng *et al.*, 2013). The strong upregulation of *ERF1* after 72 h (Fig. 5-7) suggests a continued stimulation of the ethylene signalling pathway even after 3 d K^+ starvation.

It is important to note that the *ERF1* gene can also be rapidly activated by jasmonate (JA) (Lorenzo *et al.*, 2003). It is therefore possible that this upregulation of *ERF1* is, in part, due to increased JA in response to low K^+ (Fig. 4-7) (Armengaud *et al.*, 2004). Taken together with previously published data, and RNA-Seq data (Chapter 4), there is a compelling case for a rapid increase in ethylene biosynthesis followed by a prolonged increase in ethylene signalling in response to low K^+.

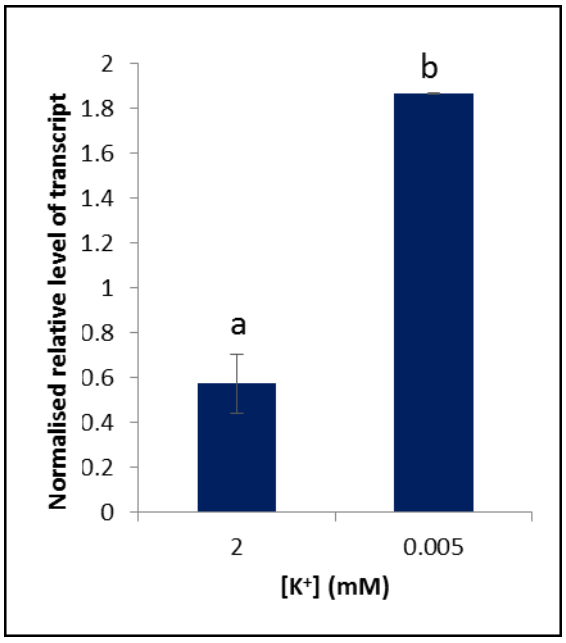

Fig. 5-7: Normalised relative level of transcript of *ERF1* after 72 h K^+ treatment (2 mM or 0.005 mM [K^+]). Samples taken from seedlings 14 days after germination Determined by qRT-PCR. Normalised against *AT1G13320.* Values are means ± SE. Three biological repeats and three technical repeats used. Letters indicate significance with independent samples *t* test (*P*-value <0.05).

5.3.2 Role of ethylene in LR growth in response to low K^+

Ethylene is known to inhibit root growth in both auxin dependent and independent ways. Ethylene is known to increase biosynthesis and transport of auxin leading to inhibition of cell elongation and cell proliferation (Ruzicka *et al.*, 2007; Swarup *et al.*, 2007; Strader *et al.*, 2010; Street *et al.*, 2015). Ethylene is also thought to regulate cell proliferation at the root meristem in an auxin-independent way, whereby ethylene treatment reduces cell proliferation and reduces meristem size in the PR (Street *et al.*, 2015). Work in this thesis has identified a similar response in the LRs of seedlings grown on low K^+, which display reduced cell division and meristem size. It was therefore hypothesised that an increase in ethylene signalling in response to low K^+ could lead to the reduced growth of LRs.

It is possible to investigate the role of ethylene in plant responses by blocking signalling and perception. This can be done using the ethylene-insensitive mutants *ein2* and *etr1-1* (Guzmán & Ecker, 1990; Chang *et al.*, 1993), and with silver ions (Ag^{2+}), which block the activity of the ethylene receptor complex (Rodriguez *et al.*, 1999). To investigate how increased ethylene signalling and biosynthesis might affect LR growth in response to low K^+, a LR progression analysis was used to count the LRs and lateral root primordia (LRP) at each stage of development when ethylene was blocked in the *ein2* mutant (Fig. 5-8B) and by using Ag^{2+} (Fig.

5-8A) to block ethylene perception. Analysis of seedlings was conducted on Col-0 or *ein2* seedlings 12 d after germination (DAG), after a total of 8 d growth on K^+ treatment (2 mM or 0.005 mM). The growth medium of the Col-0 seedlings was supplemented with 1 µM Ag^{2+}. In the WT with no supplementation, there was no difference in the numbers of LRs and LRP present in each developmental stage between high and low K^+ conditions until after the LR has emerged from the primary root (PR) (Fig. 3-4). After emergence LRs under low K^+ do not elongate to the same extent as they do under high K^+ conditions. This translates to a larger number of LRs in the length categories from 100 µm to 1 mm, and more LRs in the high K^+ are longer than 1 mm (Fig. 3-4). When ethylene signalling is blocked, either in the *ein2* mutant, or by supplementing the media with (1 µM) Ag^{2+}, this pattern is not altered, again displaying a larger number of LRs elongating past 1 mm in the high [K^+] compared with the low [K^+] (Fig. 5-8A,B). This suggests that ethylene is not playing a role in reducing LR growth in response to low K^+. To investigate this further, LR length was measured in the mutants *ein2* and *etr1-1* after 8 d growth on low K^+. No difference was observed in the length of LRs on low K^+ compared with the WT (Fig. 5-9).

5.3.3 Ethylene summary

These data suggest that there is an increase in ethylene signalling in response to low K^+. However, blocking ethylene signalling through gene mutation, or supplementing the media with silver ions, was not able to rescue LR growth under low K^+ conditions. This suggests that that reduced LR growth in response to low K^+ is coordinated through an ethylene-independent mechanism.

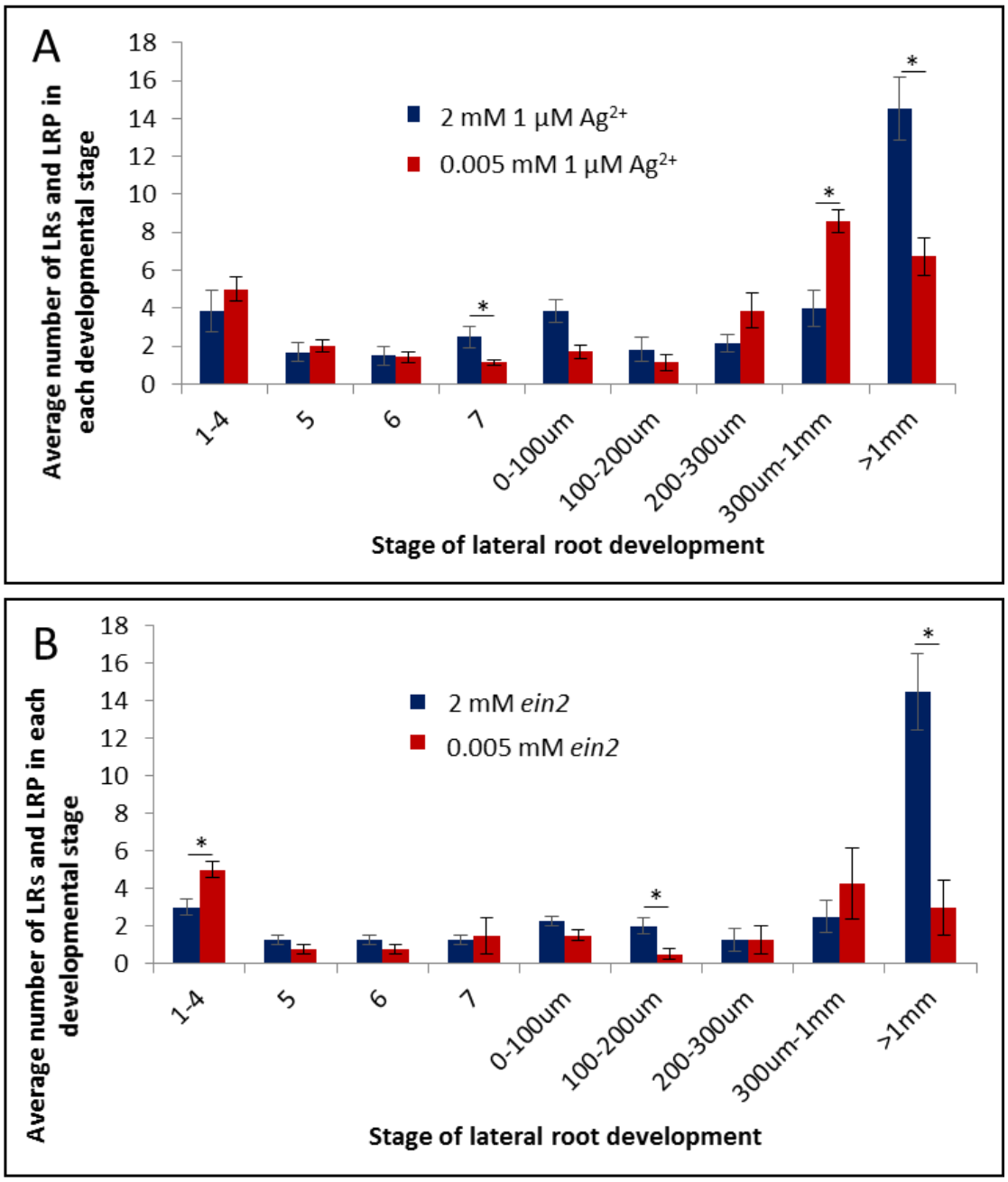

Fig. 5-8: Lateral root progression analysis. Light microscopy and the auxin-responsive *DR5::GUS* reporter line (A) and lugol staining (B) allow all lateral root primordia (LRP) and lateral roots (LRs) to be counted along the length of the primary root (PR). Col-0 (A) or *ein2* (B) seedlings analysed 12 d after germination (DAG), 8 days of K^+ treatment (2 mM or 0.005 mM). Primordial stage as defined in Malamy & Benfey (1997). Media supplemented with 1 µM Ag^{2+}. Values are averages taken from at least 7 individual seedlings (A) or 4 individual seedlings (B) ± SE. Asterisks indicate significance with independent samples *t* test (*P*-value <0.05).

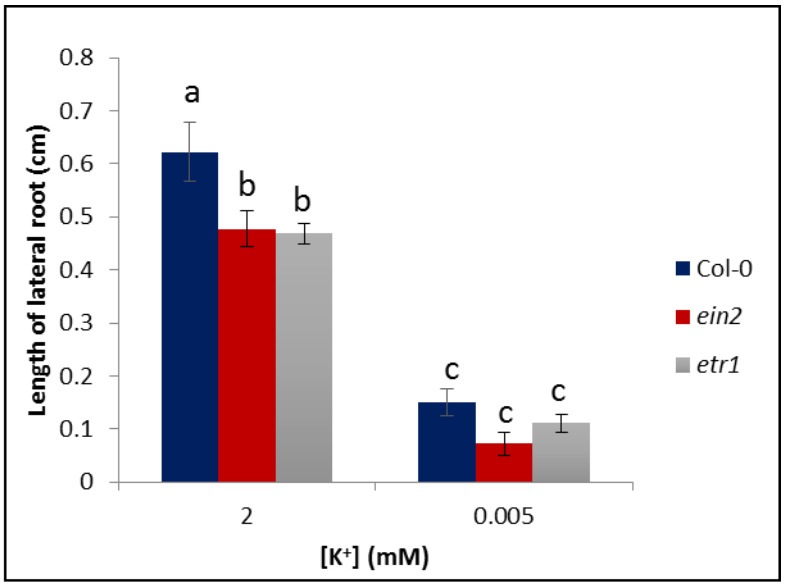

Fig. 5-9: Average length of lateral roots after 8 d K^+ treatment (2 mM or 0.005 mM), (12 d after germination (DAG) seedlings) of Col-0 and ethylene mutants *ein2* and *etr1.* Values are averages of at least 10 individual seedlings ± SE. Letters indicate significance with a Tukey Pairwise comparison $P< 0.05$.

5.4 Reactive oxygen species (ROS)

5.4.1 Introduction

The RNA-Seq experiment identified an overrepresentation of gene ontology (GO) terms relating to ROS metabolism (Figs 4-3,4-5), a larger number of downregulated scavenging genes (Fig. 4-15A) and upregulation of ROS-responsive genes (Fig. 4-15B). These data suggest that in response to low K^+ there is an increase in ROS levels. Previous transcriptomic data also suggested an increased expression of ROS-related genes in low K^+ conditions (Ma *et al.*, 2012). ROS has been identified as playing a key role in the induction of the *HAK5* K^+ transporter in response to low K^+ (Shin & Schachtman, 2004). ROS have also been implicated in the control of root elongation (Foreman *et al.*, 2003; Renew *et al.*, 2005), meristem size (Tsukagoshi, 2012), cell expansion (Hohl *et al.*, 1995; Fry, 1998; Potikha *et al.*, 1999; Ros-Barceló *et al.*, 2002; Liszkay *et al.*, 2004), and LR emergence (Manzano *et al.*, 2014). It was therefore hypothesised that changes in cellular ROS levels could be involved in reducing LR growth in Col-0 in response to low K^+. Work described in this section aimed to investigate this hypothesis. The role of ROS in the upregulation of the *HAK5* transporter in LRs was also investigated in response to low K^+.

5.4.2 ROS accumulates in LRs in response to low K^+

Fluorescence microscopy was used to investigate whether low K^+ induces changes in ROS levels in LRs. The fluorescent dye H2DCFDA has previously been used to identify increased levels of ROS in the PR of K^+-starved seedlings (Shin & Schachtman, 2004). However, more recently a molecular probe, HyPer, has been developed to allow the live imaging of H_2O_2 (Belousov *et al.*, 2006). HyPer is a cell probe that works through a YFP inserted into an *Escherichia coli* H_2O_2-binding protein called OxyR. Exposure to H_2O_2 causes a shift in the YFP excitation peak but not in the emission peak, and this can therefore be used as a quantitative ratiometric biosensor (Belousov *et al.*, 2006). As a transgenic line rather than a dye-based system, live imaging of seedlings can be conducted without disrupting their growth environment. HyPer has previously been used to measure H_2O_2 levels in the elongation zones of Arabidopsis roots (Hernandez-Barrera *et al.*, 2015), thereby displaying its applicability for use in the low K^+ system.

A fluorescence stereo microscope was used to investigate localization and levels of ROS in LRs of seedlings grown on low K^+ for 30 h, 54 h and 8 d (seedlings 12, 13 and 12 DAG respectively). Images were analysed by drawing a line down the centre of the LR and the average grey profile was plotted using ImageJ (Fig. 5-10A). The grey value indicates the brightness of each pixel, used as a measure for HyPer fluorescence. This produced a profile of the average levels of ROS at different points along the length of the LR (Fig. 5-10). LRs were grouped into size classes and profiles were transformed to give an average fluorescence value per relative distance from PR (see methods for details on the normalisation).

The profiles, in general, followed the same trend, irrespective of the length of the LR, with a high level of fluorescence in the PR at the site of attachment of the LR, then a decrease to a semi constant low level along the LR, with an increase at the tip (Figs 5-11–5-13). Despite variation in the different lengths of the LRs and at different time points, H_2O_2 levels were either similar, or increased in the LRs of plants grown on low K^+ compared with control conditions (Figs 5-11–5-13). Higher levels were not seen in the seedlings grown on control conditions for any of the timepoints tested. A region of increased H_2O_2 was also observed between approx. 20–50 % of the distance down the LR from the PR, in a number of the size categories at various timepoints (Figs 5-11B,C; 5-12C,D; 5-13C,D)(Fig. 5-10B,C), suggesting an area of accumulation along the LR. This region of accumulation was not seen in all length categories, or at all timepoints, and there appeared to be no cohesive pattern.

Results from HyPer analysis suggest that there may be increased levels of ROS in the LRs of seedlings grown on low K^+, with some showing an increase in accumulation in a region between the oldest part of the LR and the central region.

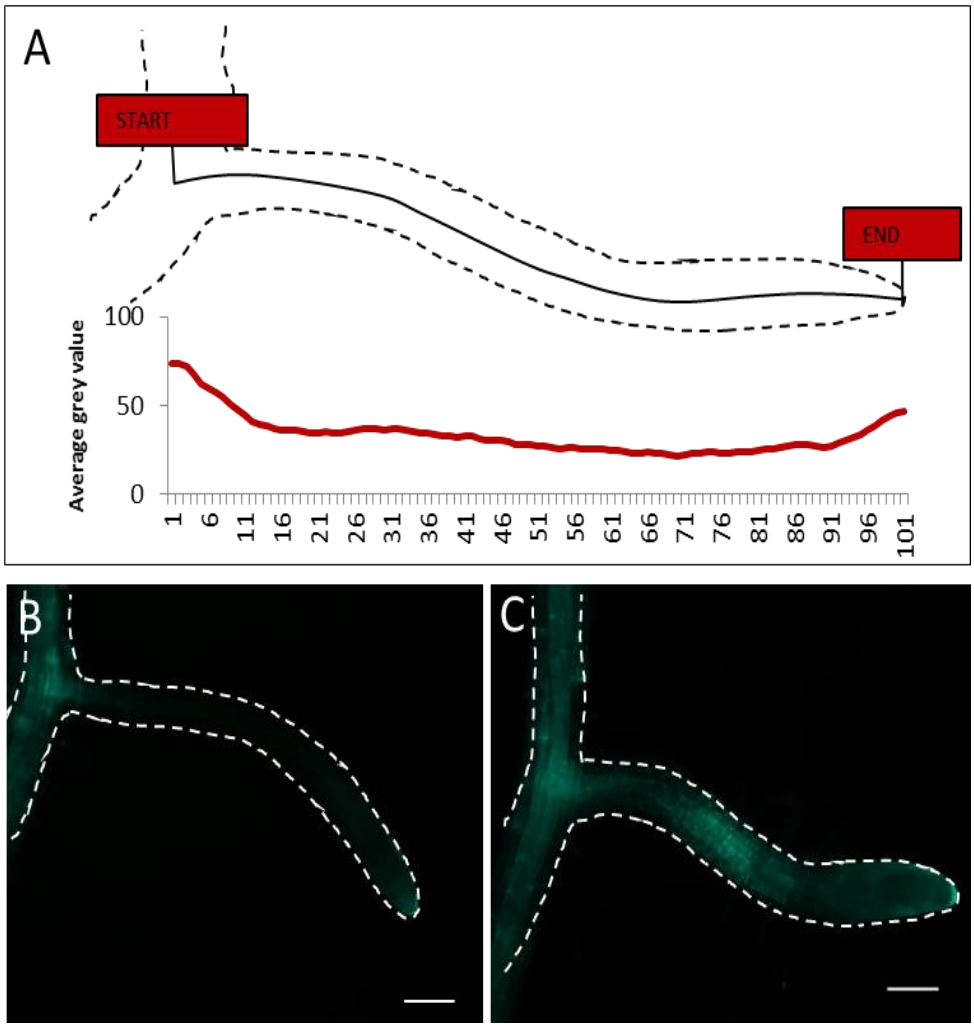

Fig. 5-10: Fluorescence stereo microscopy was used to investigate localization and levels of reactive oxygen species (ROS) in lateral roots (LRs) of seedlings grown on high or low K^+ using the transgenic molecular probe HyPer (Belousov *et al.,* 2006). (A) Diagram of the method of analysis of images. Image opened in ImageJ, a line drawn down the centre of the LR starting at the centre of the primary root (PR) and ending at the LR tip. The average grey value (brightness of each pixel) measured at every point and normalised into LR size groups, so that profiles along the LRs could be compared with similar sized LRs. (B, C) Representative images of HyPer fluorescence in LRs of seedlings grown for 8 d on 2 mM (B) or 0.005 mM (C) $[K^+]$. Scale bars = 100 µm.

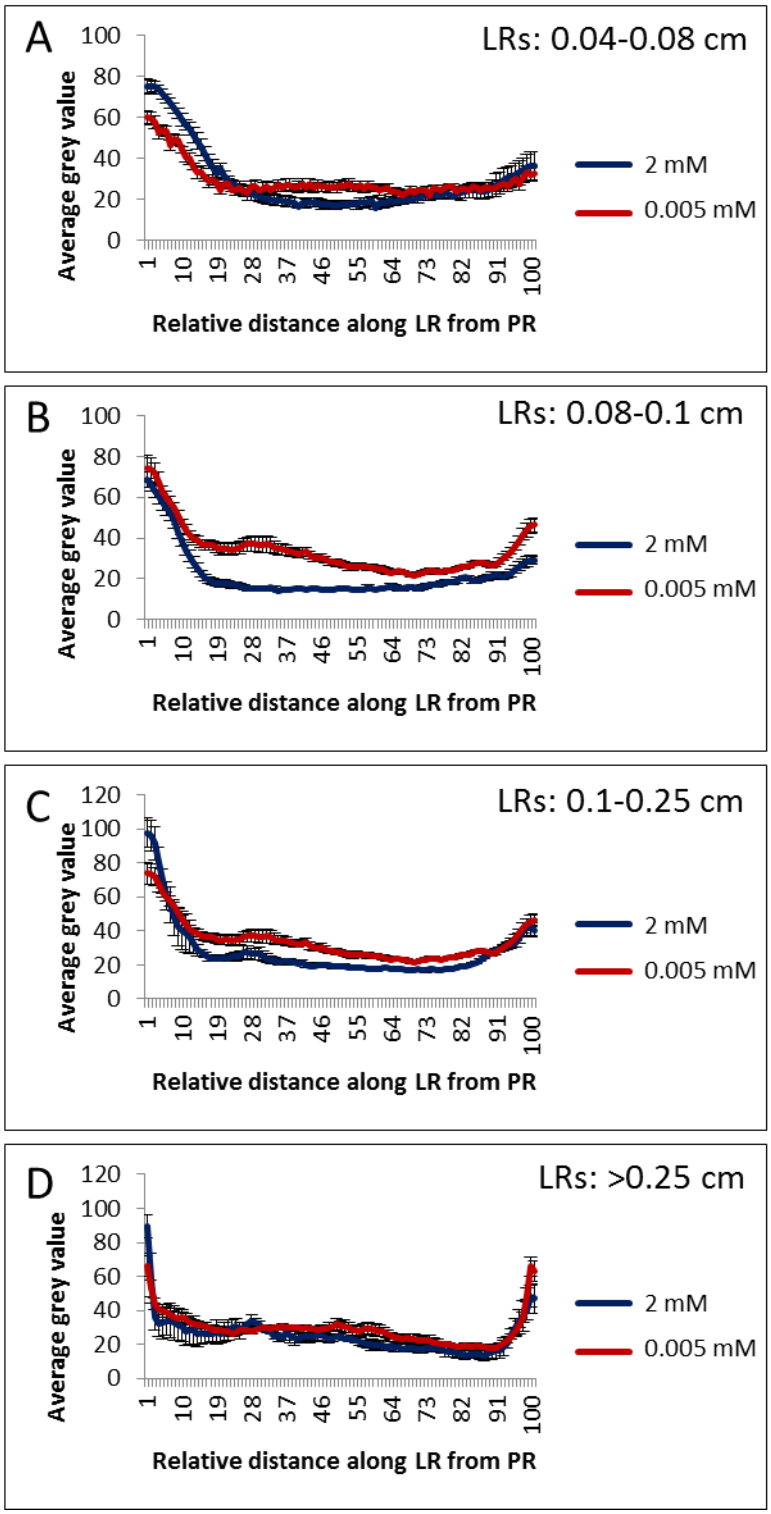

Fig. 5-11: Fluorescence stereo microscopy was used to investigate localization and levels of reactive oxygen species (ROS) in lateral roots (LRs) of seedlings grown for 11 d ½ MS10 followed by 30 h on high or low K^+ using the transgenic molecular probe HyPer (Belousov *et al.,* 2006). (See Fig 5-10 for analysis method.) (A-D) Average grey values (defined as the brightness of each pixel) of HyPer along the length of LRs, normalised for each LR length category; (A) 0.04-0.08 cm, (B) 0.08-0.1 cm, (C) 0.1-0.25 cm, (D) >0.25 cm. Points are averages of at least 5 individual seedlings ± SE.

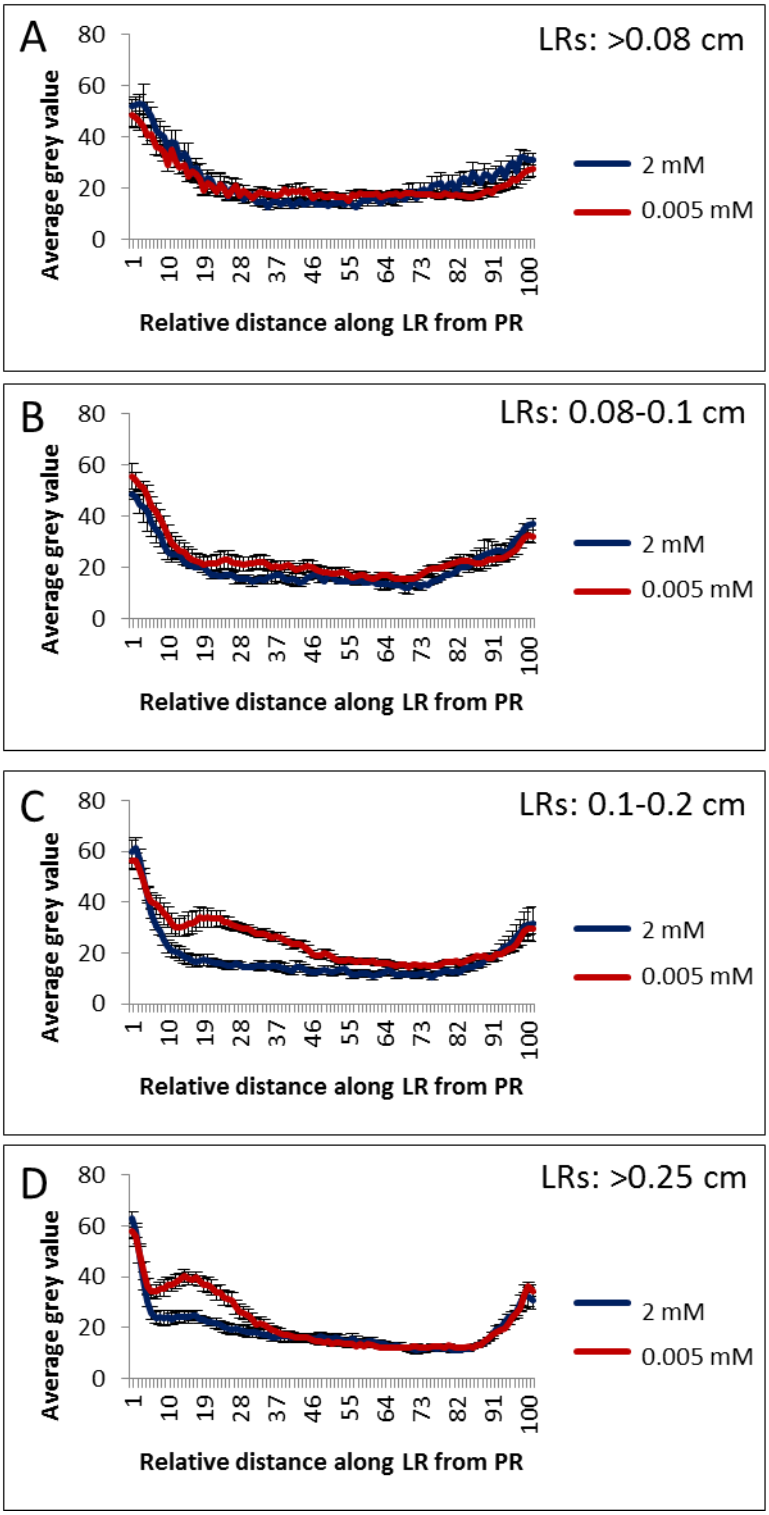

Fig. 5-12: Fluorescence stereo microscopy was used to investigate localization and levels of reactive oxygen species (ROS) in lateral roots (LRs) of seedlings grown for 11 d ½ MS10 followed by 54 h on high or low K^+ using the transgenic molecular probe HyPer (Belousov *et al.,* 2006). (See Fig. 5-10 for analysis method.) (A-D) Average grey values (defined as the brightness of each pixel) of HyPer along the length of LRs, normalised for each LR length category; (A) >0.08 cm, (B) 0.08-0.1 cm, (C) 0.1-0.2 cm, (D) >0.25 cm. Points are averages of at least 5 individual seedlings ± SE.

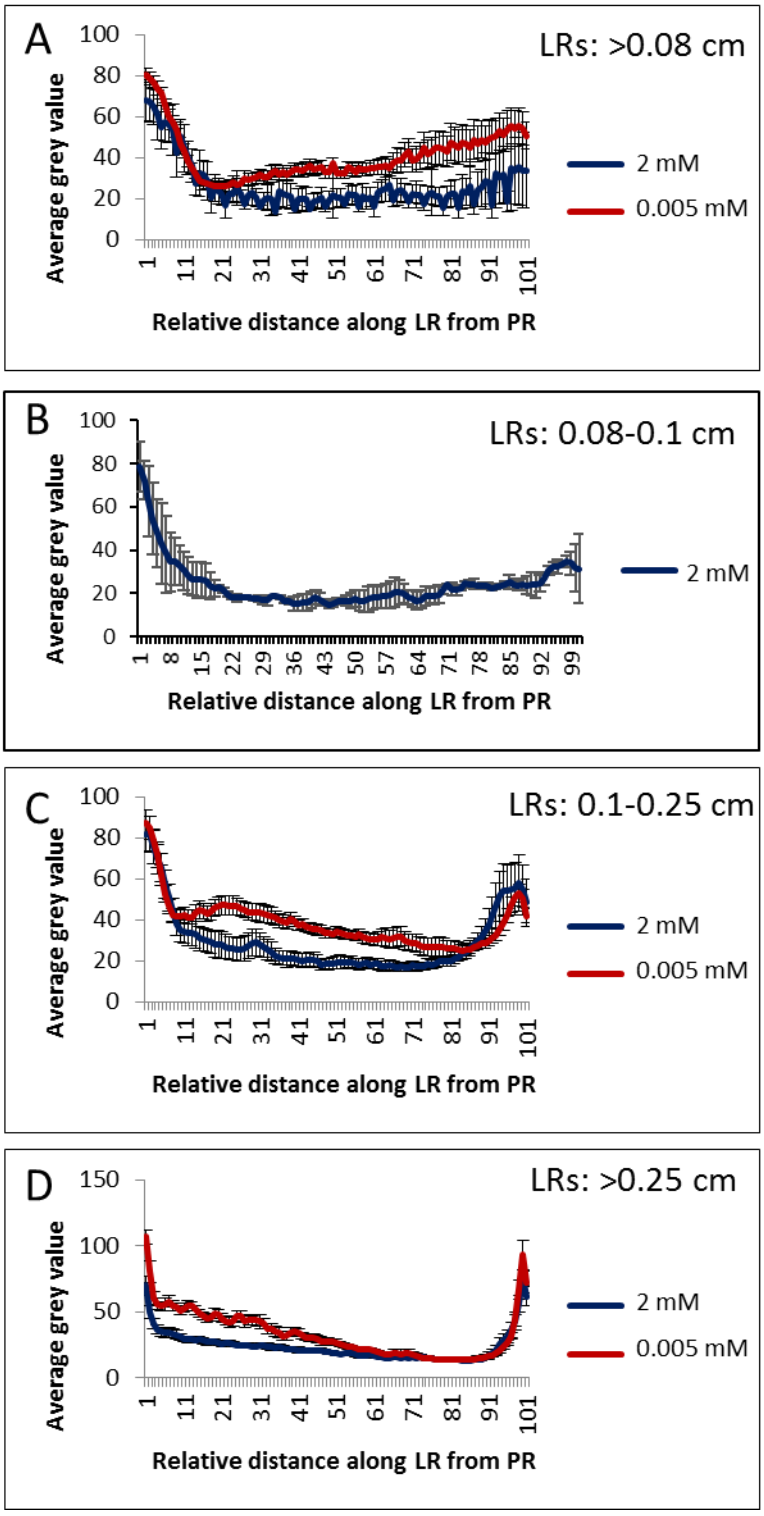

Fig. 5-13: Fluorescence stereo microscopy was used to investigate localization and levels of reactive oxygen species (ROS) in lateral roots (LRs) of seedlings grown for 4 d ½ MS10 followed by 8 d on high or low K^+ using the transgenic molecular probe HyPer (Belousov *et al.,* 2006). (See Fig. 5-10 for analysis method.) (A-D) Average grey values (defined as the brightness of each pixel) of HyPer along the length of LRs, normalised for each LR length category; (A) >0.08 cm, (B) 0.08-0.1 cm, (C) 0.1-0.25 cm, (D) >0.25 cm. Points are averages of at least 5 individual seedlings ± SE.

5.4.3 Inhibition of ROS does not restore LR growth under low K^+

A change in the localization of ROS accumulation in the LR exposed to low K^+ may suggest that ROS is playing a role in reducing LR growth. ROS can be produced in plants from a multitude of different sources but the best studied is through the NADPH oxidases, otherwise known as respiratory burst oxidase homologs (Rbohs; see Sagi & Fluhr, 2006 and Marino *et al.*, 2012 for reviews). Arabidopsis has 10 NADPH oxidase catalytic subunit genes, designated *AtrbohA–J.* The *AtrbohD* and *AtrbohF* genes were selected for investigation in this study as they have been identified as playing a role in the regulation of ABA-mediated repression of PR growth (Kwak *et al.*, 2003; Jiao *et al.*, 2013) as well as the regulation of LR formation (Li *et al.*, 2015a). Analysis using the Arabidopsis eFP Browser at bar.untoronto.ca (Winter *et al.,* 2007) also identified higher expression of the *AtrbohD* and *AtrbohF* genes in developing LR primordia than the other *Atrboh* genes. These data highlighting a role for *AtrbohD* and *AtrbohF* in root development and specifically LR growth.

The LR growth of the *atrbohD* and *atrbohF* mutants was measured after 8 d growth on high or low K^+ (Fig. 5-14A,B). The double mutant *atrbohDF* was also analysed (Fig. 5-14A), based on previously reported levels of partial redundancy (Kwak *et al.*, 2003). Mutating these genes did not rescue LR growth under low K^+ (Fig. 5-14A,B) suggesting that ROS derived from these 2 NADPH oxidases is not required in the reduction of LR growth in response to low K^+. It is not possible to conclude that NADPH oxidases are not playing a role however, as there may be redundancies between other members of the family in response to low K^+. Inhibiting ROS using the inhibitor of NADPH oxidase and other flavoenzymes, diphenylene iodonium (DPI; Bolwell & Wojtaszek, 1997) dramatically reduces the growth of the PR (Appendix VI) supporting work done by Foreman *et al.* (2003). However, DPI does not restore LR growth in low K^+ conditions (Fig. 5-14C). This suggests that the DPI-sensitive ROS pathway is having no effect on the LR growth reduction in response to K^+ starvation. Interestingly, the data suggest that ROS is needed for LR growth under normal conditions, as seen by the reduction in LR growth under 2 mM K^+ when grown on 1 µM and 200 nM DPI (Fig. 5-14C). However, in the *atrbohDF* and *atrbohD* mutants (but not *atrbohF*) there is an increase in LR growth under control conditions compared with WT (Fig. 5-14A,B), suggesting complex pathways of control in root growth.

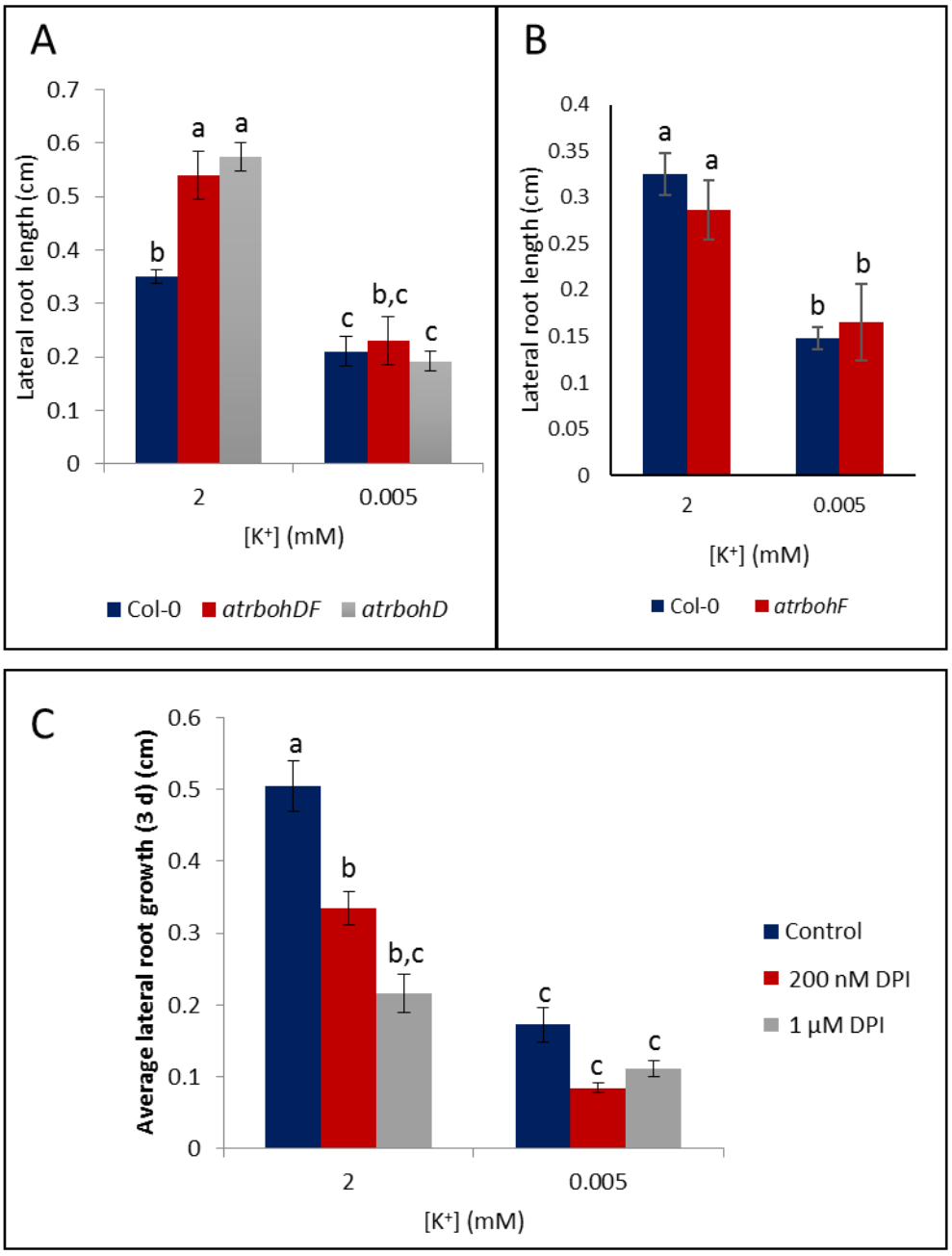

Fig. 5-14: Average lateral root (LR) length after 4 d growth on ½ MS10 followed by 8 d K^+ treatment (2 mM or 0.005 mM) of Col-0 and reactive oxygen species (ROS) mutants *atrbohD* and *atrbohDF* (A), and *atrbohF* (B). Average LR growth over 3 d following treatment when media supplemented with 200 nM or 1 µM DPI (C). Values are averages taken from at least 12 individual seedlings (A,B) and at least 6 seedlings (C) ± SE. Letters indicate significance with a Tukey Pairwise comparison $P< 0.05$.

5.4.4 ROS and *HAK5* activation

ROS has been shown to accumulate in a region of active K^+ uptake in the PR in response to low K^+ (Moritsugu *et al.,* 1993; Shin & Schachtman, 2004). As ROS is known to act in the upregulation of the *HAK5* K^+ transporter in response to low K^+ (Shin & Schachtman, 2004; Kim

et al., 2012), it has been suggested that this ROS accumulation leads to the upregulation of *HAK5* in a specific region of the PR, distal to the elongation zone. It was hypothesised that this could also be occurring in the LRs, potentially explaining the accumulation of ROS seen using the HyPer line in response to low K^+ (Fig. 5-10C). Studies investigating the localization of the HAK5 transporter have described an increase in promoter activity of *HAK5* in the LRs in response to K^+ starvation (Fig. 5-15A) (Gierth *et al.*, 2005). Images of LRs expressing the GUS reporter (*pAtHAK5::GUS/GFP)* suggested that this region of HAK5 accumulation may overlap with the region of ROS accumulation found in this thesis (Fig. 5-15A; 5-10). To investigate the link between ROS accumulation and HAK5 in the LRs in response to low K^+ the *pAtHAK5::GUS/GFP* line described in Gierth *et al.* (2005) was used. The *pAtHAK5::GUS/GFP* line was imaged using confocal microscopy. However the expression pattern of *HAK5* in the PRs did not correspond with the localization shown in the Gierth *et al.* (2005) paper (Fig. 5-15A3,B). Specifically, HAK5 localized mainly to the stele and cortex (Fig. 5-15B), rather than the epidermis as was reported in the paper (Fig. 5-15A3). The localization in the LRs corresponded better with the published data with high expression in the epidermal cells at the base of the LR (Fig. 5-1514,C). The fluorescence of GFP in the LRs of the *pAtHAK5::GUS/GFP* line increased after 3 d K^+ starvation (Fig. 5-15E), however no difference was seen in the PR after 3 d (Fig. 5-15D). The reporter was not sufficiently sensitive to see changes after short time periods. As *HAK5* is upregulated very quickly after K^+ starvation (3 h Fig. 6-3), investigating its upregulation would require a more sensitive reporter. In the future a luciferase marker driven by *HAK5* (Kim *et al.*, 2012) may allow the system to be probed further.

5.4.5 Conclusion

The work presented here suggests that ROS does not play a key role in the reduction in LR growth seen in response to low K^+, as blocking ROS through mutants and DPI is not able to restore LR growth under low K^+. Despite this, work here has identified that there is a small increase in ROS accumulation in LRs in response to low K^+. Comparing this accumulation pattern with previously published literature suggests that there may be a link between ROS and HAK5 upregulation in the LRs in response to low K^+. This would fit with previously published work investigating the PR; however, further work needs to be conducted to identify whether the same effect occurs in the LRs under K^+ starvation. The accumulation pattern observed in the LRs in response to low K^+ is also not consistent across LR lengths or low K^+ time treatments, and again, more work must be conducted to establish if this is a low K^+ response.

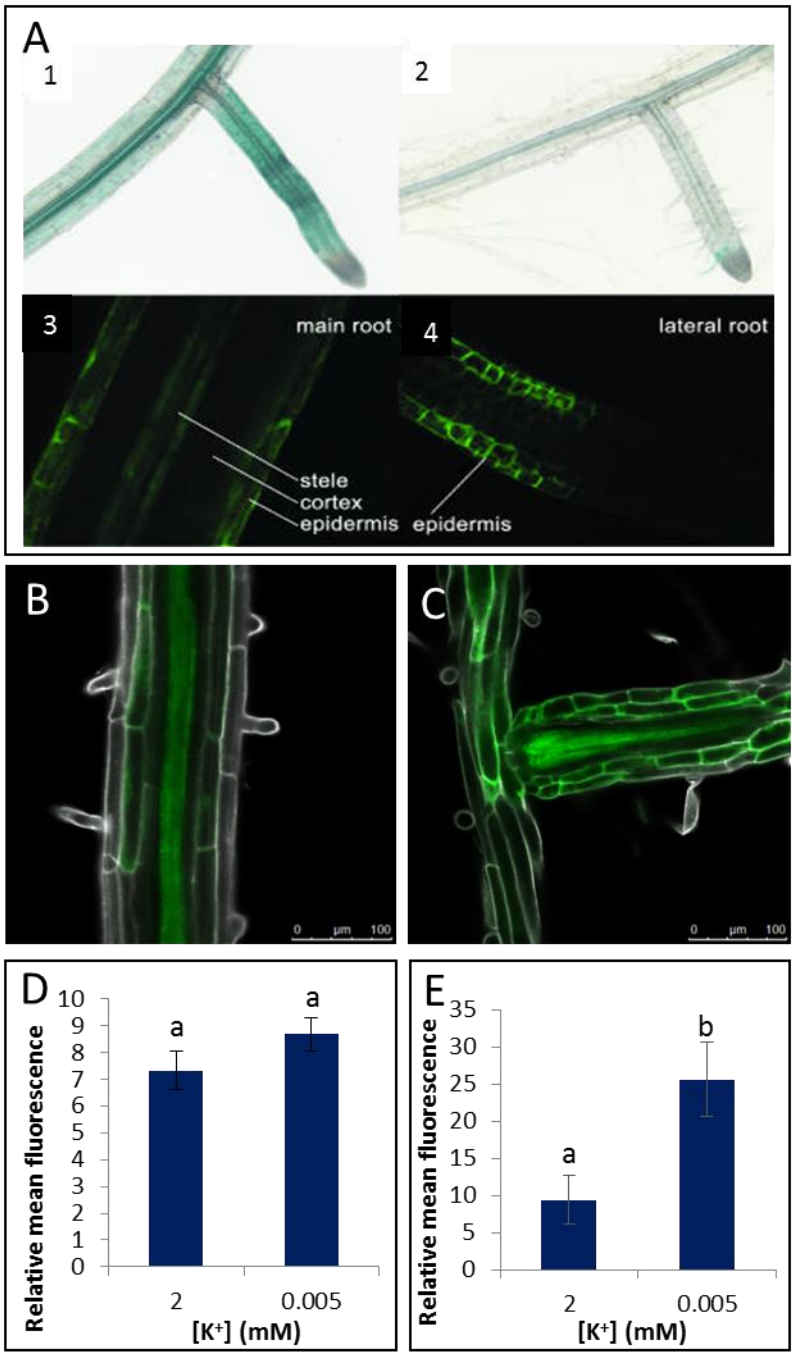

Fig. 5-15: Roots of transgenic plants expressing the GUS and GFP reporter gene driven by the *AtHAK5* promoter, p*AtHAK5::GUS/GFP.* (A) Figure adapted from Gierth *et al.* (2005). (A1,2) GUS activity in lateral roots (LRs) of seedlings grown on low K^+ (A1) and after resupply with K^+ (A2). (A3,4) Confocal microscopy identifying the GFP localization in the primary root (PR) and LRs of K^+ starved roots. (B) *pAtHAK5::GUS/GFP* fluorescence in the PR after 3 d low K^+ (0.005 mM) showing different localization compared with (A3). (C) *pAtHAK5::GUS/GFP* fluorescence in a LR where it meets the PR. White is propidium iodide stain, green is GFP. (D, E) Relative mean fluorescence of *pAtHAK5::GUS/GFP* in the PR (D) or the LR (measurements taken from the epidermis and cortex cell files) (E) of seedlings grown for 3 d on either 2 mM or 0.005 mM K^+. Values are averages taken from at least 6 individual seedlings ± SE. Letters indicate significance with a Tukey Pairwise comparison $P< 0.05$. (D) $P=0.161$, (E) $P=0.009$.

5.5 Gibberellin (GA) and DELLA signalling

Analysis of the RNA-Seq data suggested that in response to low K^+ there is downregulation of a GA biosynthesis gene, *GA3ox2.* Transcription factors (TFs) with known roles in GA degradation and reduced GA signalling were also identified as being upregulated in response to low K^+. From these data, it was hypothesised that there is a reduction in GA in response to low K^+ and this was investigated in the following experiments.

5.5.1 Increased transcription of *GA2ox6* in response to low K^+

5.5.1.1 Selection of genes for further transcriptional analysis

GA homeostasis is controlled through biosynthesis and deactivation, with three families of dioxygenase genes, namely the GA3oxs, GA20oxs and the GA2oxs, playing a key role in the regulation of this pathway in response to many developmental and environmental cues (Colebrook *et al.*, 2014). To investigate further if K^+ starvation is causing a reduction in GA, the expression levels of the GA biosynthesis genes *GIBBERELLIN-3-OXIDASE 2 (GA3ox2*)*,* and *GA3ox1,* and the GA deactivation gene *GIBBERELLIN-2-OXIDASE 6* (*GA2ox6*) were quantified using qRT-PCR, after 30 h, 54 h and 72 h of K^+ starvation (samples taken from seedlings 12, 13 and 14 DAG respectively). *GA3ox2* was chosen due to its downregulation after 30 h K^+ starvation in the RNA-Seq data, and *GA3ox1* was chosen because it is known to be downregulated by the TF *JUB1*, which was upregulated in the RNA-Seq data (Shahnejat-Bushehri *et al.*, 2016) (Fig. 4-14). The *GA2ox* genes deactivate bioactive GAs (Thomas *et al.*, 1999) and the upregulation of *GA2oxs* has been reported in response to a number of abiotic stresses (Achard *et al.*, 2008a; Magome *et al.*, 2008; Dubois *et al.*, 2013; Colebrook *et al.*, 2014). Of these *GA2ox* genes, *GA2ox6* was selected for analysis in the qRT-PCR due to its upregulation in response to many abiotic stresses and also because it is known to be transcriptionally induced by the TF ERF6*,* which was upregulated in the RNA-Seq data (Dubois *et al.*, 2013) (Table 4-1).

5.5.1.2 qRT-PCR analysis of *GA2ox6*, *GA3ox2* and *GA3ox1*

qRT-PCR was used to investigate the expression levels of GA dioxygenase genes in response to low K^+. RNA was extracted from seedlings grown for 11 d on ½MS10 media followed by 30 h, 54 h or 72 h K^+ treatment (2 mM or 0.005 mM). qRT-PCR revealed that the expression of the GA deactivation gene, *GA2ox6*, was upregulated after 54 h and 72 h of low K^+ treatment (Fig. 5-16A). This suggests an increase in the deactivation of bioactive GAs in response to low K^+. The GA biosynthesis gene *GA3ox2* was found in the RNA-Seq data to be downregulated after 30 h (-0.51 $\log_2$fc). However, the qRT-PCR data showed no significant difference between the

expression level of this gene at any timepoint following transfer to low K^+ media (Fig. 5-16B). qRT-PCR analysis of the *GA3ox1* biosynthesis gene, showed a small upregulation after 54 h and 72 h low K^+ treatment (Fig. 5-16C).

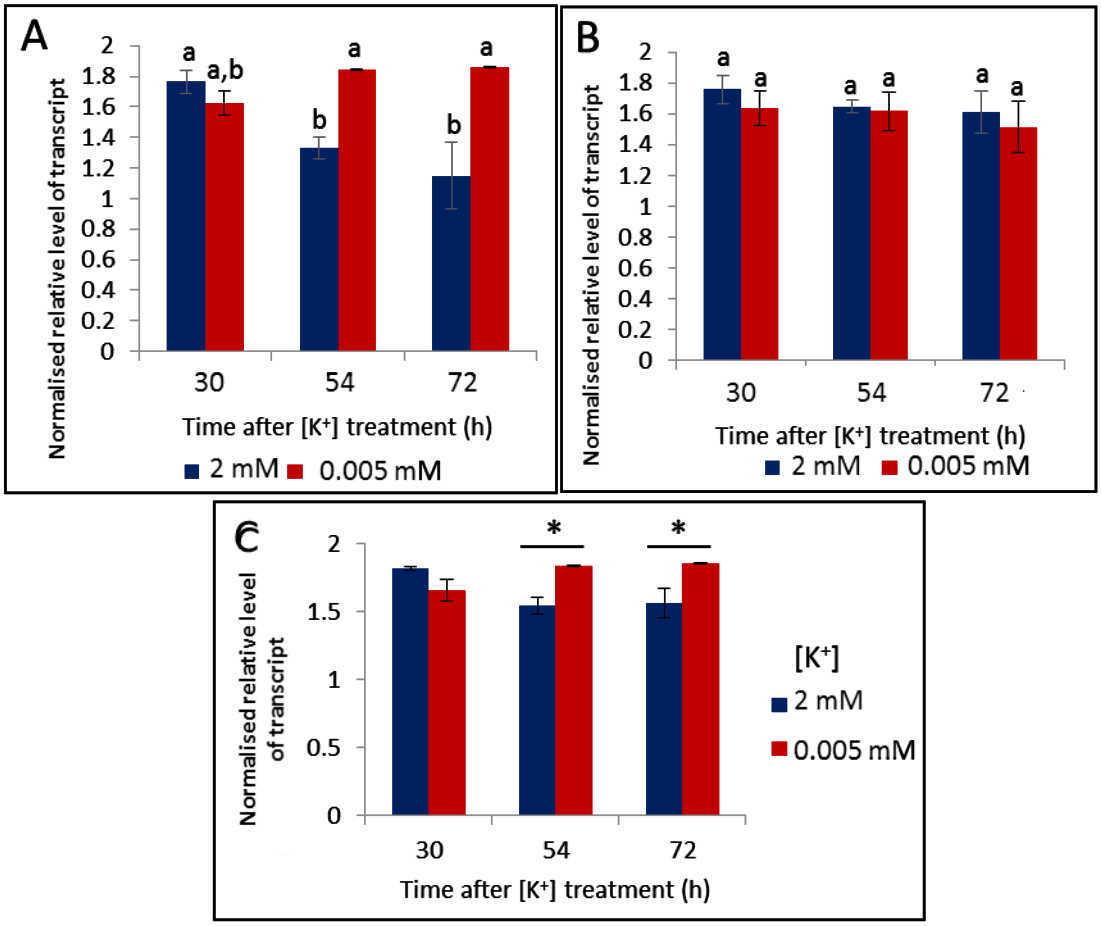

Fig. 5-16: Normalised relative level of transcript of *GA2ox6* (A), *GA3ox2* (B), and *GA3ox1* (C) after 30 h, 54 h and 72 h K^+ treatment (2 mM or 0.005 mM) determined by qRT-PCR. Seedlings grown for 11 d on ½ MS10 followed by movement to K^+ treatment. Normalised against *AT1G13320.* Values are means ± SE. Three biological repeats and three technical repeats (A,C), 6 biological repeats and 6 technical reps (B). Letters indicate significance with a Tukey Pairwise comparison $P < 0.05$ (A,B). Asterisks indicate significance with independent samples *t* test (*P*-value <0.05) (C).

5.5.2 Low K^+ induces DELLA stabilization in LR meristems

A decrease in GA levels is known to lead to the stabilization of DELLA proteins (see introduction section 1.7.3), and consequently levels of DELLA in LRs were investigated using the DELLA reporter line *proRGA::GFP:RGA* and confocal microscopy. Seedlings were grown for 9 d on ½MS10 media followed by 3 d K^+ treatment (2 mM or 0.005 mM), before being imaged. Average relative fluorescence levels of *proRGA::GFP:RGA* were higher in LRs that had been exposed to low K^+ for 3 d compared to the control seedlings (Fig. 5-17A,B). This suggests that a

decrease in GA levels leads to a stabilization of DELLA proteins. Interestingly the increase in DELLA levels was not seen after 8 d K^+ treatment (2 mM or 0.005 mM) (Fig. 5-17C). Gene expression changes of the DELLAs were not investigated as it has been found that most DELLA genes are not upregulated at the transcriptional level in response to stress (Colebrook *et al.*, 2014).

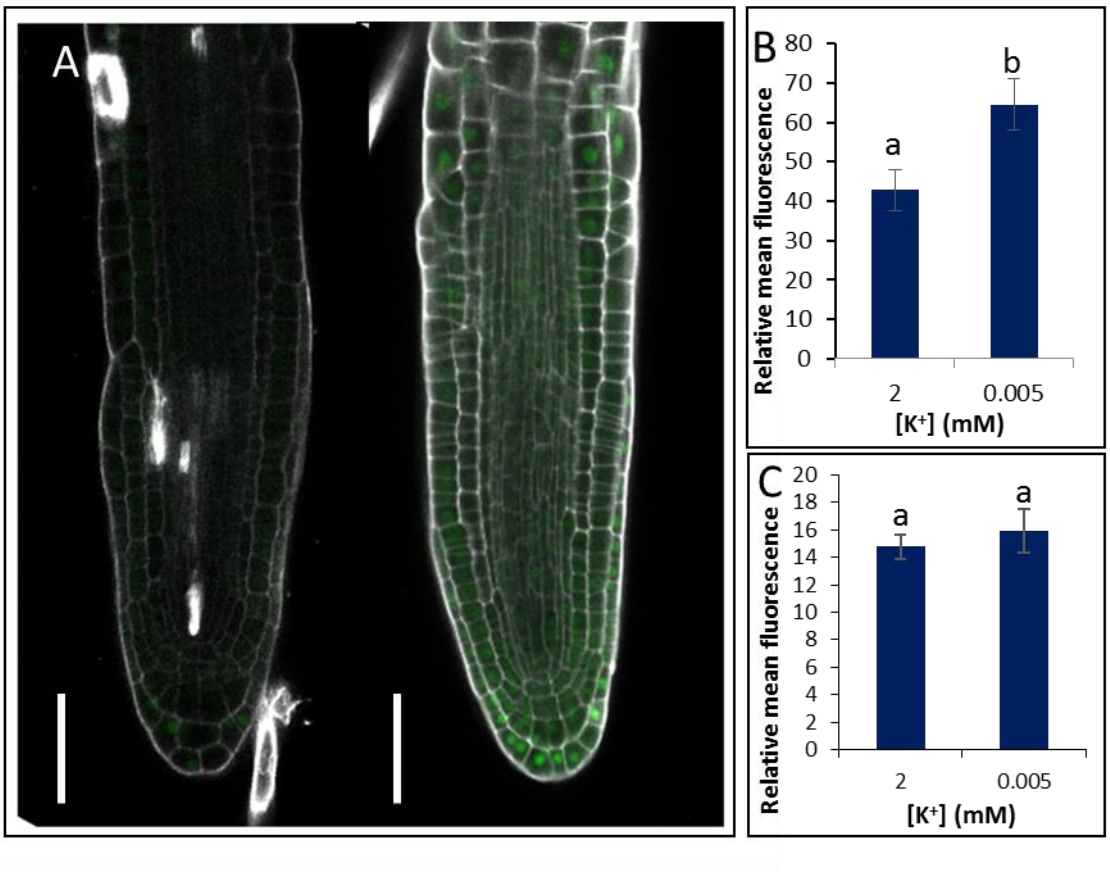

Fig. 5-17: (A) Representative confocal images of *proRGA::GFP:RGA* in lateral roots (LRs) grown for 9 d on ½ MS10 followed by 2 mM (left) or 0.005 mM (right) [K^+] for 3 d. Scale bars = 100 µm. Relative mean fluorescence of RGA GFP LRs after 3 d K^+ treatment (2 mM or 0.005 mM) (B), after 8 d K^+ treatment (2 mM or 0.005 mM) (C). Images taken from at least 6 different seedlings, *n* represents individual LRs analysed. Values are means ± SE. (B) $n \geq 18$ (C) $n \geq 14$. Letters indicate significance from independent samples *t* test $P < 0.05$.

5.2.3 Supplementing the medium with GA restores the length of LR meristems under low K^+

DELLA proteins are known to be involved in the reductions in growth by restraining cell proliferation and expansion (Peng *et al.*, 1997, 1999; Fleet & Sun, 2005). It was therefore hypothesised that the reduction in LR growth in response to low K^+ could be due to a reduction in GA leading to a stabilization of DELLAs. This was investigated by measuring meristem size using *CYCB1;2:GUS* expression as a proxy, in seedlings grown for 4 d on ½ MS10 followed by 8

d on K^+ treatment (2 mM or 0.005 mM) medium containing either GA or the GA inhibitor paclobutrazol (PAC). In the LRs of length over 1 mm, the application of 10 µM GA restored the size of the LR meristem under low K^+ (Fig. 5-18A), and application of 0.1 µM PAC reduced LR length under the control conditions (Fig. 5-18A). These results were also seen in the lateral roots 100 µm–1 mm, however the differences were less prominent and were not statistically significant (Fig. 5-18B).

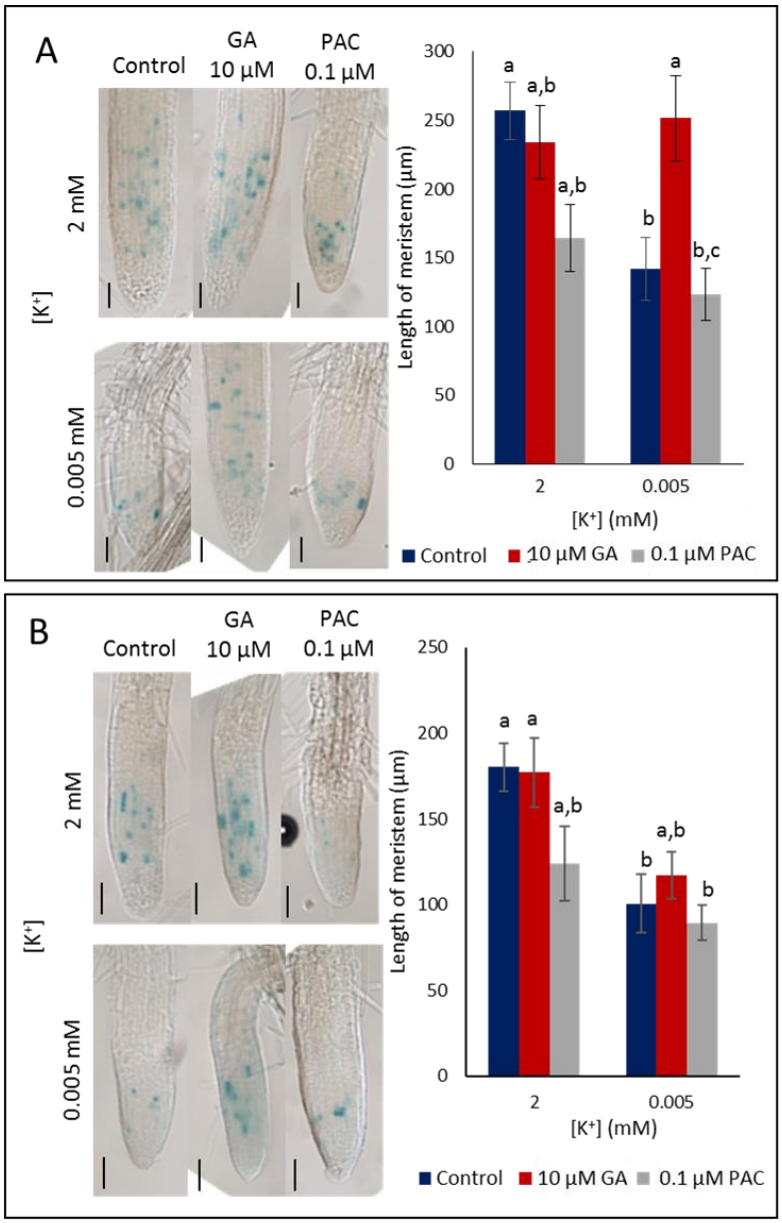

Fig. 5-18: Typical GUS staining pattern of *CYCB1;2:GUS;* the staining shows a reduced area of cell division in low [K^+]. Scale bars = 50 µM. Average length of meristem measured as the length of area with dividing cells (stained blue in *CYCB1;2:GUS* line). (A) Lateral roots (LRs) >1 mm, (B) LRs 100 µm-1 mm. Media supplemented with either 10 µM GA or 0.1 µM PAC for 8 d. Analysis carried out on seedlings 12 d after germination (DAG). Values are averages of

measurements taken from at least 6 individual seedlings per treatment ± SE, Letters indicate significance with a Tukey Pairwise comparison $P< 0.05$.

5.2.4 Supplementing the medium with GA restores LR growth under low K^+

To investigate this further, the average LR growth was measured in roots grown on media supplemented either with 10 µM GA or 0.1 µM PAC. Seedlings were grown on ½MS10 for 9 d, then transferred to K^+ treatment media (2 mM or 0.005 mM) for 3 d. These results were essentially the same as for the previous experiment, with root growth restored with the addition of GA, and root growth restricted in the control conditions when PAC was added (Fig. 5-19). Blocking GA deactivation in the *ga2ox quintuple* mutant (Rieu *et al.*, 2008) partially restored LR over 3 d of low K^+ treatment (Fig. 5-20A); however, this did not result in the restoration of growth over an 8-d low K^+ treatment (Fig. 5-20B). The 8-d growth analysis needs to be repeated because the WT was measured in a separate experiment.

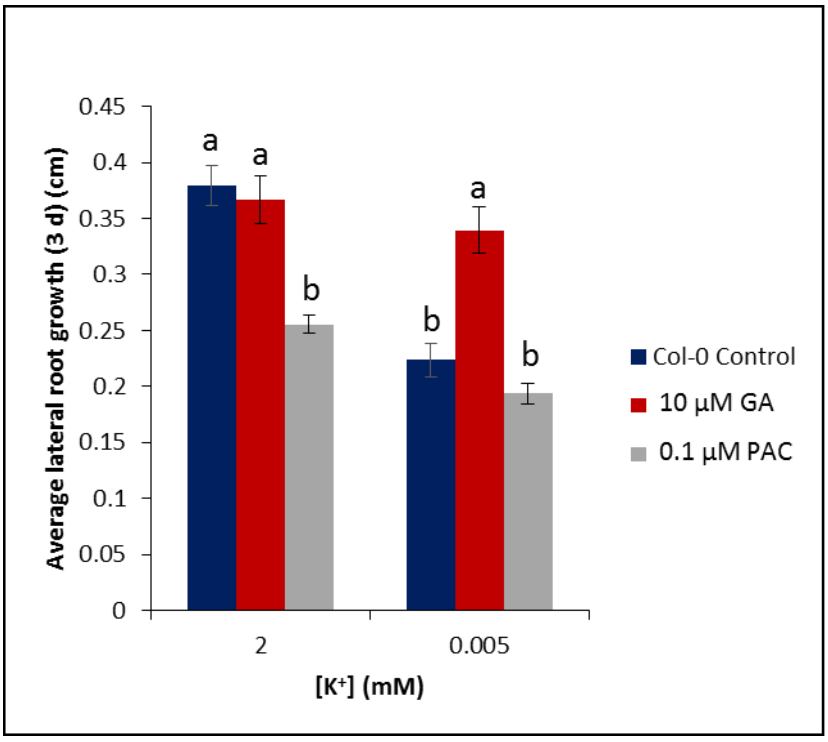

Fig. 5-19: Average lateral root growth over 3 d growth on high or low K^+ treatment (2 mM or 0.005 mM). Seedlings grown for 9 d on ½ MS10 before movement to K^+ treatment. Values are averages taken from at least 17 individual seedlings per treatment ± SE. Letters indicate significance with a Tukey Pairwise comparison $P< 0.05$.

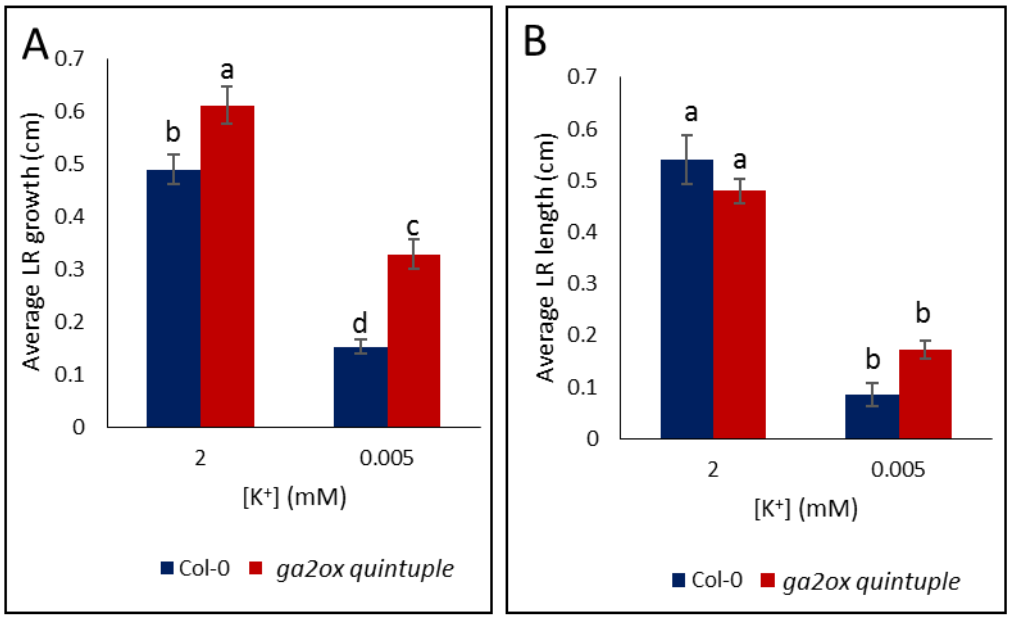

Fig. 5-20: Average lateral root (LR) growth of Col-0 or *ga2ox quintuple* mutant (Rieu *et al.,* 2008) grown on 2 mM or 0.005 mM K^+ for 3 d (A) or after 8 d (B). Seedlings all 12 days after germination. Values are averages of at least 10 individual seedlings per treatment ± SE. Letters indicate significance with a Tukey Pairwise comparison $P< 0.05$. Control for 8 d analysis (B) taken from another experiment.

5.2.5 GA and DELLA signalling summary

These data suggest that in response to K^+ starvation, there is an increase in GA deactivation, through the upregulation of the GA deactivating gene *GA2ox6*. This then reduces the levels of GA in the LRs which leads to the stabilization of DELLA proteins, as was seen using the *proRGA::GFP:RGA* reporter line. DELLA protein accumulation is known to lead to reduced cell division and growth. In this chapter it was shown that the addition of GA to the medium restores the meristem size under low K^+ conditions. Overall these data suggest an important role for GA and DELLA signalling in the reduced LR growth response to low K^+.

5.6 Summary

Work in this chapter has investigated the roles of hormones and ROS in reducing the LR growth in response to low K^+. Transcriptomic analysis and literature searches provided the basis for the hypotheses that the hormones auxin, ethylene and GA, as well as ROS, may be playing a role in the reduced LR growth response to low K^+ (Fig. 5-1). The work in this chapter has systematically investigated each of these hypotheses experimentally.

The results reported in this chapter show that the hormones ethylene and auxin, as well as ROS signalling, do not play a significant role in the reduction of LR growth in response to low K^+; disrupting their signalling, genetically, through the addition of phytohormones or the use of chemical inhibitors, was unable to restore the LR growth under low K^+. It was shown that accumulation of ROS in the LRs may be linked to the upregulation of the *HAK5* K^+ transporter in response to low K^+. However, further work is needed to establish the significance of any link. This chapter reported data suggesting that in response to low K^+ there is a reduction in GA levels, which leads to the stabilization of DELLA proteins in the LRs. It has been hypothesised that this increase in DELLAs in the LRs causes the reduction in cell division, meristem size and growth in the LRs in response to low K^+.

Chapter 6 Upstream signalling of LR response

6.1 Introduction

Results in previous chapters in this thesis have shown that in response to low K^+, lateral root (LR) growth in the Arabidopsis accession Col-0 is reduced. Further, it has been suggested that, in part, this is due to reduced gibberellic acid (GA) and increased stabilization of DELLA proteins in the LRs. This final experimental chapter will investigate the possible upstream factors which could result in reduced GA levels and stabilized DELLAs. The RNA-Seq data (Chapter 4) were revisited and analysed with the intention of seeking signals and genes that are capable of influencing GA/DELLA levels in response to low K^+. The factors chosen for further analysis were the hormone abscisic acid (ABA) and the transcription factors (TFs) CBF1 and ERF6. Genes were also chosen due to their significant upregulation after both 3 h and 30 h low K^+ treatment. Specifically, these were *WRKY40, STZ,* and a probable calcium binding protein *AT5G39670*.

6.2 The regulation of GA signalling in response to low K^+

6.2.1 The role of ABA in regulating reduced GA/ increased DELLA in response to low K^+

On the basis of the existing literature, it was hypothesised that ABA might be playing a role in the reduced LR phenotype at two different stages of the response. The first possibility is that ABA acts upstream of the GA response and causes a reduction in GA levels in response to low K^+. This possibility was suggested because ABA treatment has been shown to inhibit GA-induced degradation of the GFP-RGA protein (Achard *et al.*, 2006) and to upregulate *GA2ox6* and downregulate *GA20ox1* (Zentella *et al.*, 2007). The second possibility is that ABA action is downstream of the GA response. It has been suggested that GA inhibits ABA biosynthesis (Zentella *et al.*, 2007) and that DELLA proteins can lead to ABA accumulation through the putative DELLA target XERICO (Ko *et al.*, 2006; Zentella *et al.*, 2007). It was therefore hypothesised that reduced GA and increased DELLA could lead to increased ABA and ABA-mediated responses. WT plants grown on ABA have been shown to display a phenotype similar to the low K^+ LR phenotype: lateral root primordia (LRP) form and LRs emerge from the primary root (PR), but do not elongate (De Smet *et al.*, 2003). In addition, ABA is also known to regulate (LR) growth (Signora *et al.*, 2001; Ariel *et al.*, 2010; Van Norman *et al.*, 2014). Analysis of the RNA-Seq data did not identify changes in the expression of characterised ABA

biosynthesis genes in response to low K^+. However, the transcription factor (TF) ORA47 (upregulated 1.28 log_2fc 3 h), was identified by Agris AtTFDB, as being associated with a suite of ABA signalling genes (Fig. 4-13). This suggests that there may be changes in ABA signalling and possibly changes in biosynthesis after periods of K^+ starvation longer than 30 h. Together these results suggest that increased ABA in response to low K^+ could lead to reduced LR growth. A role for ABA in the reduced LR phenotype in response to low K^+ was therefore investigated by supplementing the growth media with 0.1 µM ABA, 1 µM ABA or 0.1 µM of the ABA biosynthesis inhibitor fluridon. Seedlings were grown for 9 d on ½ MS10 then LRs were measured upon transfer to the supplemented media and then again after 3 d growth. If the reduction in LR growth in response to K^+ starvation is due to ABA, then blocking ABA synthesis with fluridon would restore LR growth under low K^+. This is not seen however, and blocking ABA has no effect on LR growth compared with the control (Fig. 6-1). Addition of ABA to the growth medium reduces LR growth (Fig. 6-1) which supports the results of De Smet *et al.* (2003). However, ABA is not able to restore LR growth under low K^+ conditions (Fig. 6-1). These results suggest that reduced LR growth in response to low K^+ is occurring through an ABA-independent mechanism. Interestingly, the ethylene-responsive gene *ERF1* has also been shown to be negatively regulated by ABA (Cheng *et al.*, 2013), and so the significant increase in *ERF1* expression (Fig. 5-7) supports the view that there is no early increase in ABA signalling in response to low K^+.

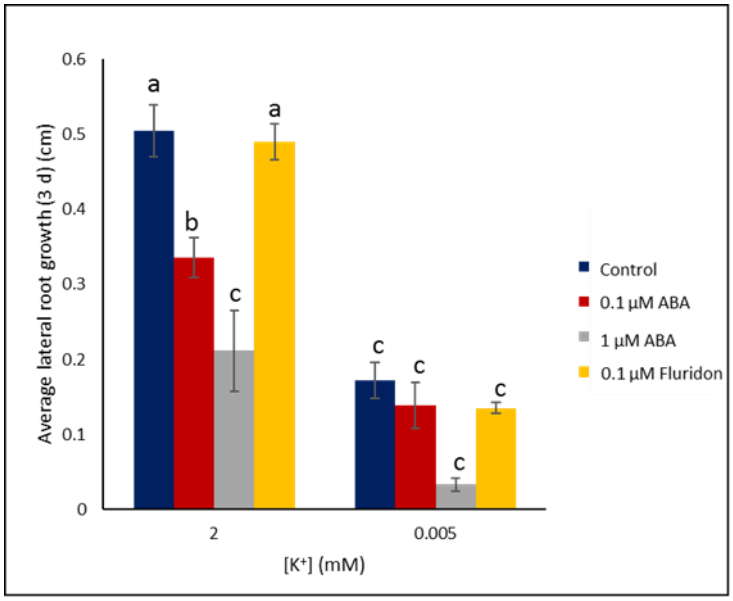

Fig. 6-1: Average lateral root growth per root over 3 d following K^+ treatment (2 mM or 0.005 mM), of Col-0 seedlings grown on media containing 0.1 µM ABA, 1 µM ABA or 0.1 µM fluridon. Seedlings grown for 9 d on ½ MS10 before transferral to K^+ treatment. Values are averages of at least 8 individual seedlings ± SE. Letters indicate significance with a Tukey Pairwise comparison $P< 0.05$.

6.2.2 The role of *CBF1* in regulating reduced GA/increased DELLA in response to low K^+

The C-repeat-binding factor (CBF)/dehydration-responsive element-binding factor (DREB1) family are a small family of TFs known to regulate cold acclimation through the activation of *COR* (*Cold On-Regulated*) genes. There are three CBF/DREB1 proteins, two of which are represented in the RNA-Seq data. *CBF3 (DREB1A)* is downregulated after 3 h K^+ starvation (-0.93 log_2fc), whilst *CBF1 (DREB1B)* is upregulated (0.80 log_2fc), and *CBF2* is not found. The *CBF1* and *CBF3* genes are both known to act in the reduction of GA and increase of DELLAs in response to cold (Achard *et al.*, 2008a; Zhou *et al.*, 2017), though they act in different ways. CBF3 has been shown to reduce GA responses through upregulation of *GA2ox7* and *RGL* (Zhou *et al*., 2017) and CBF1 is known to reduce GA through increasing the expression of *GA2ox3*, *GA2ox6* and also through the increase in transcript levels of the DELLA gene *RGL3* (Achard *et al.*, 2008a). As one *CBF* gene displayed upregulation whilst another displayed downregulation in response to low K^+, downstream targets of the CBF regulon were investigated in response to low K^+, in order to gauge if there is an overall upregulation or downregulation of the pathway. The *COR* genes are known downstream targets in the CBF regulon. Therefore, changes in expression of these genes were investigated in the RNA-Seq data set. *COR15A* and *COR15B* are both downregulated after 3 h K^+ starvation (-0.75, -0.69 log_2fc, respectively) and upregulated after 30 h K^+ starvation (0.70, 0.71 log_2fc, respectively). *COR15A* and *COR15B* are known to be CBF3 target genes (Seki *et al.*, 2002; Maruyama *et al.*, 2004), and Novillo *et al.* (2007) identified that *COR15A* needed simultaneous expression of both CBF1 and CBF3 for activation under cold. The upregulation of both *COR15A* and *COR15B* after 30 h K^+ starvation may suggest an overall upregulation of the CBF regulon, as the downstream *COR* genes are activated. It may also suggest however, that these genes are regulated differently in response to K^+ starvation than previously documented in response to cold.

As *CBF1* was found to be upregulated in response to low K^+, and its target *GA2ox6* was also found to be upregulated, the role of this gene in the reduced LR growth phenotype was investigated further. The SENSITIVE TO FREEZING6 (SFR6) protein, otherwise known as MED16, is known to act downstream of *CBF1* translation to recruit the core Mediator complex to cold-regulated genes in the activation of cold-responsive genes (Knight *et al.*, 2009; Hemsley *et al.,* 2014). It was hypothesised that in the *sfr6-1* mutant (Knight *et al.*, 1999), the activation of *GA2oxs* and DELLAs by CBF1 may be blocked in response to low K^+. The reduction in LR growth in response to low K^+ is partially attenuated in the *sfr6-1* mutant when LR growth is measured over 3 d low K^+ treatment (Fig. 6-2A). An attenuated LR growth response was also seen after 8 d growth (Fig. 6-2B). However, this 8 d experiment needs to be repeated before any firm conclusions can be drawn because the WT was measured in a separate experiment. This

attenuation of the reduced LR growth response in the *sfr6-1* mutant may suggest a role for *CBF1* and *SFR6* in the regulation of LR growth in response to low K^+. SFR6 (MED16) has also been shown to function in the regulation of iron uptake gene expression (Yang *et al.,* 2014; Zhang *et al.,* 2014) therefore it could suggest a possible pathway for the iron and K^+ starvation transcriptional profile overlap.

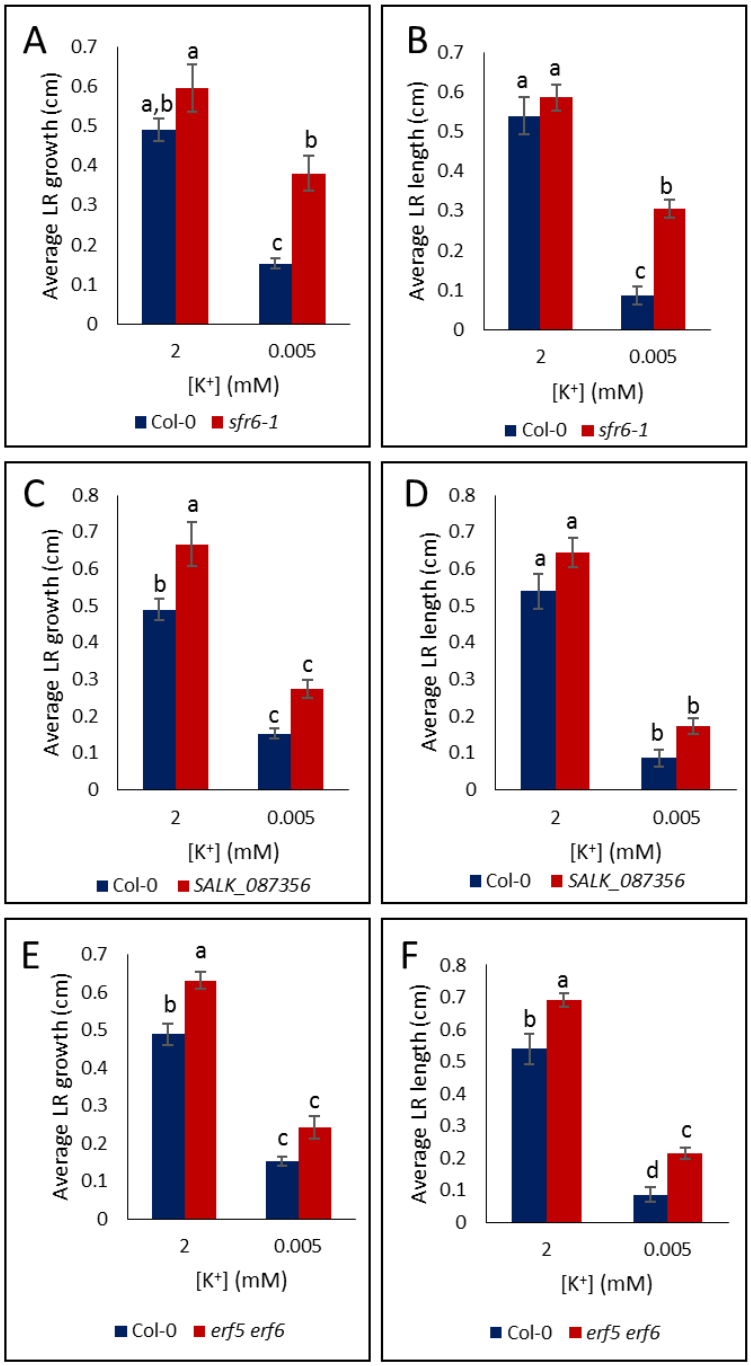

Fig. 6-2: Average LR growth over 3 d K^+ treatment (A,C,E) and LR length after 8 d K^+ treatment (2 mM or 0.005 mM) (B,D,F). Mutant seedlings of *sfr6-1* (A,B)*, SALK_087356* (mutant in the *ERF6* gene) (C,D) and *erf5 erf6* double mutant (E,F) compared with WT (Col-0). Seedlings grown for 9 d (A, C, E) or 4 d (B, D, F) on ½ MS10 before transferral to K^+ treatment. Values are averages taken from at least 9 individual seedlings ± SE. Letters indicate significance with a Tukey Pairwise comparison $P< 0.05$. Control for 8 d analysis (B,D,F) taken from another experiment.

6.2.3 The role of *ERF6* in regulating reduced GA/ increased DELLA in response to low K^+

ETHYLENE RESPONSIVE ELEMENT BINDING FACTOR 6 (ERF6) is a member of one of the largest families of plant transcription factors, the APETALA2/ETHYLENE RESPONSE FACTORs (AP2/ERF) superfamily. Characterized as containing the AP2/ERF DNA binding domain, the ERFs contain only 1 AP2/ERF domain and make up 122/147 AP2/ERF superfamily in Arabidopsis (Moffat *et al.*, 2012). The ERFs act as downstream components of the ethylene signalling pathway and are known to act as regulatory hubs integrating crosstalk between many hormone and signalling components in response to abiotic and biotic stresses (Müller & Munné-Bosch, 2015). *ERF6* was identified from the differentially expressed data in response to low K^+ due to its upregulation after both 3 h and 30 h K^+ starvation (3 h; 0.93 $\log_2$fc, 30 h 0.84 $\log_2$fc) (Fig. 6-3). Enhanced *ERF6* expression has been shown to inhibit cell proliferation and leaf growth through transcriptional induction of *GA2ox6* and a stabilisation of DELLAs (Dubois *et al.*, 2013). This has been proposed as a pathway linking ethylene with reduced growth, as ERF6 is phosphorylated by MPK3 and MPK6 (P. Wang *et al.*, 2013), which are both downstream of the ACC-independent of EIN2 signalling pathway (Yoo *et al.*, 2008).

Data in this thesis show that in response to low K^+ there is an increase in the transcription of *GA2ox6* (Fig. 5-16A) and an accumulation of DELLA proteins (Fig. 5-17). It was therefore proposed that the transcriptional increase of *ERF6* in response to low K^+ (Fig. 6-3) could lead to reduced GA, stabilised DELLAs, and therefore reduced LR growth. This hypothesis was investigated by conducting growth analyses with a SALK mutant (*SALK_087356*) which has an insertion in the exon of the *ERF6* gene (Fig. 6-4). The double mutant *erf5 erf6* was also investigated because of known redundancies between the *ERF5* and *ERF6* genes (Moffat *et al.*, 2012) and because *ERF5* was also upregulated in the RNA-seq data (3 h 0.52 $\log_2$fc).

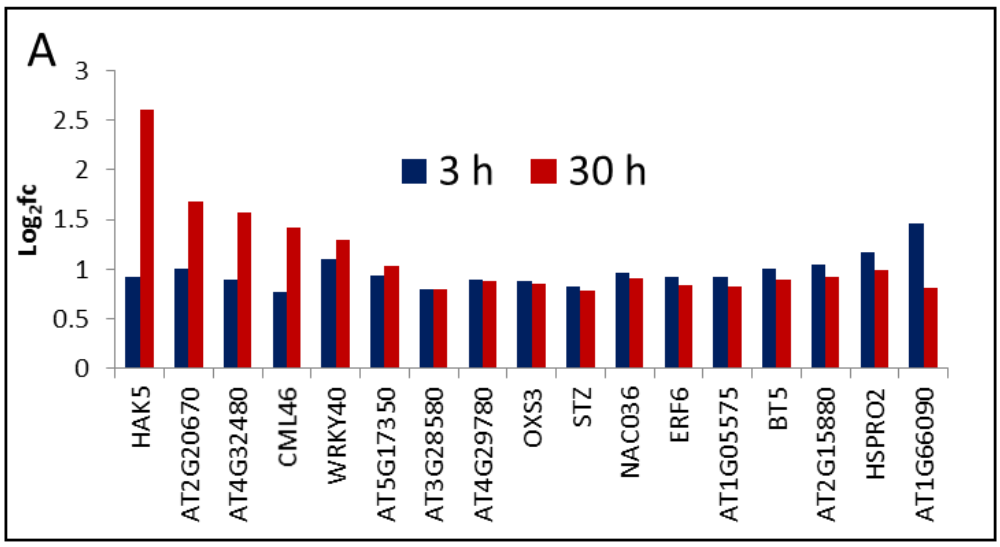

B AGI	Gene	3 h log_2fc	30 h log_2fc
AT4G13420	*High affinity K+ transporter 5 (HAK5)*	0.92	2.60
AT5G39670	*CML46 Calcium-binding EF-hand family protein*	0.77	1.41
AT1G80840	*WRKY DNA-binding protein 40(WRKY40)*	1.11	1.29
AT1G27730	*Salt tolerance zinc finger (STZ)*	0.83	0.79
AT4G17490	*Ethylene responsive element binding factor 6(ERF6)*	0.93	0.84

Fig. 6-3: (A) All genes upregulated after 3 h and 30 h K^+ starvation treatment, above 0.75 log_2 fold change (log_2fc) represented as a graph showing fold changes after both time points. (B) Table of genes selected for further analysis, as explained in text, with log_2 fold changes (log_2fc). *HAK5* K^+ transporter included for comparison.

LR growth was not restored under low K^+ treatment (after 3 d or 8 d) in either the *SALK-_087356* or the *erf5 erf6* mutants (Fig. 6-2C–F), suggesting that these genes do not play a role in the reduced LR growth phenotype in response to low K^+. The 8-d growth analysis needs to be repeated for further verification because the WT was measured in a separate experiment. However, these preliminary results support previous work in this thesis suggesting that ethylene does not play an important role in the reduced LR growth response to low K^+ (see section 5.3).

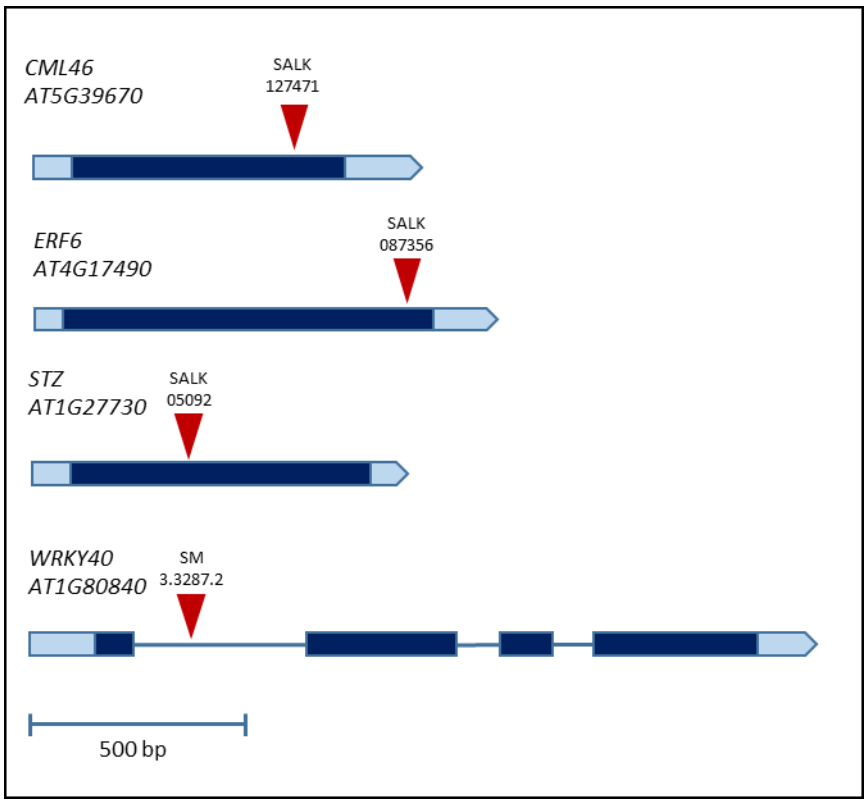

Fig. 6-4: Schematic representation of the T-DNA insertion sites for the selected genes. Sites were obtained from TAIR. Dark blue boxes represent the exons, blue lines represent introns, light blue boxes represent 5' and 3' untranslated regions (UTRs), and red triangles mark the insertion sites.

6.3 Early signalling candidates identified from the RNA-Seq data

6.3.1 Selection of candidate genes

As well as the TFs with known roles in GA signalling, the RNA-Seq data were mined for other genes that could be playing key roles in the early signalling response to low K^+. The *HAK5* high affinity K^+ transporter gene stood out immediately in the RNA-Seq data, with an increase of 0.92 $\log_2$fc after 3 h and 2.60 $\log_2$fc after 30 h, making it the second most upregulated gene after 30 h. This is not unexpected as *HAK5* is well documented for its upregulation after exposure to low K^+ conditions (Shin & Schachtman, 2004; Gierth *et al.*, 2005). Upregulation after only 3 h demonstrates that the drop in K^+ has been perceived, and signalling initiated, before the 3 h timepoint. It was proposed that the early signal perception and transduction machinery may be within the small number of differentially expressed genes found at both the 3 h and 30 h timepoints.

The Venny2.1.0 online tool was used to identify genes that were upregulated after 3 h as well as after 30 h. 17 genes were found to be upregulated over 0.75 log_2fc after both 3 h and 30 h of low K^+ treatment (Fig. 6-3A). It was decided that a smaller number of these genes would be studied in more detail. Those chosen were: *WRKY40, STZ, ERF6*, and a probable calcium binding protein *AT5G39670* (Fig. 6-3B). *AT5G39670,* was selected because it displayed a similar expression profile to *HAK5* in the RNA-Seq data (Fig. 6-3A), and *WRKY40, STZ and ERF6* were selected due to their previously characterized functions in abiotic stresses. To investigate the function of these genes in the low K^+ pathway, insertional mutants were identified and ordered from NASC (Fig. 6-4). Plants were genotyped and homozygous lines for the mutations (Fig. 2-1) were selected for *WRKY40, ERF6, STZ* and *AT5G39670*. Analysis of *ERF6* has been described in the previous section (6.2.3).

6.3.2 The role of *WRKY40* in reduced GA/increased DELLA in response to low K^+

The WRKY family of plant DNA-binding transcription factors are one of the largest families of transcriptional regulators in plants, Arabidopsis having 72 members (Bakshi & Oelmüller, 2014). They are known to play important roles in the plant defence response. They are also involved in many other biological processes, including the response to abiotic stress, nutrient deprivation and hormonal control and development (see Bakshi & Oelmüller, 2014 for a review). The *WRKY40* gene displayed strong upregulation after both 3 h (1.11 log_2fc) and 30 h (1.29 log_2fc), suggesting a strong and prolonged activation in response to low K^+. As well as a known role in ABA signalling (Chen *et al.*, 2010; Shang *et al.*, 2010; Geilen & Böhmer, 2015), WRKY40 has also been shown to bind to promoters of multiple stress inducible TFs including *DREB1A (CBF3),* repressing its expression (Shang *et al.*, 2010). The strong upregulation of *WRKY40* after 3 h K^+ starvation may therefore explain the downregulation of *CBF3* at the same timepoint. WRKYs have also been associated with reduced GA signalling and interactions with DELLAs under several conditions; OsWRKY70 is a negative regulator of GA biosynthesis during herbivore attack (Li *et al.*, 2015b), and WRKY26 has been shown to interact with the DELLA protein RGA *in planta* (Helen Riordan thesis 2015). *OsWRKY71,* which when compared to other known WRKY proteins from other species, shares the highest amino acid sequence similarity with the Wild Oat *ABF2* gene and Arabidopsis *WRKY40* (Zhang *et al.*, 2004), has been shown to act in the repression of GA signalling in aleurone cells in rice (Zhang *et al.*, 2004; Xie *et al.*, 2005). This suggests that WRKY40 may have a role in the GA response to low K^+. Mutation of the *WRKY40* gene (*SM 3.3287.2*) (Fig. 6-4) did not restore LR growth when seedlings were grown on low K^+ for 3 d or 8 d (Fig. 6-5A,B), suggesting that: (1) *WRKY40* does not play an important role in this process; (2) that there are redundancies in the pathway; or (3) that the mutation does not block gene function because the insertion site is in an intron (Fig. 6-4).

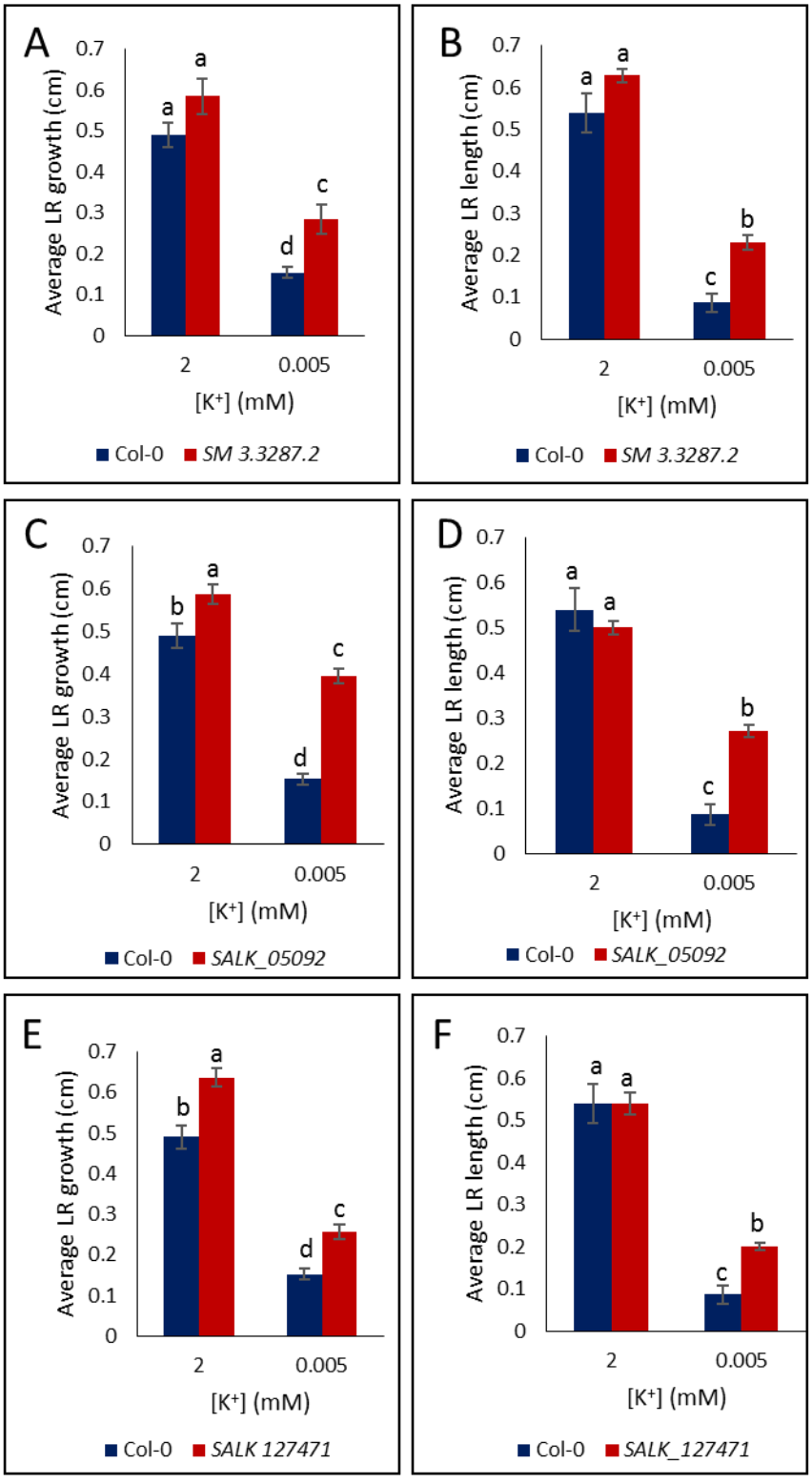

Fig. 6-5: Average lateral root (LR) growth over 3 d K^+ treatment (2 mM or 0.005 mM) (A,C,E) and LR length after 8 d K^+ treatment (B,D,F). Mutant seedlings of *SM 3.3287.2* (mutant in the *WRKY40* gene) (A,B), *SALK_05092* (mutant in the *STZ* gene) (C,D) and *SALK_127471* (mutant in the *CML46* gene) (E,F) compared to WT Col-0 (control). Seedlings grown for 9 d (A, C, E) or 4 d (B, D, F) on ½ MS10 before transferral to K^+ treatment. Values are averages of at least 9 individual seedlings ± SE. Letters indicate significance with a Tukey Pairwise comparison $P<$ 0.05. Control for 8 d analysis (B,D,F) taken from another experiment.

6.3.3 The role of *STZ* in reduced GA/ increased DELLA in response to low K^+

SALT TOLERANCE ZINC FINGER (*STZ*), also known as *ZAT10*, is a member of the C_2H_2 zinc finger family of TFs and is known to be involved in biotic and abiotic stress signalling (Sakamoto *et al.*, 2000; Sakamoto, 2004), stress tolerance, and attenuating detrimental reactive oxygen species (ROS) effects (Mittler, 2002; Davletova *et al.*, 2005; Miller *et al.*, 2008). Overexpression of *STZ* has been shown to cause a reduced growth phenotype in Arabidopsis rosette stage plants (Park *et al.*, 2015), therefore it was hypothesized that *STZ* could be playing a role in reduced growth of LRs in response to low K^+. The SALK mutant (*SALK_05092*) was used to investigate the role of *STZ* in the low K^+ response. LR growth was measured after 3 d and 8 d in the low K^+ treatment. The LRs were longer in the mutant under low K^+ than the WT, suggesting an attenuation in the reduced growth response (Fig. 6-5C,D). After 8 d growth, the PR length was also reduced under low K^+ in the *SALK_05092* mutant (Appendix VII). This was the opposite phenotype to the WT; with the mutant showing reduced PR and longer LRs, compared with the WT maintenance of PR and reduction of LRs. This suggests that the *STZ* gene may be important in regulating the root architectural response to low K^+. It is necessary however to complete further repeats on the 8 d treatment as the control was conducted in a separate experiment.

6.3.4 The role of *AT5G39670 CML46* in reduced GA/increased DELLA in response to low K^+

The intrinsic role of the calcium ion (Ca^{2+}) in the regulation of the cellular response to abiotic and biotic stress is well established (reviewed by Dodd *et al*., 2010), with documented cell type-specific responses to cold, osmotic and salt stress in the Arabidopsis root (Kiegle *et al.*, 2000). Calmodulin (CaM) and CaM-like (CML) proteins are a family of EF-hand Ca^{2+} sensors in plants (Bender & Snedden, 2013). Considerable work has been carried out characterizing the roles of CaMs as Ca^{2+} sensors, whereas less has been done looking at the large CML family, which has 50 members in Arabidopsis (McCormack & Braam, 2003).

The *AT5G39670* gene was identified from the RNA-Seq data as showing an increased level of expression after 3 h and 30 h low K^+ treatment (Fig. 6-3). The gene encodes a probable calcium binding protein defined by UniProt as *CML45* but by McCormack & Braam, (2003) as *CML46*. Many of the gene ID numbers and CaM nomenclature do not match between UniProt and McCormack & Braam (2003), and the TAIR database has not been updated with a gene name; it will hereby be referred to as *CML46*. There is also discrepancy between the number of EF-hand domains associated with the gene; however, all agree that this gene is likely to be associated with calcium binding and is a member of the CML family. McCormack & Braam (2003) identified, through expressed sequence tags (ESTs), that *CML46* is only expressed in

roots (of the tissues analysed) and in response to stress and/or hormones. It was therefore hypothesized that *CML46* could be a component of a root-specific low K^+ stress response.

The activated GID1 receptor has been shown to trigger an increase in cytoplasmic Ca^{2+} concentrations in aleurone cells (Gilroy & Jones, 1992), and McCubbin *et al.* (2004) identified a Ca^{2+}-dependent protein kinase which they suggested mediated Ca^{2+} dependent events in the GA response. These studies indicate that there may be some level of interaction between the GA/DELLA signalling pathways and Ca^{2+} signalling. CML46 may also be playing a role in the perception or early signalling of K^+ starvation, as many external signals are sensed by the plant through rapid changes in calcium levels in the cytosol (Luan *et al.*, 2002; Dodd *et al.*, 2010). The phenotype of the *SALK_127471* mutant, which has an insertion in the *CML46* gene (Fig. 6-4), was investigated in response to low K^+. It was found to have no effect on LR growth (Fig. 6-5E,F), in response to low K^+, when compared with the WT response. This suggests that *CML46* may not be playing a major role in the root architectural changes in response to low K^+, or that there are functional redundancies because of closely related members of the gene family.

6.4 Conclusion

Analyses described in this chapter have aimed to improve understanding of the upstream signalling components that cause the hormone level changes and root architectural changes in response to low K^+. A number of potential pathways to reduced GA, increased DELLA were identified from the RNA-Seq data, and literature and gene expression data were used to link previously published work to the experimental evidence presented here. More work should be carried out on all genes to conclusively identify whether they have a role in the low K^+ pathway. However, mutations in the *SFR6* and *STZ* genes cause an attenuated reduced LR growth phenotype in response to low K^+, suggesting that they may be important in this response. *SFR6* acts downstream of CBF1 which was upregulated in response to low K^+, and is also known to reduce GA levels through modulating gene expression. Therefore, the attenuated growth response of the *sfr6-1* mutant suggests that there could be a role for this regulon in the reduction of LRs in response to low K^+. *STZ* has not been linked in the literature to reduced GA signalling. Therefore, the attenuated response in the SALK mutant (*SALK_05092*) may suggest that there is an alternative pathway also reducing growth of LRs, acting through *STZ.*

7 Discussion

7.1 Introduction

K^+ starvation is a major limitation of crop yields worldwide and the root systems of plants are essential for the uptake of K^+ from the soil (Maathuis & Sanders, 1994). Understanding how plants respond to reduced K^+ levels could be important to allow manipulation of root systems for increased crop production in the future. The primary aim of the work described in this thesis was first to characterise the root architectural growth response to low K^+. Subsequent work was focused on understanding the mechanisms by which these changes (specifically the reduction in lateral root (LR) growth) occur. The approach was to use RNA-Seq to identify transcriptomic changes in response to low K^+. Using these data, hypotheses were constructed for the potential involvement of the ethylene, gibberellin (GA), auxin and reactive oxygen species (ROS) pathways in the control of changes in root architecture in response to low K^+. These hypotheses were tested experimentally in the plant, revealing a role for GA and DELLA signalling in the reduction in LR growth in response to low K^+. The final experimental chapter returns to the RNA-Seq data and uses previously published literature to construct hypotheses relating to the identity of possible upstream signalling modules involved in the control of the hormone-mediated responses.

The objectives of the current chapter are to highlight important aspects of the research in this thesis, to discuss the wider implications of the work and to suggest ideas for further investigation. The hypotheses generated from work in this thesis and analysis of published literature has allowed the construction of (Fig. 7-1), a model of hypothesised pathways resulting from exposure to low K^+. This figure will be referred to throughout this chapter and the supporting data and rationale behind each hypothesis will be discussed in greater detail in the text.

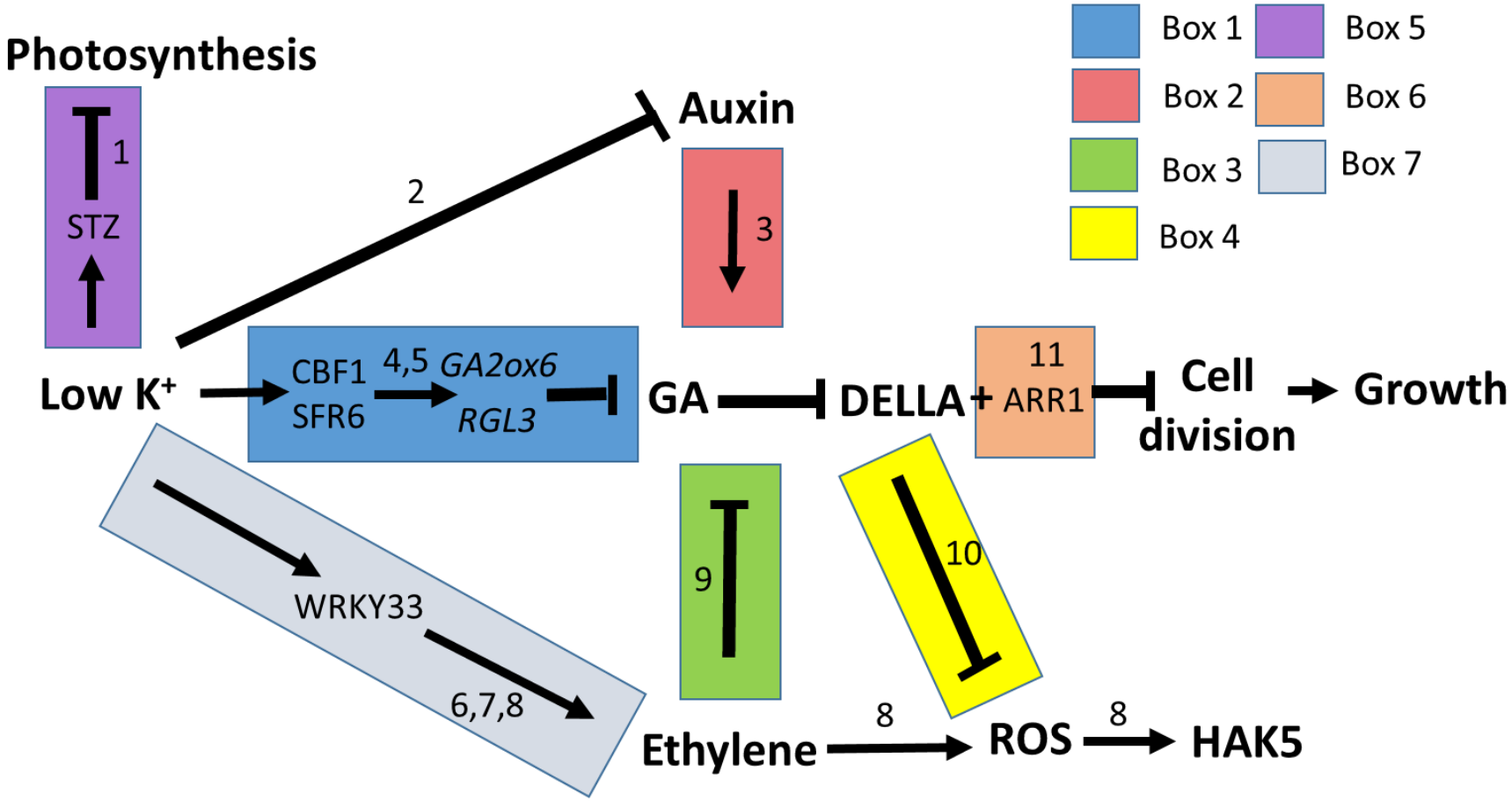

Fig. 7-1: Hypothesised pathways resulting from exposure to low K^+, in the Arabidopsis accession Col-0. Hypotheses generated from results presented throughout the thesis and from previously published literature (numbers). Arrows, hypothesised positive interaction; T-bars, inhibition or a negative relationship. GA, gibberellic acid; ROS, reactive oxygen species. Coloured boxes refer to each hypothesis and are referred to in the text. Numbers refer to published literature: 1, Maruyama *et al.* (2004); 2, Shin *et al.* (2007); 3, Fu & Harberd (2003); 4, Achard *et al.* (2008a); 5, Knight *et al.* (2009); 6, Li *et al,* (2012); 7, Shin & Schachtmann (2004); 8, Jung *et al.* (2009); 9, Achard *et al.* (2003); 10, Achard *et al.* (2008b); 11, Marín-de la Rosa *et al.* (2015). See the text for further details of hypotheses and for the rationale behind them.

7.2 Phenotypic response to low K^+

Through measurements of primary root (PR) and LR growth, it was established that, in response to low K^+, Col-0 maintains the growth of the PR. By contrast, the growth of LRs is reduced (Figs 3-1 to 3-3). It was established that LR initiation, LR primordia (LRP) development, LR emergence and LR meristem establishment were all unaffected by low K^+. However, the elongation of the LRs was impaired by K^+ starvation (Fig. 3-4). Confocal microscopy and GUS reporter studies were utilised to show that the LR meristems remain functional under low K^+, but cell division was reduced and a reduction in meristem size was observed (Figs 3-6, 3-7).

7.3 The reduction in LR growth seen in response to low K^+ requires gibberellin (GA) and DELLA signalling

As hormonal signalling is essential for growth and developmental patterning, the role of hormones was investigated in the reduced LR growth phenotype seen in Col-0 in response to low K^+. Work in this thesis suggests an important role for GA and DELLA signalling in this reduced LR growth response.

7.3.1 Reduced GA levels and increased DELLA in response to low K^+

Gene expression studies using RNA-Seq and qRT-PCR identified an increase in the expression of the GA deactivation dioxygenase gene *GA2ox6* (Fig. 5-16A), as well as an initial downregulation of a GA biosynthesis gene *GA3ox2* (Fig. 5-16B), suggesting that there is a reduction in the GA levels in response to low K^+. A reduction in GA levels was further supported by the increased levels of the DELLA protein RGA in the LRs of seedlings grown under K^+-starved conditions (Fig. 5-17A,B). As DELLAs are known to be stabilized by reduced levels of GA, this further supported a reduction in GA levels in the LRs in response to low K^+. These findings were further supported by the restoration of LR growth, and cell division under low K^+ conditions by the supplementation of GA to the growth media (Figs 5-18, 5-19). Together these data suggest that in response to K^+ starvation, there is a decrease in bioactive GA levels, which leads to the stabilization of DELLA proteins in the LRs, which then reduces cell division and growth in the LR meristems, producing the reduced growth phenotype (Fig. 7-2).

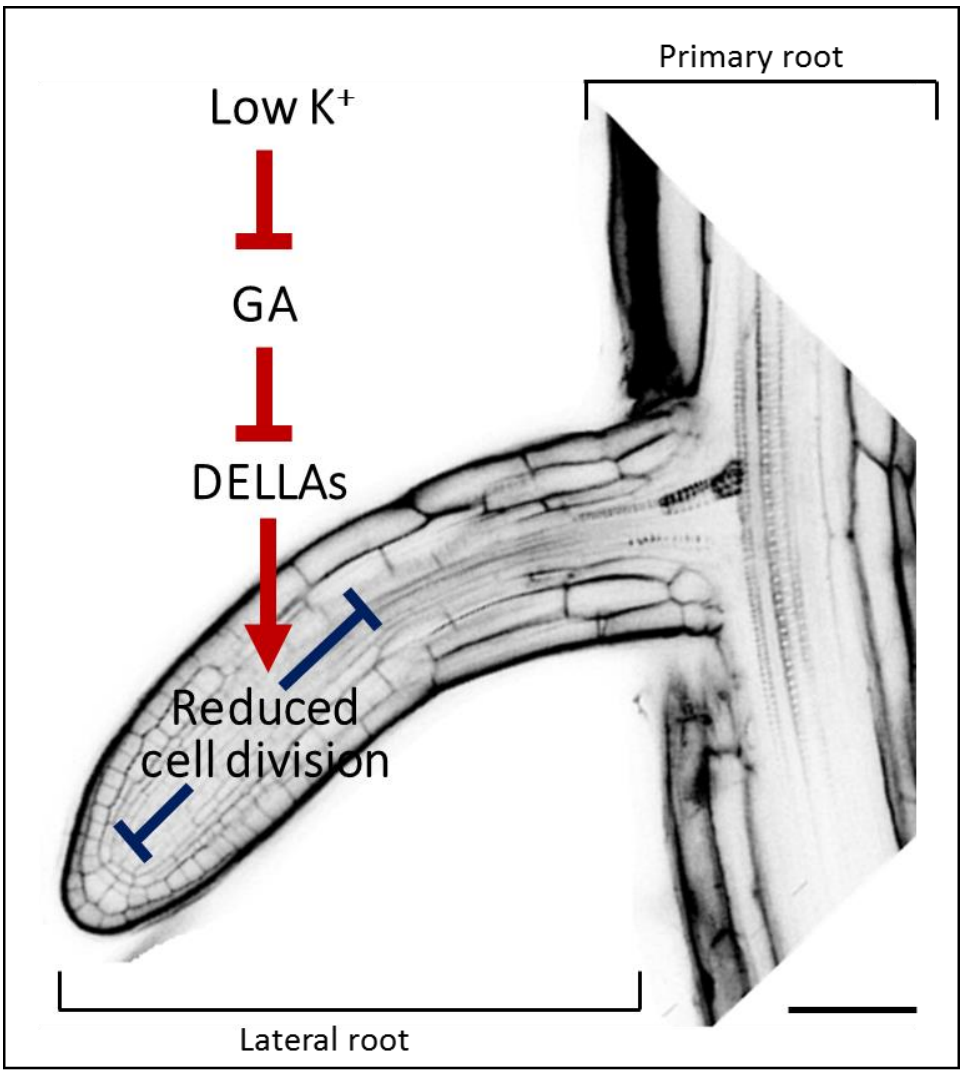

Fig. 7-2: A model for how low K^+affects lateral root growth through GA and DELLAs in the Arabidopsis accession Col-0. Arrows indicate a positive interaction, T-bars indicate inhibition or a negative relationship. Scale bar = 50 µm.

7.3.1.1 Mediation of reduction of GA levels

The data presented here suggest that the reduction in GA is being regulated at a number of levels. The first is through increased GA deactivation, as shown through increased expression of *GA2ox6* after 54 h and 72 h K^+ starvation (Fig. 5-16A). The second level is through reduced biosynthesis of GA; however the data presented here are not conclusive. An initial reduction in biosynthesis was seen in the RNA-Seq data, with a downregulation of the *GA3ox2* biosynthetic gene after 3 h. However, qRT-PCR studies did not identify a difference in expression levels of *GA3ox2* between the high and low K^+ conditions at any of the timepoints investigated (Fig. 5-16B). Data on the expression levels of *GA3ox1* showed a small increase in expression levels after 54 and 72 h K^+ starvation (Fig. 5-16C). Increased DELLA activity had been found to increase expression of *GA20ox1* and *GA3ox1* and decrease levels of *GA2ox* through a feedback

mechanism (Hedden & Kamiya, 1997; Cowling *et al.*, 1998; Thomas *et al.*, 1999; Xu *et al.*, 1999). *GA3ox1* is a known direct target of DELLA proteins (Zentella *et al.*, 2007), therefore this could suggest the reason why an increase is seen in *GA3ox1* expression in response to low K^+. This suggests that GA levels could also be being controlled through a feedback loop with DELLA proteins in response to low K^+.

7.3.2 Linking low K^+ to reduced GA levels and increased DELLA protein levels

The level of regulation of this downregulation of GA and increased DELLAs is still very speculative. The final results chapter (Chapter 6) amalgamated data from previous results chapters, bioinformatic studies and literature searches to propose hypotheses for ways in which this GA/DELLA pathway may be being regulated in response to low K^+. Only very basic phenotyping experiments were carried out to investigate proposed pathways, and further repeats are needed on the 8-d studies; however it did go some way to suggest some promising routes for further analysis.

7.3.2.1 The role of the CBF regulon

The CBF1 transcription factor was identified from the RNA-Seq data due to its upregulation after 3 h low K^+ treatment (0.80 log_2fc), and due to its known role in reducing GA and increasing DELLA signalling (Achard *et al.*, 2008a). *SFR6* is known to act downstream of *CBF1,* post translationally, and a mutation of the *SFR6* gene (*sfr6-1)* partially restored the LR growth under low K^+ stress (Fig. 6-2A,B). This suggests that *CBF1* and *SFR6* may be important in the LR growth reduction in response to low K^+. This is further supported by the upregulation of one of the *CBF1* target genes *GA2ox6* in response to low K^+ (Fig. 5-16A). *SFR6* is targeted to the nucleus, and has been hypothesised to have a direct role on the modulation of gene expression (Knight *et al.*, 2009). Therefore, it could be through *SFR6* that *CBF1* is activating GA deactivation genes. *CBF1* is also known to increase the transcript level of the DELLA gene *RGL3* (Achard *et al.*, 2008a), therefore it would be interesting to analyse the gene transcriptional levels of *RGL3* in response to low K^+ (see Fig. 7-1, box 1). It would also be interesting to look at CBF1 target gene transcription in response to low K^+ in the *sfr6-1* mutant, to suggest whether *SFR6* is also acting downstream of *CBF1* in response to low K^+. Recent advances in CRISPR/Cas9 technology (Bortesi & Fischer, 2015) has also allowed the production of *cbf* single, double and triple mutants (Jia *et al.*, 2016; Zhao *et al.*, 2016; Shi *et al.,* 2017). It would be interesting to characterize root architectural phenotypes of these mutants in order to identify if LR growth is still impaired in response to low K^+ or if the mutations block the GA/DELLA mediated growth reduction.

7.3.2.2 The role of the transcription factor STZ

A mutation in the *STZ* gene (*SALK_05092*) led to an attenuation of the reduced LR growth seen in the WT in response to low K^+ (Fig. 6-5C,D). The mutant also displayed a reduction in the growth of the PR in response to low K^+ (Appendix VII). Genetic complementation and the creation of multiple mutant alleles need to be completed to verify that it is the *STZ* gene that is causing the phenotype observed. However, these preliminary data suggest that *STZ* could play a role in reducing LR growth in response to low K^+. Although overexpression of *STZ* has previously been linked to reduced growth phenotypes, the growth response was thought to be independent of GA/DELLA signalling, as expression of *GA2ox3, GA2ox6* and *RGL3* were unchanged in the overexpressor (Park *et al.*, 2015). As the experiments reported in this thesis have shown that a mutation in this gene restores some LR growth in response to low K^+, this may suggest that in the WT, *STZ* acts in the reduction of LR growth in response to low K^+, in a GA/DELLA independent pathway. To investigate this further, gene expression levels of GA/DELLA regulating genes could be analysed in the mutant and compared with their levels in the WT.

Interestingly, it was shown in this thesis that in response to low K^+, the *SALK_05092* mutant (mutation in the *STZ* gene), appears to display a root architectural phenotype more similar to Arabidopsis accessions such as Oystese-0 (Oy-0), rather than to its background accession Col-0 (Kellermeier *et al.*, 2013) (Fig. 1-4). The *SALK_05092* mutant displayed a reduction in PR growth, but a maintenance of LR growth (Fig. 6-5C,D; Appendix VII), rather than reduced LR growth and maintained PR growth seen in Col-0 (Kellermeier *et al.*, 2013). It could therefore be hypothesised that *STZ* is an important gene in defining the root architectural response to low K^+ across different Arabidopsis accessions. It would be interesting to complete a sequence alignment of the *STZ* gene between different Arabidopsis accessions, and to also analyse the gene expression profiles in response to low K^+. By conducting these experiments, it might be possible to identify differences or patterns that are specific to different architectural responses to low K^+.

7.3.2.3 The role of *ERF6, WRKY40* and *CML46* in the low K^+ architectural response

The role of other genes in the reduced LR growth response to low K^+ were also investigated in this thesis. *ERF6, WRKY40* and *CML46* were all investigated because of their known roles in the reduction of GA levels, or due to their strong upregulation in response to both 3 h and 30 h K^+ starvation. Each gene was investigated through literature searching and LR growth analysis of an insertional mutant associated with the gene. In each case, the insertion was not able to

restore LR growth when the mutant was grown on low K^+, therefore suggesting that the gene does not play a key role in the LR growth response (Figs 6-2C–F, 6-4A,B,E,F). It is not possible, however, to rule out the involvement of the genes in the LR growth response as there may be other factors which are preventing the phenotype from being observed. For example, there may be redundancies in the pathway, which mask the role of the gene. In the case of *WRKY40*, the insertion is in the intron of the gene, and consequently the protein may still remain functional even with the insertion present. Therefore, there are many reasons why the roles of these genes cannot be discounted in the architectural response to low K^+, however work in this thesis has not provided any evidence to suggest they are playing a role.

Another transcription factor (TF) upregulated in response to low K^+, and with known roles in DELLA accumulation and reduced GA biosynthesis, was *JUNGBRUNNEN1* (*JUB1*), a H_2O_2-induced NAC TF (Wu *et al.*, 2012; Shahnejat-Bushehri *et al.*, 2016) (30 h, 1.33 log_2fc; Fig. 4-14). A mutant in this gene was not obtained for the work in this thesis, but the role of *JUB1* could be investigated in the future.

7.4 Investigating the roles of other hormones and ROS in the K^+-starvation response

The data presented in this thesis did not identify roles of other hormones or ROS in the reduced LR growth response to low K^+; however, the transcriptomic data suggests the levels of these hormones and ROS may be being affected by low K^+. As the RNA-Seq experiment was carried out on whole seedlings, responses of the whole plant to low K^+ are represented in the transcriptomic data. In this next section, I will discuss briefly the role of the hormones auxin and ethylene, and the role of ROS in the LR growth response through an overview of the data presented here. I will touch briefly on the potential roles that they may be having in the plant in response to low K^+.

7.4.1 Auxin

7.4.1.1 Auxin signalling is not sufficient to reduce LR growth in response to low K^+

Auxin is known to have important roles in the maintenance of meristem size and activity, however data in this thesis suggest that auxin signalling is not sufficient to cause the reduced LR growth phenotype in response to low K^+. No changes were observed when the media were supplemented with IAA, or NPA, or when the auxin mutant *aux1-7* was investigated. There was also no observed change in auxin distribution in the LRs in response to low K^+. This suggests that auxin signalling is unaffected in the LRs under low K^+, and that cell division in the LRs is

being modulated by an auxin-independent system. Although data in this thesis do not support a role for auxin in the reduced LR growth response to low K^+, a reduction in free IAA concentration has been identified in response to low K^+ (Shin *et al.*, 2007). Auxin is known to promote the GA-mediated deactivation of DELLAs (Fu & Harberd, 2003), and as a result reduced auxin might not be essential in the reduction of LR growth in response to low K^+, however it may contribute to the stabilization of DELLAs and therefore contribute to the overall response (see Fig. 7-1, box 2). It is also possible that changes in auxin signalling is important in the maintenance of PR growth in response to low K^+. It would be possible to investigate this hypothesis by measuring PR growth in response to low K^+ on media supplemented with IAA or with NPA.

7.4.2 Ethylene

7.4.2.1 Ethylene signalling is not sufficient to reduce LR growth in response to low K^+

Another hormone that was suggested to act in the reduction of LR growth in response to low K^+ was ethylene. Data in this thesis do not support an important role for ethylene in the LR growth reduction in response to low K^+. This was demonstrated as despite an increase in ethylene signalling in response to low K^+ (Fig. 5-7), blocking ethylene signalling using Ag^{2+} and the use of ethylene signalling mutants did not restore LR growth under low K^+ conditions (Figs 5-8, 5-9). Ethylene is known to inhibit root growth; however it has been documented that it does so primarily through its effect on cell elongation, rather than affecting cell division and meristem activity (Ruzicka *et al.*, 2007). As the reduction in LR growth in response to low K^+ was shown in this thesis to be through a reduction in cell division (Fig. 3-7) rather than a reduction in cell elongation (Fig. 3-8), this fits with the suggestion that ethylene is not playing a key role in the reduced growth phenotype.

An increase in ethylene levels is a well characterized response to low K^+ (Shin & Schachtman, 2004; Jung *et al.*, 2009). Ethylene is also known to inhibit the GA induced degradation of GFP-RGA (Achard, 2003) it is possible that an increase in ethylene may also be contributing to the higher levels of DELLA in response to low K^+ (see Fig. 7-1, box 3). Hormonal crosstalk is very complex and so it is difficult to rule out the influence of hormones such as auxin and ethylene in a role in the reduced LR response to low K^+. However, data in this thesis suggest that their individual involvement is not sufficient to create the reduced LR growth response that is seen here.

7.4.3 ROS

7.4.3.1 ROS production is not sufficient to reduce LR growth in response to low K^+

Data from this thesis suggest that an increase in ROS does not play an instrumental role in the reduced LR growth response to low K^+. This was indicated by growth of the LRs under low K^+ being unable to be restored in the ROS *rboh* mutants or when ROS was blocked using DPI (Fig. 5-14). Work has already identified a role for ROS in the upregulation of K^+ transporters in response to low K^+ (Jung *et al.*, 2009) but work in this thesis was unable to identify whether ROS was also acting in a similar role in the regulation of uptake transporters in the LRs in response to low K^+.

7.4.3.2 DELLA reducing ROS accumulation as a stress tolerance mechanism

DELLA proteins have been shown to reduce stress induced ROS accumulation by acting on the ROS scavenging system (Achard *et al.*, 2008b). It has been proposed that this is through the elevated expression levels of ROS detoxification enzymes, such as Cu/Zn-superoxide dismutases (CSDs) and catalases, which reduces ROS accumulation (Achard *et al.*, 2008b). It is possible therefore that there is not a large increase in ROS levels in the LRs in response to low K^+ due to the increased DELLA accumulation (see Fig. 7-1, box 4). It is suggested that this could be a stress tolerance mechanism, and might explain why the LR meristems remain functional, even under prolonged severe K^+ starvation. To test if DELLAs are acting to restrain ROS in response to low K^+ the HyPer line (Belousov *et al.*, 2006) could be used to visualize ROS levels in LRs. If DELLAs act to restrain ROS accumulation in response to low K^+, then addition of GA to the growth medium should cause the degradation of DELLAs and therefore an increase in ROS, because the restraint has been lifted.

7.5 Links between other stress pathways

A reduction in GA levels leading to DELLA accumulation and inhibition of growth has also been identified as a key response to salt, cold, osmotic stress and low phosphate signalling (Achard *et al.*, 2006, 2008a,b; Jiang *et al.*, 2007; Magome *et al.*, 2008; Dubois *et al.*, 2013; Rowe *et al.*, 2016). Each pathway identifies GA deactivation as a key point of control, with increased transcriptional regulation of *GA2ox* genes in each pathway (Jiang *et al.*, 2007; Achard *et al.*, 2008a; Magome *et al.*, 2008; Dubois *et al.*, 2013) (Fig. 7-3). Work in this thesis has identified another abiotic stress response mediated by reduced GA and increased DELLA action, leading to a reduction in growth (Fig. 7-3). This thesis presents a model where growth is being restricted specifically in the meristems of LRs in response to low K^+.

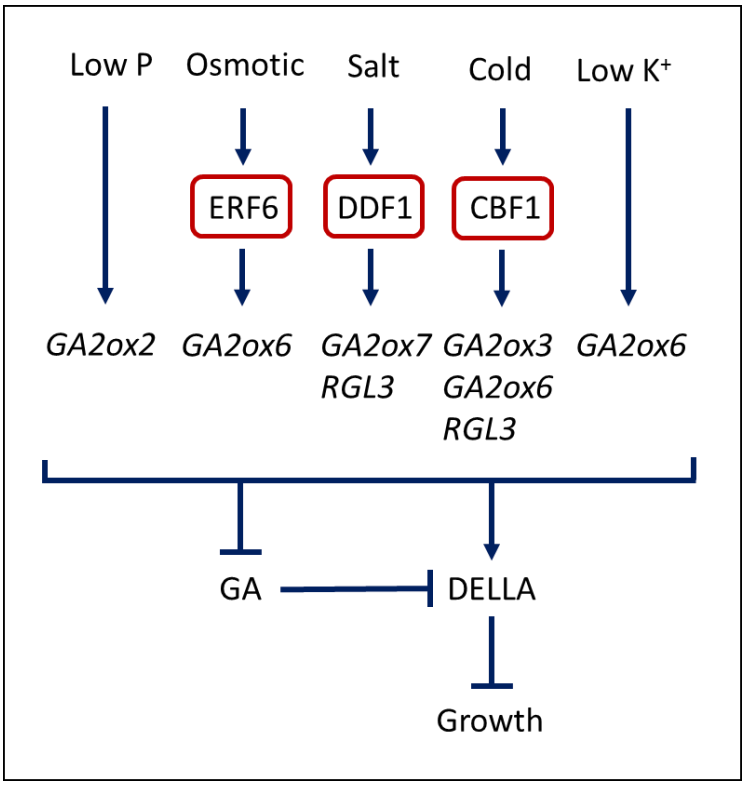

Fig. 7-3: Upregulation of members of the *GA2ox* family of GA deactivating genes and the *RGL3* DELLA gene in response to various abiotic stresses; low P (Jiang *et al.,* 2007), osmotic stress (Dubois *et al.,* 2013), salt stress (Magome *et al.,* 2008), cold (Achard *et al.,* 2008a) and low K^+ (data presented in this thesis). Transcription factors known to upregulate these genes (red rectangles). Regulation of *GA3oxs* and *GA20oxs* not included. Arrows indicate positive interactions, T-bars indicate inhibition or a negative relationship. Figure adapted from Colebrook *et al.* (2014), with data incorporated from Jiang *et al. (*2007), Achard *et al.* (2008a), Dubois *et al.* (2013), Magome *et al.* (2008) and data from this thesis.

7.5.1 Cold stress and K^+ starvation have overlapping transcript profiles

Data in this thesis suggest a link between the response to low K^+ and the response to cold, due to the upregulation of cold-responsive transcription factor *CBF1*, as well as a number of *COR* genes. A downregulation of a number of *COR* genes has previously been noted following the resupply of K^+ to K^+-starved seedlings (Armengaud *et al.*, 2004), further suggesting a link between the pathways. Interestingly, data in this thesis identified that, despite an upregulation of the *CBF1* gene in response to low K^+, there was a downregulation of another *CBF* gene, *CBF3* after 3 h K^+ starvation. The two genes have been grouped together in the past because they are regulated and function differently to the other member of the family *CBF2,* in response to cold (Novillo *et al.*, 2007); however in response to low K^+ they seem to be regulated differently. Despite this contradictory regulation, investigation of the downstream *COR* genes suggests that the pathway is being activated as both *COR15A* and *COR15B* are

upregulated after 30 h K^+ treatment. A previous report has suggested that upregulation of both *CBF1* and *CBF3* is required for the regulation of these genes under cold stress (Novillo *et al.*, 2007). As *CBF3* is downregulated after 3 h K^+, but not found to be differentially expressed from control conditions at 30 h, it could be hypothesised that after initial downregulation, the transcription is reactivated, and it just is not yet possible to observe this at the 30 h timepoint.

It would be interesting to look at the transcriptional regulation of the *CBF* genes and *COR* genes at later timepoints following K^+ starvation, to allow a larger picture of the potential integration of the two stresses, K^+ starvation and cold. Conducting root architectural analysis as well as K^+ starvation tolerance experiments on the *cbf* single, double and triple mutants (Jia *et al.*, 2016; Zhao *et al.*, 2016; Shi *et al.,* 2017) would provide clues about the roles of these genes in the K^+ response, and the links between the two pathways. These papers also conducted RNA-Seq analyses using the *cbf* mutants (Jia *et al.*, 2016; Zhao *et al.*, 2016; Shi *et al.,* 2017), and it would be interesting to conduct bioinformatic analysis comparing the transcriptional profiles with the low K^+ regulated genes to identify more overlap/differences. It would also provide more information about the differences in the regulation of the three CBF genes and how they mediate and participate in stress responses.

7.5.2 Iron and K^+ starvation transcriptional profile overlap

A link between iron (Fe) and K^+ deprivation was also identified in the RNA-Seq experiment conducted in this thesis; there was upregulation of a whole suite of genes known to be involved in in the Fe deficiency pathway in response to low K^+ (Fig. 4-9). The differentially expressed genes were not conclusive, however, as there was also downregulation of genes known to be positive regulators of the deficiency pathway, and upregulation of a number of negative regulators of Fe deficiency (Fig. 4-9).

K^+ addition is known to ameliorate the toxicity effects of Fe (Trolldenier, 1973; Becker & Asch, 2005), and this effect has been proposed to be as a result of reducing Fe uptake and translocation in the plant (Li *et al.*, 2001). It could be hypothesised that K^+ deficiency leads to a release on the inhibition of Fe uptake, thereby stimulating the Fe deficiency (or uptake) pathway. Alternatively, it could suggest that there is some level of conservation between the Fe and K^+ deficiency pathways, which has been identified within the low K^+ data as a stimulated Fe deficiency pathway. GA and DELLA activity has recently been shown to control the expression of iron regulated TFs and to limit growth in response to low Fe (Wild *et al.,* 2016), suggesting a possible link between low K^+ and low Fe, and SFR6 (MED16) was also

suggested in this thesis as a possible link between the pathways due to its known roles in gene regulation of iron homeostasis (Yang *et al.,* 2014; Zhang *et al.,* 2014). The interactions between different micro- and macro-nutrients are very complex and further work is required to investigate this proposed link between Fe and K^+.

7.6 Potassium and gravitropism

A link between potassium and gravitropism has been made a number of times in the literature (eg. Vicente-Agullo *et al.*, 2004; Ashley *et al.*, 2006), although the mechanistic details of the interaction are unknown. The work presented here, and previous analyses, provide more data to support the link. The agravitropic mutants *aux1-7* and *eir1* were shown here to display partially restored gravitropism in response to prolonged growth on low K^+ (Fig. 3-9B,D). Work here also identified a link between increased ethylene and increased degree of gravitropic growth (Fig. 3-10B). Although the work here was not able to establish a mechanism by which this is occurring, appropriate genetic resources for future study (in the form of crosses) were generated to allow further investigations into the link between K^+ and gravitropism.

7.6.1 Data in this thesis suggests that exogenous application of auxin is unable to restore gravitropism in agravitropic mutants

Vicente-Agullo *et al.* (2004) identified that supplementation of 80 nM IAA was sufficient to restore gravitropism in the *trh1* auxin mutant, however, results presented here show that application of 200 nM IAA was not able to restore gravitropism in *aux1-7* (Fig. 3-10C). It is possible that 200 nM was too high a concentration for the mutant. However, previous studies have suggested that the low diffusion rate of IAA is unable to overcome the severely disrupted auxin transport of the *aux1-7* mutant, and therefore is unable to restore the gravitropic nature (Marchant *et al.*, 1999). Gravitropism has been shown to be restored in the *aux1*-7 and *trh1* mutants through the addition of 1-NAA (Marchant *et al.*, 1999; Vicente-Agullo *et al.*, 2004), which is likely due to the fact that its distribution does not require polar auxin transport (Marchant *et al.*, 1999). It would be interesting to investigate whether the addition of 1-NAA would restore gravitropism in the *aux1-7* mutant, and how this would affect the impact of K^+ on the restoration of gravitropism.

7.6.2 Role of ethylene in the restoration of gravitropism in low K^+

The known upregulation of the hormone ethylene in response to low K^+ (Jung *et al.*, 2009) led to its investigation in this gravitropism response in this thesis. By blocking ethylene action

using Ag^{2+}, and supplementing the media with an ethylene precursor (ACC), it was possible to reveal a role for ethylene in this restoration of gravitropism. After 8 d treatment, it was shown that ACC restores gravitropism under both high and low K^+, whereas Ag^{2+} abolishes the restoration under both K^+ concentrations (Fig. 3-10B). Ethylene is upregulated under low K^+, therefore it is reasonable to hypothesise that the restoration of gravitropism under low K^+ is due in part to the increase in ethylene.

The role of ethylene in root gravitropism is controversial. Some results report a negative role for ethylene (Buer *et al.*, 2006; Ma & Ren, 2012), whilst others report a positive role (Huang *et al.*, 2013). All previous investigations have used different time points, different ways to simulate increased/decreased ethylene and different ways of characterizing the gravitropism response, and consequently it is difficult to form a clear picture of what is occurring. The previous analyses were conducted after 8 d K^+ treatment, however, when looking at a shorter timescale (Fig. 3-11B) a role for ethylene was not observed. The attenuated agravitropic phenotype under low K^+ was also not observed at this shorter timescale, (Fig. 3-11B) which suggests that the low K^+ and ethylene responses are working together at a later stage of the gravitropic response.

7.6.3 A mechanism for ethylene action in gravitropism was not established

In the response to gravity, root bending is known to be caused by a differential accumulation of auxin on the different sides of the root (Friml *et al.*, 2002b). Ethylene has been shown to modulate auxin transport through upregulation of auxin transporters such as PIN2 and AUX1 (Ruzicka *et al.*, 2007), therefore it was hypothesised that ethylene may be causing the redistribution of auxin through transporters that lead to the restoration of gravitropic bending in mutants such as *aux1* and *eir1*. Studies in this thesis looking at the accumulation of auxin and PIN2 localization in PR tip of the *aux1-7* mutant in response to low K^+ using the *aux1-7 35S::DII-VENUS-N7* auxin reporter and *aux1-7 proPIN2::PIN2::GFP* (Fig. 3-12) did not show changes in accumulation or localization pattern. However, the sample size for each was small ($n \geq 4$), and analysis was only carried out after 8 d K^+ treatment. Further investigation is needed to fully investigate the hypothesis that an increase in ethylene is causing a redistribution of auxin leading to changes in root bending. Shorter time periods need to be examined and the cell polarity of PIN2 will need to be analysed. Previous reports have also identified ectopic localization of PIN1 in agravitropic mutants (Rigas *et al.*, 2013) and therefore it would be interesting to investigate the potential role of ethylene in this response by analysing localization following ethylene treatments such as ACC and Ag^{2+}.

7.7 Reduced photosynthesis in response to low K^+

Previous studies on various crop species have observed a reduced photosynthetic rate in response to K^+ deficiency (Tomemori *et al.*, 2002; Jin *et al.*, 2011). Potassium affects photosynthesis at a number of levels; it is important in the synthesis of ATP, the activation of photosynthetic enzymes and acts as the dominant counterion to the light-induced H^+ flux across the thylakoid membranes (Marschner, 1995). There have been numerous studies linking K^+ deficiency to reduced photosynthetic rates (Bednarz *et al.*, 1998; Bednarz & Oosterhuis, 1999; Zhao *et al.*, 2001; Weng *et al.*, 2007), with links between reduced chlorophyll content, poor chloroplast ultrastructure, restricted saccharide translocation (Zhao *et al.*, 2001) reduced stomatal conductance (Bednarz *et al.*, 1998) and reduced photosynthetic enzyme activity (Weng *et al.*, 2007).

7.7.1 Downregulation of photosynthetic genes in response to low K^+

The data presented in this thesis (Chapter 4, section 4.4.2) suggest that reduced photosynthesis could be partly controlled through the downregulation of genes associated with the photosynthetic machinery (Fig. 4-8). Previous work also identified photosynthetic gene expression changes in response to salt stress and drought (Chaves *et al.*, 2009), identifying downregulation in genes relating to ATP synthesis, proton transport, light reactions and the xanthophyll cycle (Chaves *et al.*, 2009). Overexpression of *STZ* is also known to downregulate photosynthesises and carbohydrate metabolism genes (Maruyama *et al.*, 2004); therefore, the upregulation of *STZ* in response to low K^+ shown in this thesis (Table 4-1), could be leading to the downregulation of the photosynthesis genes identified in the RNA-Seq data (Fig. 4-8, Appendix III) (see Fig. 7-1, box 5). As a SALK mutant identified with an insertion in the *STZ* gene is available (Fig. 6-4), photosynthetic gene expression levels could be analysed in the mutant and compared with the WT, to determine whether the *STZ* gene is instrumental in modulating photosynthetic gene expression.

7.8 Ecological significance

7.8.1 Ecological significance of Col-0 root architectural change to low K^+

In response to low K^+ Col-0 maintains PR whilst compromising the growth of its LRs. It has been suggested that LRs are more important than the PR in the uptake of immobile nutrients, such as phosphorus and manganese, from the soil (Liu *et al*., 2013) while a deeper root system is more important for taking up mobile nutrients such as potassium and nitrogen (Maeght *et al.*,

2013). As potassium is such an essential nutrient for growth and functioning of a plant, this might explain the trade-off between PR and LR, utilising remaining resources to grow in a way more likely to find the mobile nutrient potassium, deeper in the soil.

The work by Kellermeier *et al.* (2013) described a gradient of root architectural responses to low K^+ in different Arabidopsis accessions. Some accessions displayed similar responses to Col-0, maintaining PR growth but reducing LR growth, while other accessions reduced PR growth and increased LR growth (Fig. 1-4). The ecological significance of the phenotypic gradient within the Arabidopsis species has not been investigated, and could be an interesting direction for further work. Over 7000 Arabidopsis accessions have been identified worldwide, and most live within characterized geographical boundaries (Weigel, 2012). By looking at the locations in which the accessions evolved, and the root architectural responses that they display to K^+ deprivation, causal factors such as typical soil type, precipitation and temperature may be identified. Links between the ecological niche that an accession inhabits, and the phenotypic response to potassium starvation, might provide clues as to why there is such variation in root architectural responses to an environmental factor within a single species.

7.8.2 Ecological significance of the reduced activity but maintained functionality of the LR meristem

The results in this thesis show that in response to low K^+, LR growth is reduced through modulation of meristem activity (cell division) rather than a loss of quiescent centre (QC) identity. It was also shown that LR meristem functionality is maintained even following an 8 d treatment of severe K^+ starvation (Fig. 3-6). Following the resupply of K^+, seedlings were able to regain growth of the LRs (Appendix VIII). Further experiments characterizing LR growth after resupply of K^+ need to be carried out in which LR growth after movement from low K^+ to high K^+ and high K^+ to low K^+ are investigated. These should be accompanied by control treatments to establish the level of plasticity allowing the LRs to continue growth. It would also be interesting to investigate meristem size following resupply of K^+ to determine whether the meristem is able to regain its size or if the period of K^+ starvation results in the presence of a lasting reduction in the size of the meristem. The ability to regain growth following periods of K^+ starvation would be likely beneficial to the survivability of the plant. Due to the many variables in the soil affecting K^+ availability (Jung *et al.*, 2009), it is likely that plants often experience periods of K^+ starvation in the field. It can be speculated that maintaining LR density, but not expending resources on LR growth and elongation, potentially allows the plant to conserve the limited K^+ available. It then allows the plant (in the case of Col-0) to use these remaining resources for the maintenance of downward growth of the PR. Following the lifting

of the K^+ deprivation, the LRs would then be able to continue normal growth, increasing the root surface area and increasing foraging ability of other nutrients and water.

Although not investigated in this thesis it would be interesting to examine the impact of localised areas of K^+ starvation on the root architectural growth. Classical experiments (Drew, 1975) showed that, unlike most nutrients, localized supply of K^+ to the plant did not lead to a localized proliferation of LR in the area of high $[K^+]_{ext}$. This may suggest that localized depletion zones of K^+ may not lead to reductions in LR growth in specific root zones. Investigating this further may shed more light onto the means of perception of K^+ starvation, and the signalling pathways following on from the sensing event.

7.8.3 Selective advantage of reduced growth response to abiotic stress

Work in this thesis shows that in response to low K^+, Col-0 reduces its LR growth through a DELLA-mediated pathway. In the case of salt and cold, the growth restriction mediated by DELLAs has also been linked to an increased stress tolerance (Magome *et al.*, 2004; Achard *et al.*, 2006, 2008a,b). To test the role of DELLAs in long-term stress tolerance, it would be interesting to investigate the growth of *ga2ox quintuple* mutant plants compared with the WT over a prolonged period of time. It would also be interesting to look at the tolerance of DELLA mutants; however, the creation of DELLA mutants (*rga gai*) in Col-0 causes complete male sterility (Plackett *et al.*, 2014), therefore making them difficult to work with. The advent of CRISPR/Cas9 (Bortesi & Fischer, 2015) may allow the rapid creation of GA/DELLA mutant resources in the Col-0 background.

7.9 Notes on experimental design

Through analysis of this LR growth response to low K^+ it became apparent how important experimental design is when investigating the developmental responses of LRs. Initial analyses conducted for this thesis, as well as previously published work investigating the LR response to low K^+, identified a reduced number of LRs in response to low K^+ (Fig 3-1B; Shin *et al.*, 2007; Kellermeier *et al.*, 2013). However, further characterization of this LR response (Chapter 3) identified that in contrast to the work by Shin *et al.* (2007), there was no observed reduction in LR density. The reduced number of LRs observed in initial investigations reported here (Fig. 3-1B) was shown to be due to the method of counting, which was not sensitive enough to observe the developed but not elongated roots. LR development is a very complex process and consequently it is difficult to form (well supported) conclusions concerning the influence of

external factors on root architecture if the stage of development has not been accurately characterized. For example, in the paper by Shin *et al.* (2007) a reduced LR density in Col-0 is observed in response to low K^+, and this in turn was attributed to changes in auxin signalling. However, auxin is known to act at every stage of LR development (from priming the initials through to the emergence from the PR; Lavenus *et al.*, 2013) therefore characterizing LR density in auxin signalling mutants is unlikely to accurately characterize the role of auxin in the low K^+ response. The role of auxin in the reduced LR density response to low K^+ was identified by Shin *et al.* (2007) through observations of reduced LR density in auxin signalling mutants such as *tir1-1*. However, the *tir1-1* auxin mutant was also shown to display significantly lower LR density under nutrient sufficient conditions, suggesting that the reduced density observed by Shin *et al.* (2007) was a general auxin response and not a nutrient specific response. Work in this thesis did not observe a role for auxin in the reduced LR elongation response (Chapter 5, section 5.2). It is difficult to suggest reasons why the investigations reached different conclusions without further characterization of LR development, as both used different [K^+] and different auxin signalling mutants. The current study therefore highlights the importance of experimental design when conducting LR experiments. It shows that recording the presence/absence of a visible LR does not give sufficient information to present an accurate picture of what is a complex response. The work in this thesis shows that it is important to conduct experiments such as LR progression analyses, to determine at what stage development is being influenced by the stress or stimulus.

7.10 Future prospects and further work

7.10.1 K^+ perception

Although not investigated in this thesis, the mechanisms of external K^+ perception are still unknown. As was highlighted in the Introduction (Chapter 1, section 1.2) there are a number of potential mechanisms but the K^+ channel AKT1 is the current focus of much research. There is a growing body of work suggesting a role for AKT1 in K^+ perception (see the Introduction, Chapter 1), however, despite these recent advances there is still much that is unknown. A better understanding of how plants sense external K^+ levels would be an invaluable tool to allow the further investigation of the response of the plant to low K^+.

7.10.2 Further verification of GA/ DELLA levels in response to low K^+

7.10.2.1 Analysis of GA concentration levels

Despite work in this thesis presenting compelling evidence to suggest a reduction in GA in response to low K^+ (discussed above), it was not possible to quantify cellular levels of GA. Liquid chromatography-mass spectrometry (LC-MS) can be used to measure concentrations of plant hormones (Crozier & Moritz, 1999) but attempts to do this here produced inconsistent results across biological repeats (results not shown). Another confounding factor in the measurement of GA concentrations was the need for large amounts of tissue. In response to low K^+, work in this thesis predicted a reduction in GA levels in the LRs of seedlings but not in the plant overall, due to the maintenance of PR growth. As the LRs are very short when subjected to low K^+, it was not possible in this study to collect enough tissue to complete analysis on LRs only. Further experiments could therefore focus on determining a full picture of the gene expression changes of the dioxygenase genes (*GA3oxs, GA20oxs* and the *GA2oxs*) in order to gain more evidence for reduced GA levels.

7.10.2.2 Further characterization of the DELLA accumulation response of LRs

It would also be good to investigate further the changes in DELLA levels in response to low K^+. Western blot analysis of protein levels may face the same problems as the LC-MS in the inability to look at only LR DELLA levels, therefore further confocal microscopy might be the best means of investigation. The recent advances in light sheet fluorescence microscopy (LSFM; Maizel *et al.*, 2011) could provide an exciting opportunity for further investigation of the DELLA response. LSFM allows the live imaging of a growing Arabidopsis root, and recent advances have led to the development of elegant protocols to allow the time-lapse recording of Arabidopsis LR growth over 17 h growth (Von Wangenheim *et al.,* 2017). Utilising the *proRGA::GFP:RGA* line in this system would allow the visualization of DELLA levels over prolonged periods of time following low K^+ treatment, allowing the investigation of the dynamic system.

7.10.3 How DELLA accumulation leads to reduced cell division

The mode by which DELLAs lead to growth changes is still poorly understood; however it is thought likely that DELLAs do not bind directly to DNA, but instead regulate transcription through the binding of TFs. Work looking at hypocotyl elongation in response to light demonstrated that DELLA proteins bind to bHLH TFs PIF3 and PIF4 (PHYTOCHROME INTERACTING FACTOR 3 &4), inhibiting binding to target promoters. PIFs are known to activate genes involved in cell elongation, DELLAs act to repress growth in this system (de Lucas *et al.*, 2008; Feng *et al.*, 2008). Similar mechanisms have also been demonstrated in the control of

fruit patterning and hypocotyl elongation with DELLAs binding to the bHLH TFs ALCATRAZ (ALC) and SPATULA (SPT) preventing activation of target genes (Arnaud *et al.*, 2010; Josse *et al.*, 2011), and in jasmonate (JA) signalling, with DELLAs repressing the activity of the JA ZIM-domain 1 (JAZ1) protein (Hou *et al.*, 2010).

As well as excluding TFs from promoter regions, DELLAs are also able to modulate gene expression by acting as transcriptional co-activators. In the root meristem, an interaction between cytokinin and DELLA signalling has been identified in the regulation of cell division. Cytokinin-responsive gene expression is known to be regulated by type-B ARABIDOPSIS RESPONSE REGULATORS (ARRs) transcription factors, such as ARR1 (Sakai *et al.*, 2000; Mason *et al.*, 2005). In the root meristem DELLAs have been shown to be recruited by ARRs to form transcriptionally active complexes to regulate cytokinin regulated gene expression (Marín-de la Rosa *et al.*, 2015). The presence of DELLA proteins has also been shown to be essential for the function of ARR1 in reducing cell division and meristem size in the PR meristem (Moubayidin *et al.*, 2010; Marín-de la Rosa *et al.*, 2015).

7.10.3.1 A role for cytokinin in DELLA action in response to low K^+?

The role of cytokinin in the root architectural response to low K^+ was not investigated in this thesis; however, it could be hypothesised that the DELLA-induced reduction of cell division in the LR meristem in response to low K^+ might be mediated through the interaction between DELLA proteins and TFs, such as ARR1 (see Fig. 7-1, box 6). It would therefore be interesting to investigate this interaction within the LRs of the low K^+ system. The DELLA-mediated process of cotyledon opening has been shown to be completely suppressed in the *arr1 arr12* double mutant (Marín-de la Rosa *et al.*, 2015). It would therefore be interesting to measure the LR growth response to low K^+ in this double mutant, to determine whether these response regulators are also necessary for DELLA action in this system. The use of the conditional ARR1ΔDDK:GR allele under the 35S promoter (Sakai *et al.*, 2001) may also be utilised to investigate whether ARR1 is acting with DELLAs to reduce root growth in response to low K^+. Treatment of ARR1ΔDDK:GR with dexamethasone (DEX) causes ARR1ΔDDK to translocate to the nucleus and regulate gene transcription (Sakai *et al.*, 2001). If ARR1 is necessary for the reduced growth response to low K^+, then LR growth will not be reduced if the translocation of ARR1ΔDDK is blocked by not treating seedlings with DEX.

7.10.3.2 Post translational modification of DELLAs

It has also started to come to light that post translational modifications are also important in the regulation of DELLA action. For example, SUMOylation of DELLAs is known to be important in the restraint of growth in response to salt stress (Conti *et al.*, 2014), and DELLAs have also recently been shown to be regulated through glycosylation by SPINDLY (SPY) and SECRET AGENT (SEC) (Zentella *et al.*, 2016, 2017). Post translational modifications add another layer of complexity into a system where there is still much that is unknown.

7.10.4 Gravitropism

7.10.4.1 A role for ROS in low K^+ mediated gravitropic bending?

Joo *et al.* (2001) have suggested a role for ROS in the gravitropic response. An asymmetrical accumulation of ROS on the lower cortex was observed upon a reorientation of gravity stimulus and the root bending was prevented through scavenging ROS using N-acetyl-cysteine. These data suggest that ROS acts as an inhibitor of growth in the gravitropism response (Joo *et al.*, 2001). Ethylene has been shown to act upstream of ROS in response to low K^+ (Jung *et al.*, 2009), therefore it is possible that ethylene is mediating gravitropic bending through ROS. It would be interesting to carry out vertical growth index analyses and root reorientation studies with application of H_2O_2 and ROS blocker DPI to investigate a potential role for ROS in the pathway.

7.10.4.2 The use of microscopy for future analysis of gravitropic effect

The recent advances in LSFM (Maizel *et al.*, 2011) might provide an exciting opportunity for investigating this gravitropic response. LSFM allows the live imaging of a growing Arabidopsis root. This would allow the visualization of dynamic processes such as auxin accumulation to be analysed (Ovecka *et al.*, 2015) using DII-VENUS or R2D2 Liao *et al.* (2015). This would also allow localization of proteins such as with *proPIN2::PIN2::GFP* to be observed in the response to a change in gravity stimulus. Visualization of these reporters in the PR following gravistimulation would make the elucidation of their importance in the process much easier. Light sheet technology also allows the possibility of chemical or hormonal treatments to the growth media to be carried out during imaging (Von Wangenheim *et al.,* 2017), and it could, therefore provide the perfect way to identify the role of ethylene in gravitropism through the addition of ethylene precursors or blockers.

7.10.5 Clues for the regulation of ethylene biosynthesis in response to low K^+

Despite an increase in ethylene levels and increased biosynthesis in response to low K^+ being a well characterized response, the mechanisms for this increase have not been identified.

Although not investigated in this thesis, the data presented from the RNA-Seq data did identify the WRKY TF WRKY33 as a possible candidate for activation of the *ACS6* gene expression changes. Upregulated strongly after only 3 h, then to a lesser extent after 30 h K^+ starvation, the transcription profile matches the rapid transient upregulation of *ACS6.* WRKY33 has also been shown through a chromatin-immunoprecipitation assay to directly bind to the W-box in the promoter of *ACS6 in vivo* and act in the induction of ethylene in response to pathogen attack (Li *et al.*, 2012) (see Fig. 7-1, box 7). Looking at *ACS6* expression levels in the WRKY33 mutant in the early K^+ stress response may link this TF to the ethylene response to low K^+.

7.10.6 Integration of stress pathways and construction of models

In the soil, the plant is faced with many different abiotic and biotic stress signals concurrently. The means by which these signals are integrated is of great importance in the regulation of growth conditions to increase yield of crops of the future. As discussed earlier, a reduction in growth mediated through a reduction in GA levels and subsequent stabilization of DELLAs is a common response to stresses, occurring in response to low K^+ (data shown in this thesis), salt stress (Magome *et al.*, 2008), osmotic stress (Dubois *et al.*, 2013), cold (Achard *et al.*, 2008a) and low phosphate (Jiang *et al.*, 2007) (Fig. 7-3). Understanding the specific regulation of each of these pathways is essential in uncovering the complex growth plasticity plants demonstrate to the ever-changing environment. Together, knowledge of the regulation of gene transcription, interactions with TFs and the importance of post translational modifications can be accumulated and incorporated into models. The rise of mathematical/computer modelling provides an exciting platform around which these models may be constructed. Manipulation of these models can then be undertaken in order to generate hypotheses about how multiple stress signals converge and the way in which the plant responds. Highlighting new areas of investigation in the future.

7.11 Concluding remarks

The work presented in this thesis has aimed to uncover the hormonal control of root architectural responses to low K^+ in the Arabidopsis accession Col-0. Together, the findings have identified a pathway controlling a reduction in LR in response to low K^+, as well as increasing the knowledge about differential expression changes in the early response to low K^+. Work here has identified many avenues for further research, to expand the knowledge of hormonal control of root architecture, as well as increasing the understanding of the stress tolerance responses to low K^+.

Bibliography

Achard P. **2003**. Ethylene regulates Arabidopsis eevelopment via the modulation of DELLA protein growth repressor function. *The Plant Cell Online* **15**: 2816–2825.

Achard P, Cheng H, Grauwe L De, Decat J, Schoutteten H, Moritz T, Straeten D Van Der, Peng J, Harberd NP. 2006. Integration of plant responses to environmentally activated phytohormonal signals. *Science* **311:** 91–94.

Achard P, Genschik P. **2009**. Releasing the brakes of plant growth: how GAs shutdown della proteins. *Journal of Experimental Botany* **60:** 1085–1092.

Achard P, Gong F, Cheminant S, Alioua M, Hedden P, Genschik P. **2008a**. The cold-inducible CBF1 factor-dependent signaling pathway modulates the accumulation of the growth-repressing DELLA proteins via its effect on gibberellin metabolism. *The Plant Cell* **20**: 2117–2129.

Achard P, Gusti A, Cheminant S, Alioua M, Dhondt S, Coppens F, Beemster GTS, Genschik P. **2009**. Gibberellin signaling controls cell proliferation rate in Arabidopsis. *Current Biology* **19**: 1188–1193.

Achard P, Renou JP, Berthomé R, Harberd NP, Genschik P. **2008b**. Plant DELLAs restrain growth and promote survival of adversity by reducing the levels of reactive oxygen species. *Current Biology* **18**: 656–660.

Adams F. 1971. Soil solution. In: Carson EW, ed. *The plant root and its environment.* Charlottesville, VA, USA: University Press of Virginia, 441–481.

Ahn SJ, Shin R, Schachtman DP. **2004**. Expression of KT/KUP genes in Arabidopsis and the role of root hairs in K^+ uptake. *Plant Physiology* **134**: 1135–1145.

Allakhverdiev SI, Thavasi V, Kreslavski VD, Zharmukhamedov SK, Klimov V V., Ramakrishna S, Los DA, Mimuro M, Nishihara H, Carpentier R. **2010**. Photosynthetic hydrogen production. *Journal of Photochemistry and Photobiology C: Photochemistry Reviews* **11**: 101–113.

Alonso JM, Hirayama T, Roman G, Nourizadeh S, Ecker JR. **1999**. EIN2, a bifunctional transducer of ethylene and stress responses in *Arabidopsis*. *Science* **284**: 2148–2152.

Amtmann A, Rubio F. 2012. *Potassium in plants.* eLS. John Wiley & Sons Ltd, Chichester, UK. http://www.els.net

An F, Zhao Q, Ji Y, Li W, Jiang Z, Yu X, Zhang C, Han Y, He W, Liu Y *et al.* 2010. Ethylene-induced stabilization of ETHYLENE INSENSITIVE3 and EIN3-LIKE1 is mediated by proteasomal degradation of EIN3 binding F-box 1 and 2 that requires EIN2 in *Arabidopsis*. *The Plant Cell* **22**: 2384–2401.

Anders S, Pyl PT, Huber W. **2015**. HTSeq-A Python framework to work with high-throughput sequencing data. *Bioinformatics* **31**: 166–169.

Ariel F, Diet A, Verdenaud M, Gruber V, Frugier F, Chan R, Crespi M. **2010**. Environmental regulation of lateral root emergence in *Medicago truncatula* requires the HD-Zip I transcription factor HB1. *The Plant Cell* **22**: 2171–2183.

Ariizumi T, Lawrence PK, Steber CM. **2011**. The role of two F-box proteins, SLEEPY1 and SNEEZY, in Arabidopsis gibberellin signaling. *Plant Physiology* **155**: 765–775.

Armengaud P, Breitling R, Amtmann A. **2004**. The potassium-dependent transcriptome of Arabidopsis reveals a prominent role of jasmonic acid in nutrient signaling. *Plant Physiology* **136**: 2556–2576.

Armengaud P, Breitling R, Amtmann A. **2010**. Coronatine-insensitive 1 (COI1) mediates transcriptional responses of *Arabidopsis thaliana* to external potassium supply. *Molecular Plant* **3**: 390–405.

Arnaud N, Girin T, Sorefan K, Fuentes S, Wood TA, Lawrenson T, Sablowski R, Østergaard L. **2010**. Gibberellins control fruit patterning in *Arabidopsis thaliana*. *Genes and Development* **24**: 2127–2132.

Ashley MK, Grant M, Grabov A. **2006**. Plant responses to potassium deficiencies: a role for potassium transport proteins. *Journal of Experimental Botany* **57:** 425–436.

Atkinson JA, Rasmussen A, Traini R, Voss U, Sturrock C, Mooney SJ, Wells DM, Bennett MJ. **2014**. Branching out in roots: uncovering form, function, and regulation. *Plant Physiology* **166**: 538–550.

Bakshi M, Oelmüller R. **2014**. WRKY transcription factors: Jack of many trades in plants. *Plant Signaling & Behavior* **9**: 1–18.

Becker M, Asch F. **2005**. Iron toxicity in rice-conditions and management concepts. *Journal of Plant Nutrition and Soil Science* **168**: 558–573.

Bednarz CW, Oosterhuis DM. **1999**. Physiological changes associated with potassium deficiency in cotton. *Journal of Plant Nutrition* **22**: 303–313.

Bednarz CW, Oosterhuis DM, Evans RD. **1998**. Leaf photosynthesis and carbon isotope discrimination of cotton in response to potassium deficiency. *Environmental and Experimental Botany* **39**: 131–139.

Beemster GT, Baskin TI. **1998**. Analysis of cell division and elongation underlying the developmental acceleration of root growth in *Arabidopsis thaliana*. *Plant Physiology* **116**: 1515–1526.

Behera S, Long Y, Schmitz-Thom I, Wang XP, Zhang C, Li H, Steinhorst L, Manishankar P, Ren XL, Offenborn JN *et al.* 2017. Two spatially and temporally distinct Ca^{2+} signals convey *Arabidopsis thaliana* responses to K^+ deficiency. *New Phytologist* **213**: 739–750.

Belousov VV, Fradkov AF, Lukyanov KA, Staroverov DB, Shakhbazov KS, Terskikh AV, Lukyanov S. **2006**. Genetically encoded fluorescent indicator for intracellular hydrogen peroxide. *Nature Methods* **3**: 281–286.

Bender KW, Snedden WA. **2013**. Calmodulin-related proteins step out from the shadow of their namesake. *Plant Physiology* **163**: 486–495.

Benjamins R, Ampudia CSG, Hooykaas PJJ, Offringa R. **2003**. PINOID-mediated signaling involves calcium-binding proteins. *Plant Physiology* **132**: 1623–1630.

Benková E, Michniewicz M, Sauer M, Teichmann T, Seifertová D, Jürgens G, Friml J. **2003**. Local, efflux-dependent auxin gradients as a common module for plant organ formation. *Cell* **115**: 591–602.

Bennett MJ, Marchant A, Green HG, May ST, Ward SP, Millner PA, Walker AR, Schulz B, Feldmann KA. **1996**. Arabidopsis AUX1 gene: a permease-like regulator of root gravitropism. *Science* **273**: 948–950.

Van Berg C Den, Willemsen V, Hendriks G, Weisbeek P, Scheres B. **1997**. Short-range control of cell differentiation in the Arabidopsis root meristem. *Nature* **390**: 287–289.

Van Berg C Den, Weisbeek P, Scheres B. **1998**. Cell fate and cell differentiation status in the Arabidopsis root. *Planta* **205**: 483–491.

Blilou I, Xu J, Wildwater M, Willemsen V, Paponov I, Friml J, Heidstra R, Aida M, Palme K, Scheres B. **2005**. The PIN auxin efflux facilitator network controls growth and patterning in Arabidopsis roots. *Nature* **433**: 39–44.

Boer DR, Freire-Rios A, Van Den Berg WAM, Saaki T, Manfield IW, Kepinski S, López-Vidrieo I, Franco-Zorrilla JM, De Vries SC, Solano R *et al.* 2014. Structural basis for DNA binding specificity by the auxin-dependent ARF transcription factors. *Cell* **156**: 577–589.

Bolger AM, Lohse M, Usadel B. **2014**. Trimmomatic: a flexible trimmer for Illumina sequence data. *Bioinformatics* **30**: 2114–2120.

Bolwell GP, Wojtaszek P. **1997**. Mechanisms for the generation of reactive oxygen species in plant defence – a broad perspective. *Physiological and Molecular Plant Pathology* **51**: 347–366.

Bortesi L, Fischer R. **2015**. The CRISPR/Cas9 system for plant genome editing and beyond. *Biotechnology Advances* **33**: 41–52.

Bowler C, Van Camp W, Van Montagu M, Inze D. **1994**. Superoxide dismutase in plants. *Critical Reviews in Plant Science* **13**: 199–218.

Brian PW. 1959. Effects of gibberellins on plant growth and development. *Biological Reviews of the Cambridge Philosophical Society* **34:** 37–84.

Brunoud G, Wells DM, Oliva M, Larrieu A, Mirabet V, Burrow AH, Beeckman T, Kepinski S, Traas J, Bennett MJ *et al.* 2012. A novel sensor to map auxin response and distribution at high spatio-temporal resolution. *Nature* **482**: 103–106.

Buer CS, Sukumar P, Muday GK. **2006**. Ethylene modulates flavonoid accumulation and gravitropic responses in roots of Arabidopsis. *Plant Physiology* **140**: 1384–1396.

Bulankova P, Akimcheva S, Fellner N, Riha K. **2013**. Identification of Arabidopsis meiotic cyclins reveals functional diversification among plant cyclin genes. *PLoS Genetics* **9**: e1003508.

Calderone V, Trabucco M, Vujicić A, Battistutta R, Giacometti GM, Andreucci F, Barbato R, Zanotti G. **2003**. Crystal structure of the PsbQ protein of photosystem II from higher plants. *EMBO reports* **4**: 900–905.

Canales J, Moyano TC, Villarroel E, Gutiérrez RA. **2014**. Systems analysis of transcriptome data provides new hypotheses about *Arabidopsis* root response to nitrate treatments. *Frontiers in Plant Science* **5**: 22.

Cao SQ, Su L, Fang YJ. **2006**. Evidence for involvement of jasmonic acid in the induction of leaf senescence by potassium deficiency in Arabidopsis. *Canadian Journal of Botany-Revue Canadienne De Botanique* **84**: 328–333.

Casimiro I, Marchant A, Bhalerao RP, Beeckman T, Dhooge S, Swarup R, Graham N, Inzé D, Sandberg G, Casero PJ *et al.* 2001. Auxin transport promotes Arabidopsis lateral root initiation. *The Plant Cell* **13**: 843–852.

Caverzan A, Passaia G, Rosa SB, Ribeiro CW, Lazzarotto F, Margis-Pinheiro M. **2012**. Plant responses to stresses: role of ascorbate peroxidase in the antioxidant protection. *Genetics and Molecular Biology* **35**: 1011–1019.

Chang C. **2016**. Q&A: How do plants respond to ethylene and what is its importance? *BMC Biology* **14**: 7. https://doi.org/10.1186/s12915-016-0230-0.

Chang C, Kwok S, Bleecker A, Meyerowitz E. **1993**. Arabidopsis ethylene-response gene ETR1: similarity of product to two-component regulators. *Science* **262**: 539–544.

Chang L, Ramireddy E, Schmülling T. **2013**. Lateral root formation and growth of *Arabidopsis* is redundantly regulated by cytokinin metabolism and signalling genes. *Journal of Experimental Botany* **64**: 5021–5032.

Chanroj S, Wang G, Venema K, Zhang MW, Delwiche CF, Sze H. **2012**. Conserved and diversified gene families of monovalent cation/H^+ antiporters from algae to flowering

plants. *Frontiers in Plant Science* **3**: 1–18.

Chaves MM, Flexas J, Pinheiro C. **2009**. Photosynthesis under drought and salt stress: regulation mechanisms from whole plant to cell. *Annals of Botany* **103**: 551–560.

Chee-Seng K, En Yun L, Yudi P, Kee-Seng C. 2010. *Next generation sequencing technologies and their application. eLS* John Wiley & Sons Ltd, Chichester, UK. doi: 10.1002/9780470015902.a0022508.

Chen C, Chen Z. **2002**. Potentiation of developmentally regulated plant defense response by AtWRKY18, a pathogen-induced Arabidopsis transcription factor. *Plant Physiology* **129**: 706–16.

Chen H, Lai Z, Shi J, Xiao Y, Chen Z, Xu X. **2010**. Roles of arabidopsis WRKY18, WRKY40 and WRKY60 transcription factors in plant responses to abscisic acid and abiotic stress. *BMC Plant Biology* **10**: 281.

Chen R, Hilson P, Sedbrook J, Rosen E, Caspar T, Masson PH. **1998**. The *Arabidopsis thaliana AGRAVITROPIC 1* gene encodes a component of the polar-auxin-transport efflux carrier. *Proceedings of the National Academy of Sciences, USA* **95**: 15112–15117.

Cheng M-C, Liao P-M, Kuo W-W, Lin T-P. **2013**. The Arabidopsis ETHYLENE RESPONSE FACTOR1 regulates abiotic stress-responsive gene expression by binding to different *cis*-acting elements in response to different stress signals. *Plant Physiology* **162**: 1566–1582.

Cheong YH, Pandey GK, Grant JJ, Batistic O, Li L, Kim BG, Lee SC, Kudla J, Luan S. **2007**. Two calcineurin B-like calcium sensors, interacting with protein kinase CIPK23, regulate leaf transpiration and root potassium uptake in Arabidopsis. *Plant Journal* **52**: 223–239.

Chérel I, Lefoulon C, Boeglin M, Sentenac H. **2014**. Molecular mechanisms involved in plant adaptation to low K^+ availability. *Journal of Experimental Botany* **65**: 833–848.

Choi HI, Hong JH, Ha JO, Kang JY, Kim SY. **2000**. ABFs, a family of ABA-responsive element binding factors. *Journal of Biological Chemistry* **275**: 1723–1730.

Clark KL, Larsen PB, Wang X, Chang C. **1998**. Association of the *Arabidopsis* CTR1 Raf-like kinase with the ETR1 and ERS ethylene receptors. *Proceedings of the National Academy of Sciences* **95:** 5401–5406.

Cloonan N, Forrest ARR, Kolle G, Gardiner BBA, Faulkner GJ, Brown MK, Taylor DF, Steptoe AL, Wani S, Bethel G *et al.* 2008. Stem cell transcriptome profiling via massive-scale mRNA sequencing. *Nature Methods* **5**: 613–619.

Colangelo EP. **2004**. The essential basic helix-loop-helix protein FIT1 is required for the iron deficiency response. *The Plant Cell Online* **16**: 3400–3412.

Colebrook EH, Thomas SG, Phillips AL, Hedden P. **2014**. The role of gibberellin signalling in plant responses to abiotic stress. *The Journal of Experimental Biology* **217**: 67–75.

Comas LH, Becker SR, Cruz VM V, Byrne PF, Dierig DA. **2013**. Root traits contributing to plant productivity under drought. *Frontiers in Plant Science* **4**: 442.

Conti L, Nelis S, Zhang C, Woodcock A, Swarup R, Galbiati M, Tonelli C, Napier R, Hedden P, Bennett M *et al.* 2014. Small Ubiquitin-like Modifier Protein SUMO enables plants to control growth independently of the phytohormone gibberellin. *Developmental Cell* **28**: 102–110.

Cowling RJ, Kamiya Y, Seto H, Harberd NP. **1998**. Gibberellin dose-response regulation of *GA4* gene transcript levels in Arabidopsis. *Plant Physiology* **117**: 1195–1203.

Crozier A, Moritz T. 1999. Physico-chemical methods of plant hormone analysis. In: Hooykaas PJJ, Hall MA, Libbenga KR, eds. *Biochemistry and molecular biology of plant hormones.* New York, USA: Elsevier Science, 23–60.

Cutler SR, Rodriguez PL, Finkelstein RR, Abrams SR. **2010**. Abscisic acid: emergence of a core signaling network. *Annual Review of Plant Biology* **61**: 651–679.

Czechowski T, Stitt M, Altmann T, Udvardi MK, Scheible W-R. **2005**. Genome-wide identification and testing of superior reference genes for transcript normalization in Arabidopsis. *Plant Physiology* **139**: 5–17.

Darwin C. 1880. *The power of movement in plants (assisted by F. Darwin)*. London, UK: John Murray.

Davletova S, Rizhsky L, Liang H, Shengqiang Z, Oliver DJ, Coutu J, Shulaev V, Schlauch K, Mittler R. 2005. Cytosolic ascorbate peroxidase 1 is a central component of the reactive oxygen gene network of Arabidopsis. *The Plant Cell Online* **17**: 268–281.

Davuluri RV, Sun H, Palaniswamy SK, Matthews N, Molina C, Kurtz M, Grotewold E. **2003**. AGRIS: Arabidopsis gene regulatory information server, an information resource of Arabidopsis *cis*-regulatory elements and transcription factors. *BMC Bioinformatics* **4**: 25.

De Lucas M, Davière J-M, Rodríguez-Falcón M, Pontin M, Iglesias-Pedraz JM, Lorrain S, Fankhauser C, Blázquez MA, Titarenko E, Prat S *et al.* 2008. A molecular framework for light and gibberellin control of cell elongation. *Nature* **451**: 480–484.

De Rybel B, Vassileva V, Parizot B, Demeulenaere M, Grunewald W, Audenaert D, Van Campenhout J, Overvoorde P, Jansen L, Vanneste S *et al.* 2010. A novel Aux/IAA28 signaling cascade activates GATA23-dependent specification of lateral root founder cell identity. *Current Biology* **20**: 1697–1706.

De Smet I, Signora L, Beeckman T, Inzé D, Foyer CH, Zhang H. **2003**. An abscisic acid-sensitive checkpoint in lateral root development of Arabidopsis. *Plant Journal* **33**: 543–555.

De Smet I, Tetsumura T, De Rybel B, Frei dit Frey N, Laplaze L, Casimiro I, Swarup R, Naudts M, Vanneste S, Audenaert D *et al.* 2007. Auxin-dependent regulation of lateral root positioning in the basal meristem of Arabidopsis. *Development (Cambridge, England)* **134**: 681–690.

De Smet I, Vassileva V, De Rybel B, Levesque MP, Grunewald W, Van Damme D, Van Noorden G, Naudts M, Van Isterdael G, De Clercq R *et al.* 2008. Receptor-like kinase ACR4 restricts formative cell divisions in the *Arabidopsis* root. *Science* **322**: 594–597.

De Smet S, Cuypers A, Vangronsveld J, Remans T. **2015**. Gene networks involved in hormonal control of root development in *Arabidopsis thaliana*: a framework for studying its disturbance by metal stress. *International Journal of Molecular Sciences* **16**: 19195–19224.

Dello Ioio R, Linhares FS, Scacchi E, Casamitjana-Martinez E, Heidstra R, Costantino P, Sabatini S. 2007. Cytokinins determine Arabidopsis root-meristem size by controlling cell differentiation. *Current Biology* **17**: 678–682.

Dello Ioio R, Nakamura K, Moubayidin L, Perilli S, Taniguchi M, Morita MT, Aoyama T, Costantino P, Sabatini S. **2008**. A genetic framework for the control of cell division and differentiation in the root meristem. *Science (New York, N.Y.)* **322**: 1380–1384.

Desbrosses G, Josefsson C, Rigas S, Hatzopoulos P, Dolan L. **2003**. *AKT1* and *TRH1* are required during root hair elongation in *Arabidopsis*. *Journal of Experimental Botany* **54**: 781–788.

Dharmasiri N, Dharmasiri S, Estelle M. **2005**. The F-box protein TIR1 is an auxin receptor. *Nature* **435**: 441–445.

Dill A, Thomas SG, Hu J, Steber CM, Sun T. **2004**. The Arabidopsis F-box protein SLEEPY1 targets gibberellin signaling repressors for gibberellin-induced degradation. *The Plant*

Cell **16**: 1392–1405.

Dodd AN, Kudla J, Sanders D. **2010**. The language of calcium signaling. *Annual Review of Plant Biology* **61**: 593–620.

Dohmann EMN, Nill C, Schwechheimer C. **2010**. DELLA proteins restrain germination and elongation growth in *Arabidopsis thaliana* COP9 signalosome mutants. *European Journal of Cell Biology* **89**: 163–168.

Dolan L, Janmaat K, Willemsen V, Linstead P, Poethig S, Roberts K, Scheres B. **1993**. Cellular organisation of the *Arabidopsis thaliana* root. *Development* **119**: 71–84.

Dos Santos Maraschin F, Memelink J, Offringa R. **2009**. Auxin-induced, SCFTIR1-mediated poly-ubiquitination marks AUX/IAA proteins for degradation. *Plant Journal* **59**: 100–109.

Drew M. **1975**. Comparison of the effects of a localised supply of phosphate, nitrate, ammonium and potassium on the growth of the seminal root system, and the shoot, in barley. *New Phytologist* **75**: 479–490.

Du Z, Zhou X, Ling Y, Zhang Z, Su Z. **2010**. agriGO: a GO analysis toolkit for the agricultural community. *Nucleic Acids Research* **38**: W64–W70.

Dubois M, Van den Broeck L, Claeys H, Van Vlierberghe K, Matsui M, Inzé D. **2015**. The ETHYLENE RESPONSE FACTORs ERF6 and ERF11 antagonistically regulate mannitol-induced growth inhibition in Arabidopsis. *Plant Physiology* **169**: 166–179.

Dubois M, Skirycz A, Claeys H, Maleux K, Dhondt S, De Bodt S, Vanden Bossche R, De Milde L, Yoshizumi T, Matsui M *et al.* 2013. The ETHYLENE RESPONSE FACTOR 6 acts as central regulator of leaf growth under water limiting conditions in *Arabidopsis thaliana*. *Plant Physiology* **162**: 319–332.

Dubrovsky JG, Rost TL, Colón-Carmona a, Doerner P. **2001**. Early primordium morphogenesis during lateral root initiation in *Arabidopsis thaliana*. *Planta* **214**: 30–36.

Edwards K, Johnstone C, Thompson C. **1991**. A simple and rapid method for the preparation of plant DNA for PCR analysis. *Nucleic Acids Research* **19**: 1349–1349.

Eide D, Broderius M, Fett J, Guerinot ML. **1996**. A novel iron-regulated metal transporter from plants identified by functional expression in yeast. *Proceedings of the National Academy of Sciences* **93**: 5624–5628.

Eliasson L, Bertell G, Bolander E. **1989**. Inhibitory action of auxin on root elongation not mediated by ethylene. *Plant Physiology* **91**: 310–314.

Epstein E, Rains D, Elzam O. 1963. Resolution of dual mechanisms of potassium absorption by barley roots. *Proceedings of the National Academy of Sciences* **49:** 684–692.

FAO. **2015**. *World fertilizer trends and outlook to 2018*. ISBN 978-92-5-108692-6 http://www.fao.org/3/a-i4324e.pdf. [accessed August 2017].

Feng S, Martinez C, Gusmaroli G, Wang Y, Zhou J, Wang F, Chen L, Yu L, Iglesias-Pedraz JM, Kircher S *et al.* 2008. Coordinated regulation of *Arabidopsis thaliana* development by light and gibberellins. *Nature* **451**: 475–479.

Fleet CM, Sun TP. **2005**. A DELLAcate balance: the role of gibberellin in plant morphogenesis. *Current Opinion in Plant Biology* **8**: 77–85.

Foreman J, Demidchik V, Bothwell JH, Mylona P, Miedema H, Torres MA, Linstead P, Costa S, Brownlee C, Jones JD *et al.* 2003. Reactive oxygen species produced by NADPH oxidase regulate plant cell growth. *Nature* **422**: 442–446.

Forzani C, Aichinger E, Sornay E, Willemsen V, Laux T, Dewitte W, Murray JH. **2014**. WOX5

suppresses *CYCLIN D* activity to establish quiescence at the center of the root stem cell niche. *Current Biology* **24:** 1939–1944.

Friml J. **2003**. Auxin transport – shaping the plant. *Current Opinion in Plant Biology* **6**: 7–12.

Friml J, Benková E, Blilou I, Wisniewska J, Hamann T, Ljung K, Woody S, Sandberg G, Scheres B, Jürgens G *et al.* 2002a. AtPIN4 mediates sink-driven auxin gradients and root patterning in *Arabidopsis*. *Cell* **108**: 661–673.

Friml J, Wiśniewska J, Benková E, Mendgen K, Palme K. **2002b**. Lateral relocation of auxin efflux regulator PIN3 mediates tropism in *Arabidopsis*. *Nature* **415**: 806–809.

Fry SC. **1998**. Oxidative scission of plant cell wall polysaccharides by ascorbate-induced hydroxyl radicals. *Biochemical Journal* **332**: 507–515.

Fu X, Harberd NP. **2003**. Auxin promotes *Arabidopsis* root growth by modulating gibberellin response. *Nature* **421**: 740–743.

Fu X, Richards DE, Fleck B, Xie D, Burton N, Harberd NP. **2004**. The Arabidopsis mutant sleepy1gar2-1 protein promotes plant growth by increasing the affinity of the SCFSLY1 E3 ubiquitin ligase for DELLA protein substrates. *Plant Cell* **16**: 1406–1418.

Fujii H, Chinnusamy V, Rodrigues A, Rubio S, Antoni R, Park S-Y, Cutler SR, Sheen J, Rodriguez PL, Zhu J-K. **2009**. *In vitro* reconstitution of an abscisic acid signalling pathway. *Nature* **462**: 660–664.

Fujimoto SY, Ohta M, Usui A, Shinshi H, Ohme-Takagi M. **2000**. Arabidopsis ethylene-responsive element binding factors act as transcriptional activators or repressors of GCC box-mediated gene expression. *The Plant Cell* **12**: 393–404.

Fukaki H, Nakao Y, Okushima Y, Theologis A, Tasaka M. **2005**. Tissue-specific expression of stabilized SOLITARY-ROOT/IAA14 alters lateral root development in Arabidopsis. *Plant Journal* **44**: 382–395.

Fukaki H, Tameda S, Masuda H, Tasaka M. **2002**. Lateral root formation is blocked by a gain-of-function mutation in the *SOLITARY-ROOT/IAA14* gene of *Arabidopsis*. *Plant Journal* **29**: 153–168.

Furihata T, Maruyama K, Fujita Y, Umezawa T, Yoshida R, Shinozaki K, Yamaguchi-Shinozaki K. **2006**. Abscisic acid-dependent multisite phosphorylation regulates the activity of a transcription activator AREB1. *Proceedings of the National Academy of Sciences, USA* **103**: 1988–1993.

Gadjev I, **Vanderauwera S, Gechev TS, Laloi C, Minkov IN, Shulaev V, Apel K, Inzé D, Mittler R, Van Breusegem F. 2006**. Transcriptomic footprints disclose specificity of reactive oxygen species signaling in Arabidopsis. *Plant Physiology* **141**: 436–445.

Galvan-Ampudia CS, Julkowska MM, Darwish E, Gandullo J, Korver RA, Brunoud G, Haring MA, Munnik T, Vernoux T, Testerink C. **2013**. Halotropism is a response of plant roots to avoid a saline environment. *Current Biology* **23**: 2044–2050.

Gälweiler L, Guan C, Müller A, Wisman E, Mendgen K, Yephremov A, Palme K. **1998**. Regulation of polar auxin transport by AtPIN1 in *Arabidopsis* vascular tissue. *Science* **282**: 2226–2230.

Gao XH, Xiao SL, Yao QF, Wang YJ, Fu XD. **2011**. An updated GA signaling 'relief of repression' regulatory model. *Molecular Plant* **4**: 601–606.

Geilen K, Böhmer M. **2015**. Dynamic subnuclear relocalisation of WRKY40 in response to abscisic acid in *Arabidopsis thaliana*. *Scientific Reports* **5**: 13369.

Gierth M, Mäser P. **2007**. Potassium transporters in plants – involvement in K^+ acquisition, redistribution and homeostasis. *FEBS Letters* **581**: 2348–2356.

Gierth M, Mäser P, Schroeder JI. **2005**. The potassium transporter *AtHAK5* functions in K^+ deprivation-induced high-affinity K^+ uptake and AKT1 K^+ channel contribution to K^+ uptake kinetics in Arabidopsis roots. *Plant Physiology* **137**: 1105–1114.

Gilroy S, Jones RL. **1992**. Gibberellic acid and abscisic acid coordinately regulate cytoplasmic calcium and secretory activity in barley aleurone protoplasts. *Proceedings of the National Academy of Sciences, USA* **89**: 3591–3595.

Giovannoni JJ. **2007**. Fruit ripening mutants yield insights into ripening control. *Current Opinion in Plant Biology* **10**: 283–289.

Glawischnig E, Hansen BG, Olsen CE, Halkier BA. **2004**. Camalexin is synthesized from indole-3-acetaldoxime, a key branching point between primary and secondary metabolism in Arabidopsis. *Proceedings of the National Academy of Sciences, USA* **101**: 8245–8250.

Gomez-Porras JL, Riaño-Pachón DM, Benito B, Haro R, Sklodowski K, Rodríguez-Navarro A, Dreyer I. **2012**. Phylogenetic analysis of K^+ transporters in Bryophytes, Lycophytes, and flowering plants indicates a specialization of vascular plants. *Frontiers in Plant Science* **3**: 1–13.

González-García M-P, Vilarrasa-Blasi J, Zhiponova M, Divol F, Mora-García S, Russinova E, Caño-Delgado AI. **2011**. Brassinosteroids control meristem size by promoting cell cycle progression in Arabidopsis roots. *Development (Cambridge, England)* **138**: 849–859.

Gray WM, Kepinski S, Rouse D, Leyser O, Estelle M. **2001**. Auxin regulates SCF(TIR1)-dependent degradation of AUX/IAA proteins. *Nature* **414**: 271–276.

Griffiths J, Murase K, Rieu I, Zentella R, Zhang Z-L, Powers SJ, Gong F, Phillips AL, Hedden P, Sun T *et al.* 2006. Genetic characterization and functional analysis of the GID1 gibberellin receptors in Arabidopsis. *The Plant Cell* **18**: 3399–3414.

Guyomarc'h S, Léran S, Suzon-Cape M, Perrine-Walker F, Lucas M, Laplaze L. 2012. Early development and gravitropic response of lateral roots in *Arabidopsis thaliana. Philosophical Transactions of the Royal Society B* **367:** 1509–1516.

Guzmán P, Ecker JR. **1990**. Exploiting the triple response of Arabidopsis to identify ethylene-related mutants. *The Plant Cell* **2**: 513–523.

Hammer GL, Dong Z, McLean G, Doherty A, Messina C, Schussler J, Zinselmeier C, Paszkiewicz S, Cooper M. **2009**. Can changes in canopy and/or root system architecture explain historical maize yield trends in the U.S. corn belt? *Crop Science* **49**: 299–312.

Harris J. **2015**. Abscisic acid: hidden architect of root system structure. *Plants* **4**: 548–572.

Haydon MJ, Kawachi M, Wirtz M, Hillmer S, Hell R, Kramer U. **2012**. Vacuolar nicotianamine has critical and distinct roles under iron deficiency and for zinc sequestration in Arabidopsis. *The Plant Cell Online* **24**: 724–737.

He XJ, Mu RL, Cao WH, Zhang ZG, Zhang JS, Chen SY. **2005**. AtNAC2, a transcription factor downstream of ethylene and auxin signaling pathways, is involved in salt stress response and lateral root development. *Plant Journal* **44**: 903–916.

Hedden P, Kamiya Y. **1997**. Gibberellin biosynthesis: enzymes, genes and their regulation. *Annual Review of Plant Physiology and Plant Molecular Biology* **48**: 431–460.

Hedden P, Phillips AL. 2000. Gibberellin metabolism: new insights revealed by the genes. *Trends in Plant Science* **5**: 523–530.

Heisler MG, Ohno C, Das P, Sieber P, Reddy G V., Long JA, Meyerowitz EM. **2005**. Patterns of auxin transport and gene expression during primordium development revealed by live imaging of the Arabidopsis inflorescence meristem. *Current Biology* **15**: 1899–1911.

Hemsley PA, Hurst CH, Kaliyadasa E, Lamb R, Knight MR, De Cothi EA, Steele JF, Knight H.

2014. The Arabidopsis mediator complex subunits MED16, MED14 and MED2 regulate mediator and RNA polymerase II recruitment to CBF-responsive cold-regulated genes. *The Plant Cell* **26:** 465–484.

Henriques R, Jásik J, Klein M, Martinoia E, Feller U, Schell J, Pais MS, Koncz C. **2002**. Knock-out of *Arabidopsis* metal transporter gene *IRT1* results in iron deficiency accompanied by cell differentiation defects. *Plant Molecular Biology* **50**: 587–597.

Hentrich M, Böttcher C, Düchting P, Cheng Y, Zhao Y, Berkowitz O, Masle J, Medina J, Pollmann S. **2013**. The jasmonic acid signaling pathway is linked to auxin homeostasis through the modulation of *YUCCA8* and *YUCCA9* gene expression. *Plant Journal* **74**: 626–637.

Heo J-O, Chang KS, Kim IA, Lee M-H, Lee SA, Song S-K, Lee MM, Lim J. **2011**. Funneling of gibberellin signaling by the GRAS transcription regulator SCARECROW-LIKE 3 in the *Arabidopsis* root. *Proceedings of the National Academy of Sciences, USA* **108**: 2166–2171.

Herder G Den, Van Isterdael G, Beeckman T, De Smet I. **2010**. The roots of a new green revolution. *Trends in Plant Science* **15**: 600–607.

Hernandez-Barrera A, Velarde-Buendia A, Zepeda I, Sanchez F, Quinto C, Sanchez-Lopez R, Cheung AY, Wu HM, Cardenas L. **2015**. Hyper, a hydrogen peroxide sensor, indicates the sensitivity of the Arabidopsis root elongation zone to aluminum treatment. *Sensors (Switzerland)* **15**: 855–867.

Himmelbach A, Hoffmann T, Leube M, Höhener B, Grill E. **2002**. Homeodomain protein ATHB6 is a target of the protein phosphatase ABI1 and regulates hormone responses in *Arabidopsis*. *The EMBO Journal* **21**: 3029–3038.

Hirota A, Kato T, Fukaki H, Aida M, Tasaka M. **2007**. The auxin-regulated AP2/EREBP gene *PUCHI* is required for morphogenesis in the early lateral root primordium of *Arabidopsis*. *Plant Cell* **19**: 2156–2168.

Hirsch RE, Lewis BD, Spalding EP, Sussman MR. **1998**. A role for the AKT1 potassium channel in plant nutrition. *Science (New York, N.Y.)* **280**: 918–921.

Ho CH, Lin SH, Hu HC, Tsay YF. **2009**. CHL1 functions as a nitrate sensor in plants. *Cell* **138**: 1184–1194.

Hohl M, Greiner H, Schopfer P. **1995**. The cryptic-growth response of maize coleoptiles and its relationship to H_2O_2-dependent cell wall stiffening. *Physiologia Plantarum* **94**: 491–498.

Hou X, Lee LYC, Xia K, Yan Y, Yu H. **2010**. DELLAs modulate jasmonate signaling via competitive binding to JAZs. *Developmental Cell* **19**: 884–894.

Hua J, Meyerowitz EM. **1998**. Ethylene responses are negatively regulated by a receptor gene family in *Arabidopsis thaliana*. *Cell* **94**: 261–271.

Huang SJ, Chang CL, Wang PH, Tsai MC, Hsu PH, Chang IF. **2013**. A type III ACC synthase, ACS7, is involved in root gravitropism in *Arabidopsis thaliana*. *Journal of Experimental Botany* **64**: 4343–4360.

Huang DW, Lempicki RA, Sherman BT. **2009a**. Systematic and integrative analysis of large gene lists using DAVID bioinformatics resources. *Nature Protocols* **4**: 44–57.

Huang DW, Sherman BT, Lempicki RA. **2009b**. Bioinformatics enrichment tools: paths toward the comprehensive functional analysis of large gene lists. *Nucleic Acids Research* **37**: 1–13.

Hulsen T, de Vlieg J, Alkema W. **2008**. BioVenn – a web application for the comparison and

visualization of biological lists using area-proportional Venn diagrams. *BMC Genomics* **9**: 488. https://doi.org/10.1186/1471-2164-9-488.

Huxley JS. 1935. Chemical regulation and the hormone concept. *Biological Reviews* **10**: 427–441.

Ikeda A, Ueguchi-Tanaka M, Sonoda Y, Kitano H, Koshioka M, Futsuhara Y, Matsuoka M, Yamaguchi J. **2001**. slender rice, a constitutive gibberellin response mutant, is caused by a null mutation of the SLR1 gene, an ortholog of the height-regulating gene GAI/RGA/RHT/D8. *The Plant Cell* **13**: 999–1010.

Ingram P, Dettmer J, Helariutta Y, Malamy JE. **2011**. *Arabidopsis Lateral Root Development 3* is essential for early phloem development and function, and hence for normal root system development. *Plant Journal* **68**: 455–467.

Ishida T, Adachi S, Yoshimura M, Shimizu K, Umeda M, Sugimoto K. **2010**. Auxin modulates the transition from the mitotic cycle to the endocycle in Arabidopsis. *Development* **137**: 63–71.

Jakoby M, Wang HY, Reidt W, Weisshaar B, Bauer P. **2004**. *FRU* (*BHLH029*) is required for induction of iron mobilization genes in *Arabidopsis thaliana*. *FEBS Letters* **577**: 528–534.

Jefferson RA, Kavanagh TA, Bevan MW. **1987**. GUS fusions: beta-glucuronidase as a sensitive and versatile gene fusion marker in higher plants. *The EMBO Journal* **6**: 3901–3907.

Jia Y, Ding Y, Shi Y, Zhang X, Gong Z, Yang S. **2016**. The *cbfs* triple mutants reveal the essential functions of *CBFs* in cold acclimation and allow the definition of CBF regulons in *Arabidopsis*. *New Phytologist* **212**: 345–353.

Jiang C, Gao X, Liao L, Harberd NP, Fu X. **2007**. Phosphate starvation root architecture and anthocyanin accumulation responses are modulated by the gibberellin-DELLA signaling pathway in Arabidopsis. *Plant Physiology* **145**: 1460–1470.

Jiao Y, Sun L, Song Y, Wang L, Liu L, Zhang L, Liu B, Li N, Miao C, Hao F. **2013**. AtrbohD and AtrbohF positively regulate abscisic acid-inhibited primary root growth by affecting Ca^{2+} signalling and auxin response of roots in *Arabidopsis*. *Journal of Experimental Botany* **64**: 4183–4192.

Jin SH, Huang JQ, Li XQ, Zheng BS, Wu J Sen, Wang ZJ, Liu GH, Chen M. **2011**. Effects of potassium supply on limitations of photosynthesis by mesophyll diffusion conductance in *Carya cathayensis*. *Tree Physiology* **31**: 1142–1151.

Johansson I, Wulfetange K, Porée F, Michard E, Gajdanowicz P, Lacombe B, Sentenac H, Thibaud JB, Mueller-Roeber B, Blatt MR *et al.* 2006. External K^+ modulates the activity of the Arabidopsis potassium channel SKOR via an unusual mechanism. *Plant Journal* **46**: 269–281.

Joo JH, Bae YS, Lee JS. **2001**. Role of auxin-induced reactive oxygen species in root gravitropism. *Plant Physiology* **126**: 1055–1060.

Josse E-M, Gan Y, Bou-Torrent J, Stewart KL, Gilday AD, Jeffree CE, Vaistij FE, Martínez-García JF, Nagy F, Graham IA *et al.* 2011. A DELLA in disguise: SPATULA restrains the growth of the developing *Arabidopsis* seedling. *The Plant Cell* **23**: 1337–1351.

Ju C, Yoon GM, Shemansky JM, Lin DY, Ying ZI, Chang J, Garrett WM, Kessenbrock M, Groth G, Tucker ML *et al.* 2012. CTR1 phosphorylates the central regulator EIN2 to control ethylene hormone signaling from the ER membrane to the nucleus in *Arabidopsis*. *Proceedings of the National Academy of Sciences, USA* **109**: 19486–19491.

Jung J-Y, Shin R, Schachtman DP. **2009**. Ethylene mediates response and tolerance to potassium deprivation in Arabidopsis. *The Plant Cell* **21**: 607–621.

Kanyanjua SM, Ayaga GO. 2006. A guide to choice of mineral fertilisers in Kenya. *KARI Technical Note*. http://www.kalro.org:8080/dspace/handle/0/9242. [accessed August 2017].

Kellermeier F, Chardon F, Amtmann A. 2013. Natural variation of Arabidopsis root architecture reveals complementing adaptive strategies to potassium starvation. *Plant Physiology* **161**: 1421–1432.

Kepinski S, Leyser O. 2005. The *Arabidopsis* F-box protein TIR1 is an auxin receptor. *Nature* **435:** 446-451.

Kieber JJ, Rothenberg M, Roman G, Feldmann KA, Ecker JR. 1993. *CTR1*, a negative regulator of the ethylene response pathway in arabidopsis, encodes a member of the Raf family of protein kinases. *Cell* **72**: 427–441.

Kiegle E, Moore CA, Haseloff J, Tester MA, Knight MR. 2000. Cell-type-specific calcium responses to drought, salt and cold in the Arabidopsis root. *Plant Journal* **23**: 267–278.

Kim D, Pertea G, Trapnell C, Pimentel H, Kelley R, Salzberg SL. 2013. TopHat2: accurate alignment of transcriptomes in the presence of insertions, deletions and gene fusions. *Genome Biology* **14**: R36.

Kim MJ, Ciani S, Schachtman DP. 2010. A peroxidase contributes to ROS production during Arabidopsis root response to potassium deficiency. *Molecular Plant* **3**: 420–427.

Kim MJ, Ruzicka D, Shin R, Schachtman DP. 2012. The *Arabidopsis* AP2/ERF transcription factor RAP2.11 modulates plant response to low-potassium conditions. *Molecular Plant* **5**: 1042–1057.

Kleine-Vehn J, Ding Z, Jones AR, Tasaka M, Morita MT, Friml J. 2010. Gravity-induced PIN transcytosis for polarization of auxin fluxes in gravity-sensing root cells. *Proceedings of the National Academy of Sciences, USA* **107**: 22344–22349.

Knight H, Mugford SG, Ülker B, Gao D, Thorlby G, Knight MR. 2009. Identification of SFR6, a key component in cold acclimation acting post-translationally on CBF function. *Plant Journal* **58**: 97–108.

Ko J-H, Yang SH, Han K-H. 2006. Upregulation of an Arabidopsis RING-H2 gene, *XERICO*, confers drought tolerance through increased abscisic acid biosynthesis. *Plant Journal* **47**: 343–355.

Kou X, Liu C, Han L, Wang S, Xue Z. 2016. NAC transcription factors play an important role in ethylene biosynthesis, reception and signaling of tomato fruit ripening. *Molecular Genetics and Genomics* **291**: 1205–1217.

Křeček P, Skůpa P, Libus J, Naramoto S, Tejos R, Friml J, Zažímalová E. 2009. The PIN-FORMED (PIN) protein family of auxin transporters. *Genome Biology* **10**: 249.

Kwak JM, Mori IC, Pei ZM, Leonhard N, Angel Torres M, Dangl JL, Bloom RE, Bodde S, Jones JDG, Schroeder JI. 2003. NADPH oxidase *AtrbohD* and *AtrbohF* genes function in ROS-dependent ABA signaling in *Arabidopsis*. *EMBO Journal* **22**: 2623–2633.

Lagarde D, Basset M, Lepetit M, Conejero G, Gaymard F, Astruc S, Grignon C. 1996. Tissue-specific expression of Arabidopsis *AKT1* gene is consistent with a role in K^+ nutrition. *The Plant Journal: for Cell and Molecular Biology* **9**: 195–203.

Lavenus J, Goh T, Roberts I, Guyomarc'h S, Lucas M, De Smet I, Fukaki H, Beeckman T, Bennett M, Laplaze L. 2013. Lateral root development in Arabidopsis: fifty shades of auxin. *Trends in Plant Science* **18**: 1360–1385.

Lee DJ, Park JW, Lee HW, Kim J. 2009. Genome-wide analysis of the auxin-responsive transcriptome downstream of iaa1 and its expression analysis reveal the diversity and

complexity of auxin-regulated gene expression. *Journal of Experimental Botany* **60**: 3935–3957.

Lee S, Cheng H, King KE, Wang W, He Y, Hussain A, Lo J, Harberd NP, Peng J. **2002**. Gibberellin regulates *Arabidopsis* seed germination via *RGL2*, a *GAI/RGA*-like gene whose expression is up-regulated following imbibition. *Genes and Development* **16**: 646–658.

Leigh RA, Jones RGW. **1984**. A hypothesis relating critical potassium concentrations for growth to the distribution and functions of this ion in the plant cell. *New Phytologist* **97**: 1–13.

Lewis DR, Negi S, Sukumar P, Muday GK. **2011**. Ethylene inhibits lateral root development, increases IAA transport and expression of PIN3 and PIN7 auxin efflux carriers. *Development (Cambridge, England)* **138**: 3485–3495.

Li G, Meng X, Wang R, Mao G, Han L, Liu Y, Zhang S. **2012**. Dual-level regulation of ACC synthase activity by MPK3/MPK6 cascade and its downstream WRKY transcription factor during ethylene induction in arabidopsis. *PLoS Genetics* **8**: e1002767.

Li G, Xu W, Kronzucker HJ, Shi W. **2015a**. Ethylene is critical to the maintenance of primary root growth and Fe homeostasis under Fe stress in Arabidopsis. *Journal of Experimental Botany* **66**: 2041–2054.

Li H, Handsaker B, Wysoker A, Fennell T, Ruan J, Homer N, Marth G, Abecasis G, Durbin R. **2009**. The Sequence Alignment/Map format and SAMtools. *Bioinformatics* **25**: 2078–2079.

Li H, Yang X, Luo A. **2001**. Ameliorating effect of potassium on iron toxicity in hybrid rice. *Journal of Plant Nutrition* **24**: 1849–1860.

Li J, Wu W-H, Wang Y. 2017. Potassium channel AKT1 is involved in the auxin-mediated root growth inhibition in *Arabidopsis* response to low K^+ stress. *Journal of Integrative Plant Biology*. doi: 10.1111/jipb.12575.

Li L, Hou X, Tsuge T, Ding M, Aoyama T, Oka A, Gu H, Zhao Y, Qu LJ. **2008**. The possible action mechanisms of indole-3-acetic acid methyl ester in Arabidopsis. *Plant Cell Reports* **27**: 575–584.

Li L, Kim BG, Cheong YH, Pandey GK, Luan S. **2006**. A Ca^{2+} signaling pathway regulates a K^+ channel for low-K response in Arabidopsis. *Proceedings of the National Academy of Sciences, USA* **103**: 12625–12630.

Li R, Zhang J, Li J, Zhou G, Wang Q, Bian W, Erb M, Lou Y. **2015b**. Prioritizing plant defence over growth through WRKY regulation facilitates infestation by non-target herbivores. *eLife* **4:**.e04805.

Li X, Zhang H, Ai Q, Liang G, Yu D. **2016**. Two bHLH transcription factors, bHLH34 and bHLH104, regulate iron homeostasis in *Arabidopsis thaliana*. *Plant Physiology* **170**: 2478–2493.

Liao C-Y, Smet W, Brunoud G, Yoshida S, Vernoux T, Weijers D. **2015**. Reporters for sensitive and quantitative measurement of auxin response. *Nature Methods* **12**: 207–210.

Lister R, O'Malley RC, Tonti-Filippini J, Gregory BD, Berry CC, Millar AH, Ecker JR. **2008**. Highly integrated single-base resolution maps of the epigenome in Arabidopsis. *Cell* **133**: 523–536.

Liszkay A, van der Zalm E, Schopfer P. **2004**. Production of reactive oxygen intermediates ($O2^{\cdot-}$, H_2O_2, and OH) by maize roots and their role in wall loosening and elongation growth. *Plant Physiology* **136**: 3114–3123.

Liu Y, Donner E, Lombi E, Li RY, Wu ZC, Zhao FJ, Wu P. 2013. Assessing the contributions of lateral roots to element uptake in rice using an auxin-related lateral root mutant. *Plant*

Soil **372:** 125–136.

Lobet G, Pagès L, Draye X. **2011**. A novel image-analysis toolbox enabling quantitative analysis of root system architecture. *Plant Physiology* **157**: 29–39.

Long TA, Tsukagoshi H, Busch W, Lahner B, Salt DE, Benfey PN. **2010**. The bHLH transcription factor POPEYE regulates response to iron deficiency in Arabidopsis roots. *The Plant Cell* **22**: 2219–2236.

López-Bucio J, Cruz-Ramírez A, Herrera-Estrella L. **2003**. The role of nutrient availability in regulating root architecture. *Current Opinion in Plant Biology* **6**: 280–287.

Lorenzo O, Piqueras R, Sánchez-Serrano JJ, Solano R. **2003**. ETHYLENE RESPONSE FACTOR1 integrates signals from ethylene and jasmonate pathways in plant defense. *The Plant Cell* **15**: 165–178.

Luan S, Kudla JJ, Rodriguez-concepcion M, Yalovsky S, Gruissem W, Yalovsky CS, Gruissem W, Yalovsky S, Gruissem W, Yalovsky CS *et al.* 2002. Calmodulins and calcineurin B-like proteins: calcium sensors for specific signal response coupling in plants. *The Plant Cell Online* **14:** S389–S400.

Lucas M, Davière J-M, Rodríguez-Falcón M, Pontin M, Iglesias-Pedraz JM, Lorrain S, Fankhauser C, Blázquez MA, Titarenko E, Prat S *et al.* 2008. A molecular framework for light and gibberellin control of cell elongation. *Nature* **451**: 480–484.

Luschnig C, Gaxiola RA, Grisafi P, Fink GR. **1998**. EIR1, a root-specific protein involved in auxin transport, is required for gravitropism in *Arabidopsis thaliana*. *Genes and Development* **12**: 2175–2187.

Lynch J. **1995**. Root architecture and plant productivity. *Plant Physiology* **109**: 7–13.

Lynch JP. **2007**. Roots of the second green revolution. *Australian Journal of Botany* **55**: 493–512.

Lynch JP, Brown KM. **2012**. New roots for agriculture: exploiting the root phenome. *Philosophical transactions of the Royal Society of London. Series B, Biological Sciences* **367**: 1598–1604.

Ma T-L, Wu W-H, Wang Y. **2012**. Transcriptome analysis of rice root responses to potassium deficiency. *BMC Plant Biology* **12**: 161.

Ma Y, Szostkiewicz I, Korte A, Moes D, Yang Y, Christmann A, Grill E. **2009**. Regulators of PP2C phosphatase activity function as abscisic acid sensors. *Science (New York, N.Y.)* **324**: 1064–1068.

Ma Z, Ren YY. **2012**. Ethylene interacts with auxin in regulating developmental attenuation of gravitropism in flax root. *Journal of Plant Growth Regulation* **31**: 509–518.

Maathuis FJM, Filatov V, Herzyk P, Krijger GC, Axelsen KB, Chen S, Green BJ, Li Y, Madagan KL, Sánchez-Fernández R *et al.* 2003. Transcriptome analysis of root transporters reveals participation of multiple gene families in the response to cation stress. *Plant Journal* **35**: 675–692.

Maathuis FJM, Sanders D. **1993**. Energization of potassium uptake in *Arabidopsis thaliana*. *Planta* **191**: 302–307.

Maathuis FJ, Sanders D. **1994**. Mechanism of high-affinity potassium uptake in roots of Arabidopsis thaliana. *Proceedings of the National Academy of Sciences, USA* **91**: 9272–9276.

MacMillan J. **2002**. Occurrence of gibberellins in vascular plants, fungi, and bacteria. *Journal of Plant Growth Regulation* **20**: 387–442.

Maeght J-L, Rewald B, Pierret A. **2013**. How to study deep roots—and why it matters. *Frontiers in Plant Science* **4**: 299.

Magome H, Yamaguchi S, Hanada A, Kamiya Y, Oda K. **2004**. *dwarf and delayed-flowering 1*, a novel Arabidopsis mutant deficient in gibberellin biosynthesis because of overexpression of a putative AP2 transcription factor. *Plant Journal* **37**: 720–729.

Magome H, Yamaguchi S, Hanada A, Kamiya Y, Oda K. **2008**. The DDF1 transcriptional activator upregulates expression of a gibberellin-deactivating gene, *GA2ox7*, under high-salinity stress in Arabidopsis. *Plant Journal* **56**: 613–626.

Maizel A, Von Wangenheim D, Federici F, Haseloff J, Stelzer EHK. **2011**. High-resolution live imaging of plant growth in near physiological bright conditions using light sheet fluorescence microscopy. *Plant Journal* **68**: 377–385.

Malamy JE, Benfey PN. **1997**. Organization and cell differentiation in lateral roots of *Arabidopsis thaliana*. *Development (Cambridge, England)* **124**: 33–44.

Mandadi KK, Misra A, Ren S, McKnight TD. **2009**. BT2, a BTB protein, mediates multiple responses to nutrients, stresses, and hormones in Arabidopsis. *Plant Physiology* **150**: 1930–1939.

Manzano C, Pallero-Baena M, Casimiro I, De Rybel B, Orman-Ligeza B, Van Isterdael G, Beeckman T, Draye X, Casero P, Del Pozo JC. **2014**. The emerging role of reactive oxygen species signaling during lateral root development. *Plant Physiology* **165**: 1105–1119.

Marcel D, Müller T, Hedrich R, Geiger D. **2010**. K^+ transport characteristics of the plasma membrane tandem-pore channel TPK4 and pore chimeras with its vacuolar homologs. *FEBS Letters* **584**: 2433–2439.

Marchant A, Kargul J, May ST, Muller P, Delbarre A, Perrot-Rechenmann C, Bennett MJ. **1999**. AUX1 regulates root gravitropism in *Arabidopsis* by facilitating auxin uptake within root apical tissues. *The EMBO Journal* **18**: 2066–2073.

Marín-de la Rosa N, Pfeiffer A, Hill K, Locascio A, Bhalerao RP, Miskolczi P, Grønlund AL, Wanchoo-Kohli A, Thomas SG, Bennett MJ *et al.* 2015. Genome wide binding site analysis reveals transcriptional coactivation of cytokinin-responsive genes by DELLA proteins. *PLoS Genetics* **11**: e1005337.

Marino D, Dunand C, Puppo A, Pauly N. **2012**. A burst of plant NADPH oxidases. *Trends in Plant Science* **17**: 9–15.

Marschner H. **1995**. *Mineral nutrition of higher plants.* Amsterdam, the Netherlands: Academic Press.

Maruyama K, Sakuma Y, Kasuga M, Ito Y, Seki M, Goda H, Shimada Y, Yoshida S, Shinozaki K, Yamaguchi-Shinozaki K. **2004**. Identification of cold-inducible downstream genes of the Arabidopsis DREB1A/CBF3 transcriptional factor using two microarray systems. *Plant Journal* **38**: 982–993.

Mashiguchi K, Tanaka K, Sakai T, Sugawara S, Kawaide H, Natsume M, Hanada A, Yaeno T, Shirasu K, Yao H *et al.* 2011. The main auxin biosynthesis pathway in Arabidopsis. *Proceedings of the National Academy of Sciences* **108**: 18512–18517.

Mason MG, Mathews DE, Argyros DA, Maxwell BB, Kieber JJ, Alonso JM, Ecker JR, Schaller GE. **2005**. Multiple type-B response regulators mediate cytokinin signal transduction in Arabidopsis. *The Plant Cell* **17**: 3007–3018.

McCarthy DJ, Chen Y, Smyth GK. **2012**. Differential expression analysis of multifactor RNA-Seq experiments with respect to biological variation. *Nucleic Acids Research* **40**: 4288–4297.

McCormack E, Braam J. **2003**. Calmodulins and related potential calcium sensors of Arabidopsis. *New Phytologist* **159**: 585–598.

McCubbin AG, Ritchie SM, Swanson SJ, Gilroy S. **2004**. The calcium-dependent protein kinase HvCDPK1 mediates the gibberellic acid response of the barley aleurone through regulation of vacuolar function. *Plant Journal* **39**: 206–218.

McGinnis KM, Thomas SG, Soule JD, Strader LC, Zale JM, Sun T, Steber CM. **2003**. The Arabidopsis *SLEEPY1* gene encodes a putative F-box subunit of an SCF E3 ubiquitin ligase. *The Plant Cell* **15**: 1120–1130.

Miller G, Shulaev V, Mittler R. **2008**. Reactive oxygen signaling and abiotic stress. *Physiologia Plantarum* **133**: 481–489.

Mironova V V, Omelyanchuk N a, Wiebe DS, Levitsky VG. **2014**. Computational analysis of auxin responsive elements in the *Arabidopsis thaliana* L. genome. *BMC Genomics* **15 Suppl 12**: S4.

Mittler R. **2002**. Oxidative stress, antioxidants and stress tolerance. *Trends in Plant Science* **7**: 405–410.

Mittler R, Vanderauwera S, Gollery M, Van Breusegem F. **2004**. Reactive oxygen gene network of plants. *Trends in Plant Science* **9**: 490–498.

Moffat CS, Ingle RA, Wathugala DL, Saunders NJ, Knight H, Knight MR. **2012**. ERF5 and ERF6 play redundant roles as positive regulators of JA/Et-mediated defense against *Botrytis cinerea* in Arabidopsis. *PLoS ONE* **7:** e35995.

Morita MT, Tasaka M. 2010. *Tropism*. eLS. John Wiley & Sons Ltd, Chichester, UK. http://www.els.net

Moritsugu M, Shibasaka M, Kawasaki T. 1993. Where is the most important and efficient site for absorption and translocation of cations in excised barley roots? *Soil Science & Plant Nutrition* **39:** 299–307.

Mortazavi A, Williams BA, McCue K, Schaeffer L, Wold B. **2008**. Mapping and quantifying mammalian transcriptomes by RNA-Seq. *Nature Methods* **5**: 621–628.

Moubayidin L, Perilli S, Dello Ioio R, Di Mambro R, Costantino P, Sabatini S. **2010**. The rate of cell differentiation controls the *Arabidopsis* root meristem growth phase. *Current Biology* **20**: 1138–1143.

Mounier E, Pervent M, Ljung K, Gojon A, Nacry P. **2014**. Auxin-mediated nitrate signalling by NRT1.1 participates in the adaptive response of *Arabidopsis* root architecture to the spatial heterogeneity of nitrate availability. *Plant, Cell & Environment* **37**: 162–174.

Mravec J, Kubes M, Bielach A, Gaykova V, Petrasek J, Skupa P, Chand S, Benkova E, Zazimalova E, Friml J. **2008**. Interaction of PIN and PGP transport mechanisms in auxin distribution-dependent development. *Development* **135**: 3345–3354.

Muller O, Lightfoot S, Schroeder A. 2016. RNA integrity number (RIN) – standardization of RNA quality control. Application Agilent Technologies. 5989-1165EN. https://www.agilent.com/cs/library/applications/5989-1165EN.pdf. [accessed 1 August 2017]

Müller A, Guan C, Gälweiler L, Tänzler P, Huijser P, Marchant A, Parry G, Bennett MJ, Wisman E, Palme K. **1998**. *AtPIN2* defines a locus of *Arabidopsis* for root gravitropism control. *The EMBO Journal* **17**: 6903–6911.

Müller M, Munné-Bosch S. **2015**. Ethylene response factors: a key regulatory hub in hormone and stress signaling. *Plant Physiology* **169**: 32–41.

Müller TM, Böttcher C, Morbitzer R, Götz CC, Lehmann J, Lahaye T, Glawischnig E. **2015**.

TRANSCRIPTION ACTIVATOR-LIKE EFFECTOR NUCLEASE-mediated generation and metabolic analysis of camalexin-deficient *cyp71a12 cyp71a13* double knockout lines. *Plant Physiology* **168**: 849–858.

Murase K, Hirano Y, Sun T, Hakoshima T. **2008**. Gibberellin-induced DELLA recognition by the gibberellin receptor GID1. *Nature* **456**: 459.

Murashige T, Skoog F. **1962**. A revised medium for rapid growth and bio assays with tobacco tissue cultures. *Physiologia Plantarum* **15**: 473–497.

NAAIAP report. 2014. Soil suitability valuation for maize production in Kenya. A Report by National Accelerated Agricultural Inputs Access Programme (NAAIAP) in collaboration with Kenya Agricultural Research Institute (KARI) Department of Kenya Soil Survey. http://www.africafertilizer.org/wp-content/uploads/2017/04/Soil-Suitability-Evaluation-for-Maize-Prod.-in-Kenya.pdf. [accessed 1 August 2017].

Nagalakshmi U, Wang Z, Waern K, Shou C, Raha D, Gerstein M, Snyder M. **2008**. The transcriptional landscape of the yeast genome defined by RNA sequencing. *Science* **320**: 1344–1349.

Naithani S, Preece J, D'Eustachio P, Gupta P, Amarasinghe V, Dharmawardhana PD, Wu G, Fabregat A, Elser JL, Weiser J *et al.* 2017. Plant Reactome: a resource for plant pathways and comparative analysis. *Nucleic Acids Research* **45**: D1029–D1039.

Nakajima M, Shimada A, Takashi Y, Kim YC, Park SH, Ueguchi-Tanaka M, Suzuki H, Katoh E, Iuchi S, Kobayashi M *et al.* 2006. Identification and characterization of Arabidopsis gibberellin receptors. *Plant Journal* **46**: 880–889.

Nam YJ, Tran LSP, Kojima M, Sakakibara H, Nishiyama R, Shin R. **2012**. Regulatory roles of cytokinins and cytokinin signaling in response to potassium deficiency in *Arabidopsis*. *PLoS ONE* **7**: e47797.

Nechushtai R, Conlan AR, Harir Y, Song L, Yogev O, Eisenberg-Domovich Y, Livnah O, Michaeli D, Rosen R, Ma V *et al.* 2012. Characterization of *Arabidopsis* NEET reveals an ancient role for NEET proteins in iron metabolism. *The Plant Cell* **24**: 2139–2154.

Negi S, Ivanchenko MG, Muday GK. **2008**. Ethylene regulates lateral root formation and auxin transport in *Arabidopsis thaliana*. *Plant Journal* **55**: 175–187.

Nieves-Cordones M, Miller AJ, Alemán F, Martínez V, Rubio F. **2008**. A putative role for the plasma membrane potential in the control of the expression of the gene encoding the tomato high-affinity potassium transporter HAK5. *Plant Molecular Biology* **68**: 521–532.

Normanly J, Grisafi P, Fink GR, Bartel B. **1997**. Arabidopsis mutants resistant to the auxin effects of indole-3-acetonitrile are defective in the nitrilase encoded by the NIT1 gene. *The Plant Cell* **9**: 1781–1790.

Novillo F, Medina J, Salinas J. **2007**. *Arabidopsis* CBF1 and CBF3 have a different function than CBF2 in cold acclimation and define different gene classes in the CBF regulon. *Proceedings of the National Academy of Sciences, USA* **104**: 21002–21007.

Okushima Y, Overvoorde PJ, Arima K, Alonso JM, Chan A, Chang C, Ecker JR, Hughes B, Lui A, Nguyen D *et al.* 2005. Functional genomic analysis of the *AUXIN RESPONSE FACTOR* gene family members in *Arabidopsis thaliana*: unique and overlapping functions of *ARF7* and *ARF19*. *Plant Cell* **17**: 444–463.

Ortega-Martínez O, Pernas M, Carol RJ, Dolan L. **2007**. Ethylene modulates stem cell division in the *Arabidopsis thaliana* root. *Science (New York, N.Y.)* **317**: 507–510.

Ovecka M, Vaskebova L, Komis G, Luptovciak I, Smertenko A, Samaj J. **2015**. Preparation of plants for developmental and cellular imaging by light-sheet microscopy. *Nature*

Protocols **10**: 1234–1247.

Overvoorde P, Fukaki H, Beeckman T. **2010**. Auxin control of root development. *Cold Spring Harbor Perspectives in Biology* **2:** a001537.

Pacifici E, Polverari L, Sabatini S. **2015**. Plant hormone cross-talk: the pivot of root growth. *Journal of Experimental Botany* **66**: 1113–1121.

Paez-Garcia A, Motes C, Scheible W-R, Chen R, Blancaflor E, Monteros M. **2015**. Root traits and phenotyping strategies for plant improvement. *Plants* **4**: 334–355.

Park S, Lee CM, Doherty CJ, Gilmour SJ, Kim Y, Thomashow MF. **2015**. Regulation of the Arabidopsis CBF regulon by a complex low-temperature regulatory network. *Plant Journal* **82**: 193–207.

Park S-Y, Fung P, Nishimura N, Jensen DR, Fujii H, Zhao Y, Lumba S, Santiago J, Rodrigues A, Chow T-FF *et al.* 2009. Abscisic acid inhibits type 2C protein phosphatases via the PYR/PYL family of START proteins. *Science (New York, N.Y.)* **324**: 1068–1071.

Passardi F, Tognolli M, De Meyer M, Penel C, Dunand C. **2006**. Two cell wall associated peroxidases from Arabidopsis influence root elongation. *Planta* **223**: 965–974.

Peng J, Carol P, Richards DE, King KE, Cowling RJ, Murphy GP, Harberd NP. **1997**. The Arabidopsis *GAI* gene defines a signaling pathway that negatively regulates gibberellin responses. *Genes and Development* **11**: 3194–3205.

Peng JR, Richards DE, Hartley NM, Murphy GP, Devos KM, Flintham JE, Beales J, Fish LJ, Worland AJ, Pelica F *et al.* 1999. 'Green revolution' genes encode mutant gibberellin response modulators. *Nature* **400**: 256–261.

Peng L, Yamamoto H, Shikanai T. **2011**. Structure and biogenesis of the chloroplast NAD(P)H dehydrogenase complex. *Biochimica et Biophysica Acta - Bioenergetics* **1807**: 945–953.

Péret B, Li G, Zhao J, Band LR, Voß U, Postaire O, Luu D-T, Da Ines O, Casimiro I, Lucas M *et al.* 2012. Auxin regulates aquaporin function to facilitate lateral root emergence. *Nature Cell Biology* **14**: 991–998.

Perilli S, Moubayidin L, Sabatini S. **2010**. The molecular basis of cytokinin function. *Current Opinion in Plant Biology* **13**: 21–26.

Perrot-Rechenmann C. **2010**. Cellular responses to auxin: division versus expansion. *Cold Spring Harbor Perspectives in Biology* **2**: a001446.

Petrášek J, Mravec J, Bouchard R, Blakeslee JJ, Abas M, Seifertová D, Wisniewska J, Tadele Z, Kubes M, Covanová M *et al.* 2006. PIN proteins perform a rate-limiting function in cellular auxin efflux. *Science* **312**: 914–918.

Petricka JJ, Winter CM, Benfey PN. **2012**. Control of Arabidopsis root development. *Annual review of plant biology* **63**: 563–90.

Pitts RJ, Cernac A, Estelle M. **1998**. Auxin and ethylene promote root hair elongation in Arabidopsis. *Plant Journal* **16**: 553–560.

Plackett ARG, Ferguson AC, Powers SJ, Wanchoo-Kohli A, Phillips AL, Wilson ZA, Hedden P, Thomas SG. **2014**. DELLA activity is required for successful pollen development in the Columbia ecotype of Arabidopsis. *New Phytologist* **201**: 825–836.

Potikha TS, Collins CC, Johnson DI, Delmer DP, Levine A. **1999**. The involvement of hydrogen peroxide in the differentiation of secondary walls in cotton fibers. *Plant Physiology* **119**: 849–858.

Prajapati K, Modi HA. **2012**. The importance of potassium in plant growht – a review. *Indian Journal of Plant Sciences Jul.-Sept. & Oct.-Dec* **1**: 2319–382402.

Qiao H, Shen Z, Huang S-sC, Schmitz RJ, Urich MA, Briggs SP, Ecker JR. **2012**. Processing and subcellular trafficking of ER-tethered EIN2 control response to ethylene gas. *Science* **338**: 390–393.

Qin G, Gu H, Zhao Y, Ma Z, Shi G, Yang Y, Pichersky E, Chen H, Liu M, Chen Z *et al.* 2005. An indole-3-acetic acid carboxyl methyltransferase regulates Arabidopsis leaf development. *The Plant Cell* **17**: 2693–2704.

Queval G, Foyer CH. **2012**. Redox regulation of photosynthetic gene expression. *Philosophical Transactions of the Royal Society of London. Series B, Biological Sciences* **367**: 3475–3485.

Romheld V, Kirkby EA. **2010**. Research on potassium in agriculture: needs and prospects. *Plant and Soil* **335**: 155–180.

Ragel P, Ródenas R, García-Martín E, Andrés Z, Villalta I, Nieves-Cordones M, Rivero RM, Martínez V, Pardo JM, Quintero FJ *et al.* 2015. The CBL-interacting protein kinase CIPK23 regulates HAK5-mediated high-affinity K^+ uptake in Arabidopsis roots. *Plant Physiology* **169**: doi: https://doi.org/10.1104/pp.15.01401.

Rahman A, Hosokawa S, Oono Y, Amakawa T, Goto N, Tsurumi S. **2002**. Auxin and ethylene response interactions during Arabidopsis root hair development dissected by auxin influx modulators. *Plant Physiology* **130**: 1908–1917.

Ramakers C, Ruijter JM, Lekanne Deprez RH, Moorman AFM. **2003**. Assumption-free analysis of quantitative real-time polymerase chain reaction (PCR) data. *Neuroscience Letters* **339**: 62–66.

Raven JA. 1975. Transport of indoleacetic acid in plant calls in relation to pH and electrical potential gradients, and its significance for polar IAA transport. *New Phytologist* **74**: 163–172.

Ravet K, Touraine B, Boucherez J, Briat JF, Gaymard F, Cellier F. **2009**. Ferritins control interaction between iron homeostasis and oxidative stress in Arabidopsis. *Plant Journal* **57**: 400–412.

Renew S, Heyno E, Schopfer P, Liszkay A. **2005**. Sensitive detection and localization of hydroxyl radical production in cucumber roots and Arabidopsis seedlings by spin trapping electron paramagnetic resonance spectroscopy. *The Plant journal : for cell and molecular biology* **44**: 342–347.

Rieu I, Eriksson S, Powers SJ, Gong F, Griffiths J, Woolley L, Benlloch R, Nilsson O, Thomas SG, Hedden P *et al.* 2008. Genetic analysis reveals that C19-GA 2-oxidation is a major gibberellin inactivation pathway in *Arabidopsis*. *The Plant Cell* **20**: 2420–2436.

Rigas S, Ditengou FA, Ljung K, Daras G, Tietz O, Palme K, Hatzopoulos P. **2013**. Root gravitropism and root hair development constitute coupled developmental responses regulated by auxin homeostasis in the Arabidopsis root apex. *New Phytologist* **197**: 1130–1141.

Riordan HE. 2015. *Studies into the link between plant development and abiotic stress tolerance in* Arabidopsis thaliana. PhD thesis, Durham University, Durham, UK. (http://etheses.dur.ac.uk/11149/)

Robinson MD, McCarthy DJ, Smyth GK. **2010**. edgeR: a bioconductor package for differential expression analysis of digital gene expression data. *Bioinformatics (Oxford, England)* **26**: 139–140.

Robinson NJ, Procter CM, Connolly EL, Guerinot ML. **1999**. A ferric-chelate reductase for iron uptake from soils. *Nature* **397**: 694–697.

Rodriguez FI, Esch JJ, Hall AE, Binder BM, Schaller GE, Bleecker AB. **1999**. A copper cofactor

for the ethylene receptor ETR1 from *Arabidopsis*. *Science* **283**: 996–998.

Ros-Barceló A, Pomar F, López-Serrano M, Martínez P, Pedreño MA. **2002**. Developmental regulation of the H_2O_2-producing system and of a basic peroxidase isoenzyme in the *Zinnia elegans* lignifying xylem. *Plant Physiology and Biochemistry* **40**: 325–332.

Rowe JH, Topping JF, Liu J, Lindsey K. **2016**. Abscisic acid regulates root growth under osmotic stress conditions via an interacting hormonal network with cytokinin, ethylene and auxin. *New Phytologist* **211**: 225–239.

Rubery PH, Sheldrake AR. **1974**. Carrier-mediated auxin transport. *Planta* **118**: 101–121.

Ruzicka K, Ljung K, Vanneste S, Podhorska R, Beeckman T, Friml J, Benkova E. **2007**. Ethylene regulates root growth through effects on auxin biosynthesis and transport-dependent auxin distribution. *The Plant Cell Online* **19**: 2197–2212.

De Rybel B, Vassileva V, Parizot B, Demeulenaere M, Grunewald W, Audenaert D, Van Campenhout J, Overvoorde P, Jansen L, Vanneste S *et al.* 2010. A novel Aux/IAA28 signaling cascade activates GATA23-dependent specification of lateral root founder cell identity. *Current Biology* **20**: 1697–1706.

Sabatini S, Beis D, Wolkenfelt H, Murfett J, Guilfoyle T, Malamy J, Benfey P, Leyser O, Bechtold N, Weisbeek P *et al.* 1999. An auxin-dependent distal organizer of pattern and polarity in the Arabidopsis root. *Cell* **99**: 463–472.

Sabatini S, Heidstra R, Wildwater M, Scheres B. **2003**. SCARECROW is involved in positioning the stem cell niche in the Arabidopsis root meristem. *Genes and Development* **17**: 354–358.

Sagi M, Fluhr R. **2006**. Production of reactive oxygen species by plant NADPH oxidases. *Plant Physiology* **141**: 336–340.

Sakai H, Aoyama T, Oka A. **2000**. *Arabidopsis* ARR1 and ARR2 response regulators operate as transcriptional activators. *Plant Journal* **24**: 703–711.

Sakai H, Honma T, Aoyama T, Sato S, Kato T, Tabata S, Oka A. **2001**. ARR1, a transcription factor for genes immediately responsive to cytokinins. *Science* **294**: 1519–1521.

Sakamoto H. **2004**. Arabidopsis Cys2/His2-type zinc-finger proteins function as transcription repressors under drought, cold, and high-salinity stress conditions. *Plant Physiology* **136**: 2734–2746.

Sakamoto H, Araki T, Meshi T, Iwabuchi M. **2000**. Expression of a subset of the Arabidopsis Cys2/His2-type zinc-finger protein gene family under water stress. *Gene* **248**: 23–32.

Sanz L, Murray JAH, Dewitte W. **2009**. Regulating cell division in roots during post-embryonic growth. *Progress in Botany* **73**: 57–81.

Sarkar AK, Luijten M, Miyashima S, Lenhard M, Hashimoto T, Nakajima K, Scheres B, Heidstra R, Laux T. **2007**. Conserved factors regulate signalling in *Arabidopsis thaliana* shoot and root stem cell organizers. *Nature* **446**: 811–814.

Scheres B, Dilaurenzio L, Willemsen V, Hauser MT, Janmaat K, Weisbeek P, Benfey PN. **1995**. Mutations affecting the radial organisation of the Arabidopsis root display specific defects throughout the embryonic axis. *Development* **121**: 53–62.

Schneider CA, Rasband WS, Eliceiri KW. **2012**. NIH Image to ImageJ: 25 years of image analysis. *Nature Methods* **9**: 671–675.

Schroeder JI, Fang HH. **1991**. Inward-rectifying K^+ channels in guard cells provide a mechanism for low-affinity K^+ uptake. *Proceedings of the National Academy of Sciences, USA* **88**: 11583–11587.

Schroeder JI, Ward JM, Gassmann W. **1994**. Perspectives on the physiology and structure of inward-rectifying K^+ channels in higher plants: biophysical implications for K^+ uptake. *Annual Review of Biophysics and Biomolecular Structure* **23**: 441–471.

Seki M, Narusaka M, Ishida J, Nanjo T, Fujita M, Oono Y, Kamiya A, Nakajima M, Enju A, Sakurai T *et al.* 2002. Monitoring the expression profiles of 7000 Arabidopsis genes under drought, cold and high-salinity stresses using a full-length cDNA microarray. *Plant Journal* **31**: 279–292.

Selote D, Samira R, Matthiadis A, Gillikin JW, Long TA. **2015**. Iron-binding E3 ligase mediates iron response in plants by targeting basic helix-loop-helix transcription factors. *Plant Physiology* **167**: 273–286.

Sentenac H, Bonneaud N, Minet M, Lacroute F, Salmon J, Gaymard F, Grignon C. **1992**. Cloning and expression in yeast of a plant potassium-ion transport-system. *Science* **256**: 663–665.

Shahnejat-Bushehri S, Tarkowska D, Sakuraba Y, Balazadeh S. **2016**. *Arabidopsis* NAC transcription factor JUB1 regulates GA/BR metabolism and signalling. *Nature Plants* **2**: 16013.

Shahzad Z, Amtmann A. **2017**. Food for thought: how nutrients regulate root system architecture. *Current Opinion in Plant Biology* **39**: 80–87.

Shan W, Kuang JF, Chen L, Xie H, Peng HH, Xiao YY, Li XP, Chen WX, He QG, Chen JY *et al.* 2012. Molecular characterization of banana NAC transcription factors and their interactions with ethylene signalling component EIL during fruit ripening. *Journal of Experimental Botany* **63**: 5171–5187.

Shang Y, Yan L, Liu Z-Q, Cao Z, Mei C, Xin Q, Wu F-Q, Wang X-F, Du S-Y, Jiang T *et al.* 2010. The Mg-chelatase H subunit of *Arabidopsis* antagonizes a group of WRKY transcription repressors to relieve ABA-responsive genes of inhibition. *The Plant Cell* **22**: 1909–1935.

Sharp RE, Poroyko V, Hejlek LG, Spollen WG, Springer GK, Bohnert HJ, Nguyen HT. **2004**. Root growth maintenance during water deficits: physiology to functional genomics. *Journal of Experimental Botany* **55:** 2343–2351.

Sharp RE, Wu YJ, Voetberg GS, Saab IN, Lenoble ME. 1994. Confirmation that abscisic-acid accumulation is required for maize primary root elongation at low water potentials. *Journal of Experimental Botany* **45:** 1743–1751.

Sheard LB, Zheng N. **2009**. Signal advance for abscisic acid. *Nature* **462**: 575–576.

Shi Y, Huang J, Sun T, Wang X, Zhu C, Ai Y, Gu H. **2017.** The precise regulation of different *COR* genes by individual CBF transcription factors in *Arabidopsis thaliana*. *Journal of Integrative Plant Biology* **59:** 118–133.

Shin R, Burch AY, Huppert KA, Tiwari SB, Murphy AS, Guilfoyle TJ, Schachtman DP. **2007**. The Arabidopsis transcription factor MYB77 modulates auxin signal transduction. *The Plant Cell* **19**: 2440–2453.

Shin R, Schachtman DP. **2004**. Hydrogen peroxide mediates plant root cell response to nutrient deprivation. *Proceedings of the National Academy of Sciences, USA* **101**: 8827–8832.

Signora L, De Smet I, Foyer CH, Zhang H. **2001**. ABA plays a central role in mediating the regulatory effects of nitrate on root branching in *Arabidopsis*. *Plant Journal* **28**: 655–662.

Silverstone AL, Jung HS, Dill A, Kawaide H, Kamiya Y, Sun TP. **2001**. Repressing a repressor: gibberellin-induced rapid reduction of the RGA protein in Arabidopsis. *The Plant Cell* **13**: 1555–1566.

Smalle J, Vierstra RD. **2004**. The ubiquitin 26S proteasome proteolytic pathway. *Annual Review of Plant Biology* **55**: 555–590.

Smith S, De Smet I. **2012**. Root system architecture: insights from Arabidopsis and cereal crops. *Philosophical Transactions of the Royal Society B: Biological Sciences* **367**: 1441–1452.

Sofo A, Scopa A, Nuzzaci M, Vitti A. **2015**. Ascorbate peroxidase and catalase activities and their genetic regulation in plants subjected to drought and salinity stresses. *International Journal of Molecular Sciences* **16**: 13561–13578.

Solano R, Stepanova A, Chao Q, Ecker JR. **1998**. Nuclear events in ethylene signaling: A transcriptional cascade mediated by ETHYLENE-INSENSITIVE3 and ETHYLENE-RESPONSE-FACTOR1. *Genes and Development* **12**: 3703–3714.

Sønderby IE, Geu-Flores F, Halkier BA. **2010**. Biosynthesis of glucosinolates – gene discovery and beyond. *Trends in Plant Science* **15**: 283–290.

Spalding EP, Hirsch RE, Lewis DR, Qi Z, Sussman MR, Lewis BD. **1999**. Potassium uptake supporting plant growth in the absence of AKT1 channel activity: Inhibition by ammonium and stimulation by sodium. *The Journal of General Physiology* **113**: 909–918.

Sponsel VM, Hedden P. **2010**. Gibberellin biosynthesis and inactivation. In: Davies PJ, ed. *Plant hormones*. *Biosynthsis, signal transduction, action!* Dordrecht, the Netherlands: Springer, 63–94.

Stepanova AN, Robertson-Hoyt J, Yun J, Benavente LM, Xie DY, Doležal K, Schlereth A, Jürgens G, Alonso JM. **2008**. TAA1-mediated auxin biosynthesis is essential for hormone crosstalk and plant development. *Cell* **133**: 177–191.

Strader LC, Chen GL, Bartel B. **2010**. Ethylene directs auxin to control root cell expansion. *Plant Journal* **64**: 874–884.

Street IH, Aman S, Zubo Y, Ramzan A, Wang X, Shakeel SN, Kieber JJ, Schaller GE. **2015**. Ethylene inhibits cell proliferation of the Arabidopsis root meristem. *Plant Physiology* **169**: 338–350.

Sugawara S, Hishiyama S, Jikumaru Y, Hanada A, Nishimura T, Koshiba T, Zhao Y, Kamiya Y, Kasahara H. **2009**. Biochemical analyses of indole-3-acetaldoxime-dependent auxin biosynthesis in Arabidopsis. *Proceedings of the National Academy of Sciences, USA* **106**: 5430–5435.

Sun T. 2010. Gibberellin-GID1-DELLA: a pivotal regulatory module for plant growth and development. *Plant Physiology* **154**: 567–570.

Sun T, Gubler F. **2004**. Molecular mechanism of gibberellin signaling in plants. *Annual Review of Plant Biology* **55**: 197–223.

Supek F, Bošnjak M, Škunca N, Šmuc T. **2011**. Revigo summarizes and visualizes long lists of gene ontology terms. *PLoS ONE* **6**: e21800.

Swarup K, Benkova E, Swarup R, Casimiro I, Peret B, Yang Y, Parry G, Nielsen E, De Smet I, Vanneste S *et al.* 2008. The auxin influx carrier LAX3 promotes lateral root emergence. *Nature Cell Biology* **10**: 946–954.

Swarup R, Friml J, Marchant A, Ljung K, Sandberg G, Palme K, Bennett M. **2001**. Localization of the auxin permease AUX1 suggests two functionally distinct hormone transport pathways operate in the *Arabidopsis* root apex. *Genes and Development* **15**: 2648–2653.

Swarup R, Perry P, Hagenbeek D, Van Der Straeten D, Beemster GTS, Sandberg G, Bhalerao

R, Ljung K, Bennett MJ. **2007**. Ethylene upregulates auxin biosynthesis in *Arabidopsis* seedlings to enhance inhibition of root cell elongation. *The Plant Cell* **19**: 2186–2196.

Szklarczyk D, Morris JH, Cook H, Kuhn M, Wyder S, Simonovic M, Santos A, Doncheva NT, Roth A, Bork P *et al.* 2017. The STRING database in 2017: quality-controlled protein–protein association networks, made broadly accessible. *Nucleic Acids Research* **45**: D362–D368.

Takatsuka H, Umeda M. **2014**. Hormonal control of cell division and elongation along differentiation trajectories in roots. *Journal of Experimental Botany* **65**: 2633–2643.

Tan X, Calderon-Villalobos LI a, Sharon M, Zheng C, Robinson C V, Estelle M, Zheng N. **2007**. Mechanism of auxin perception by the TIR1 ubiquitin ligase. *Nature* **446**: 640–645.

The Arabidopsis Genome Initiative. **2000**. Analysis of the genome sequence of the flowering plant *Arabidopsis thaliana*. *Nature* **408**: 796–815.

Thomas SG, Phillips AL, Hedden P. **1999**. Molecular cloning and functional expression of gibberellin 2- oxidases, multifunctional enzymes involved in gibberellin deactivation. *Proceedings of the National Academy of Sciences, USA* **96**: 4698–4703.

Tian T, Liu Y, Yan H, You Q, Yi X, Du Z, Xu W, Su Z. 2017. agriGO v2.0: a GO analysis toolkit for the agricultural community, 2017 update. *Nucleic Acids Research.* doi: 10.1093/nar/gkx382.

Tigchelaar EC. 1978. Tomato ripening mutants. *HortScience* **13:** 502–502.

Tomemori H, Hamamura K, Tanabe K. **2002**. Interactive effects of sodium and potassium on the growth and photosynthesis of spinach and komatsuna. *Plant Production Science* **5**: 281–285.

Topping JF, Lindsey K. **1997**. Promoter trap markers differentiate structural and positional components of polar development in Arabidopsis. *The Plant Cell* **9**: 1713–1725.

Trolldenier G. 1973. Secondary effects of potassium and nitrogen nutrition of rice: change in microbial activity and iron reduction in the rhizosphere. *Plant and Soil* **38:** 267–279.

Tsay Y-F, Ho C-H, Chen H-Y, Lin S-H. **2011**. Integration of nitrogen and potassium signaling. *Annual Review of Plant Biology* **62**: 207–226.

Tsukagoshi H. **2012**. Defective root growth triggered by oxidative stress is controlled through the expression of cell cycle-related genes. *Plant Science* **197**: 30–39.

Tsukagoshi H, Busch W, Benfey PN. **2010**. Transcriptional regulation of ROS controls transition from proliferation to differentiation in the root. *Cell* **143**: 606–616.

Ubeda-Tomás S, Swarup R, Coates J, Swarup K, Laplaze L, Beemster GTS, Hedden P, Bhalerao R, Bennett MJ. **2008**. Root growth in Arabidopsis requires gibberellin/DELLA signalling in the endodermis. *Nature Cell Biology* **10**: 625–628.

Ueguchi-Tanaka M, Ashikari M, Nakajima M, Itoh H, Katoh E, Kobayashi M, Chow TY, Hsing YI, Kitano H, Yamaguchi I *et al.* 2005. *GIBBERELLIN INSENSITIVE DWARF1* encodes a soluble receptor for gibberellin. *Nature* **437**: 693–698.

Ulmasov T, Murfett J, Hagen G, Guilfoyle TJ. **1997**. Aux/IAA proteins repress expression of reporter genes containing natural and highly active synthetic auxin response elements. *The Plant Cell* **9**: 1963–1971.

Uno Y, Furihata T, Abe H, Yoshida R, Shinozaki K, Yamaguchi-Shinozaki K. **2000**. Arabidopsis basic leucine zipper transcription factors involved in an abscisic acid-dependent signal transduction pathway under drought and high-salinity conditions. *Proceedings of the National Academy of Sciences, USA* **97**: 11632–11637.

Vaahtera L, Brosché M, Wrzaczek M, Kangasjärvi J. **2013**. Specificity in ROS signaling and transcript signatures. *Antioxidants and Redox Signaling* **21**: 1422–1441.

Van Norman JM, Zhang J, Cazzonelli CI, Pogson BJ, Harrison PJ, Bugg TDH, Chan KX, Thompson AJ, Benfey PN. **2014**. Periodic root branching in *Arabidopsis* requires synthesis of an uncharacterized carotenoid derivative. *Proceedings of the National Academy of Sciences, USA* **111**: E1300–E1309.

Varotto C, Maiwald D, Pesaresi P, Jahns P, Salamini F, Leister D. **2002**. The metal ion transporter IRT1 is necessary for iron homeostasis and efficient photosynthesis in *Arabidopsis thaliana*. *Plant Journal* **31**: 589–599.

Verbelen J-P, De Cnodder T, Le J, Vissenberg K, Baluska F. **2006**. The root apex of *Arabidopsis thaliana* consists of four distinct zones of growth activities: meristematic zone, transition zone, fast elongation zone and growth terminating zone. *Plant Signaling & Behavior* **1**: 296–304.

Vert G, Grotz N, Dédaldéchamp F, Gaymard F, Guerinot M Lou, Briat J-F, Curie C. **2002**. IRT1, an Arabidopsis transporter essential for iron uptake from the soil and for plant growth. *Plant Cell* **14**: 1223–1233.

Vicente-Agullo F, Rigas S, Desbrosses G, Dolan L, Hatzopoulos P, Grabov A. **2004**. Potassium carrier TRH1 is required for auxin transport in Arabidopsis roots. *Plant Journal* **40**: 523–535.

Voelker C, Gomez-Porras JL, Becker D, Hamamoto S, Uozumi N, Gambale F, Mueller-Roeber B, Czempinski K, Dreyer I. **2010**. Roles of tandem-pore K^+ channels in plants – a puzzle still to be solved. *Plant Biology* **12**: 56–63.

Von Wangenheim D, Hauschild R, Friml J. 2017. Light sheet fluorescence microscopy of plant roots growing on the surface of a gel. *Journal of Visualized Experiments* **119:** 55044.

Wang H, Caruso LV, Downie AB, Perry SE. **2004**. The embryo MADS domain protein AGAMOUS-Like 15 directly regulates expression of a gene encoding an enzyme involved in gibberellin metabolism. *The Plant Cell* **16**: 1206–1219.

Wang M, Zheng Q, Shen Q, Guo S. **2013**. The critical role of potassium in plant stress response. *International Journal of Molecular Sciences* **14**: 7370–7390.

Wang N, Cui Y, Liu Y, Fan H, Du J, Huang Z, Yuan Y, Wu H, Ling HQ. **2013**. Requirement and functional redundancy of Ib subgroup bHLH proteins for iron deficiency responses and uptake in *Arabidopsis thaliana*. *Molecular Plant* **6**: 503–513.

Wang P, Du Y, Zhao X, Miao Y, Song C-P. **2013**. The MPK6-ERF6-ROS-responsive *cis*-acting element7/GCC box complex modulates oxidative gene transcription and the oxidative response in Arabidopsis. *Plant Physiology* **161**: 1392–1408.

Wang Y, Wu WH. **2010**. Plant sensing and signaling in response to K^+-deficiency. *Molecular Plant* **3**: 280–287.

Weigel D. 2012. Natural variation in *Arabidopsis*: from molecular genetics to ecological genomics. *Plant Physiology* **158:** 2–22.

Wen CK, Chang C. **2002**. Arabidopsis *RGL1* encodes a negative regulator of gibberellin responses. *Plant Cell* **14**: 87–100.

Wen X, Zhang C, Ji Y, Zhao Q, He W, An F, Jiang L, Guo H. 2012. Activation of ethylene signaling is mediated by nuclear translocation of the cleaved EIN2 carboxyl terminus. *Cell Research* **22:** 1613.

Weng XY, Zheng CJ, Xu HX, Sun JY. **2007**. Characteristics of photosynthesis and functions of the water-water cycle in rice (*Oryza sativa*) leaves in response to potassium deficiency.

Physiologia Plantarum **131**: 614–621.

Wild M, Daviere J-M, Regnault T, Sakvarelidze-Achard L, Carrera E, Lopez Diaz I, Cayrel A, Dubeaux G, Vert G, Achard P. 2016. Tissue-specific regulation of gibberellin signalling fine-tunes iron-deficiency responses. *Developmental Cell* **37:** 190–200.

Wilhelm BT, Marguerat S, Watt S, Schubert F, Wood V, Goodhead I, Penkett CJ, Rogers J, Bähler J. **2008**. Dynamic repertoire of a eukaryotic transcriptome surveyed at single-nucleotide resolution. *Nature* **453**: 1239–1243.

Winter D, Vinegar B, Nahal H, Ammar R, Wilson GV, Provart NJ. 2007. An 'Electronic Fluorescent Pictograph' browser for exploring and analyzing large-scale biological data sets. *PLoS ONE* **2**: e718.

Wisniewska J, Xu J, Seifertova D, Brewer PB, Ruzicka K, Blilou I, Rouquie D, Benkova E, Scheres B, Friml J. **2006**. Polar PIN localization directs auxin flow in plants. *Science* **312**: 883–883.

Wolverton C, Ishikawa H, Evans ML. **2002**. The kinetics of root gravitropism: Dual motors and sensors. *Journal of Plant Growth Regulation* **21**: 102–112.

World Health Organization. **2012**. *Guideline: Potassium intake for adults and children.* World Health Organization. ISBN-13: 978-924-150482-9.

Wu A, Allu AD, Garapati P, Siddiqui H, Dortay H, Zanor M-I, Asensi-Fabado MA, Munne-Bosch S, Antonio C, Tohge T *et al.* 2012. *JUNGBRUNNEN1*, a reactive oxygen species-responsive NAC transcription factor, regulates longevity in *Arabidopsis*. *The Plant Cell Online* **24**: 482–506.

Xie Z, Zhang Z-L, Zou X, Huang J, Ruas P, Thompson D, Shen QJ. **2005**. Annotations and functional analyses of the rice *WRKY* gene superfamily reveal positive and negative regulators of abscisic acid signaling in aleurone cells. *Plant Physiology* **137**: 176–189.

Xie Z, Zhang ZL, Zou X, Yang G, Komatsu S, Shen QJ. **2006**. Interactions of two abscisic-acid induced *WRKY* genes in repressing gibberellin signaling in aleurone cells. *Plant Journal* **46**: 231–242.

Xu J, Li HD, Chen LQ, Wang Y, Liu LL, He L, Wu WH. **2006**. A protein kinase, interacting with two calcineurin B-like proteins, regulates K^+ transporter AKT1 in Arabidopsis. *Cell* **125**: 1347–1360.

Xu Y-H. **2004**. Characterization of GaWRKY1, a cotton transcription factor that regulates the sesquiterpene synthase gene (+)-δ-cadinene synthase-A. *Plant Physiology* **135**: 507–515.

Xu YL, Li L, Gage DA, Zeevaart JA. **1999**. Feedback regulation of *GA5* expression and metabolic engineering of gibberellin levels in Arabidopsis. *The Plant Cell* **11**: 927–936.

Xuan W, Band LR, Kumpf RP, Van Damme D, Parizot B, De Rop G, Opdenacker D, Moller BK, Skorzinski N, Njo MF *et al.* 2016. Cyclic programmed cell death stimulates hormone signaling and root development in Arabidopsis. *Science* **351**: 384–387.

Yamaguchi S. 2008. Gibberellin metabolism and its regulation. *Annual Review of Plant Biology* **59:** 225–251.

Yang Y, Ou B, Zhang J, Si W, Gu H, Qin G, Qu L-J. 2014. The Arabidopsis Mediator subunit MED16 regulates iron homeostasis by associating with EIN3/EIL1 through subunit MED25. *The Plant Journal* **77:** 838–851.

Yang Y, Hammes UZ, Taylor CG, Schachtman DP, Nielsen E. **2006**. High-affinity auxin transport by the AUX1 influx carrier protein. *Current Biology* **16**: 1123–1127.

Yilmaz A, Mejia-Guerra MK, Kurz K, Liang X, Welch L, Grotewold E. **2011**. AGRIS: the

Arabidopsis gene regulatory information server, an update. *Nucleic Acids Research* **39**: D1118–D1122.

Yoo S-D, Cho Y-H, Tena G, Xiong Y, Sheen J. **2008**. Dual control of nuclear EIN3 by bifurcate MAPK cascades in C_2H_4 signalling. *Nature* **451**: 789–795.

Yoshida R, Umezawa T, Mizoguchi T, Takahashi S, Takahashi F, Shinozaki K. **2006**. The regulatory domain of SRK2E/OST1/SnRK2.6 interacts with ABI1 and integrates abscisic acid (ABA) and osmotic stress signals controlling stomatal closure in *Arabidopsis*. *Journal of Biological Chemistry* **281**: 5310–5318.

Yoshida T, Fujita Y, Maruyama K, Mogami J, Todaka D, Shinozaki K, Yamaguchi-Shinozaki K. **2015**. Four *Arabidopsis* AREB/ABF transcription factors function predominantly in gene expression downstream of SnRK2 kinases in abscisic acid signalling in response to osmotic stress. *Plant, Cell & Environment* **38**: 35–49.

Young DB. 2001. *Role of potassium in preventive cardiovascular medicine.* Boston, MA, USA & London, UK: Kluwer Academic Publishers.

Yuan Y, Wu H, Wang N, Li J, Zhao W, Du J, Wang D, Ling H-Q. **2008**. FIT interacts with AtbHLH38 and AtbHLH39 in regulating iron uptake gene expression for iron homeostasis in *Arabidopsis*. *Cell Research* **18**: 385–397.

Yuan YX, Zhang J, Wang DW, Ling HQ. **2005**. AtbHLH29 of *Arabidopsis thaliana* is a functional ortholog of tomato FER involved in controlling iron acquisition in strategy I plants. *Cell Research* **15**: 613–621.

Zentella R, Hu J, Hsieh WP, Matsumoto PA, Dawdy A, Barnhill B, Oldenhof H, Hartweck LM, Maitra S, Thomas SG *et al.* 2016. O-GlcNAcylation of master growth repressor DELLA by SECRET AGENT modulates multiple signaling pathways in *Arabidopsis*. *Genes and Development* **30**: 164–176.

Zentella R, Sui N, Barnhill B, Hsieh W-P, Hu J, Shabanowitz J, Boyce M, Olszewski NE, Zhou P, Hunt DF *et al.* 2017. The *Arabidopsis* O-fucosyltransferase SPINDLY activates nuclear growth repressor DELLA. *Nature Chemical Biology* **13**: 479–485.

Zentella R, Zhang Z-L, Park M, Thomas SG, Endo A, Murase K, Fleet CM, Jikumaru Y, Nambara E, Kamiya Y *et al.* 2007. Global analysis of DELLA direct targets in early gibberellin signaling in Arabidopsis. *The Plant Cell* **19**: 3037–3057.

Zhang B, Liu H, Ding X, Qiu J, Zhang M, Chu Z. 2017. *AtACS8* plays a critical role in the early biosynthesis of ethylene elicited by copper ions in *Arabidopsis*. *Journal of Cell Science*. doi: 10.1242/jcs.202424.

Zhang H, Han W, De Smet I, Talboys P, Loya R, Hassan A, Rong H, Jürgens G, Paul Knox J, Wang MH. **2010**. ABA promotes quiescence of the quiescent centre and suppresses stem cell differentiation in the Arabidopsis primary root meristem. *Plant Journal* **64**: 764–774.

Zhang Y, Wu H, Wang N, Fan H, Chen C, Cui Y, Liu H, Ling H-Q. 2014. Mediator subunit 16 functions in the regulation of iron uptake gene expression in Arabidopsis. *New Phytologist* **203:** 770–783.

Zhang Z-L, Ogawa M, Fleet CM, Zentella R, Hu J, Heo J-O, Lim J, Kamiya Y, Yamaguchi S, Sun T. **2011**. SCARECROW-LIKE 3 promotes gibberellin signaling by antagonizing master growth repressor DELLA in Arabidopsis. *Proceedings of the National Academy of Sciences, USA* **108**: 2160–2165.

Zhang Z-L, Xie Z, Zou X, Casaretto J, Ho T-HD, Shen QJ. **2004**. A rice *WRKY* gene encodes a transcriptional repressor of the gibberellin signaling pathway in aleurone cells. *Plant Physiology* **134**: 1500–1513.

Zhao Y, Hull AK, Gupta NR, Goss KA, Alonso J, Ecker JR, Normanly J, Chory J, Celenza JL. **2002**. Trp-dependent auxin biosynthesis in Arabidopsis: involvement of cytochrome P450s CYP79B2 and CYP79B3. *Genes and Development* **16**: 3100–3112.

Zhao D, Oosterhuis DM, Bednarz CW. **2001**. Influence of potassium deficiency on photosynthesis, chlorophyll content, and chloroplast ultrastructure of cotton plants. *Photosynthetica* **39**: 103–109.

Zhao C, Zhang Z, Xie S, Si T, Li Y, Zhu J-K. **2016**. Mutational evidence for the critical role of CBF genes in cold acclimation in Arabidopsis. *Plant Physiology* **171:** 2744–2759.

Zheng Y, Ren N, Wang H, Stromberg AJ, Perry SE. **2009**. Global identification of targets of the *Arabidopsis* MADS domain protein AGAMOUS-Like15. *The Plant Cell Online* **21**: 2563–2577.

Zhou M, Chen H, Wei D, Ma H, Lin J. **2017**. Arabidopsis CBF3 and DELLAs positively regulate each other in response to low temperature. *Scientific Reports* **7**: 39819.

Appendices

Appendix I Primer sequences

Primers used for genotyping:

AGI	Gene name	Forward Primer	Reverse Primer	Tm (°C)
AT5G39670	*CML46*	AACTTCCTCTCTTTTGCCTCG	AGTGATGGAGAGCTCTTG CAC	60
AT1G80840	*WRKY40*	CTTTCTTCCTCAGCTTACGGG	TTTGACAGAACAGCTTGGA GC	50
AT4G17490	*ERF6*	TCTGAATTTGAAACCAAACC G	CGAGCATATTACATGCCAT TG	58
AT1G27730	*STZ*	TATTTTGTAAGGCGGCATCA G	AAGTCAAACCGAGGCTTCT TC	60
AT5G47910	*AtrbohD*	CGGATGGGAGACAGCAGGA TACTTAGTC	GAGCTTGATACCATGGAC AATGAGAAGAGC	62
AT1G64060	*AtrbohF*	ACTTCCGATATCCTTCAACCA ACTCTTTG	CTCTCGTCGTTGATTTGTG ACCAATACT	60

TDNA insert specific border primers:

T-DNA insert	Specific border primer sequence	Tm (°C)
Spm32_JICSM	TACGAATAAGAGCGTCCATTTTAGAGTGA	62
dSpm1	CTTATTTCAGTAAGAGTGTGGGGTTTTGG	62
dSpm11	GGTGCAGCAAAACCCACACTTTTACTTC	65
LBb1.3 SALK border	ATTTTGCCGATTTCGGAAC	52

Primers used qRT-PCR:

	Forward Primer	Reverse Primer	Tm (°C)
HK1 *AT1G13320*	TAACGTGGCCAAAATGATGC	GTTCTCCACAACCGCTTGGT	55 59
ACT2	GGATCGGTGGTTCCATTCTTGC	AGAGTTTGTCACACACAAGTGCA	56 55
HAK5	CGAGACGGACAAAGAAGAGGAACC	CACGACCCTTCCCGACCTAATCT	64 64
ERF6	TCGAATCCTCCTCGCGTTACTG	TTCGGTGGTGCGATCTTCAACG	62 62
STZ	TCACAAGGCAAGCCACCGTAAG	TTGTCGCCGACGAGGTTGAATG	62 62
IAA2	CCTCCTACCAAAACTCAAATCGTT	CGTAGCTCACACTGTTGTTGTTCT	59 61
ERF1	GGTATTAGGGTTTGGCTCGG	CCGAAAGCGACTCTTGAACT	58 58
GA2ox6	TGGATCCCAATCCCATCTGACC	TCTCCCATTCGTCAATGCCTGAAG	62 62
GA3ox2	CTGCCGCTCATCGACCTC	AGCATGGCCCACAAGAGTG	60 58
GA3ox1	GATCTCCTCTTCTCCGCTGCT	GAGGGATGTTTTCACCGGTG	61 59

Appendix II Analysis of RNA quality for use in RNA-Seq experiment

A

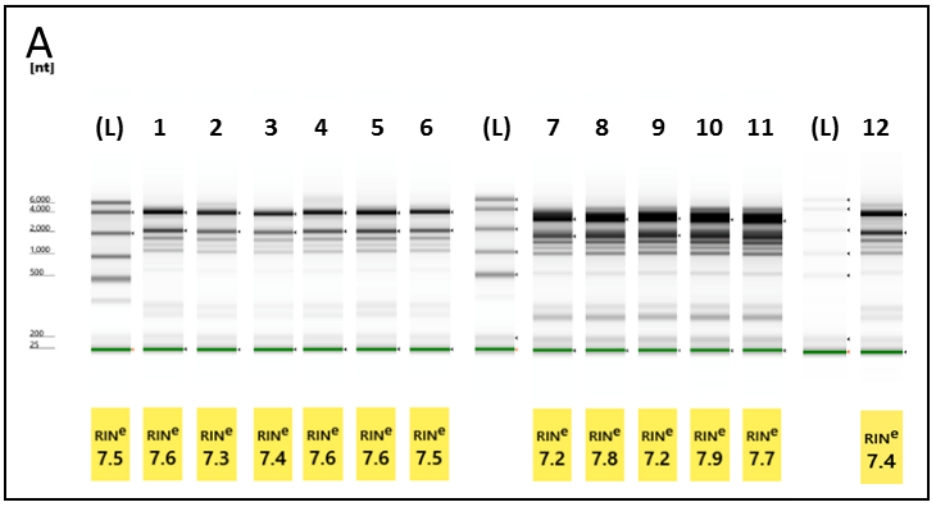

B

Sample Description	Well	RINe	28S/18S (Height)	28S/18S (Area)	Conc. (ng μl^{-1})	Total RNA Area	rRNA Area
3 h 2 mM 1	1	7.6	2.1	1.8	345	10.07	3.17
3 h 2 mM 2	2	7.3	2.2	1.9	279	8.14	2.39
3 h 2 mM 3	3	7.4	2.3	1.9	250	7.30	2.31
3 h 0.005 mM 1	4	7.6	2.2	2.0	313	9.12	2.66
3 h 0.005 mM 2	5	7.6	2.1	1.8	352	10.28	3.22
3 h 0.005 mM 3	6	7.5	2.1	1.9	280	8.17	2.46
30 h 2 mM 1	7	7.2	2.1	1.6	824	15.69	4.45
30 h 2 mM 2	8	7.8	-	-	574	21.84	-
30 h 2 mM 3	9	7.2	2.3	1.5	614	23.36	6.49
0.005 mM 30 h 1	10	7.9	-	-	666	25.36	-
0.005 mM 30 h 2	11	7.7	-	-	659	25.06	-
0.005 mM 30 h 3	12	7.4	2.2	1.9	372	10.85	3.21

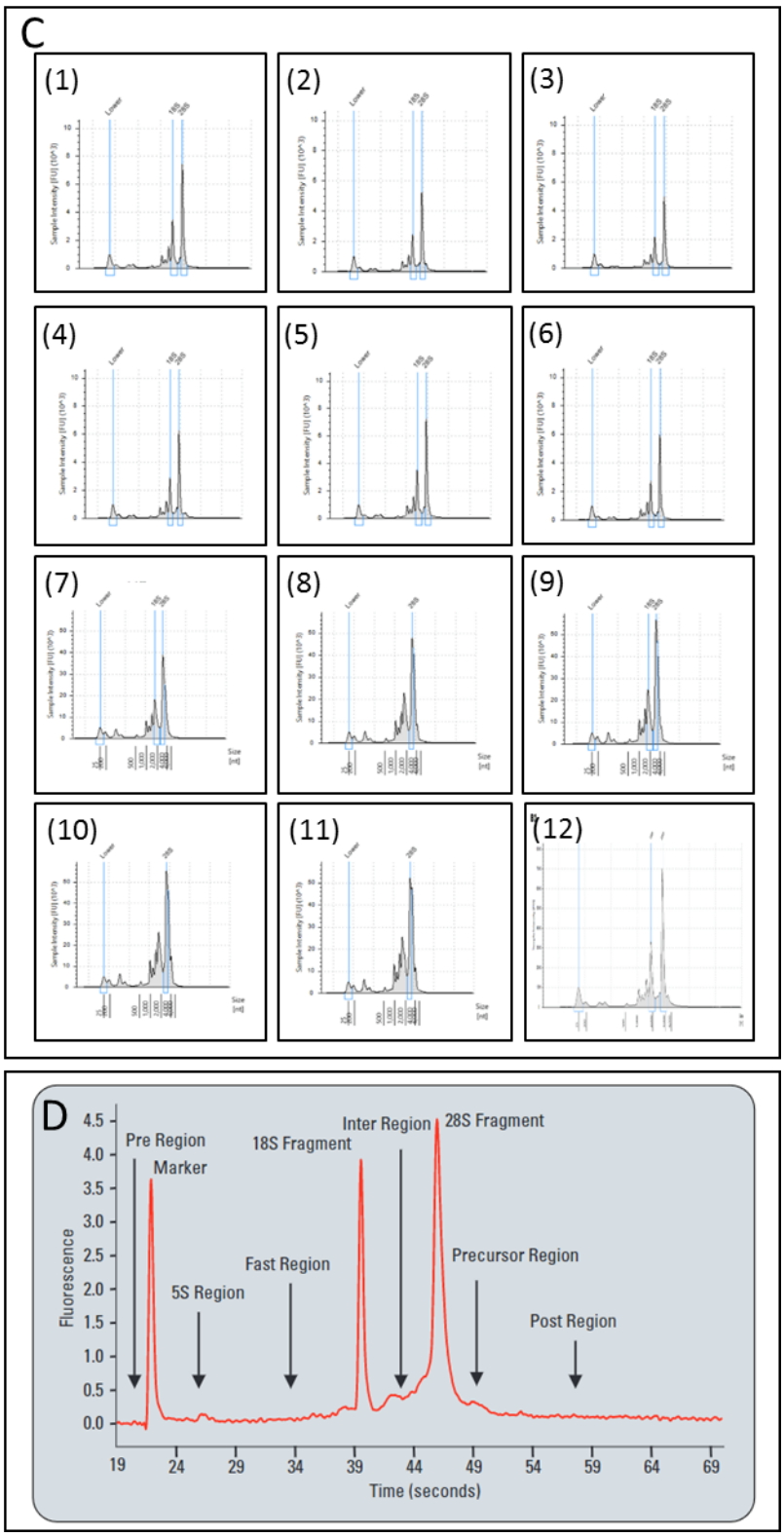

Appendix II: Analysis of the quality of the RNA Samples used in the RNA-Seq experiment. Results obtained from samples run on an RNA ScreenTape. Figure shows composite of results, run on different tapes. (A) Gel- like image of total RNA sample. (B) Full sample metrics. (C) Electropherograms showing quality of RNA levels. (D) Representative electropherogram detailing regions indicative of RNA quality. Figure from Mueller *et al., (*2016).

Appendix III Photosynthetic gene changes in response to low K^+

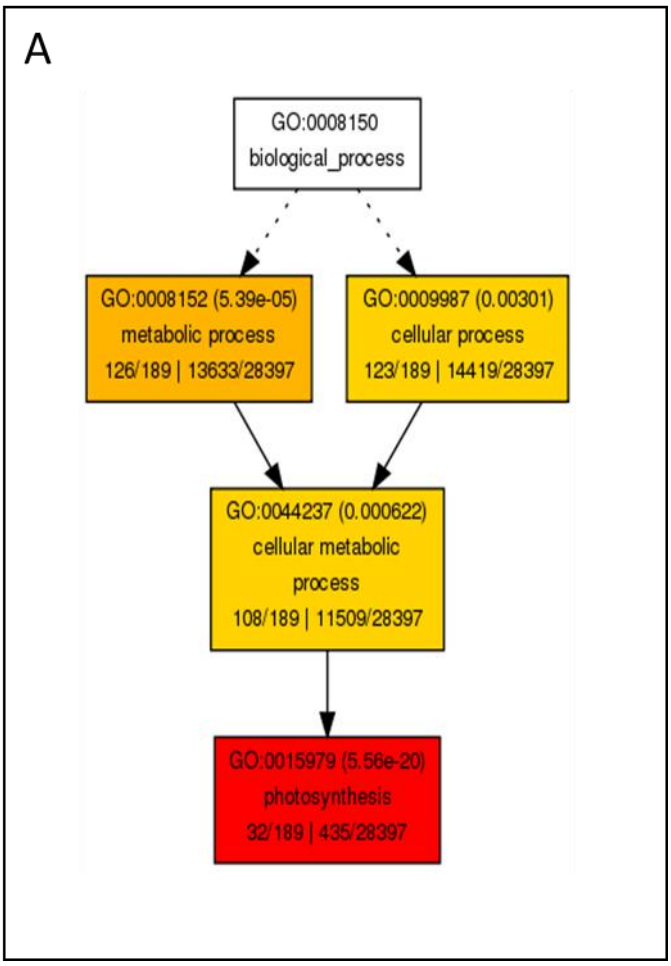

B AGI	Gene name	log_2fc 30 h
AT1G60950	2Fe-2S ferredoxin-like superfamily protein(FED A)	-0.64
AT2G40100	Light harvesting complex photosystem II(LHCB4.3)	-0.54
AT2G40300	Ferritin 4(FER4)	-0.99
AT3G47070	Thylakoid soluble phosphoprotein(AT3G47070)	-0.52
AT3G56090	Ferritin 3(FER3)	-0.59
AT3G61870	Plant/protein (AT3G61870)	-0.53
AT4G12480	Bifunctional inhibitor/lipid-transfer protein/seed storage 2S albumin superfamily protein(EARLI1)	-0.56
AT5G01600	Ferretin 1(FER1)	-1.76
AT5G13630	Magnesium-chelatase subunit chlH, chloroplast, putative / Mg-protoporphyrin IX chelatase, putative (CHLH)(GUN5)	-0.51
AT5G17170	Rubredoxin family protein(ENH1)	-1.09
ATCG00040	MATK, MATURASE K	-2.06
ATCG00065	RIBOSOMAL PROTEIN S12	-1.89
ATCG00160	RIBOSOMAL PROTEIN S2, RPS2	-0.68
ATCG00170	RPOC2 RNA polymerase beta' subunit-2	-0.56
ATCG00270	PHOTOSYSTEM II REACTION CENTER PROTEIN D, PSBD	-2.08
ATCG00280	PHOTOSYSTEM II REACTION CENTER PROTEIN C, PSBC	-1.82
ATCG00300	YCF9 encodes PsbZ, which is a subunit of photosystem II	-1.74
ATCG00380	CHLOROPLAST RIBOSOMAL PROTEIN S4	-1.19
ATCG00420	NADH DEHYDROGENASE SUBUNIT J, NDHJ	-1.08
ATCG00430	NDHK, PHOTOSYSTEM II REACTION CENTER PROTEIN G, PSBG	-0.89
ATCG00440	NDHC Encodes NADH dehydrogenase D3 subunit o	-1.39
ATCG00470	ATP SYNTHASE EPSILON CHAIN, ATPE	-0.62
ATCG00480	ATHCF1BETA, ATP SYNTHASE SUBUNIT BETA, ATPB, CF1BETA, PB	-0.58
ATCG00550	PHOTOSYSTEM II REACTION CENTER PROTEIN J, PSBJ	-0.86
ATCG00640	RIBOSOMAL PROTEIN L33, RPL33	-1.05
ATCG00650	RIBOSOMAL PROTEIN S18, RPS18	-2.34
ATCG00660	RIBOSOMAL PROTEIN L20, RPL20	-0.61
ATCG00670	CASEINOLYTIC PROTEASE P 1, CLPP1, PCLPP, PLASTID-ENCODED CLP P	-1.55
ATCG00820	RIBOSOMAL PROTEIN S19	-0.53
ATCG01020	RIBOSOMAL PROTEIN L32, RPL32	-0.96
ATCG01040	YCF5 respiratory chain complex IV assembly	-1.13
ATCG01310	RIBOSOMAL PROTEIN L2, RPL2.2	-0.69

Appendix III: (A) Gene ontology analysis (agriGO) of genes dowregulated after 30 h K^+ deprivation treatment. Significant GO term 'Photosynthesis' selected and graphed. (B) Table of genes identified in the AgriGO analysis with gene expression changes in response to 30 h low K^+, identified by RNA-Seq.

Appendix IV Fe related gene expression changes in response to low K^+

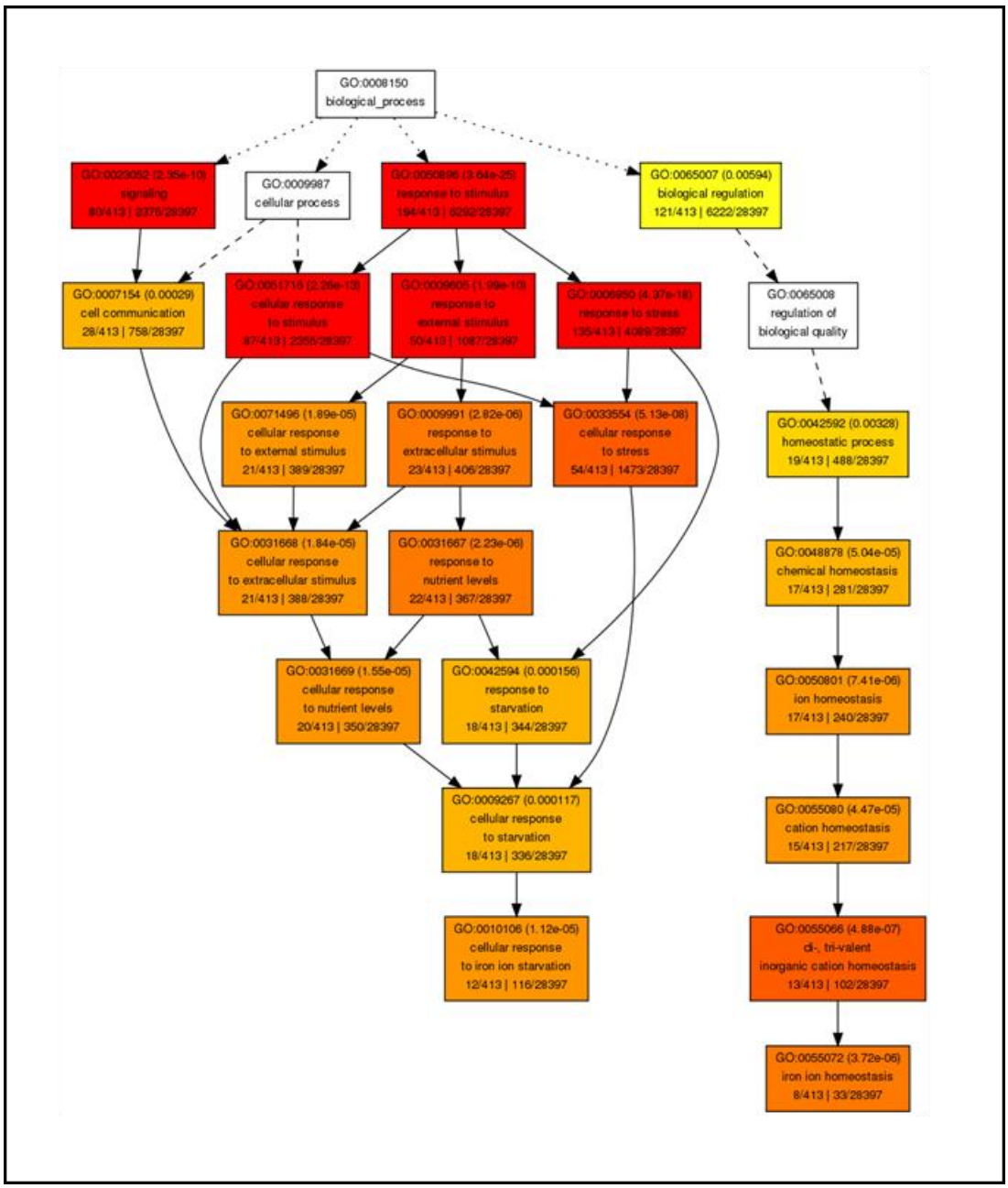

Appendix IV: Gene ontology analysis (agriGO) of genes upregulated after 30 h K^+ deprivation treatment (from RNA-Seq experiment). Significant GO term 'Iron ion homeostasis' and 'cellular response to iron ion starvation' selected and graphed.

Appendix V Genes upregulated in response to low K^+ and various ROS stimuli

A		K^+ starvation		ROS Transcriptomic Footprint							
AGI	Gene name	30 h log_2fc		KD-SOD	APX1-1.5 h	flu-2 h	OZONE	MV-24 h	CAT2HP 1-8 h	AAL-48 h	AT
AT2G43510	IT1	1.14		5.58	15.44	6.53	11.90	8.04	6.06	8.49	14.03
AT3G13610	AT3G13610	0.75		2.22	2.32	1.01	4.22	2.20	31.37	53.35	12.09
AT4G29780	AT4G29780	0.88		0.63	2.97	312.95	30.74	6.98	0.82	0.56	0.56
AT1G80840	WRKY40	1.29		**0.89**	**2.87**	**262.56**	**123.50**	**36.46**	**0.72**	**1.18**	**1.85**
AT5G04340	ZAT6	0.58		**2.04**	**1.96**	**147.10**	**23.29**	**44.81**	**1.71**	**0.48**	**0.92**
AT5G59820	ZAT12	0.59		**1.36**	**1.35**	**130.86**	**65.98**	**45.34**	**4.88**	**4.03**	**3.06**
AT1G27730	STZ	0.79		**1.51**	**2.61**	**126.29**	**72.22**	**85.18**	**0.86**	**0.61**	**0.81**
AT2G38470	WRKY33	0.60		**1.29**	**3.59**	**90.32**	**23.93**	**21.25**	**2.87**	**1.62**	**1.34**
AT4G17500	ERF-1	0.66		**0.99**	**0.92**	**46.66**	**13.31**	**19.23**	**0.59**	**1.56**	**4.05**
AT4G27280	AT4G27280	0.74		0.69	2.20	25.58	10.82	5.09	0.61	0.80	0.89
AT3G50260	CEJ1	0.57		**1.08**	**0.91**	**22.21**	**13.96**	**12.35**	**1.35**	**0.93**	**3.42**
AT3G55980	SZF1	0.63		**0.94**	**1.64**	**16.94**	**9.44**	**6.14**	**0.36**	**0.27**	**0.41**
AT5G47220	ERF2	0.98		**1.07**	**0.78**	**15.02**	**31.78**	**11.39**	**0.26**	**0.64**	**0.47**
AT1G72900	AT1G72900	0.53		1.04	2.77	14.32	26.19	15.07	2.19	0.71	1.27
AT1G18570	MYB51	0.52		**2.81**	**1.35**	**13.79**	**23.65**	**5.19**	**4.72**	**1.76**	**1.31**
AT2G04040	DTX1	0.58		1.17	0.93	12.06	22.11	30.80	3.40	0.97	1.00
AT4G17490	ERF6	0.84		**1.98**	**0.98**	**6.40**	**18.54**	**7.21**	**0.35**	**0.70**	**0.71**
AT1G26420	AT1G26420	1.04		0.89	0.88	5.93	38.32	8.82	20.70	48.14	6.54
AT5G13080	WRKY75	0.74		**0.91**	**0.91**	**9.68**	**64.32**	**19.97**	**48.20**	**68.03**	**27.39**
AT1G26380	AT1G26380	1.32		0.97	1.02	18.28	82.73	56.10	102.60	57.12	12.86
AT4G37370	CYP81D8	0.72		1.91	1.17	45.50	152.07	220.79	47.58	13.39	19.14

B		K^+ starvation		ROS Transcriptomic Footprint							
AGI	Gene name	3 h log_2fc		KD-SOD	APX1-1.5 h	flu-2 h	OZONE	MV-24 h	CAT2HP 1-8 h	AAL-48 h	AT
AT4G29780	AT4G29780	0.89		0.63	2.97	312.95	30.74	6.98	0.82	0.56	0.56
AT1G80840	WRKY40	1.11		**0.89**	**2.87**	**262.56**	**123.50**	**36.46**	**0.72**	**1.18**	**1.85**
AT1G27730	STZ	0.83		**1.51**	**2.61**	**126.29**	**72.22**	**85.18**	**0.86**	**0.61**	**0.81**
AT2G38470	WRKY33	0.94		**1.29**	**3.59**	**90.32**	**23.93**	**21.25**	**2.87**	**1.62**	**1.34**
AT1G61340	FBS1	0.56		0.81	0.34	54.74	58.74	6.74	2.04	0.18	1.42
AT4G24570	DIC2	1.21		0.97	2.33	28.99	7.98	5.01	0.43	0.43	0.51
AT4G27280	AT4G27280	0.67		0.69	2.20	25.58	10.82	5.09	0.61	0.80	0.89
AT3G10930	AT3G10930	0.61		2.11	0.98	23.14	24.97	6.49	1.39	0.80	1.47
AT3G55980	SZF1	1.09		**0.94**	**1.64**	**16.94**	**9.44**	**6.14**	**0.36**	**0.27**	**0.41**
AT1G18570	MYB51	0.73		**2.81**	**1.35**	**13.79**	**23.65**	**5.19**	**4.72**	**1.76**	**1.31**
AT2G40140	CZF1	0.51		**2.27**	**2.05**	**13.67**	**12.30**	**15.42**	**2.23**	**0.81**	**0.97**
AT4G11280	ACS6	0.71		0.75	1.53	12.96	6.54	8.05	2.42	0.59	0.66
AT2G41100	TCH3	0.59		0.96	3.04	11.17	27.14	11.40	1.72	1.33	2.42
AT4G17490	ERF6	0.93		**1.98**	**0.98**	**6.40**	**18.54**	**7.21**	**0.35**	**0.70**	**0.71**

Appendix V: (A) 21 genes upregulated after 30 h K^+ starvation (blue) also upregulated by over 5-fold in at least 3 of the ROS experiments in the ROS transcriptomics footprint Gadjev *et al.* (2006). (B) 14 genes upregulated after 3 h K^+ starvation (blue) also upregulated by over 5-fold in at least 3 of the ROS experiments in the ROS transcriptomics footprint (red) Gadjev *et al.* (2006).

Appendix VI Effect of DPI on primary root growth

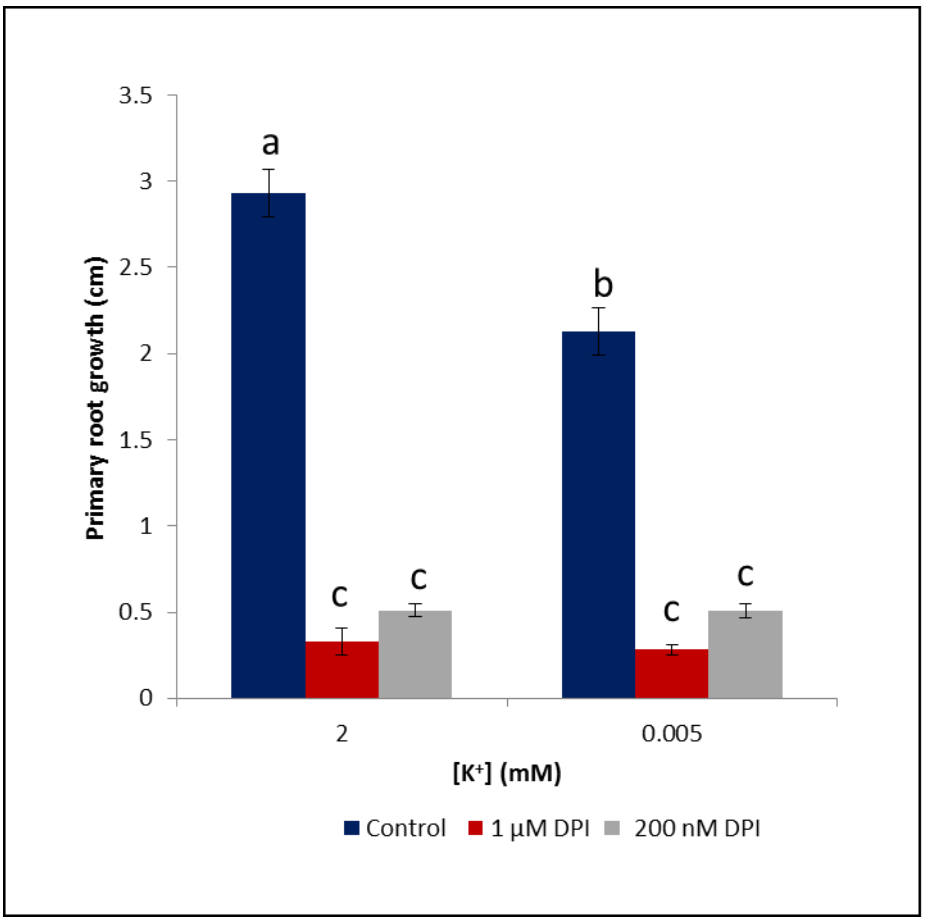

Appendix VI: Average primary root growth over 3 d following treatment when media supplemented with 200 nM or 1 µM DPI. Values are averages taken from at least 6 individual seedlings ± SE. Letters indicate significance with a Tukey Pairwise comparison $P < 0.05$.

Appendix VII *SALK_05092* primary root growth on low K^+

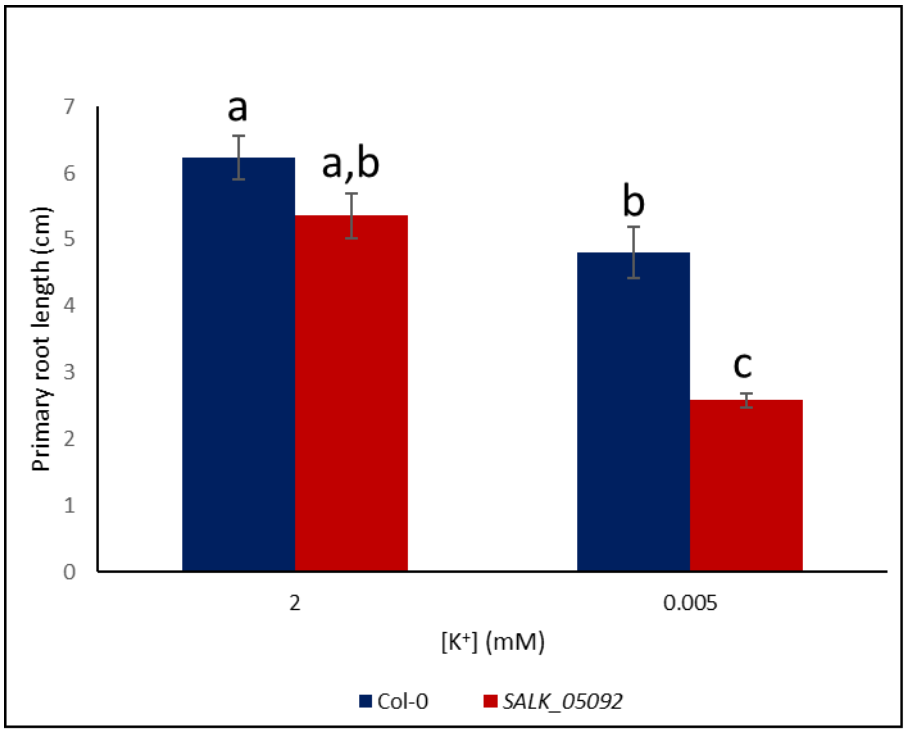

Appendix VII: Primary root length after 8 d K^+ treatment (2 mM or 0.005 mM) of Col-0 and *SALK_05092.* Values are averages taken from at least 16 individual seedlings ± SE. Letters indicate significance with a Tukey Pairwise comparison $P< 0.05$. Control taken from another experiment.

Appendix VIII Restoration of growth following resupply of K^+

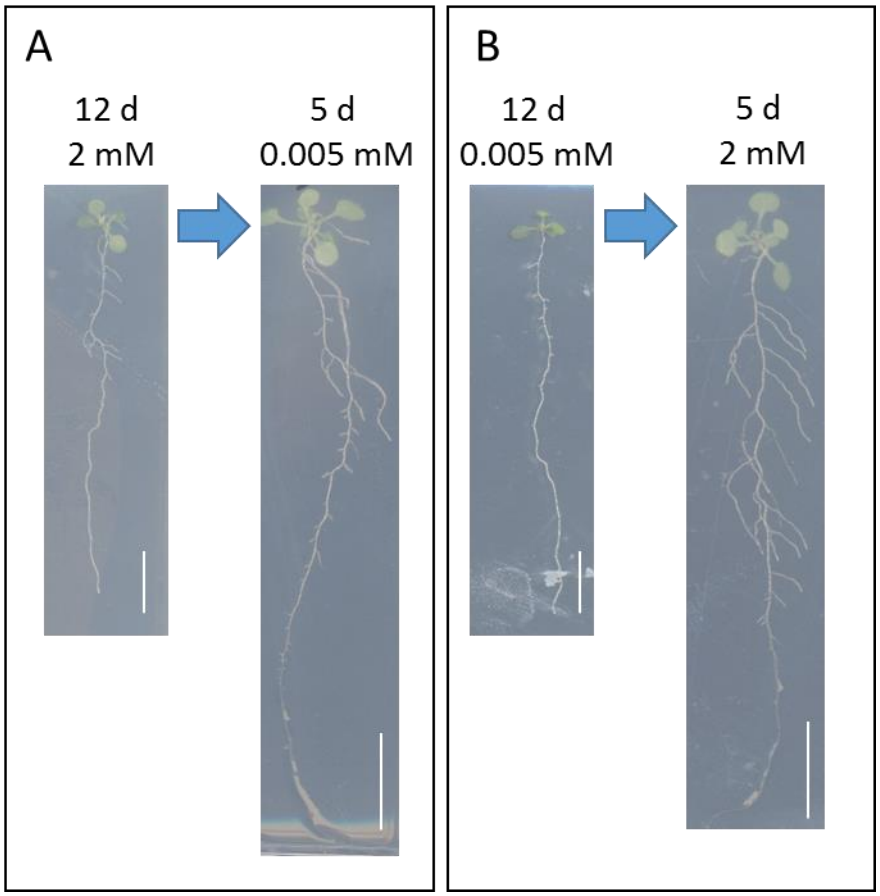

Appendix VIII: Preliminary data: representative images of growth response after 12 d growth on either 2 mM or 0.005 mM [K^+], then swapped to the opposite [K^+] and a further 5 d growth. (A) Grown for 12 d on 2 mM then moved to 0.005 mM for 5 d. (B) Grown for 12 d on 0.005 mM then moved to 2 mM for 5 d. Scale bar = 1 cm. *n = 5* individual seedlings for each treatment.

Appendix IX Differentially expressed gene list

The following file can be found on the enclosed CD-ROM.

Appendix IX DEGs Excel spreadsheet:

Page 1: Genes upregulated by at least 0.5 log_2fc in response to 3 h K^+ starvation

Page 2: Genes downregulated by at least 0.5 log_2fc in response to 3 h K^+ starvation

Page 3: Genes upregulated by at least 0.5 log_2fc in response to 30 h K^+ starvation

Page 4: Genes downregulated by at least 0.5 log_2fc in response to 30 h K^+ starvation